



**NARASARAOPETA**  
**ENGINEERING COLLEGE**  
(AUTONOMOUS)

**DEPARTMENT OF ELECTRONICS AND COMMUNICATION ENGINEERING**

# **COURSE FILE**

## **DIGITAL IMAGE PROCESSING**

### **III B.TCH, II SEMESTER**

### **R16 REGULATION**



**NARASARAOPETA**  
**ENGINEERING COLLEGE**  
(AUTONOMOUS)

Department of Electronics and Communication Engineering

**COURSE FILE CONTENTS**

S.No	CONTENTS
1	Institute, Department Vision and Mission
2	Programme Educational Objectives and Programme Specific Outcomes
3	Program Outcomes
4	Bloom's Taxonomy levels
5	Course Objectives & Course Outcomes
6	Course Information Sheet
7	Academic calendar
8	Time tables
9	Syllabus copy
10	Lesson Plan
11	CO-PO& PSO Mapping and assessment
12	Web references & other pedagogical initiatives details
13	Student's Roll list
14	Hand Written / Printed Lecture Notes / Material given to the Students
15	Power Point Presentation Slides
16	Mid & Assignment Examination Question Papers with scheme and solutions (for problems)
17	Unit wise important questions
18	Previous University Question Papers
19	Missing Topics(Course gaps) and Topics beyond Syllabus
20	Remedial/corrective actions

Submitted By

Approved By



Institute Vision  
and  
Mission



Department of Electronics and Communication Engineering

## Institute Vision and Mission

### **Vision**

To emerge a Centre of excellence in technical education with a blend of effective student centric teaching learning practices as well as research for the transformation of lives and community,

### **Mission**

M1: Provide the best class infra- structure to explore the field of engineering and research

M2: Build a passionate and a determined team of faculty with student centric teaching, imbibing experiential, innovative skills

M3: Imbibe lifelong learning skills, entrepreneurial skills and ethical values in students for addressing societal problems

  
**PRINCIPAL**

PRINCIPAL  
NARASARAOPETA ENGINEERING COLLEGE  
(AUTONOMOUS)  
NARASARAOPET - 522 601  
Guntur (Dist.), A.P.

# Department Vision and Mission

 **NARASARAOPETA**  
**ENGINEERING COLLEGE**  
(AUTONOMOUS)

Department of Electronics and Communication Engineering

DEPARTMENT VISION AND MISSION

**VISION:**

To produce creative communication engineers by imparting technical education with ethical and moral values to meet the global standards.

**MISSION:**

1. To impart technical education theoretically and practically with discipline through dedicated staff.
2. To develop state-of-the-art laboratories and research facilities for effective teaching learning process to produce globally competent ECE graduates.
3. To empower the students with up to date technical trends and establishing industry interactions through consultancy and sponsored research.

  
**HOD**

**HEAD OF THE DEPARTMENT**  
**DEPT. OF ELECTRONICS AND COMMUNICATION**  
**ENGG**  
**NARASARAOPETA ENGINEERING COLLEGE**  
**NARASARAOPET-522 601**

PEOs

&

PSOs



# NARASARAOPETA ENGINEERING COLLEGE

(AUTONOMOUS)

Department of Electronics and Communication Engineering

## PROGRAM EDUCATIONAL OBJECTIVES:

PEO1: To train the students to design and analyze the electronic circuits and equipment for societal benefits.

PEO2: To inculcate in the students the desire for lifelong learning to obtain thorough knowledge in their chosen fields and also to motivate them for higher studies/research.

PEO3: To train the students so that they can effectively perform the duties assigned to them as team leaders or project managers in the industry/organization with ethical and moral values.

## PROGRAM SPECIFIC OUTCOMES:

PSO1: Analyze and Design Analog and Digital circuits for a given specification and function.

PSO2: Design a variety of Electronic Systems for applications including Signal Processing, Communications, Computer Networks and Control Systems.

  
HOD

HEAD OF THE DEPARTMENT  
DEPT. OF ELECTRONICS AND COMMUNICATION  
ENGG  
NARASARAOPETA ENGINEERING COLLEGE  
NARASARAOPET-522 601



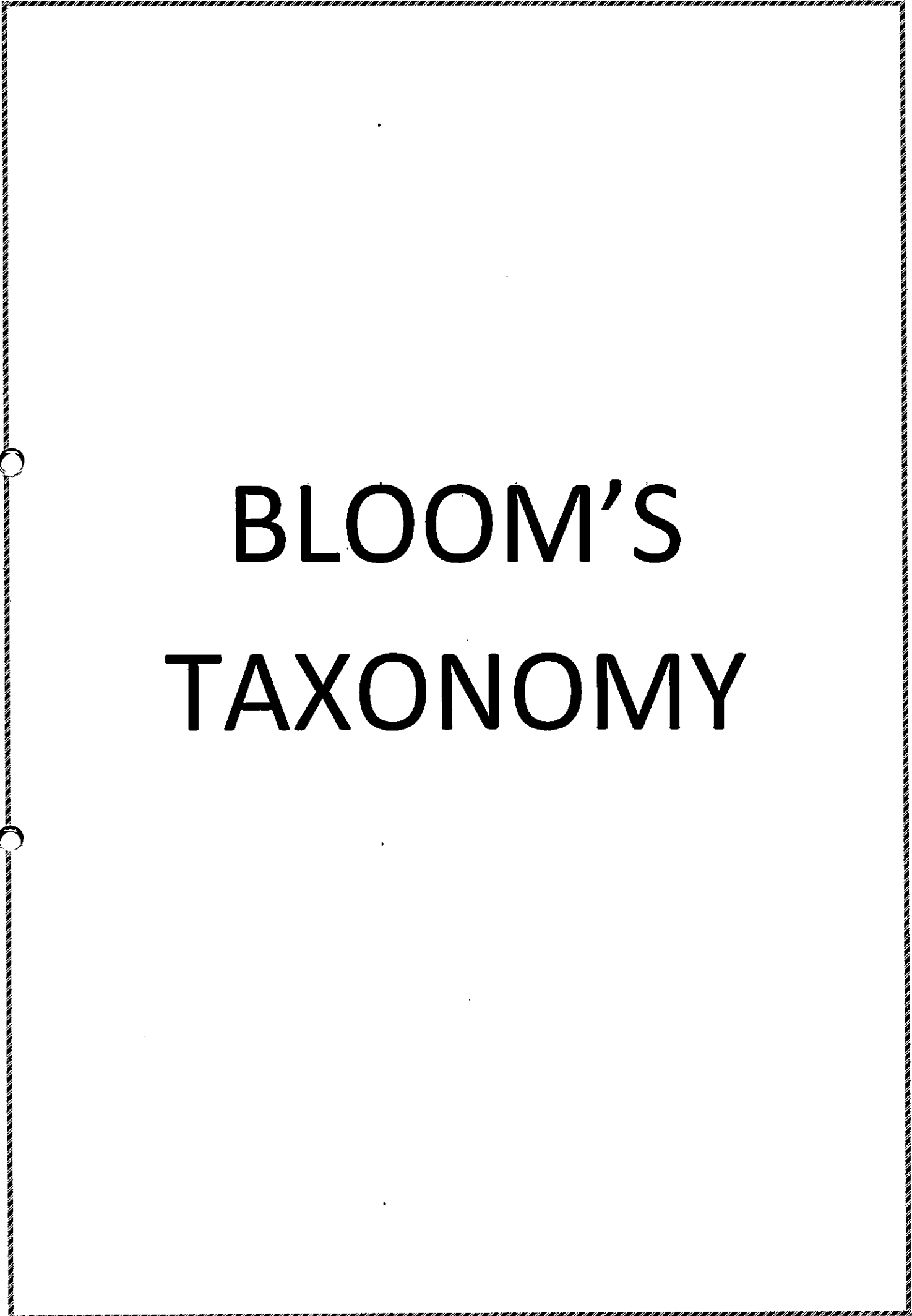
# PROGRAM OUTCOMES

DEPARTMENT OF ELECTRONICS AND COMMUNICATION ENGINEERING

**PROGRAM OUTCOMES**

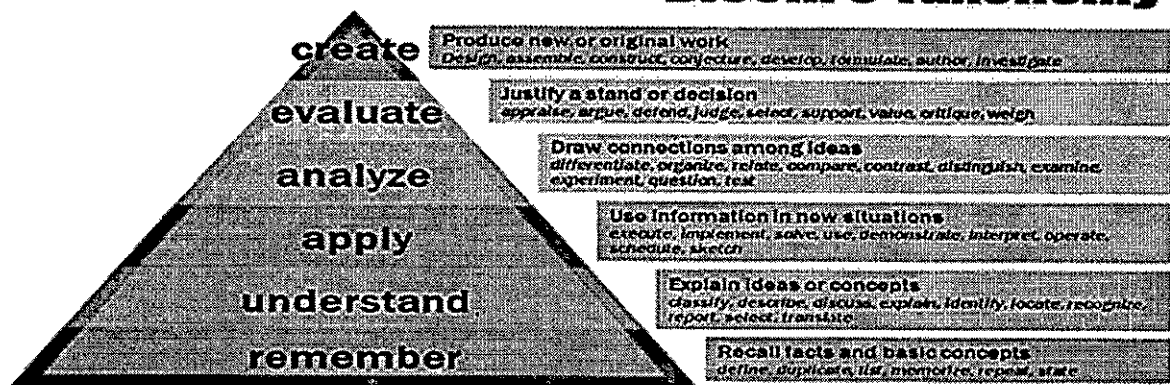
Narasaraopeta Engineering College follows the Program Outcomes (PO) as defined by NBA  
Engineering Graduates will be able to:

<b>PO1</b>	<b>1. Engineering knowledge:</b> Apply the knowledge of mathematics, science, engineering fundamentals, and an engineering specialization to the solution of complex engineering problems.
<b>PO2</b>	<b>2. Problem analysis:</b> Identify, formulate, review research literature, and analyze complex engineering problems reaching substantiated conclusions using first principles of mathematics, natural sciences, and engineering sciences
<b>PO3</b>	<b>3. Design/development of solutions:</b> Design solutions for complex engineering problems and design system components or processes that meet the specified needs with appropriate consideration for the public health and safety, and the cultural, societal, and environmental considerations.
<b>PO4</b>	<b>4. Conduct investigations of complex problems:</b> Use research-based knowledge and research methods including design of experiments, analysis and interpretation of data, and synthesis of the information to provide valid conclusions
<b>PO5</b>	<b>5. Modern tool usage:</b> Create, select, and apply appropriate techniques, resources, and modern engineering and IT tools including prediction and modeling to complex engineering activities with an understanding of the limitations.
<b>PO6</b>	<b>6. The engineer and society:</b> Apply reasoning informed by the contextual knowledge to assess societal, health, safety, legal and cultural issues and the consequent responsibilities relevant to the professional engineering practice
<b>PO7</b>	<b>7. Environment and sustainability:</b> Understand the impact of the professional engineering solutions in societal and environmental contexts, and demonstrate the knowledge of, and need for sustainable development.
<b>PO8</b>	<b>8. Ethics:</b> Apply ethical principles and commit to professional ethics and responsibilities and norms of the engineering practice
<b>PO9</b>	<b>9. Individual and team work:</b> Function effectively as an individual, and as a member or leader in diverse teams, and in multidisciplinary settings
<b>PO10</b>	<b>10. Communication:</b> Communicate effectively on complex engineering activities with the engineering community and with society at large, such as, being able to comprehend and write effective reports and design documentation, make effective presentations, and give and receive clear instructions
<b>PO11</b>	<b>11. Project management and finance:</b> Demonstrate knowledge and understanding of the engineering and management principles and apply these to one's own work, as a member and leader in a team, to manage projects and in multidisciplinary environments
<b>PO12</b>	<b>12. Life-long learning:</b> Recognize the need for, and have the preparation and ability to engage in independent and life-long learning in the broadest context of technological change.



# **BLOOM'S TAXONOMY**

# Bloom's Taxonomy



**COURSE  
OBJECTIVES  
&  
COURSE  
OUTCOMES**

**COURSE OBJECTIVES:**

1. Give the students a taste of the applications of the theories taught in the subject. This will be achieved through the project and some selected lab sessions.
2. Introduce the students to some advanced topics in digital image processing.
3. Give the students a useful skill base that would allow them to carry out further study should they be interested and to work in the field.

**COURSE OUTCOMES:**

On completion of the course, the student will be able to

**CO1:** Recall the Digital Image Fundamentals & Image Transforms.

**CO2:** Implement basic image processing algorithms or techniques (Spatial Domain & Frequency Domain

**CO3:** Summarize Image Restoration using Degradation Model, Algebraic Approach, Inverse Filtering, Least Mean Square Filters, and Constrained Least Squares Filters

**CO4:** Compare three (RGB, CMY and HIS) color models, pseudo color image processing and full color image processing,

**CO5:** Illustrate wavelets multi-resolution processing and different image compression techniques.

**CO6:** Demonstrate the Image Segmentation and Morphological Image Processing.

# **Course Information Sheet**



**Narasaraopeta Engineering College**  
(Autonomous)  
Yallmanda(Post), Narasaraopet- 522601  
Department of Electronics & Communication  
Engineering

### COURSE INFORMATION SHEET

<b>PROGRAMME: B.Tech Electronics &amp; Communication Engineering</b>	
<b>COURSE: DIGITAL IMAGE PROCESSING</b>	Semester : VI      CREDITS: 3
<b>COURSE CODE: R16EC3209 (C323)</b> REGULATION: R1	<b>COURSE TYPE (CORE /ELECTIVE / BREADTH/ S&amp;H): CORE</b>
<b>COURSE AREA/DOMAIN: Image Processing</b>	<b>PERIODS: 6 Per Week.</b>

**COURSE PRE-REQUISITES:**

C.CODE	COURSE NAME	DESCRIPTION	SEM
R21041	Amplifiers	Knowledge of filters is required	III
R32043	Signal Processing	Knowledge of transformations	VI

**COURSE OUTCOMES:**

SNO	Course Outcome Statement
CO1	Recall the Digital Image Fundamentals & Explain Image Transforms-K1 & K2
CO2	Implement basic image processing algorithms or techniques (Spatial Domain & Frequency Domain)-K3
CO3	Summarize Image Restoration using Degradation Model, Algebraic Approach, Inverse Filtering, Least Mean Square Filters, and Constrained Least Squares Filters-K2
CO4	Compare three (RGB, CMY and HIS) color models, pseudo color image processing and full color image processing-K4
CO5	Illustrate wavelets multi-resolution processing and different image compression techniques-K4
CO6	Demonstrate the Image Segmentation and Morphological Image Processing-K3

**SYLLABUS:**

UNIT	DETAILS
I	<p><b>UNIT-1</b></p> <p><b>Introduction:</b> Origins of digital image processing, uses digital image processing, fundamental steps in digital image processing, components of an image processing system, digital image fundamentals, Elements of visual perception, light and electromagnetic spectrum, imaging sensing and acquisition, image sampling and quantization. Some basic relationships between pixels, an introduction to the mathematical tools used in digital image processing.</p> <p><b>Image Transforms:</b> Need for image transforms, Spatial Frequencies in image processing, introduction to Fourier transform, discrete Fourier transform, fast Fourier transform and its algorithm, properties of Fourier transform. Discrete sine transforms. Walsh Transform. Hadamard transform, Haar Transform. Slant transforms, SVD and KL Transforms or Hotelling Transform</p>
II	<p><b>UNIT-2</b></p> <p><b>Intensity Transformations and Spatial Filtering:</b> Background, Some basic intensity transformation functions, histogram processing, fundamentals of spatial filtering, smoothing spatial filters, sharpening spatial filters, Combining spatial enhancement methods, using fuzzy techniques for intensity transformations and spatial filtering.</p> <p><b>Filtering in the frequency domain:</b> Preliminary concepts, Sampling and the Fourier transform of sampled functions, the discrete Fourier transform (DFT) of one variable, Extension to functions of two</p>



	variables, some properties of the 2-D Discrete Fourier transform. The Basic of filtering in the frequency domain, image smoothing using frequency domain filters, Selective filtering, Implementation.
III	<b>Image restoration and Reconstruction:</b> A model of the image degradation /Restoration process, Noise models, restoration in the presence of noise only-Spatial Filtering, Periodic Noise Reduction by frequency domain filtering, Linear, Position –Invariant Degradations, Estimation the degradation function, Inverse filtering, Minimum mean square error(Wiener) filtering ,constrained least squares filtering ,geometric mean filtering ,image reconstruction from projections.
IV	<b>Color image processing:</b> color fundamentals, color models, pseudo color image processing, basic of full color image processing, color transformations, smoothing and sharpening. Image segmentation based on color, noise in color images, color image compression.
V	<b>Wavelets and Multi-resolution Processing:</b> image pyramids, sub band coding & Haar transforms multi resolution expressions, wavelet transforms in one dimensions. The fast wavelets transform, wavelet transforms in two dimensions, wavelet packets. <b>Image compression:</b> Fundamentals, various compression methods-coding techniques, digital image water marking.
VI	<b>Morphological image processing:</b> preliminaries Erosion and dilation, opening and closing, the Hit-or-miss transformation, some Basic Morphological algorithms, grey –scale morphology <b>Image segmentation:</b> Fundamentals, point, line, edge detection thresholding, region –based segmentation, segmentation using Morphological watersheds, the use of motion in segmentation.

### TEXT BOOKS

T	BOOK TITLE/AUTHORS/PUBLISHER
T1	Digital Image Processing -R. C. Gonzalez and R. E. Woods, , 3rd edition, Prentice Hall, 2008.
T2	Fundamentals of Digital Image Processing -Anil K.Jain, , Prentice Hall of India, 9th Edition, Indian Reprint, 2002.

### REFERENCE BOOKS

R	BOOK TITLE/AUTHORS/PUBLISHER
R1	Digital Image Processing Using MATLAB -R. C. Gonzalez, R. E. Woods and Steven L. Eddins , 2rd edition, Prentice Hall, 2009.
R2	Digital Image Processing -Jayaraman, S. Esakkirajan, and T. Veerakumar. Tata McGraw-Hill Education, 2011.

### TOPICS BEYOND SYLLABUS/ADVANCED TOPICS:

SNO	DESCRIPTION	Associated PO & PSO
1	Image Segmentation techniques	PO4 & PSO1
2	Principle Component analysis	PO1,PO3& PO4

### WEB SOURCE REFERENCES:

1	<a href="https://nptel.ac.in/courses/106105032">https://nptel.ac.in/courses/106105032</a> by Prof . G. Harit
2	<a href="https://www.tutorialspoint.com/dip/">https://www.tutorialspoint.com/dip/</a>
3	<a href="http://textofvideo.nptel.ac.in/117105135/lec1.pdf">http://textofvideo.nptel.ac.in/117105135/lec1.pdf</a>
4	<a href="https://www.digimat.in/nptel/courses/video/117105135/L01.html">https://www.digimat.in/nptel/courses/video/117105135/L01.html</a>

### DELIVERY/INSTRUCTIONAL METHODOLOGIES:

Chalk & Talk	PPT	Active Learning
Web Resources	Students Seminars	Case Study
Blended Learning	Quiz	Tutorials
Project based learning	NPTEL/MOOCs	Simulation
Flipped Learning	Industrial Visit	Model Demonstration
Brain storming	Role Play	Virtual Labs

MAPPING CO'S WITH PO'S

COs	PO1	PO2	PO3	PO4	PO5	PO6	PO7	PO8	PO9	PO10	PO11	PO12	PSO1	PSO2
C325.1	1	1	2	2										
C325.2	2	2	2	1										
C325.3	3	2	2	1										
C325.4	3	2	2	2										
C325.5	1	1	-	3										
C325.6	1	-		3										
C325	1.8	1.6	2	2										

**COURSE OUTCOME RUBRIC (ASSESSMENT PER STUDENT):**

ASSESSMENT TOOL WITH WEIGHTAGE	METHOD	ATTAINMENT LEVEL 3 (EXCELLENT)	ATTAINMENT LEVEL 2 (GOOD)	ATTAINMENT LEVEL 1 (AVERAGE)	ATTAINMENT LEVEL 0 (POOR)
Internal tests (40%)	Direct	Student secured $\geq$ 60% marks of allocated marks for that CO	Student secured $\leq$ 60% and $>$ 50% marks of allocated marks for that CO	Student secured $\leq$ 50% and $>$ 40% marks of allocated marks for that CO	Student secured $<$ 40% marks of allocated marks for that CO
Assignments (20%)	Direct	Student secured $\geq$ 80% marks allocated for that CO	Student secured $\geq$ 70% and $<$ 80% marks allocated for that CO	Student secured $\geq$ 60% and $<$ 70% marks allocated for that CO	Student secured $<$ 60% of marks allocated for that CO
End Semester Examination (30%)	Direct	Student secured grades A*&S* in External Exam	Student secured grades C*&B* in External Exam	Student secured grades D*&E* in External Exam	Student secured grades F* in External Exam
Course end Survey (10%)	Indirect	Student selected option	Student selected option	Student selected option	Student selected option
* Grade Definition: S: $\geq$ 90%; A: 80%-89%; B: 70%-79%; C: 60%-69%; D: 50%-59%; E: 40%-49%; F: $<$ 40%					

*RNL*  
Course Coordinator

*BA*  
Module Coordinator

*CS*  
Head of the Department

**ANNEXURE I:**

**(A) PROGRAM OUTCOMES(POs) Engineering Graduates will be able to:**

- 1. Engineering knowledge:** Apply the knowledge of mathematics, science, engineering fundamentals, and an engineering specialization to the solution of complex engineering problems.
- 2. Problem analysis:** Identify, formulate, review research literature, and analyze complex engineering problems reaching substantiated conclusions using first principles of mathematics, natural sciences, and engineering sciences.

**3. Design/development of solutions:** Design solutions for complex engineering problems and design system components or processes that meet the specified needs with appropriate consideration for the public health and safety, and the cultural, societal, and environmental considerations.

**4. Conduct investigations of complex problems:** Use research-based knowledge and research methods including design of experiments, analysis and interpretation of data, and synthesis of the information to provide valid conclusions.

**5. Modern tool usage:** Create, select, and apply appropriate techniques, resources, and modern engineering and IT tools including prediction and modeling to complex engineering activities with an understanding of the limitations.

**6. The engineer and society:** Apply reasoning informed by the contextual knowledge to assess societal, health, safety, legal and cultural issues and the consequent responsibilities relevant to the professional engineering practice.

**7. Environment and sustainability:** Understand the impact of the professional engineering solutions in societal and environmental contexts, and demonstrate the knowledge of, and need for sustainable development.

**8. Ethics:** Apply ethical principles and commit to professional ethics and responsibilities and norms of the engineering practice.

**9. Individual and team work:** Function effectively as an individual, and as a member or leader in diverse teams, and in multidisciplinary settings.

**10. Communication:** Communicate effectively on complex engineering activities with the engineering community and with society at large, such as, being able to comprehend and write effective reports and design documentation, make effective presentations, and give and receive clear instructions.

**11. Project management and finance:** Demonstrate knowledge and understanding of the engineering and management principles and apply these to one's own work, as a member and leader in a team, to manage projects and in multidisciplinary environments.

**12. Life-long learning:** Recognize the need for, and have the preparation and ability to engage in independent and life-long learning in the broadest context of technological change.

**(B) PROGRAM SPECIFIC OUTCOMES (PSOs) :**

1. Design, model, simulate and analyze various mechanical systems or processes.

2. Obtain additional skills and knowledge to develop and implement thermal engineering systems

**Cognitive levels as per Revised Blooms Taxonomy:**

Cognitive Domain	LEVEL	Key words
Remember	K1	Defines, describes, identifies, knows, labels, lists, matches, names, outlines, recalls, recognizes, reproduces, selects, states.
Understand	K2	Comprehends, converts, defends, distinguishes, estimates, explains, extends, generalizes, gives an example, infers, interprets, paraphrases, predicts, rewrites, summarizes, translates.
Apply	K3	Applies, changes, computes, constructs, demonstrates, discovers, manipulates, modifies, operates, predicts, prepares, produces, relates, shows, solves, uses.
Analyse	K4	Analyzes, breaks down, compares, contrasts, diagrams, deconstructs, differentiates, discriminates, distinguishes, identifies, illustrates, infers, outlines, relates, selects, separates.
Evaluate	K5	Appraises, compares, concludes, contrasts, criticizes, critiques, defends, describes, discriminates, evaluates, explains, interprets, justifies, relates, summarizes, supports
Create	K6	Categorizes, combines, compiles, composes, creates, devises, designs, explains, generates, modifies, organizes, plans, rearranges, reconstructs, relates, reorganizes, revises, rewrites, summarizes, tells, write

**COURSE OUTCOMES: Students are able to**

CO1: Recall the Digital Image Fundamentals & Explain Image Transforms-K1 & K2

CO2: Implement basic image processing algorithms or techniques (Spatial Domain & Frequency Domain)-K3

CO3: Summarize Image Restoration using Degradation Model, Algebraic Approach, Inverse Filtering, Least Mean Square Filters, and Constrained Least Squares Filters-K2

CO4: Compare three (RGB, CMY and HIS) color models, pseudo color image processing and full color image processing-K4

CO5: Illustrate wavelets multi-resolution processing and different image compression techniques-K4

CO6: Demonstrate the Image Segmentation and Morphological Image Processing-K3

**Unit wise Sample assessment questions**

S NO	QUESTION	KNOWLEDGE LEVEL	CO
<b>UNIT I</b>			
1	What is the need of image transform? List out various transform used in image processing.	K2	CO1
2	Explain the following terms: (i) Adjacency (ii) Connectivity (iii) Regions (iv) Boundaries	K2	CO1
3	Explain the basic concepts of sampling and quantization in the generation of digital image.	K2	CO1
4	Discuss about KL Transform and write its applications in image processing		
<b>UNIT 2</b>			
1	Explain the following filters: (i) Band reject and Band pass filters (ii) Notch filters	K2	CO2
2	Explain the use of histogram statistics for image enhancement.	K3	CO2
3	With an example, explain the concept of histogram equalization.	K3	CO2
4	State 2D sampling theorem and explain about aliasing in images.	K4	CO2
<b>UNIT 3</b>			
1	Explain the image degradation model	K2	CO3
2	Explain the following. a) Minimum Mean square error filtering. b) Inverse filtering.	K2	CO3
3	Define all the noise models.	K1	CO3
<b>UNIT 4</b>			
1	Explain about RGB color model and write its applications.	K1	CO3
2	State the expression for conversion of HIS to RGB color model. Explain the terms involved in it.	K1&K2	CO3
3	Demonstrate CMY and CMYK color models.	K2	CO3
<b>UNIT 5</b>			
1	Model a general image compression system and explain it.	K3	CO3
2	Explain the concept of wavelet packets and write its advantages.	K2	CO3
3	What is meant by block transform coding? Explain.	K1	CO3

UNIT 6			
1	Explain about morphological hit-or-miss transform.	K2	CO4
2	Distinguish Erosion & Dilation	K4	CO4
3	Explain the basics of intensity thresholding in image segmentation.	K2	CO4

Code: RT41043

Model Question Paper  
R13

Narasaraopeta Engineering College  
(Autonomous)  
Yallmanda(Post), Narasaraopet- 522601  
B. Tech VII Semester Regular Examinations  
DIGITAL IMAGE PROCESSING  
[OUTCOME BASED EDUCATION PATTERN]

Time: 3 Hrs

Max. Marks: 70

- Note: 1. Question Paper consists of two parts (Part-A and Part-B)  
2. Answering the question in Part-A is compulsory  
3. Answer any THREE Questions from Part-B

Execution Plan

Sl. No	Activities	Time (Minutes)
1	To study the Question Paper and choose to attempt	5
2	Part-A 5 Minutes x 6 Questions	30
3	Part-B 45 Minutes x 3 Questions	135
4	Quick revision & Winding up	10
	Total	180

PART-A (22 Marks)  
Answer ALL Questions.

S No	Question	Cognitive Level	CO	Marks
1	a Define Walsh Transform and write its properties.	K1	1	4
	b List out some important noise probability density functions	K4	2	4
	c List out different masks used to compute the gradient.	K1	2	3
	d Write short notes on RGB to CMY conversion.	K1	3	3
	e Explain the effect of noise in edge detection.	K2	3	4
	f Explain the duality of erosion and dilation operations	K2	4	4

PART-B (48 Marks)  
Answer any THREE Questions

S. No	Question	Cognitive Level	CO	Marks
1	a What are the various fundamental steps in digital image processing?	K1	1	8
	b Find the Haar transformation matrix for $N = 8$ .	K1	1	8
2	a Explain the concept of histogram equalization	K2	1	8

	<b>b</b>	Write a short note on the following i) Smoothing spatial filters ii) Sharpening spatial filters	<b>K1</b>	<b>1</b>	<b>8</b>
<b>3</b>	<b>a</b>	Model an image degradation process and explain it.	<b>K3&amp;K2</b>	<b>2</b>	<b>8</b>
	<b>b</b>	List out some important noise probability density functions used in image processing and sketch their plots.	<b>K4</b>	<b>2</b>	<b>8</b>
<b>4</b>	<b>a</b>	Distinguish Full color and pseudo color image processing	<b>K4</b>	<b>3</b>	<b>8</b>
	<b>b</b>	Define the following terms i) Radiance ii) Luminance iii) Primary colors iv) Secondary colors	<b>K1</b>	<b>3</b>	<b>8</b>
<b>5</b>	<b>a</b>	Explain transform coding	<b>K1</b>	<b>3</b>	<b>6</b>
	<b>b</b>	Write a short note on the following i) Image pyramids ii) Sub band coding	<b>K1</b>	<b>3</b>	<b>10</b>
<b>6</b>	<b>a</b>	Explain about morphological hit-or-miss transform.	<b>K2</b>	<b>4</b>	<b>8</b>
	<b>b</b>	Demonstrate region based segmentation.	<b>K2</b>	<b>4</b>	<b>8</b>



ACADEMIC  
CALENDAR



Narasaraopeta Engineering College (Autonomous)  
Kotappakonda Road, Yellamanda (P.O), Narasaraopet- 522601, Guntur District, AP.

### ACADEMIC CALENDAR

(B.Tech. 2019, 2018 and 2017 admitted batches, Academic Year 2020-21)

2019 Batch 2 <sup>nd</sup> Year 1 <sup>st</sup> Semester, 2018 Batch 3 <sup>rd</sup> Year 1 <sup>st</sup> Semester and 2017 Batch 4 <sup>th</sup> Year 1 <sup>st</sup> Semester			
Description	From Date	To Date	Duration
Commencement of Class Work	02-11-2020		4 Weeks
1 <sup>st</sup> Spell of Instructions	02-11-2020	30-11-2020	
I Mid examinations	01-12-2020	05-12-2020	1 Week
2 <sup>nd</sup> Spell of Instructions	07-12-2020	20-02-2021	11 Weeks
II Mid examinations	22-02-2021	27-02-2021	1 Week
Preparation & Practicals	01-03-2021	06-03-2021	1 Week
Semester End Examinations	08-03-2021	20-03-2021	2 Weeks
2019 Batch 2 <sup>nd</sup> Year 2 <sup>nd</sup> semester, 2018 Batch 3 <sup>rd</sup> Year 2 <sup>nd</sup> Semester and 2017 Batch 4 <sup>th</sup> Year 2 <sup>nd</sup> Semester			
Commencement of Class Work	22-03-2021		7 Weeks
1 <sup>st</sup> Spell of Instructions	22-03-2021	08-05-2021	
I Assignment Test	12-04-2021	17-04-2021	
II Assignment Test	26-04-2021	30-04-2021	
I Mid examinations	10-05-2021	15-05-2021	1 Week
2 <sup>nd</sup> Spell of Instructions	17-05-2021	03-07-2021	7 Weeks
III Assignment Test	31-05-2021	05-06-2021	
IV Assignment Test	21-06-2021	26-06-2021	
II Mid examinations	05-07-2021	10-07-2021	1 Week
Preparation & Practicals	12-07-2021	17-07-2021	1 Week
Semester End Examinations	19-07-2021	31-07-2021	2 Weeks

  
PRINCIPAL



# TIME TABLES



# NARASARAOPETA ENGINEERING COLLEGE

(AUTONOMOUS)

DEPARTMENT OF ELECTRONICS AND COMMUNICATION ENGINEERING

III B.Tech., II semester, ECE-A Class TimeTable for the A.Y. 2020-21

Room No.: 3308


w.e.f: 24-03-2021

DAY	1	2	3		4	12:40 to 1:30	5	6	7
	9:10 to 10:00	10:00 to 10:50	10:50 to 11:00	11:00 to 11:50	11:50 to 12:40		1:30 to 2:20	2:20 to 3:10	3:10 to 4:00
MON	DIP	DSP / MW&OC LAB				L U N C H  B R E A K	MW&OC	DSP	EMI
TUE	MW&OC	DSP / MW&OC LAB					DIP	VLSI	IoT
WED	EMI	VLSI	B R E A K	DSP	/DSP		IoT	MW&OC	DIP
THU	VLSI	IoT		DIP	EMI		VLSI	DSP	MW&OC
FRI	EMI	MW&OC		VLSI	DIP		DSP	IoT	MENTORING
SAT	IoT	EMI		MW&OC	DSP		VLSI	DIP	LIBRARY/ SPORTS

VLSID	: VLSI Design	Dr. B. Raghavaiah
MW&OC	: Microwave & Optical Communications	Ms. K. Sheela
DSP	: Digital Signal Processing	Mr. G. Srinivasa Rao
EMI	: Electronic Measurements & Instrumentation	Mr. A. Venkata Siva
DIP	: Digital Image Processing	Mr. J. Narasimha Rao
IoT	: Internet of Things	Mr. N. Narayana
ACS	: Advanced Communication Skills	Mr. Ch. Krishna

DSP Lab : Digital Signal Processing Lab  
Dr. B. Raghavaiah, Dr. T. Santhi  
Mr. G. Srinivasa Rao/ Mr. A. Kanchana,  
Mr. Ch. Karthik, Dr. Amit Gupta/  
Dr.A.V.Nageswara Rao

MW&OC Lab : Microwave and Optical Communications Lab  
Mr. J. Narasimha Rao/Mrs. B. Suneetha.  
Mr. A. Venkata Siva / Ms. K. Sheela,  
Mr. N. Narayana Mr. V. R. Krishna Reddy

  
HEAD OF THE DEPARTMENT  
(Dr. V. VENKATA RAO)

  
PRINCIPAL  
(Dr. M. SREENIVASA KUMAR)

HEAD OF THE DEPARTMENT  
DEPT. OF ELECTRONICS AND COMMUNICATION  
NARASARAOPETA ENGINEERING COLLEGE  
NARASARAOPETA-522 601

PRINCIPAL  
NARASARAOPETA ENGINEERING COLLEGE  
(AUTONOMOUS)  
NARASARAOPETA - 522 601.  
Guntur (Dist.), A.P.


**NARASARAOPETA**  
**ENGINEERING COLLEGE**  
 (AUTONOMOUS)

**DEPARTMENT OF ELECTRONICS AND COMMUNICATION ENGINEERING**

**III B.Tech., II semester, ECE-B Class TimeTable for the A.Y. 2020-21**


Room No.: 3314

w.e.f: 24-03-2021

DAY	1	2		3	4		5	6	7	
	9:10 to 10:00	10:00 to 10:50	10:50 to 11:00	11:00 to 11:50	11:50 to 12:40	12:40 to 1:30	1:30 to 2:20	2:20 to 3:10	3:10 to 4:00	
MON	VLSI	EMI	B R E A K	DSP	IoT	L U N C H  B R E A K	DSP	DIP	MW&OC	
TUE	EMI	DSP		VLSI	MENTORING		VLSI	MW&OC	DIP	
WED	IoT	DSP / MW&OC LAB					MW&OC	VLSI	LIBRARY/ SPORTS	
THU	DIP	DSP / MW&OC LAB					EMI	IoT	DSP	
FRI	DSP	IoT		MW&OC	EMI		DIP	MW&OC	VLSI	
SAT	MW&OC	DIP		DSP	IoT		EMI	VLSI	DIP	

VLSID	: VLSI Design	Dr. T. Santhi
MW&OC	: Microwave & Optical Communications	Mrs. B. Suneetha
DSP	: Digital Signal Processing	Mr. Ch. Karthik
EMI	: Electronic Measurements & Instrumentation	Dr. Amit Gupta
DIP	: Digital Image Processing	Mr. V. R. Krishna Reddy
IoT	: Internet of Things	Dr.A.V.Nageswara Rao
ACS	: Advanced Communication Skills	Mr. Ch. Krishna

DSP Lab	: Digital Signal Processing Lab	Dr. B. Raghavaiah/ Dr. Amit Gupta/ Dr. T. Santhi Mr. G. Srinivasa Rao Mr. A. Kanchana Mr. Ch. Karthik Dr.A.V.Nageswara Rao
MW&OC Lab	: Microwave and Optical Communications Lab	Mr. J. Narasimha Rao/ Mrs. B. Suneetha/ Mr. A. Venkata Siva Ms. K. Sheela, Mr. N. Narayana

  
**HEAD OF THE DEPARTMENT**  
 (Dr. V. VENKATA RAO)

**HEAD OF THE DEPARTMENT**  
 DEPT.OF ELECTRONICS AND COMMUNICATION  
 ENGG.  
 NARASARAOPETA ENGINEERING COLLEGE  
 NARASARAOPET-522 601

  
**PRINCIPAL**  
 (Dr. M. SREENIVASA/KUMAR)

**PRINCIPAL**  
 NARASARAOPETA ENGINEERING COLLEGE  
 (AUTONOMOUS)  
 NARASARAOPET - 522 601.  
 Guntur (Dist.), A.P.

**DEPARTMENT OF ELECTRONICS AND COMMUNICATION ENGINEERING**

**III B.Tech., II semester, ECE-C Class TimeTable for the A.Y. 2020-21**

Room No.: 3315

w.e.f: 24-03-2021

DAY	1	2		3	4		5	6	7
	9:10 to 10:00	10:00 to 10:50	10:50 to 11:00	11:00 to 11:50	11:50 to 12:40	12:40 to 1:30	1:30 to 2:20	2:20 to 3:10	3:10 to 4:00
MON	IoT	EMI	B R E A K	DIP	DSP	L U N C H  B R E A K	MW&OC	VLSI	DSP
TUE	MW&OC	DIP		IoT	MENTORING		DSP	VLSI	LIBRARY/ SPORTS
WED	IoT	DSP		MW&OC	EMI		DIP	VLSI	MW&OC
THU	DSP	DIP		IoT	VLSI		EMI	DSP	MW&OC
FRI	DIP	DSP / MW&OC LAB			VLSI		MW&OC	EMI	
SAT	IoT	DSP / MW&OC LAB			EMI		DIP	VLSI	

VLSID	: VLSI Design	Mr. A. Kanchana
MW&OC	: Microwave & Optical Communications	Mr. B. Srinivasa Rao
DSP	: Digital Signal Processing	Dr. R. Sambasiva Nayak
EMI	: Electronic Measurements & Instrumentation	Mr. N. Srinivasa Rao
DIP	: Digital Image Processing	Ms. G. Bhavani
IoT	: Internet of Things	Mr. Sk. Zuber Basha
ACS	: Advanced Communication Skills	Mr. Ch. Krishna

DSP Lab : Digital Signal Processing Lab  
 Mr. M. Srinivasa Rao/Dr. R. Sambasiva Nayak  
 Mr. A. Charles Stud/ Mr. N. Srinivasa Rao ,  
 Mr. A. Kanchana/Mr. B. Naga Ganesh

MW&OC Lab : Microwave and Optical Communications Lab  
 Mr. B. Srinivasa Rao / Mr. Sk.MD.Umar,  
 Mr. Sk. Zuber Basha Mr. V. R. Krishna Reddy,  
 Mr. P. Bhagya Raju.Ms. G. Bhavani,  
 Mr. N. Syed Khasim, Ms. M.Amulya Bhanu

  
**HEAD OF THE DEPARTMENT**  
 (Dr. V. VENKATA RAO)

  
**PRINCIPAL**  
 (Dr. M. SREENIVASA KUMAR)

**HEAD OF THE DEPARTMENT**  
 DEPT.OF ELECTRONICS AND COMMUNICATION  
 ENGG.  
 NARASARAOPETA ENGINEERING COLLEGE  
 NARASARAOPET-522 601



# NARASARAOPETA ENGINEERING COLLEGE (AUTONOMOUS)

DEPARTMENT OF ELECTRONICS AND COMMUNICATION ENGINEERING

III B.Tech., II semester, ECE-D Class TimeTable for the A.Y. 2020-21

Room No.: 3316

w.e.f: 24-03-2021

DAY	1	2		3	4		5	6	7	
	9:10 to 10:00	10:00 to 10:50	10:50 to 11:00	11:00 to 11:50	11:50 to 12:40	12:40 to 1:30	1:30 to 2:20	2:20 to 3:10	3:10 to 4:00	
MON	VLSI	DIP	B R E A K	EMI	MW&OC	L U N C H  B R E A K	DSP / MW&OC LAB			
TUE	IoT	EMI		DSP	MENTORING		DSP / MW&OC LAB			
WED	DIP	MW&OC		DSP	IoT		VLSI	EMI	LIBRARY/ SPORTS	
THU	EMI	DSP		DIP	MW&OC		VLSI	DIP	VLSI	
FRI	IoT	VLSI		DSP	IoT		MW&OC	DIP	VLSI	
SAT	DSP	IoT		MW&OC	DSP		DIP	MW&OC	EMI	

VLSID	: VLSI Design	Mr. M. Srinivasa Rao
MW&OC	: Microwave & Optical Communications	Mr. N. Syed Khasim
DSP	: Digital Signal Processing	Mr. B. Naga Ganesh
EMI	: Electronic Measurements & Instrumentation	Ms. M.Amulya Bhanu
DIP	: Digital Image Processing	Mr. A. Charles Stud
IoT	: Internet of Things	Mr. Sk.MD.Umar
ACS	: Advanced Communication Skills	Mr. Ch. Krishna

DSP Lab	: Digital Signal Processing Lab	Mr. B. Naga Ganesh/Mr. A. Charles Stud / Dr. R. Sambasiva Nayak/Mr. N. Srinivasa Rao, Mr. M. Srinivasa Rao, Mr. A. Kanchana
MW&OC Lab	: Microwave and Optical Communications Lab	Mr. B. Srinivasa Rao /Mr. P. Bhagya Raju, Mr. N. Syed Khasim, Mr. Sk.MD.Umar, Mr. Sk. Zuber Basha, Ms. M.Amulya Bhanu Ms. G. Bhavani

*(Signature)*  
**HEAD OF THE DEPARTMENT**  
(Dr. V. VENKATA RAO)

*(Signature)*  
**PRINCIPAL**  
(Dr. M. SREENIVASA KUMAR)  
**PRINCIPAL**

**HEAD OF THE DEPARTMENT**  
DEPT. OF ELECTRONICS AND COMMUNICATION  
NARASARAOPETA ENGINEERING COLLEGE  
NARASARAOPETA-522 601

**NARASARAOPETA ENGINEERING COLLEGE**  
(AUTONOMOUS)  
NARASARAOPETA - 522 601  
Guntur (Dist.), A.P.

**SYLLABUS**  
**COPY**

III B.TECH-II-SEMESTER	L	T	P	INTERNAL MARKS	EXTERNAL MARKS	TOTAL MARKS	CREDITS
	4	0	0	40	60	100	3

**DIGITAL IMAGE PROCESSING**  
*(Professional Elective – I)*

**COURSE OBJECTIVES:**

1. Give the students a taste of the applications of the theories taught in the subject. This will be achieved through the project and some selected lab sessions.
2. Introduce the students to some advanced topics in digital image processing.
3. Give the students a useful skill base that would allow them to carry out further study should they be interested and to work in the field.

**COURSE OUTCOMES:**

On completion of the course, the student will be able to

**CO1:** Recall the Digital Image Fundamentals & Image Transforms.

**CO2:** Implement basic image processing algorithms or techniques (Spatial Domain & Frequency Domain)

**CO3:** Summarize Image Restoration using Degradation Model, Algebraic Approach, Inverse Filtering, Least Mean Square Filters, and Constrained Least Squares Filters

**CO4:** Compare three (RGB, CMY and HIS) color models, pseudo color image processing and full color image processing,

**CO5:** Illustrate wavelets multi-resolution processing and different image compression techniques.

**CO6:** Demonstrate the Image Segmentation and Morphological Image Processing.

**UNIT-I: DIGITAL IMAGE FUNDAMENTALS & IMAGE TRANSFORMS**

Digital Image Fundamentals, Sampling and Quantization, Relationship between Pixels, Image Transforms: 2-D FFT, Properties, Walsh Transform, Hadamard Transform, Discrete Cosine Transform, Haar Transform, Slant Transform, Hotelling Transform.

**UNIT-II: IMAGE ENHANCEMENT (SPATIAL & FREQUENCY DOMAIN)**

Introduction, Image Enhancement in Spatial Domain, Enhancement Through Point Operation, Types of Point Operation, Histogram Manipulation, Linear and Non — Linear Gray Level Transformation, Local or Neighborhood Operation, Median Filter, Spatial Domain High-Pass Filtering. Image Enhancement (Frequency Domain): Filtering in Frequency Domain, Obtaining Frequency Domain Filters from Spatial Filters, Generating Filters Directly in the Frequency Domain, Low Pass (Smoothing) and High Pass (Sharpening) Filters in Frequency Domain.

**UNIT-III: IMAGE RESTORATION AND RECONSTRUCTION**

Degradation and Restoration Model, Noise models, Restoration in the presence of noise only, Spatial filtering, Periodic noise reduction by frequency domain filtering, Linear Position Invariant degradations, Estimation of degradation, Restoration, Inverse Filtering, Least Mean Square Filters, Constrained Least Squares Restoration, Interactive Restoration.

**UNIT-IV: COLOR IMAGE PROCESSING**

Color fundamentals, color models, pseudo color image processing, Basics of full color image Processing, Color transforms, Smoothing and Sharpening, image segmentation based on color, Noise in color images, Color image Compression

**UNIT-V: WAVELETS AND MULTI-RESOLUTION PROCESSING**

Image pyramids, Sub band coding & Haar transforms, Multi resolution expressions, Wavelet transforms in one dimensions, Fast wavelet transform dimensions, Wavelet packet. Image Compression: Fundamentals, Various compression methods-coding techniques, digital image

water marking.

**UNIT-VI: MORPHOLOGICAL IMAGE PROCESSING**

Dilation and Erosion: Dilation, Structuring Element Decomposition, Erosion, Combining Dilation and Erosion, Opening and Closing, the Hit or Miss Transformation. Image Segmentation: Detection of Discontinuities, Edge Linking And Boundary Detection, Thresholding, Region Oriented Segmentation.

**Text Books:**

1. Rafael C. Gonzalez, Richard E. Woods, "Digital Image Processing", 3<sup>rd</sup> Edition, Pearson, 2008
2. S Jayaraman, S Esakkirajan and T Veerakumar, "Digital Image Processing", TMH, 2010.

**Reference Books:**

1. Scotte Umbaugh, "Digital Image Processing and Analysis-Human and Computer Vision Application with using CVIP Tools", 2<sup>nd</sup> Edition, CRC Press, 2011
2. Rafael C. Gonzalez, Richard E Woods and Steven L. Eddings, "Digital Image Processing using MATLAB", 2<sup>nd</sup> Edition, TMH, 2010.
3. A.K. Jain, "Fundamentals of Digital Image Processing" PHI, 1989
4. Somka, Hlavac Boyle, "Digital Image Processing and Computer Vision", Cengage Learning (Indian edition) 2008.
5. Adrian low, "Introductory Computer Vision Imaging Techniques and Solutions", 2<sup>nd</sup> Edition, 2008
6. John C. Russ, J. Christian Russ, "Introduction to Image Processing & Analysis", CRC Press, 2010.
7. Vipula Singh, "Digital Image Processing with MATLAB & Lab view", Elsevier, 2012.



# LESSON PLAN



**NARASARAOPETA ENGINEERING COLLEGE, NARASARAOPETA**  
 (Approved by AICTE, Affiliated to JNTUK, Kakinada, Accredited by NBA, ISO 9001:2008 Certified Institution)  
 Kotappakonda Road, Vallamanda (Post), Narasaraopeta - 522601, Guntur District, Andhra Pradesh  
 Phone No.: 08647-239914, 9441127485, Fax No.: 08647-239902  
 E-mail: nrtec\_ece@yahoo.com, Website: <http://www.nrteggcollege.com>

**DEPARTMENT OF ELECTRONICS & COMMUNICATION ENGINEERING**

Academic year : 2020-21  
 Class : ECE-A & B  
 Year & Semester : III-II  
 Subject : DIGITAL IMAGE PROCESSING.  
 Date of Commencement :  
 Faculty Name : Mr.J. NARASIMHA RAO

**COURSE OBJECTIVES:**

1. Give the students a taste of the applications of the theories taught in the subject. This will be achieved through the project and some selected lab sessions.
2. Introduce the students to some advanced topics in digital image processing.
3. Give the students a useful skill base that would allow them to carry out further study should they be interested and to work in the field.

**LESSON PLAN**

S.No	Name of the Topic	No. of Periods Required	Cumulative Periods
<b>UNIT I : Introduction</b>			
1	Origins of digital image processing, Uses of digital image processing, Fundamental steps in digital image processing	1	1
2	Components of an image processing system, Elements of visual perception, Digital image fundamentals, Light and electromagnetic spectrum ,	1	2
3	Imaging sensing and acquisition, image sampling and quantization, some basic relationships between pixels, An introduction to mathematical tools used in digital image processing	1	3
4	Tutorial	1	4
5	<b>Image transforms:</b> Need for image transform, spatial frequencies in image processing, Introduction to Fourier Transform, Discrete Fourier Transform,	1	5
6	Fast Fourier Transform and its algorithms, Properties of Fourier Transform-Sampling theorem ,Parseval's theorem, Discrete cosine transform, Discrete sine transform	1	6
7	Walsh transform, Haar transform, Hadmard transform, Slant transform, SVD and KL transforms or Hotelling transform	1	7
8	Tutorial	1	8
<b>UNIT II :Intensity transformations and spatial filtering</b>			
9	Back ground, some basic intensity transformation functions, Histogram processing	1	9
10	Fundamentals of spatial filtering	1	10
11	Smoothing spatial filters	1	11

12	Tutorial	1	12
13	Sharpening spatial filters	1	13
14	Combining spatial Enhancement methods	1	14
15	Using Fuzzy Techniques for intensity transformations and spatial filtering	1	15
16	Tutorial	1	16
<b>UNIT III : Filtering in the Frequency Domain</b>			
16	Preliminary concepts, Sampling and the Fourier Transform of sampled functions,	1	17
17	The discrete Fourier Transform(DFT) of one variable, Extension functions of two variables	1	18
18	Some properties of the 2-D Discrete Fourier Transform	1	19
19	Tutorial	1	20
20	The basic of filtering in the Frequency Domain	1	21
21	Image smoothing using Frequency Domain Filters, Selective filtering and Implementation	1	22
<b>UNIT IV : Image Restoration Reconstruction</b>			
22	A model of the image Degradation/Reconstruction process, Noise models, Restoration in the presence of noise only –spatial filtering,	1	23
	Tutorial	1	24
23	Periodic Noise Reduction by frequency Domain Filtering, Linear position invariant Degradations	1	25
24	Estimation the degradation function, Inverse filtering, Minimum Mean square Error(Weiner)Filtering, Constrained Least squares filtering	1	26
25	Geometric Mean Filtering, Image reconstruction from projections	1	27
26	Tutorial	1	28
<b>UNIT V : Color Image Processing</b>			
27	Color Fundamentals color models, Pseudo color image processing, Basic of full image processing	1	29
28	Color Transformations	1	30
29	Smoothing and sharpening, Image segmentation based on color	1	31
30	Tutorial	1	32
31	Noise in color images, color image compression	1	33
<b>UNIT VI: Wavelets and Multi Resolution Processing</b>			
32	Image pyramids, Sub band coding & Transform	1	34
33	Multi resolution expansions, Wavelet transform in one Dimension	1	35
34	Tutorial	1	36
35	The Fast wavelet transform in two Dimensions Wavelet packets	1	37
36	Image compression: Fundamentals, Various compression methods –coding techniques ,Digital image water marking	1	38
<b>UNIT VII: Morphological Image Processing</b>			
37	Preliminaries, Erosion and Dilation, Opening and closing	1	39
38	Tutorial	1	40

39	The Hit –or –Miss Transformation,	1	41
40	some Basic Morphological Algorithms, Grey scale Morphology	1	42
<b>UNIT VIII: Image Segmentation</b>			
41	Fundamentals, Point, Line, Edge Detection Thresholding, Region based Segmentation,	1	43
42	Tutorial	1	44
43	Segmentation using Morphological watersheds, The use of motion in segmentation	1	45

**COURSE OUTCOMES:**

**COURSE OUTCOMES: Students are able to**

CO1: Recall the Digital Image Fundamentals & Explain Image Transforms-K1 & K2

CO2: Implement basic image processing algorithms or techniques (Spatial Domain & Frequency Domain)-K3

CO3: Summarize Image Restoration using Degradation Model, Algebraic Approach, Inverse Filtering, Least Mean Square Filters, and Constrained Least Squares Filters-K2

CO4: Compare three (RGB, CMY and HIS) color models, pseudo color image processing and full color image processing-K4

CO5: Illustrate wavelets multi-resolution processing and different image compression techniques-K4

CO6: Demonstrate the Image Segmentation and Morphological Image Processing-K3

**TEACHING AIDS:**

1. Chalk and Board
2. Laptop and LCD Projector

**TEXTBOOKS:**

1. RafaelC Gonzalez and Richard E Woods, "Digital Image Processing" Pearson Education 2011
2. S.Sridhar, "Digital Image Processing" Oxford Publishers 2011

**REFERENCES:**

- 1.S Jayaraman,S.Esakkairajan, T.Veerakumar, "Digital Image Processing and analysis" Prentice Hall of India2011/2012(print)
- 2.B.Chanda and D.Dutta Majumder, "Digital Image Processing" -McGraw Hill
- 3.Anil K.Jain, "Fundamentals of Digital Image Processing"Prentice Hall of India,2012
- 4.Milan Sonka,Hlavac &Boyle , "Digital Image Processing and Computer Vision" Cengage Learning Publishers,2010(Reprinted)

**Course outcomes:**

After going through this course the student will be able to

- Perform different transforms on image useful for image processing applications
- Perform spatial and frequency domain filtering on image and can implement all smoothing and sharpening operations on images
- Perform image restoration operations/techniques on images
- Operate effectively on color images and different color conversions on images and can code images to achieve good compression
- Do wavelet based image processing and image compression using wavelets
- Perform all morphological operations on images and can be able to do image segmentation also.
- Develop simple algorithms for image processing and use the various techniques involved in Bio Medical applications, etc



**Signature of the Faculty**



**Signature of H.O.D**

# CO-PO MAPPING

## CO-PO Mapping

COs	POs											
	PO1	PO2	PO3	PO4	PO5	PO6	PO7	PO8	PO9	PO10	PO11	PO12
C325.1: Recall the Digital Image Fundamentals & Image Transforms.	1	1	2	2								
C325.2: Implement basic image processing algorithms or techniques (Spatial Domain & Frequency domain	2	2	2	1								
C325.3: Summarize Image Restoration using Degradation Model, Algebraic Approach, Inverse Filtering, Least Mean Square Filters, and Constrained Least Squares Filters	3	2	2	1								
C325.4: Compare three (RGB, CMY and HIS) color models, pseudo color image processing and full color image	3	2	2	2								
C325.5: Illustrate wavelets multi-resolution processing and different image compression techniques.	1	1	-	3								
C325.6: Demonstrate the Image Segmentation and Morphological Image Processing.	1	-		3								
<b>C325</b>	<b>18</b>	<b>11.6</b>	<b>2</b>	<b>2</b>								

## Total CO Attainment through Direct & Indirect Assessment

CO Attainment	2.5
---------------	-----

## PO Attainment

PO Attainment	PO1	PO2	PO3	PO4	PO5	PO6	PO7	PO8	PO9	PO10	PO11	PO12
		1.5	13	1.7	1.7							

1. Copy CO - PO matrix and CO attainment matrix from previous pages and find PO attainment.

2. PO attainment is calculated as per the following formula:

POi \* Total CO attainment Level / 3 where 'i' ranges from 1 to 12.

# CO-PSO MAPPING



### Criteria 3

### CO-PSO Mapping

COs	PSOs	
	PSO1	PSO2
C325.1	-	-
C325.2	3	-
C325.3	3	-
C325.4	3	-
C325.5	3	-
C325.6	3	-
C325	3	-

### Attainment through Direct & Indirect

CO Attainment	2.5
1. Slight(2. Moderate(Medium)	
3. Substantial(High)	
If there is no correlation put '1'	

### PSO Attainment

COs	PSOs	
	PSO1	PSO2
PSO Attainment	2.5	-

1. Copy CO - PSO matrix and CO attainment matrix from previous pages and find PSO attainment.
2. PSO attainment is calculated as per the following formula:

1

2

# CO ATTAINMENTS

3

4

### Criteria 3: CO Attainment through Direct Assessment

	CO Attainment Level (Mid)	CO Attainment Level (External)	Direct CO Attainment Level (Internal * 30%) + (External * 70%)	Indirect CO Attainment Level	Total CO Attainment Level (Direct CO Attainment * 90% + Indirect CO Attainment * 10%)
CO1	3	1	2	3	3
CO2	1	0	1	2	2
CO3	3	1	2	2	2
CO4	3	2	3	3	3
CO5	3	1	2	2	2
CO6	3	3	3	2	3
					2.5

1. Copy the Direct CO Attainment Level (Internal) and Direct CO Attainment Level (External) from the previous sheets and then find the Direct CO Attainment Level.
2. Find Direct CO attainment level using the formula:  

$$\text{CO Attainment Level (Internal)} * 30\% + \text{CO Attainment Level (External)} * 70\%$$
3. Copy Indirect CO Attainment Level.
4. Find the CO attainment level using the formula:  

$$\text{Direct CO Attainment Level} * 80\% + \text{Indirect CO Attainment Level} * 20\%$$

### WEB SOURCE REFERENCES

1	<a href="https://nptel.ac.in/courses/106105032">https://nptel.ac.in/courses/106105032</a> .by Prof . G. Harit
2	<a href="https://www.tutorialspoint.com/dip/">https://www.tutorialspoint.com/dip/</a>
3	<a href="http://textofvideo.nptel.ac.in/117105135/lec1.pdf">http://textofvideo.nptel.ac.in/117105135/lec1.pdf</a>
4	<a href="https://www.digimat.in/nptel/courses/video/117105135/L01.html">https://www.digimat.in/nptel/courses/video/117105135/L01.html</a>

STUDENT'S  
ROLL LIST

**DEPARTMENT OF ELECTRONICS AND COMMUNICATION ENGINEERING**  
**YEAR AND SEMESTER: III YEAR II SEMESTER**

S.No.	H.T.No.	NAME OF THE STUDENT
1	17471A0402	ANNAM PRABHU CHAITANYA
2	18471A0401	ANUMALASETTY DHARANI
3	18471A0402	AVULA NAVEEN
4	18471A0403	BADUGU PRAKASH BABU
5	18471A0405	BALLI PALLI SAI VENKAT
6	18471A0406	BANDARU SAI KUMAR
7	18471A0407	BATHULA SRINU
8	18471A0408	BEERAM UPENDRA REDDY
9	18471A0409	BHUVANAM NAGA VAMSI
10	18471A0410	BOBBILLA KARTHIK
11	18471A0411	BODLAPATI SRAVYA
12	18471A0412	BURRI NAGA VENI
13	18471A0413	CHAKKA MANOJ KUMAR
14	18471A0414	CHITTINENI SIDDHARDHA
15	18471A0415	CHOPPARA MANOJ KUMAR
16	18471A0416	DASIREDDY NAGI REDDY
17	18471A0417	DEVARAKONDA NITISH KUMAR REDDY
18	18471A0418	DEVARAPALLI KUSUMITHA
19	18471A0419	GADIBOYINA JAYENDRA KUMAR
20	18471A0420	GAYAM RAMYA
21	18471A0421	GOPU GANESH SIVA SAI
22	18471A0422	GOPU SAI MOULI
23	18471A0423	GOTTIPATI VAMSI
24	18471A0424	GUMMALAMPATI MANOJ KUMAR
25	18471A0425	INAGANTI BHARATH TEJA
26	18471A0426	JALADI SAI KRISHNA
27	18471A0427	JILLELLAMUDI SRINIVASU
28	18471A0428	JUPUDI PAVAN KUMAR
29	18471A0429	KANAMARLAPUDI LAKSHMI SAI SUBHASH
30	18471A0430	KARNAM SREE DEVI
31	18471A0431	KASIREDDY NAGAMAHENDRA
32	18471A0432	KOLLU SAI SURYA
33	18471A0433	KOMMALAPATI CHINNI KRISHNA
34	18471A0434	KUNAGU ASLESHASAIKUMAR
35	18471A0435	KUNCHAPU SRIKANTH
36	18471A0436	MADASU VIVEK
37	18471A0437	MADHAVARAPU MANOHAR
38	18471A0438	MARELLA VENKATA SIVA RAVI TEJA
39	18471A0439	MATLAPUDI ANIL KUMAR

40	18471A0440	MEDISETTY MANOHAR
41	18471A0441	MIRIYALA VENKATESH
42	18471A0442	MURAM SASIDHAR REDDY
43	18471A0443	MUTHINENI ANJI BABU
44	18471A0444	PAPASANI NAGA MANIKANTA REDDY
45	18471A0445	PARELLA POOJITHA
46	18471A0446	PATHAN MAHABOOB KHAN
47	18471A0447	PONDUGULA BHAVYA LAKSHMI
48	18471A0448	PULIPATI DEVI SRI SRESHTA
49	18471A0449	SENAGALA CHAITANYA REDDY
50	18471A0450	SHAIK AYESHA SIDDIKA
51	18471A0451	SHAIK BURUHAN JANI
52	18471A0452	SHAIK KARISHMA
53	18471A0453	SHAIK MAHAMMAD ASHRAF
54	18471A0454	SHAIK SHAJAHAN
55	18471A0455	SIDDABATHUNI VENKATA HARSHITHA
56	18471A0456	SURE YASWANTH REDDY
57	18471A0457	TALLURI ANJALI
58	18471A0458	UPPUTHOLLA TABITHA
59	18471A0459	VEDANTHAM LAKSHMI MOULYA SRI
60	18471A0460	VEERAMSETTY SWATHI
61	18471A0461	ALAPATI KIRAN BABU
62	18471A0463	ANNAPAREDDY ROHINI
63	18471A0464	BADAM HARINI
64	18471A0465	BATHULA DEVA RAJU
65	18471A0466	BETHALA BULLI BABU
66	18471A0467	BHUKYA SALAMMA
67	18471A0468	BIJJAM PRASANNA
68	18471A0470	BUDDA VENKATA SAI DURGA PRASAD
69	18471A0471	BUSI NARAYANA
70	18471A0472	CHILAKALA DIVYA
71	18471A0473	CHILAKALA PRABHAVATHI
72	18471A0474	DARIVEMULA EBINEZAR
73	18471A0475	DEVARASETTY VENKATA SATYA SUBHASH
74	18471A0476	ESKA RAMANJI REDDY
75	18471A0477	GADE MANOJ KUMAR REDDY
76	18471A0478	GAVIRIBOINA SANJAY
77	18471A0479	GELLI HEMA SUNDARI
78	18471A0480	GERA SANDHYA
79	18471A0481	SARAYU SHAIK
80	18471A0482	GUTHA VENKATESH
81	18471A0483	INAVOLU HARISH
82	18471A0484	JAJJARA AMULYA
83	18471A0485	JEEDIMALLA VENKATA PAVAN KALYAN
84	18471A0486	KAREDLA VENKATA SAI NUBYA
85	18471A0487	KARNATA GAYATHRI

86	18471A0488	KASUKURTHI KIRAN KUMAR
87	18471A0489	KOTHAPALLI CHARAN
88	18471A0490	KOTHURI JASWANTHI
89	18471A0491	KOTHURI UHA VENKATA SAI UJWALA
90	18471A0492	KUNCHALA SAITEJA
91	18471A0493	KUNISETTY V N S P L MAMATHA
92	18471A0494	LAKKIMSETTY MANOJ VENKAT
93	18471A0495	MADDI LEELA GOWRI LAVANYA
94	18471A0496	MADDIRALA MANOJ KUMAR
95	18471A0497	MAGULURU RAJASHEKAR
96	18471A0498	MARRI SRINIVASARAO
97	18471A0499	MEDIDA TEJA
98	18471A04A1	MUKKU SUSHMA
99	18471A04A2	NARISETTY SOWJANYA
100	18471A04A3	NARU MARUTHI REDDY
101	18471A04A4	NEELAM JYOTHIRMAI
102	18471A04A5	PILLI AKHIL
103	18471A04A6	POLISETTI SUSMITHA
104	18471A04A7	RAVURI RAMA NAIDU
105	18471A04A8	SHAIK ARSHATH
106	18471A04A9	SHAIK KAREEM
107	18471A04B0	SHAIK MADDIRALA NAZIROON
108	18471A04B1	SHAIK MOHAMMAD AAQIL ASHRAF
109	18471A04B2	SHAIK NAZEER AHMAD
110	18471A04B3	SINGAMSETTY HANUMANTHA RAO
111	18471A04B4	THONDAPI BHARGAVI
112	18471A04B5	VELAGADA HEMA SUNDAR
113	18471A04B6	VENNA NAGENDRA REDDY
114	18471A04B7	VITTALADEVUNI AKHILKRISHNA
115	18471A04B8	VUTUKURI SRAVANI
116	18471A04B9	YAKKALA NIKILESH
117	18471A04C0	YARRA NAVEEN
118	18471A04C1	ALLADI GOPALA KRISHNA
119	18471A04C2	AMIRISETTY VENKATA SAI LAKSHMI
120	18471A04C3	ANIKALA ROHITH REDDY
121	18471A04C4	ANNEM SRINIVASA RAO
122	18471A04C5	ANUMALASETTY SRAVANI
123	18471A04C6	BADDULA RAVI TEJA
124	18471A04C7	BANDARU RAVI TEJA
125	18471A04C9	BITTU NARESH
126	18471A04D0	BODDAPATI PAVANI
127	18471A04D1	BOGIRI YAMALAI AH
128	18471A04D2	BOILLA PAVAN KALYAN REDDY
129	18471A04D3	BOPPUDI ROHITH SURYA
130	18471A04D4	CHAKKA V S N S L TEJASWINI
131	18471A04D5	CHILAKALA SRI HANUMAN SANJAY GUPTHA



132	18471A04D6	DUDDUKURI SOWJANYA
133	18471A04D7	EDULA MEGHANA
134	18471A04D8	GADE MALLESWARI
135	18471A04D9	GATTINENI YASHWANTH
136	18471A04E0	GOTTIPATI AKHILA
137	18471A04E1	GUDA VISHNU GOVARDHAN REDDY
138	18471A04E2	INJAPALLI ISSAC
139	18471A04E3	IRLAPATI SUDHEER
140	18471A04E4	IRRI SRAVANI
141	18471A04E5	KADEM DHANA LAKSHMI
142	18471A04E7	KOTU SAIKRISHNA
143	18471A04E8	KUNCHEPU HARIKRISHNA
144	18471A04E9	KURRA YASWANTH SAI RAM
145	18471A04F0	MADDU CHAITHANYA KUMAR
146	18471A04F1	MALLEMSETTI REVATHI
147	18471A04F2	MANDALI RAVI TEJA
148	18471A04F3	MEKAPOTHU NARSI REDDY
149	18471A04F4	MELAM SINDHU
150	18471A04F5	MINDALA RAJA
151	18471A04F6	MODADUGU VINOD BABU
152	18471A04F7	MULAVEESALA GANESH
153	18471A04F8	NAMBURI ABHISHEK
154	18471A04F9	PALAPARTHI RAKESH
155	18471A04G0	PATTAN ABDUL KALESHA VALI
156	18471A04G1	PEDDETI BHAGYAVATHI
157	18471A04G2	POKURI RUPESH
158	18471A04G3	PONUGOTI VIJAYKRISHNA
159	18471A04G4	POOSAPATI BHANU PRAKASH REDDY
160	18471A04G5	PURIMITLA BHAVANI
161	18471A04G6	RAGAM SHANMUKA VENKATESH
162	18471A04G7	RAMYA PRIYA MEKA
163	18471A04G8	SAI PRAVEEN REDDY BAKKA
164	18471A04G9	SHAIK JOHNVALI
165	18471A04H0	SHAIK MUZEEF
166	18471A04H1	SHAIK NASEEMA
167	18471A04H2	SHAIK NASEEMA
168	18471A04H3	SHAIK SAJID
169	18471A04H4	SHAIK VASEEM
170	18471A04H5	SINGAREDDY RAJA SEKHAR REDDY
171	18471A04H6	SRIRAMANENI SAI RAM
172	18471A04H7	SYED MASIVULLA
173	18471A04H8	THADIBOINA APARNA
174	18471A04H9	VARLA IJACK
175	18471A04I0	YENAGANDLA BALASUBRAMANYAM
176	18471A04I1	ANNALADASU PRASAD RAO
177	18471A04I2	BATCHU LEELA NAGA SASANKA

178	18471A04I3	BATHULA ANUMOHAN REDDY
179	18471A04I4	CHINTHAKUNTA SAI TEJA
180	18471A04I5	CHUPURI SAILAJA
181	18471A04I6	DAVULURI BHANU PRAKASH
182	18471A04I7	GALLA MALLIKARJUNA RAO
183	18471A04I8	GANTA GOPI KRISHNA
184	18471A04I9	GATTUPALLI LAKSHMI PRAVALLIKA
185	18471A04J0	JUNUBOYINA SRINIVASARAO
186	18471A04J1	KAMBALA NAVYA HARIKA
187	18471A04J2	KAMEPALLI HARISH
188	18471A04J3	KANAPARTHI ROHITH
189	18471A04J4	KARANAM GOPI CHANDHD
190	18471A04J5	LINGAMGUNTLA SHAIK AMEER BASHA
191	18471A04J6	MALAMPATI NAVEEN
192	18471A04J7	MANDAVA PRANAY KUMAR
193	18471A04J8	MARRIKANTI VEERA CHARY
194	18471A04J9	MUDDAPATI SAI TEJA
195	18471A04K0	NARNE PAVANESWAR
196	18471A04K1	PASAM JAYA SAI REDDY
197	18471A04K2	PERIGISETTY SURESH
198	18471A04K3	PERLA BHAVANI
199	18471A04K4	POLURI HARI PRIYA REDDY
200	18471A04K5	PONUGOTI SIVA MANIKANTA SAI
201	18471A04K6	RAJANALA KARTHIKEYA
202	18471A04K7	SARANGI VENKATA SAI
203	18471A04K8	SHAIK ABDUL BASHA
204	18471A04K9	SHAIK BAJI
205	18471A04L0	SHAIK FAREED BABA
206	18471A04L1	SHAIK HAPPSA
207	18471A04L2	SHAIK SADDAM HUSSAIN
208	18471A04L3	SHAIK TANVIR
209	18471A04L4	SHAIK UMRE FAROOQ
210	18471A04L5	SYED MOHAMMAD ALI
211	18471A04L6	TAVVA KANAKA TEJA
212	18471A04L7	THANIGUNDALA RAJASEKHAR REDDY
213	18471A04L8	THIMMISSETTY ANIL KUMAR
214	18471A04L9	VEERLA TRINADH
215	18471A04M1	YARLAGADDA NAVYA SAI
216	18471A04M2	LAKKAKULA AKASH
217	18471A04M3	NELAKURTHI HARITHA
218	18471A04M4	ANANTHA LAKSHMI RISHITHA
219	18471A04M5	PATHAN BALASAIDA
220	19475A0401	KOLAGANI TEJANJALI
221	19475A0402	SHAIK MASUDA
222	19475A0403	MUTLURI DAVID
223	19475A0404	VINUKONDA PRIYANKA

224	19475A0405	BANDARU HARIKA
225	19475A0406	BANTUPALLI SUDHEER KUMAR
226	19475A0407	KATTAMURI JAGADEESH KUMAR
227	19475A0408	TELAGATHOTI NAVEEN
228	19475A0409	UDATHA NARENDRA
229	19475A0410	PEDDISETTI PRABHU KUMAR
230	19475A0411	EEMANI LAKSHMI NARAYANA
231	19475A0412	MANNEM SAMBASIVA RAO
232	19475A0413	PARITALA SREEKANTH
233	19475A0414	VADDI NAGALAKSHMI
234	19475A0415	BOLE SRINU
235	19475A0416	ARIKATLA VENU GOPALA REDDY
236	19475A0417	KATTEKOTA JASWANTHIKA SAI KOTESWARI
237	19475A0418	PAMIDIMALLA SAMUEL JOE
238	19475A0419	GALIDINNE PAVAN KALYAN
239	19475A0420	PALAPARTHI CHANDRABABU
240	19475A0421	ALAKUNTA SRIHARI
241	19475A0422	BALIJEPAI GANGAMMA
242	19475A0423	GUDURI RAJASREE
243	19475A0424	KATIKAM MAHESH BABU
244	19475A0425	KOLA JAYANTH SAI GANESH
245	19475A0426	KOTTAPALLI SAIKUMAR

  
HOD, ECE

# LECTURE NOTES

○

○

# DIGITAL IMAGE PROCESSING

### **1. What is meant by Digital Image Processing? Explain how digital images can be represented?**

An image may be defined as a two-dimensional function,  $f(x, y)$ , where  $x$  and  $y$  are spatial (plane) coordinates, and the amplitude of  $f$  at any pair of coordinates  $(x, y)$  is called the intensity or gray level of the image at that point. When  $x$ ,  $y$ , and the amplitude values of  $f$  are all finite, discrete quantities, we call the image a digital image. The field of digital image processing refers to processing digital images by means of a digital computer. Note that a digital image is composed of a finite number of elements, each of which has a particular location and value. These elements are referred to as picture elements, image elements, pels, and pixels. Pixel is the term most widely used to denote the elements of a digital image.

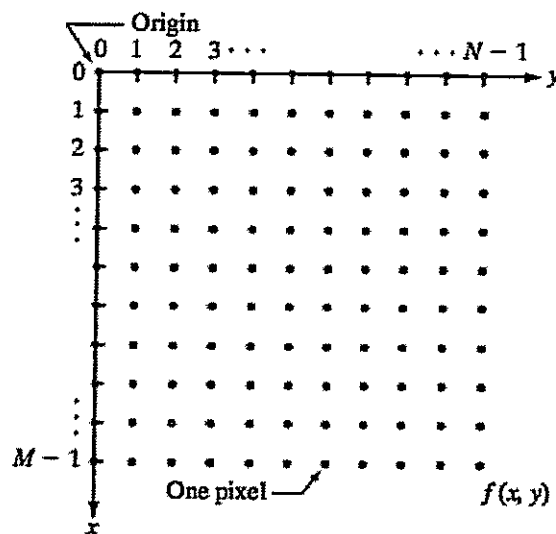
Vision is the most advanced of our senses, so it is not surprising that images play the single most important role in human perception. However, unlike humans, who are limited to the visual band of the electromagnetic (EM) spectrum, imaging machines cover almost the entire EM spectrum, ranging from gamma to radio waves. They can operate on images generated by sources that humans are not accustomed to associating with images. These include ultra-sound, electron microscopy, and computer-generated images. Thus, digital image processing encompasses a wide and varied field of applications. There is no general agreement among authors regarding where image processing stops and other related areas, such as image analysis and computer vision, start. Sometimes a distinction is made by defining image processing as a discipline in which both the input and output of a process are images. We believe this to be a limiting and somewhat artificial boundary. For example, under this definition, even the trivial task of computing the average intensity of an image (which yields a single number) would not be considered an image processing operation. On the other hand, there are fields such as computer vision whose ultimate goal is to use computers to emulate human vision, including learning and being able to make inferences and take actions based on visual inputs. This area itself is a branch of artificial intelligence (AI) whose objective is to emulate human intelligence. The field of AI is in its earliest stages of infancy in terms of development, with progress having been much slower than originally anticipated. The area of image analysis (also called image understanding) is in between image processing and computer vision.

There are no clear-cut boundaries in the continuum from image processing at one end to computer vision at the other. However, one useful paradigm is to consider three types of computerized processes in this continuum: low-, mid-, and high-level processes. Low-level processes involve primitive operations such as image preprocessing to reduce noise, contrast enhancement, and image sharpening. A low-level process is characterized by the fact that both its inputs and outputs are images. Mid-level processing on images involves tasks such as segmentation (partitioning an image into regions or objects), description of those objects to reduce them to a form suitable for computer processing, and classification (recognition) of individual objects. A mid-level process is characterized by the fact that its inputs generally are

images, but its outputs are attributes extracted from those images (e.g., edges, contours, and the identity of individual objects). Finally, higher-level processing involves “making sense” of an ensemble of recognized objects, as in image analysis, and, at the far end of the continuum, performing the cognitive functions normally associated with vision and, in addition, encompasses processes that extract attributes from images, up to and including the recognition of individual objects. As a simple illustration to clarify these concepts, consider the area of automated analysis of text. The processes of acquiring an image of the area containing the text, preprocessing that image, extracting (segmenting) the individual characters, describing the characters in a form suitable for computer processing, and recognizing those individual characters are in the scope of what we call digital image processing.

**Representing Digital Images:**

We will use two principal ways to represent digital images. Assume that an image  $f(x, y)$  is sampled so that the resulting digital image has  $M$  rows and  $N$  columns. The values of the coordinates  $(x, y)$  now become discrete quantities. For notational clarity and convenience, we shall use integer values for these discrete coordinates. Thus, the values of the coordinates at the origin are  $(x, y) = (0, 0)$ . The next coordinate values along the first row of the image are represented as  $(x, y) = (0, 1)$ . It is important to keep in mind that the notation  $(0, 1)$  is used to signify the second sample along the first row. It does not mean that these are the actual values of physical coordinates when the image was sampled. Figure 1 shows the coordinate convention used.



**Fig 1 Coordinate convention used to represent digital images**

The notation introduced in the preceding paragraph allows us to write the complete  $M \times N$  digital image in the following compact matrix form:

$$f(x, y) = \begin{bmatrix} f(0, 0) & f(0, 1) & \cdots & f(0, N - 1) \\ f(1, 0) & f(1, 1) & \cdots & f(1, N - 1) \\ \vdots & \vdots & \ddots & \vdots \\ f(M - 1, 0) & f(M - 1, 1) & \cdots & f(M - 1, N - 1) \end{bmatrix}$$

The right side of this equation is by definition a digital image. Each element of this matrix array is called an image element, picture element, pixel, or pel.

## 2. What are the fundamental steps in Digital Image Processing?

### Fundamental Steps in Digital Image Processing:

Image acquisition is the first process shown in Fig.2. Note that acquisition could be as simple as being given an image that is already in digital form. Generally, the image acquisition stage involves preprocessing, such as scaling.

Image enhancement is among the simplest and most appealing areas of digital image processing. Basically, the idea behind enhancement techniques is to bring out detail that is obscured, or simply to highlight certain features of interest in an image. A familiar example of enhancement is when we increase the contrast of an image because "it looks better." It is important to keep in mind that enhancement is a very subjective area of image processing.

Image restoration is an area that also deals with improving the appearance of an image. However, unlike enhancement, which is subjective, image restoration is objective, in the sense that restoration techniques tend to be based on mathematical or probabilistic models of image degradation. Enhancement, on the other hand, is based on human subjective preferences regarding what constitutes a "good" enhancement result.

Color image processing is an area that has been gaining in importance because of the significant increase in the use of digital images over the Internet.



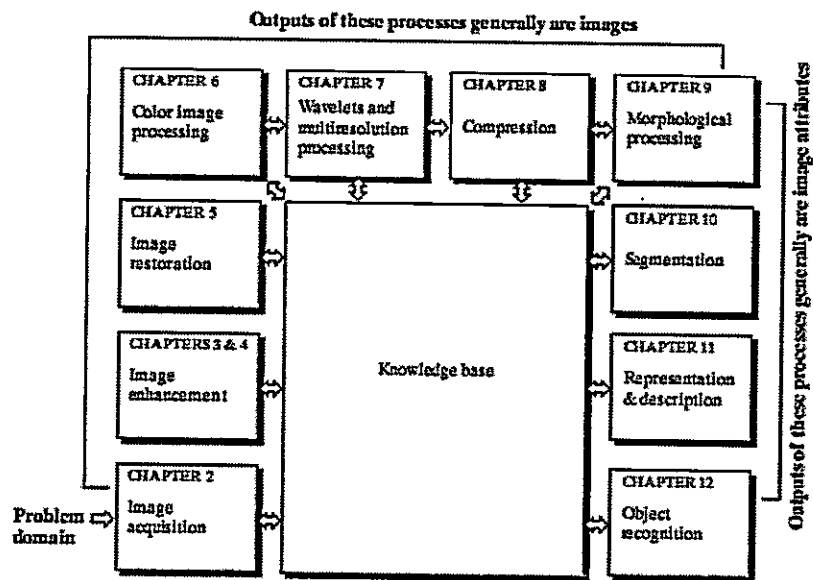


Fig.2. Fundamental steps in Digital Image Processing

Wavelets are the foundation for representing images in various degrees of resolution. Compression, as the name implies, deals with techniques for reducing the storage required to save an image, or the bandwidth required to transmit it. Although storage technology has improved significantly over the past decade, the same cannot be said for transmission capacity. This is true particularly in uses of the Internet, which are characterized by significant pictorial content. Image compression is familiar (perhaps inadvertently) to most users of computers in the form of image file extensions, such as the jpg file extension used in the JPEG (Joint Photographic Experts Group) image compression standard.

Morphological processing deals with tools for extracting image components that are useful in the representation and description of shape.

Segmentation procedures partition an image into its constituent parts or objects. In general, autonomous segmentation is one of the most difficult tasks in digital image processing. A rugged segmentation procedure brings the process a long way toward successful solution of imaging problems that require objects to be identified individually. On the other hand, weak or erratic segmentation algorithms almost always guarantee eventual failure. In general, the more accurate the segmentation, the more likely recognition is to succeed.

Representation and description almost always follow the output of a segmentation stage, which usually is raw pixel data, constituting either the boundary of a region (i.e., the set of pixels separating one image region from another) or all the points in the region itself. In either case, converting the data to a form suitable for computer processing is necessary. The first decision that must be made is whether the data should be represented as a boundary or as a complete region. Boundary representation is appropriate when the focus is on external shape characteristics, such as corners and inflections. Regional representation is appropriate when the focus is on internal properties, such as texture or skeletal shape. In some applications, these representations complement each other. Choosing a representation is only part of the solution for transforming raw data into a form suitable for subsequent computer processing. A method must also be specified for describing the data so that features of interest are highlighted. Description, also called feature selection, deals with extracting attributes that result in some quantitative information of interest or are basic for differentiating one class of objects from another.

Recognition is the process that assigns a label (e.g., "vehicle") to an object based on its descriptors. We conclude our coverage of digital image processing with the development of methods for recognition of individual objects.

### **3. What are the components of an Image Processing System?**

#### **Components of an Image Processing System:**

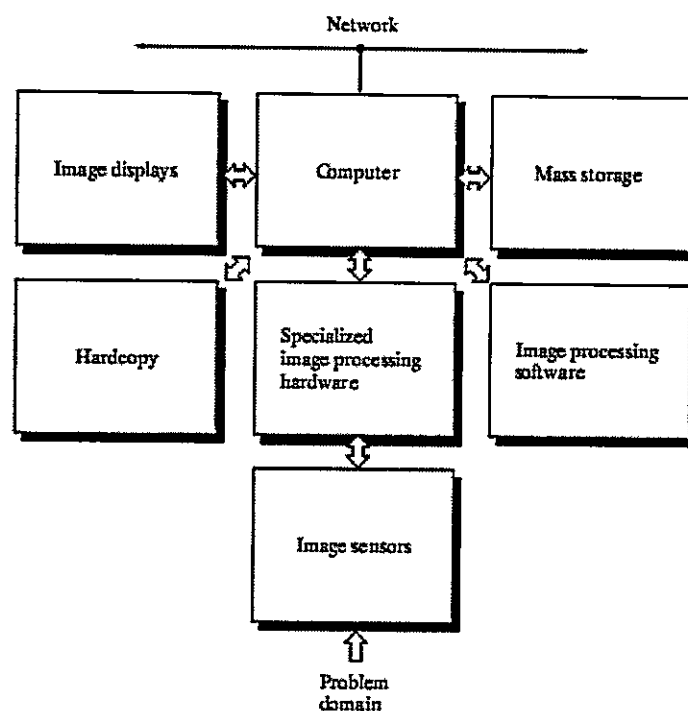
As recently as the mid-1980s, numerous models of image processing systems being sold throughout the world were rather substantial peripheral devices that attached to equally substantial host computers. Late in the 1980s and early in the 1990s, the market shifted to image processing hardware in the form of single boards designed to be compatible with industry standard buses and to fit into engineering workstation cabinets and personal computers. In addition to lowering costs, this market shift also served as a catalyst for a significant number of new companies whose specialty is the development of software written specifically for image processing.

Although large-scale image processing systems still are being sold for massive imaging applications, such as processing of satellite images, the trend continues toward miniaturizing and blending of general-purpose small computers with specialized image processing hardware. Figure 3 shows the basic components comprising a typical general-purpose system used for digital image processing. The function of each component is discussed in the following paragraphs, starting with image sensing.

With reference to sensing, two elements are required to acquire digital images. The first is a physical device that is sensitive to the energy radiated by the object we wish to image. The second, called a digitizer, is a device for converting the output of the physical sensing device into

digital form. For instance, in a digital video camera, the sensors produce an electrical output proportional to light intensity. The digitizer converts these outputs to digital data.

Specialized image processing hardware usually consists of the digitizer just mentioned, plus hardware that performs other primitive operations, such as an arithmetic logic unit (ALU), which performs arithmetic and logical operations in parallel on entire images. One example of how an ALU is used is in averaging images as quickly as they are digitized, for the purpose of noise reduction. This type of hardware sometimes is called a front-end subsystem, and its most distinguishing characteristic is speed. In other words, this unit performs functions that require fast data throughputs (e.g., digitizing and averaging video images at 30 frames) that the typical main computer cannot handle.



**Fig.3. Components of a general purpose Image Processing System**

The computer in an image processing system is a general-purpose computer and can range from a PC to a supercomputer. In dedicated applications, some times specially designed computers are used to achieve a required level of performance, but our interest here is on general-purpose

image processing systems. In these systems, almost any well-equipped PC-type machine is suitable for offline image processing tasks.

Software for image processing consists of specialized modules that perform specific tasks. A well-designed package also includes the capability for the user to write code that, as a minimum, utilizes the specialized modules. More sophisticated software packages allow the integration of those modules and general-purpose software commands from at least one computer language.

Mass storage capability is a must in image processing applications. An image of size 1024\*1024 pixels, in which the intensity of each pixel is an 8-bit quantity, requires one megabyte of storage space if the image is not compressed. When dealing with thousands, or even millions, of images, providing adequate storage in an image processing system can be a challenge. Digital storage for image processing applications falls into three principal categories: (1) short-term storage for use during processing, (2) on-line storage for relatively fast re-call, and (3) archival storage, characterized by infrequent access. Storage is measured in bytes (eight bits), Kbytes (one thousand bytes), Mbytes (one million bytes), Gbytes (meaning giga, or one billion, bytes), and Tbytes (meaning tera, or one trillion, bytes). One method of providing short-term storage is computer memory. Another is by specialized boards, called frame buffers, that store one or more images and can be accessed rapidly, usually at video rates (e.g., at 30 complete images per second). The latter method allows virtually instantaneous image zoom, as well as scroll (vertical shifts) and pan (horizontal shifts). Frame buffers usually are housed in the specialized image processing hardware unit shown in Fig.3. Online storage generally takes the form of magnetic disks or optical-media storage. The key factor characterizing on-line storage is frequent access to the stored data. Finally, archival storage is characterized by massive storage requirements but infrequent need for access. Magnetic tapes and optical disks housed in "jukeboxes" are the usual media for archival applications.

Image displays in use today are mainly color (preferably flat screen) TV monitors. Monitors are driven by the outputs of image and graphics display cards that are an integral part of the computer system. Seldom are there requirements for image display applications that cannot be met by display cards available commercially as part of the computer system. In some cases, it is necessary to have stereo displays, and these are implemented in the form of headgear containing two small displays embedded in goggles worn by the user.

Hardcopy devices for recording images include laser printers, film cameras, heat-sensitive devices, inkjet units, and digital units, such as optical and CD-ROM disks. Film provides the highest possible resolution, but paper is the obvious medium of choice for written material. For presentations, images are displayed on film transparencies or in a digital medium if image projection equipment is used. The latter approach is gaining acceptance as the standard for image presentations.

Networking is almost a default function in any computer system in use today. Because of the large amount of data inherent in image processing applications, the key consideration in image transmission is bandwidth. In dedicated networks, this typically is not a problem, but communications with remote sites via the Internet are not always as efficient. Fortunately, this situation is improving quickly as a result of optical fiber and other broadband technologies.

#### **4. Explain about elements of visual perception.**

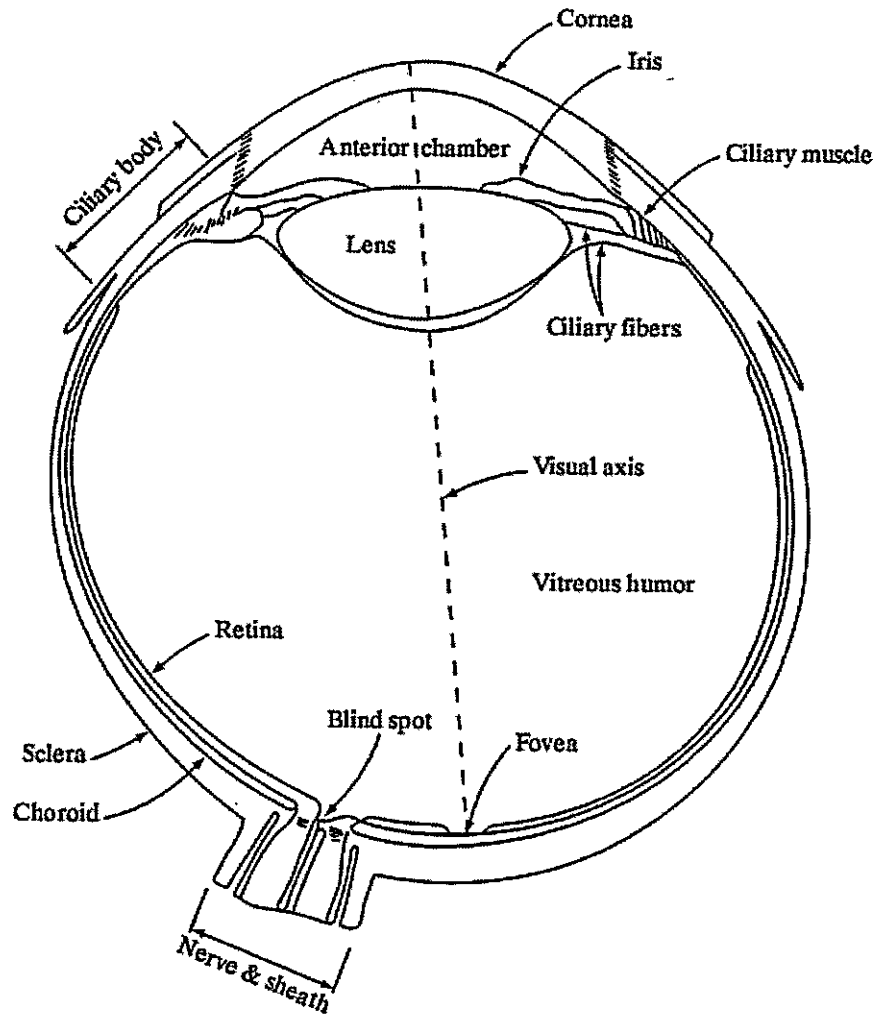
##### **Elements of Visual Perception:**

Although the digital image processing field is built on a foundation of mathematical and probabilistic formulations, human intuition and analysis play a central role in the choice of one technique versus another, and this choice often is made based on subjective, visual judgments.

##### **(1) Structure of the Human Eye:**

Figure 4.1 shows a simplified horizontal cross section of the human eye. The eye is nearly a sphere, with an average diameter of approximately 20 mm. Three membranes enclose the eye: the cornea and sclera outer cover; the choroid; and the retina. The cornea is a tough, transparent tissue that covers the anterior surface of the eye. Continuous with the cornea, the sclera is an opaque membrane that encloses the remainder of the optic globe. The choroid lies directly below the sclera. This membrane contains a network of blood vessels that serve as the major source of nutrition to the eye. Even superficial injury to the choroid, often not deemed serious, can lead to severe eye damage as a result of inflammation that restricts blood flow. The choroid coat is heavily pigmented and hence helps to reduce the amount of extraneous light entering the eye and the backscatter within the optical globe. At its anterior extreme, the choroid is divided into the ciliary body and the iris diaphragm. The latter contracts or expands to control the amount of light that enters the eye. The central opening of the iris (the pupil) varies in diameter from approximately 2 to 8 mm. The front of the iris contains the visible pigment of the eye, whereas the back contains a black pigment.

The lens is made up of concentric layers of fibrous cells and is suspended by fibers that attach to the ciliary body. It contains 60 to 70% water, about 6% fat, and more protein than any other tissue in the eye. The lens is colored by a slightly yellow pigmentation that increases with age. In extreme cases, excessive clouding of the lens, caused by the affliction commonly referred to as cataracts, can lead to poor color discrimination and loss of clear vision. The lens absorbs approximately 8% of the visible light spectrum, with relatively higher absorption at shorter wavelengths. Both infrared and ultraviolet light are absorbed appreciably by proteins within the lens structure and, in excessive amounts, can damage the eye.



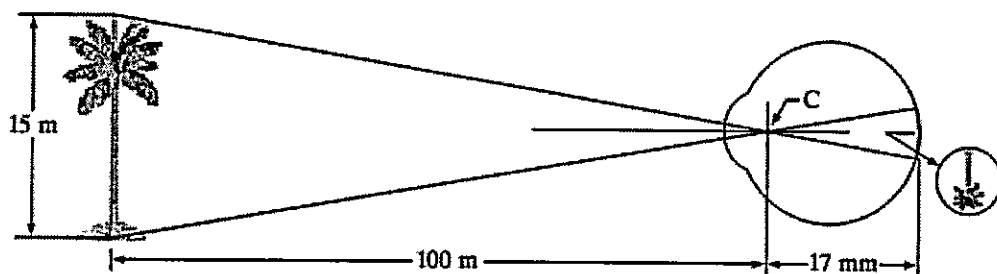
**Fig.4.1 Simplified diagram of a cross section of the human eye.**

The innermost membrane of the eye is the retina, which lines the inside of the wall's entire posterior portion. When the eye is properly focused, light from an object outside the eye is imaged on the retina. Pattern vision is afforded by the distribution of discrete light receptors over the surface of the retina. There are two classes of receptors: cones and rods. The cones in each eye number between 6 and 7 million. They are located primarily in the central portion of the

retina, called the fovea, and are highly sensitive to color. Humans can resolve fine details with these cones largely because each one is connected to its own nerve end. Muscles controlling the eye rotate the eyeball until the image of an object of interest falls on the fovea. Cone vision is called photopic or bright-light vision. The number of rods is much larger: Some 75 to 150 million are distributed over the retinal surface. The larger area of distribution and the fact that several rods are connected to a single nerve end reduce the amount of detail discernible by these receptors. Rods serve to give a general, overall picture of the field of view. They are not involved in color vision and are sensitive to low levels of illumination. For example, objects that appear brightly colored in daylight when seen by moonlight appear as colorless forms because only the rods are stimulated. This phenomenon is known as scotopic or dim-light vision.

## (2) Image Formation in the Eye:

The principal difference between the lens of the eye and an ordinary optical lens is that the former is flexible. As illustrated in Fig. 4.1, the radius of curvature of the anterior surface of the lens is greater than the radius of its posterior surface. The shape of the lens is controlled by tension in the fibers of the ciliary body. To focus on distant objects, the controlling muscles cause the lens to be relatively flattened. Similarly, these muscles allow the lens to become thicker in order to focus on objects near the eye. The distance between the center of the lens and the retina (called the focal length) varies from approximately 17 mm to about 14 mm, as the refractive power of the lens increases from its minimum to its maximum. When the eye



**Fig.4.2.** Graphical representation of the eye looking at a palm tree Point C is the optical center of the lens.

focuses on an object farther away than about 3 m, the lens exhibits its lowest refractive power. When the eye focuses on a nearby object, the lens is most strongly refractive. This information

makes it easy to calculate the size of the retinal image of any object. In Fig. 4.2, for example, the observer is looking at a tree 15 m high at a distance of 100 m. If  $h$  is the height in mm of that object in the retinal image, the geometry of Fig.4.2 yields  $15/100=h/17$  or  $h=2.55\text{mm}$ . The retinal image is reflected primarily in the area of the fovea. Perception then takes place by the relative excitation of light receptors, which transform radiant energy into electrical impulses that are ultimately decoded by the brain.

### (3) Brightness Adaptation and Discrimination:

Because digital images are displayed as a discrete set of intensities, the eye's ability to discriminate between different intensity levels is an important consideration in presenting image-processing results. The range of light intensity levels to which the human visual system can adapt is enormous—on the order of  $10^{10}$ —from the scotopic threshold to the glare limit. Experimental evidence indicates that subjective brightness (intensity as perceived by the human visual system) is a logarithmic function of the light intensity incident on the eye. Figure 4.3, a plot of light intensity versus subjective brightness, illustrates this characteristic. The long solid curve represents the range of intensities to which the visual system can adapt. In photopic vision alone, the range is about  $10^6$ . The transition from scotopic to photopic vision is gradual over the approximate range from 0.001 to 0.1 millilambert ( $-3$  to  $-1$  mL in the log scale), as the double branches of the adaptation curve in this range show.

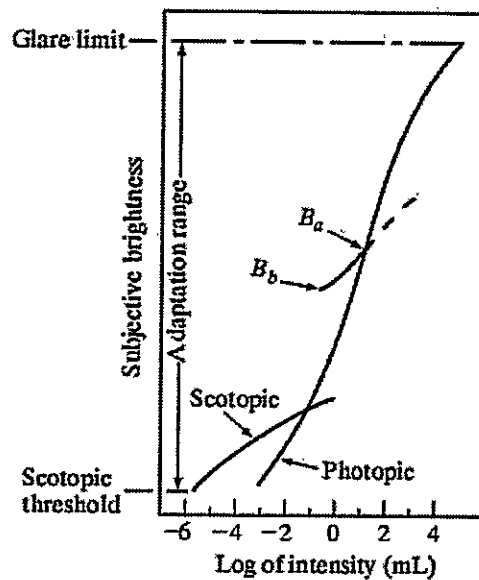


Fig.4.3. Range of Subjective brightness sensations showing a particular adaptation level.



The essential point in interpreting the impressive dynamic range depicted in Fig.4.3 is that the visual system cannot operate over such a range simultaneously. Rather, it accomplishes this large variation by changes in its overall sensitivity, a phenomenon known as brightness adaptation. The total range of distinct intensity levels it can discriminate simultaneously is rather small when compared with the total adaptation range. For any given set of conditions, the current sensitivity level of the visual system is called the brightness adaptation level, which may correspond, for example, to brightness  $B_a$  in Fig. 4.3. The short intersecting curve represents the range of subjective brightness that the eye can perceive when adapted to this level. This range is rather restricted, having a level  $B_b$  at and below which all stimuli are perceived as indistinguishable blacks. The upper (dashed) portion of the curve is not actually restricted but, if extended too far, loses its meaning because much higher intensities would simply raise the adaptation level higher than  $B_a$ .

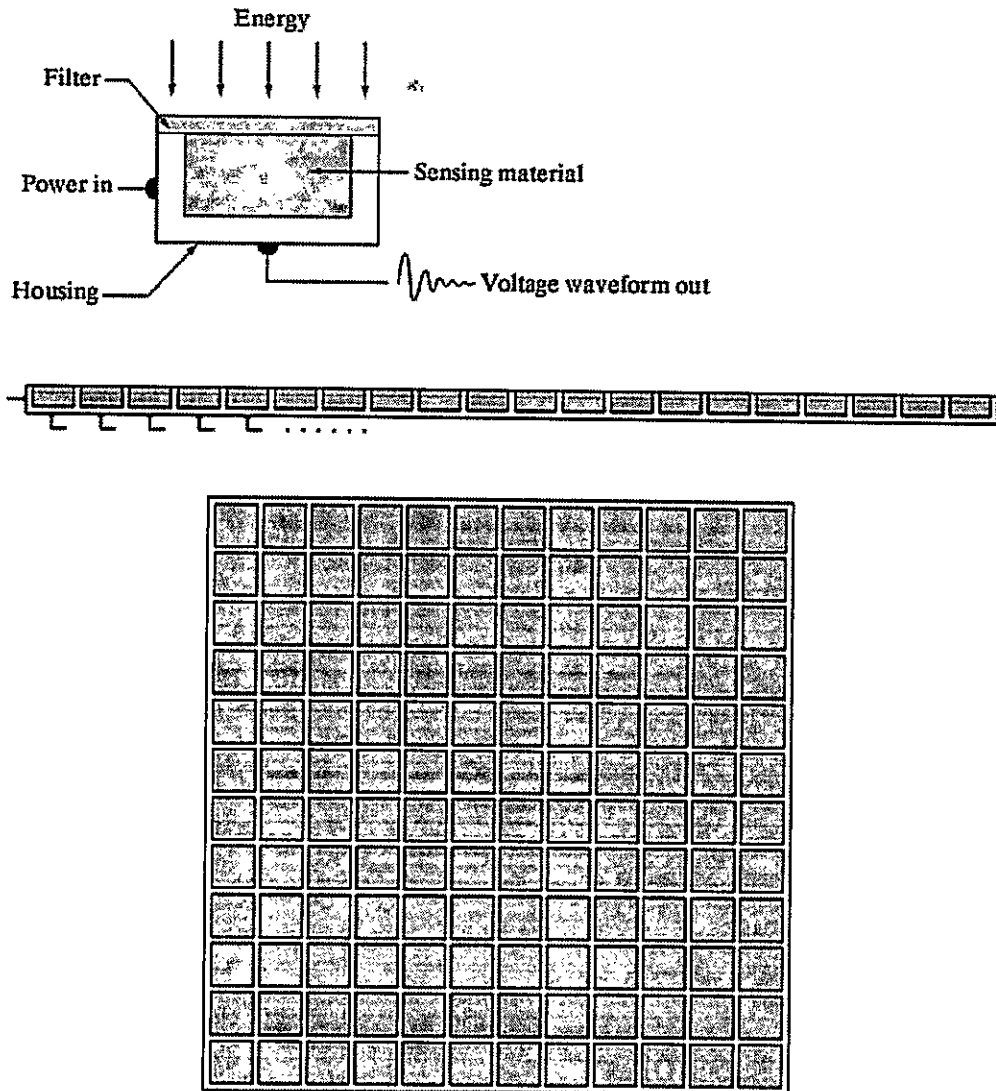
## 5. Explain the process of image acquisition.

### Image Sensing and Acquisition:

The types of images in which we are interested are generated by the combination of an "illumination" source and the reflection or absorption of energy from that source by the elements of the "scene" being imaged. We enclose illumination and scene in quotes to emphasize the fact that they are considerably more general than the familiar situation in which a visible light source illuminates a common everyday 3-D (three-dimensional) scene. For example, the illumination may originate from a source of electromagnetic energy such as radar, infrared, or X-ray energy. But, as noted earlier, it could originate from less traditional sources, such as ultrasound or even a computer-generated illumination pattern.

Similarly, the scene elements could be familiar objects, but they can just as easily be molecules, buried rock formations, or a human brain. We could even image a source, such as acquiring images of the sun. Depending on the nature of the source, illumination energy is reflected from, or transmitted through, objects. An example in the first category is light reflected from a planar surface. An example in the second category is when X-rays pass through a patient's body for the purpose of generating a diagnostic X-ray film. In some applications, the reflected or transmitted energy is focused onto a photo converter (e.g., a phosphor screen), which converts the energy into visible light. Electron microscopy and some applications of gamma imaging use this approach.

Figure 5.1 shows the three principal sensor arrangements used to transform illumination energy into digital images. The idea is simple: Incoming energy is transformed into a voltage by the combination of input electrical power and sensor material that is responsive to the particular type of energy being detected. The output voltage waveform is the response of the sensor(s), and a digital quantity is obtained from each sensor by digitizing its response.



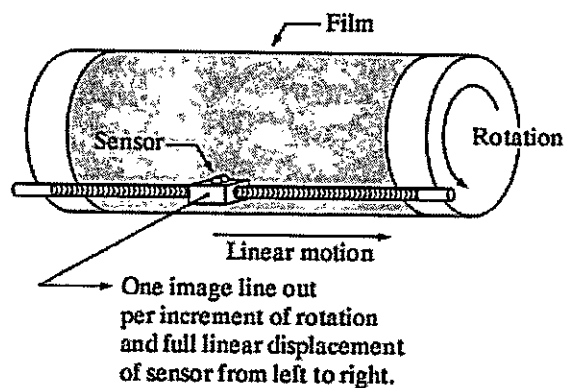
**Fig.5.1 (a) Single imaging Sensor (b) Line sensor (c) Array sensor**

**(1)Image Acquisition Using a Single Sensor:**

Figure 5.1 (a) shows the components of a single sensor. Perhaps the most familiar sensor of this type is the photodiode, which is constructed of silicon materials and whose output voltage waveform is proportional to light. The use of a filter in front of a sensor improves selectivity. For example, a green (pass) filter in front of a light sensor favors light in the green band of the color

spectrum. As a consequence, the sensor output will be stronger for green light than for other components in the visible spectrum.

In order to generate a 2-D image using a single sensor, there has to be relative displacements in both the x- and y-directions between the sensor and the area to be imaged. Figure 5.2 shows an arrangement used in high-precision scanning, where a film negative is mounted onto a drum whose mechanical rotation provides displacement in one dimension. The single sensor is mounted on a lead screw that provides motion in the perpendicular direction. Since mechanical motion can be controlled with high precision, this method is an inexpensive (but slow) way to obtain high-resolution images. Other similar mechanical arrangements use a flat bed, with the sensor moving in two linear directions. These types of mechanical digitizers sometimes are referred to as microdensitometers.



**Fig.5.2. Combining a single sensor with motion to generate a 2-D image**

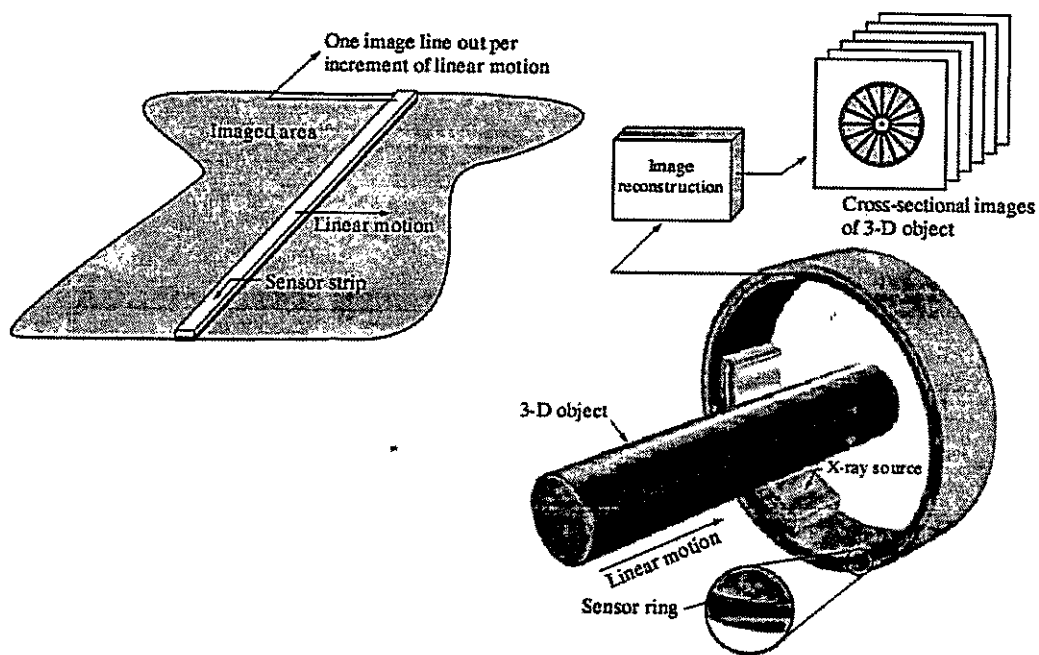
## (2) Image Acquisition Using Sensor Strips:

A geometry that is used much more frequently than single sensors consists of an in-line arrangement of sensors in the form of a sensor strip, as Fig. 5.1 (b) shows. The strip provides imaging elements in one direction. Motion perpendicular to the strip provides imaging in the other direction, as shown in Fig. 5.3 (a). This is the type of arrangement used in most flat bed scanners. Sensing devices with 4000 or more in-line sensors are possible. In-line sensors are used routinely in airborne imaging applications, in which the imaging system is mounted on an aircraft that flies at a constant altitude and speed over the geographical area to be imaged. One-dimensional imaging sensor strips that respond to various bands of the electromagnetic spectrum are mounted perpendicular to the direction of flight. The imaging strip gives one line of an image

at a time, and the motion of the strip completes the other dimension of a two-dimensional image. Lenses or other focusing schemes are used to project the area to be scanned onto the sensors.

Sensor strips mounted in a ring configuration are used in medical and industrial imaging to obtain cross-sectional ("slice") images of 3-D objects, as Fig. 5.3 (b) shows. A rotating X-ray source provides illumination and the portion of the sensors opposite the source collect the X-ray energy that pass through the object (the sensors obviously have to be sensitive to X-ray energy). This is the basis for medical and industrial computerized axial tomography (CAT). It is important to note that the output of the sensors must be processed by reconstruction algorithms whose objective is to transform the sensed data into meaningful cross-sectional images.

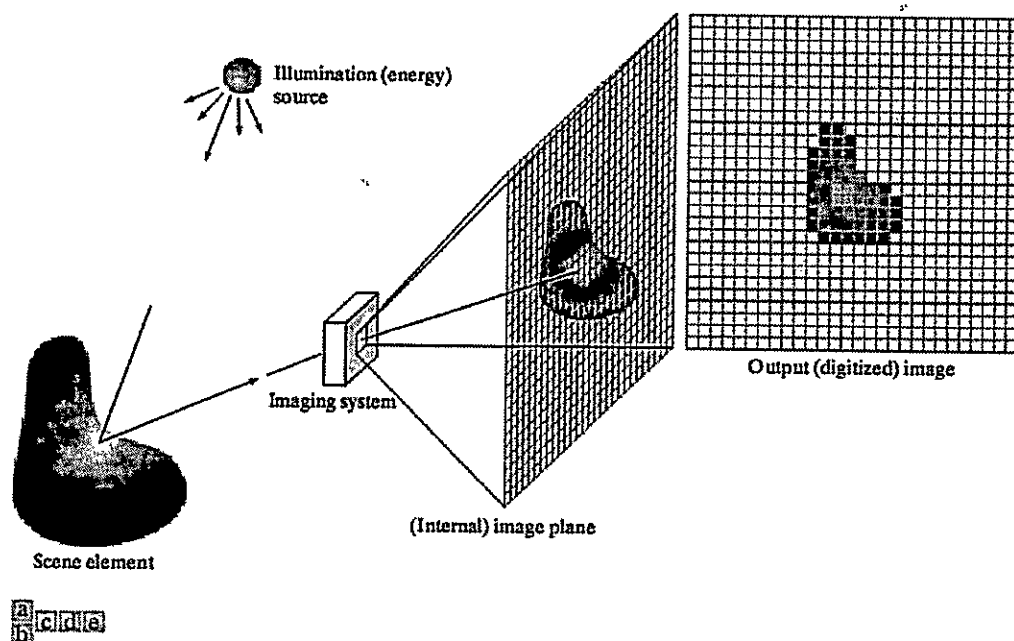
In other words, images are not obtained directly from the sensors by motion alone; they require extensive processing. A 3-D digital volume consisting of stacked images is generated as the object is moved in a direction perpendicular to the sensor ring. Other modalities of imaging based on the CAT principle include magnetic resonance imaging (MRI) and positron emission tomography (PET). The illumination sources, sensors, and types of images are different, but conceptually they are very similar to the basic imaging approach shown in Fig. 5.3 (b).



**Fig.5.3 (a) Image acquisition using a linear sensor strip (b) Image acquisition using a circular sensor strip.**

**(3) Image Acquisition Using Sensor Arrays:**

Figure 5.1 (c) shows individual sensors arranged in the form of a 2-D array. Numerous electromagnetic and some ultrasonic sensing devices frequently are arranged in an array format. This is also the predominant arrangement found in digital cameras. A typical sensor for these cameras is a CCD array, which can be manufactured with a broad range of sensing properties and can be packaged in rugged arrays of  $4000 * 4000$  elements or more. CCD sensors are used widely in digital cameras and other light sensing instruments. The response of each sensor is proportional to the integral of the light energy projected onto the surface of the sensor, a property that is used in astronomical and other applications requiring low noise images. Noise reduction is achieved by letting the sensor integrate the input light signal over minutes or even hours. Since the sensor array shown in Fig. 5.4 (c) is two dimensional, its key advantage is that a complete image can be obtained by focusing the energy pattern onto the surface of the array. The principal manner in which array sensors are used is shown in Fig.5.4. This figure shows the energy from an illumination source being reflected from a scene element, but, as mentioned at the beginning of this section, the energy also could be transmitted through the scene elements. The first function performed by the imaging system shown in Fig.5.4 (c) is to collect the incoming energy and focus it onto an image plane. If the illumination is light, the front end of the imaging system is a lens, which projects the viewed scene onto the lens focal plane, as Fig. 2.15(d) shows. The sensor array, which is coincident with the focal plane, produces outputs proportional to the integral of the light received at each sensor. Digital and analog circuitry sweep these outputs and converts them to a video signal, which is then digitized by another section of the imaging system. The output is a digital image, as shown diagrammatically in Fig. 5.4 (e).



**Fig.5.4** An example of the digital image acquisition process (a) Energy (“illumination”) source (b) An element of a scene (c) Imaging system (d) Projection of the scene onto the image plane (e) Digitized image

## 6. Explain about image sampling and quantization process.

### Image Sampling and Quantization:

The output of most sensors is a continuous voltage waveform whose amplitude and spatial behavior are related to the physical phenomenon being sensed. To create a digital image, we need to convert the continuous sensed data into digital form. This involves two processes: sampling and quantization.

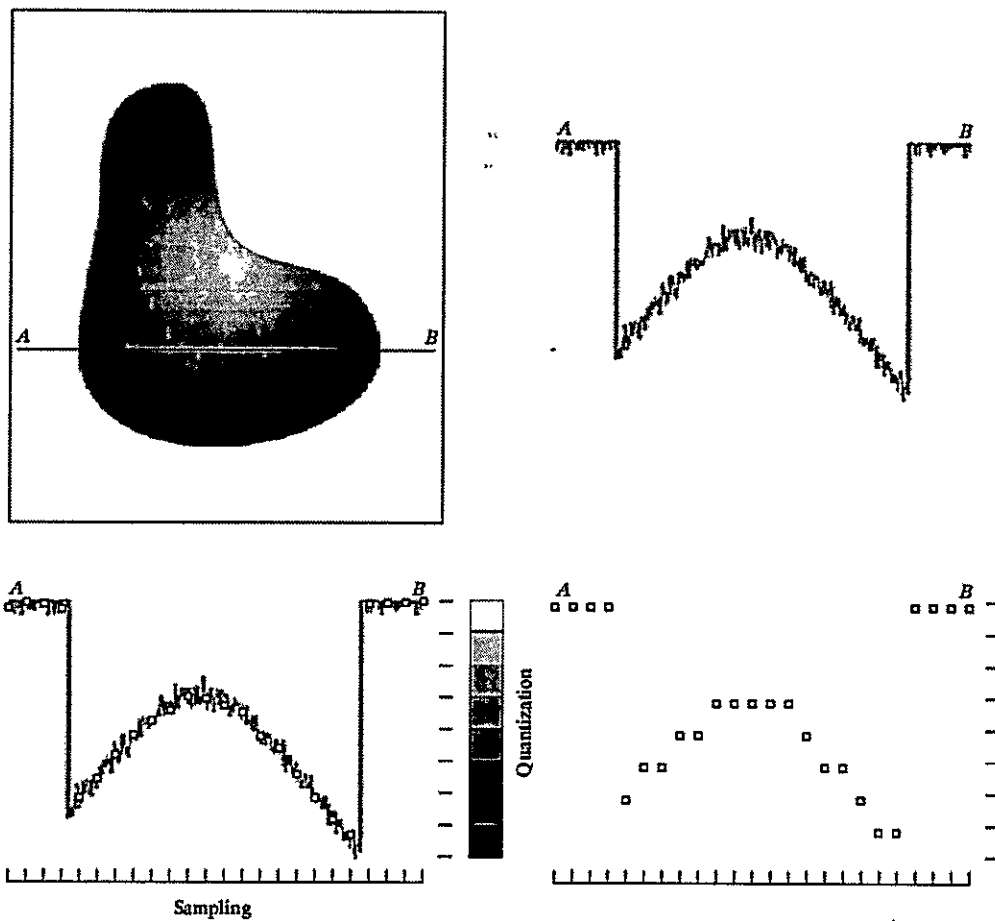
### Basic Concepts in Sampling and Quantization:

The basic idea behind sampling and quantization is illustrated in Fig.6.1. Figure 6.1(a) shows a continuous image,  $f(x, y)$ , that we want to convert to digital form. An image may be continuous with respect to the x- and y-coordinates, and also in amplitude. To convert it to digital form, we have to sample the function in both coordinates and in amplitude. Digitizing the coordinate values is called sampling. Digitizing the amplitude values is called quantization.

The one-dimensional function shown in Fig.6.1 (b) is a plot of amplitude (gray level) values of the continuous image along the line segment AB in Fig. 6.1(a). The random variations are due to image noise. To sample this function, we take equally spaced samples along line AB, as shown in Fig.6.1 (c). The location of each sample is given by a vertical tick mark in the bottom part of the figure. The samples are shown as small white squares superimposed on the function. The set of these discrete locations gives the sampled function. However, the values of the samples still span (vertically) a continuous range of gray-level values. In order to form a digital function, the gray-level values also must be converted (quantized) into discrete quantities. The right side of Fig. 6.1 (c) shows the gray-level scale divided into eight discrete levels, ranging from black to white. The vertical tick marks indicate the specific value assigned to each of the eight gray levels. The continuous gray levels are quantized simply by assigning one of the eight discrete gray levels to each sample. The assignment is made depending on the vertical proximity of a sample to a vertical tick mark. The digital samples resulting from both sampling and quantization are shown in Fig.6.1 (d). Starting at the top of the image and carrying out this procedure line by line produces a two-dimensional digital image.

Sampling in the manner just described assumes that we have a continuous image in both coordinate directions as well as in amplitude. In practice, the method of sampling is determined by the sensor arrangement used to generate the image. When an image is generated by a single

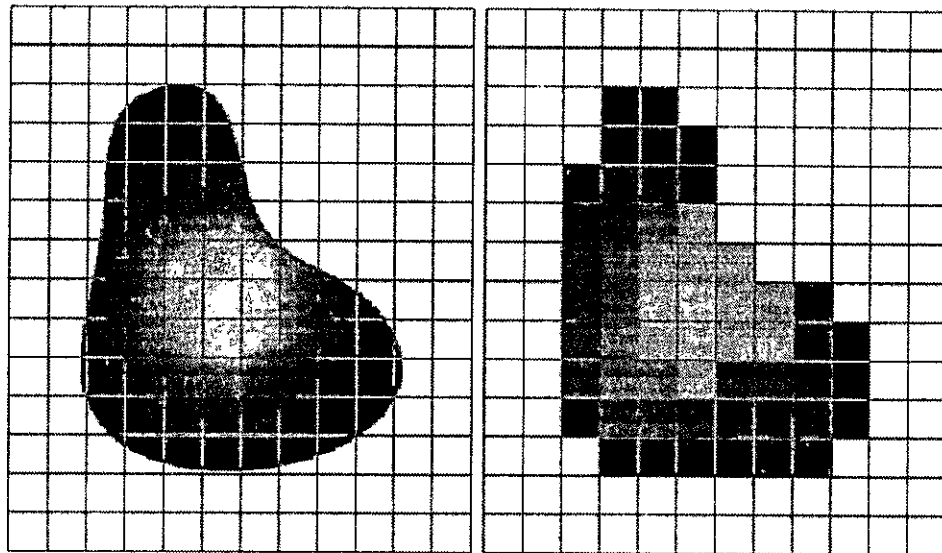
sensing element combined with mechanical motion, as in Fig. 2.13, the output of the sensor is quantized in the manner described above. However, sampling is accomplished by selecting the number of individual mechanical increments at which we activate the sensor to collect data. Mechanical motion can be made very exact so, in principle; there is almost no limit as to how fine we can sample an image. However, practical limits are established by imperfections in the optics used to focus on the



**Fig.6.1. Generating a digital image (a) Continuous image (b) A scan line from A to Bin the continuous image, used to illustrate the concepts of sampling and quantization (c) Sampling and quantization. (d) Digital scan line**

sensor an illumination spot that is inconsistent with the fine resolution achievable with mechanical displacements. When a sensing strip is used for image acquisition, the number of sensors in the strip establishes the sampling limitations in one image direction. Mechanical motion in the other direction can be controlled more accurately, but it makes little sense to try to achieve sampling density in one direction that exceeds the sampling limits established by the number of sensors in the other. Quantization of the sensor outputs completes the process of generating a digital image.

When a sensing array is used for image acquisition, there is no motion and the number of sensors in the array establishes the limits of sampling in both directions. Figure 6.2 illustrates this concept. Figure 6.2 (a) shows a continuous image projected onto the plane of an array sensor. Figure 6.2 (b) shows the image after sampling and quantization. Clearly, the quality of a digital image is determined to a large degree by the number of samples and discrete gray levels used in sampling and quantization.



**a** **b**

**Fig.6.2. (a) Continuous image projected onto a sensor array (b) Result of image sampling and quantization.**



## 7. Define spatial and gray level resolution. Explain about isopreference curves.

### Spatial and Gray-Level Resolution:

Sampling is the principal factor determining the spatial resolution of an image. Basically, spatial resolution is the smallest discernible detail in an image. Suppose that we construct a chart with vertical lines of width  $W$ , with the space between the lines also having width  $W$ . A line pair consists of one such line and its adjacent space. Thus, the width of a line pair is  $2W$ , and there are  $1/2W$  line pairs per unit distance. A widely used definition of resolution is simply the smallest number of discernible line pairs per unit distance; for example, 100 line pairs per millimeter. Gray-level resolution-similarly refers to the smallest discernible change in gray level. We have considerable discretion regarding the number of samples used to generate a digital image, but this is not true for the number of gray levels. Due to hardware considerations, the number of gray levels is usually an integer power of 2.

The most common number is 8 bits, with 16 bits being used in some applications where enhancement of specific gray-level ranges is necessary. Sometimes we find systems that can digitize the gray levels of an image with 10 or 12 bit of accuracy, but these are the exception rather than the rule. When an actual measure of physical resolution relating pixels and the level of detail they resolve in the original scene are not necessary, it is not uncommon to refer to an  $L$ -level digital image of size  $M*N$  as having a spatial resolution of  $M*N$  pixels and a gray-level resolution of  $L$  levels.

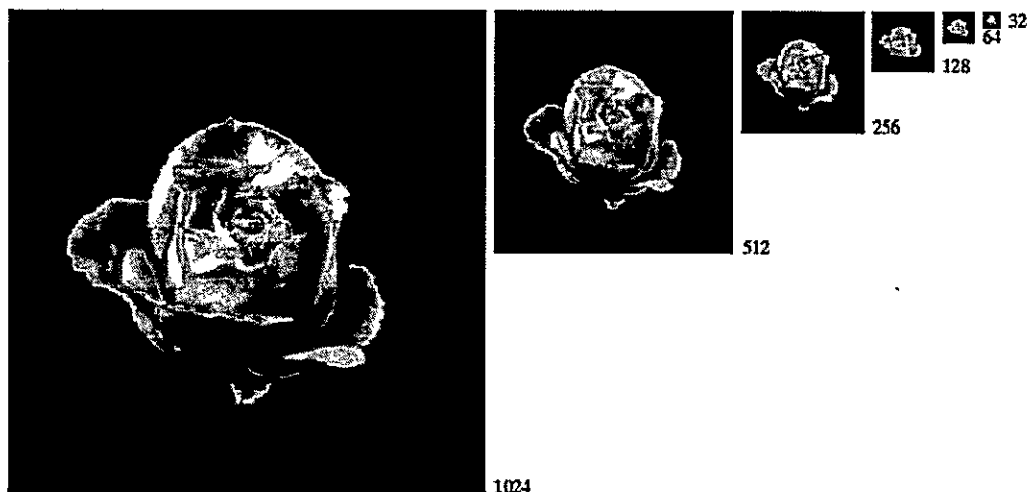
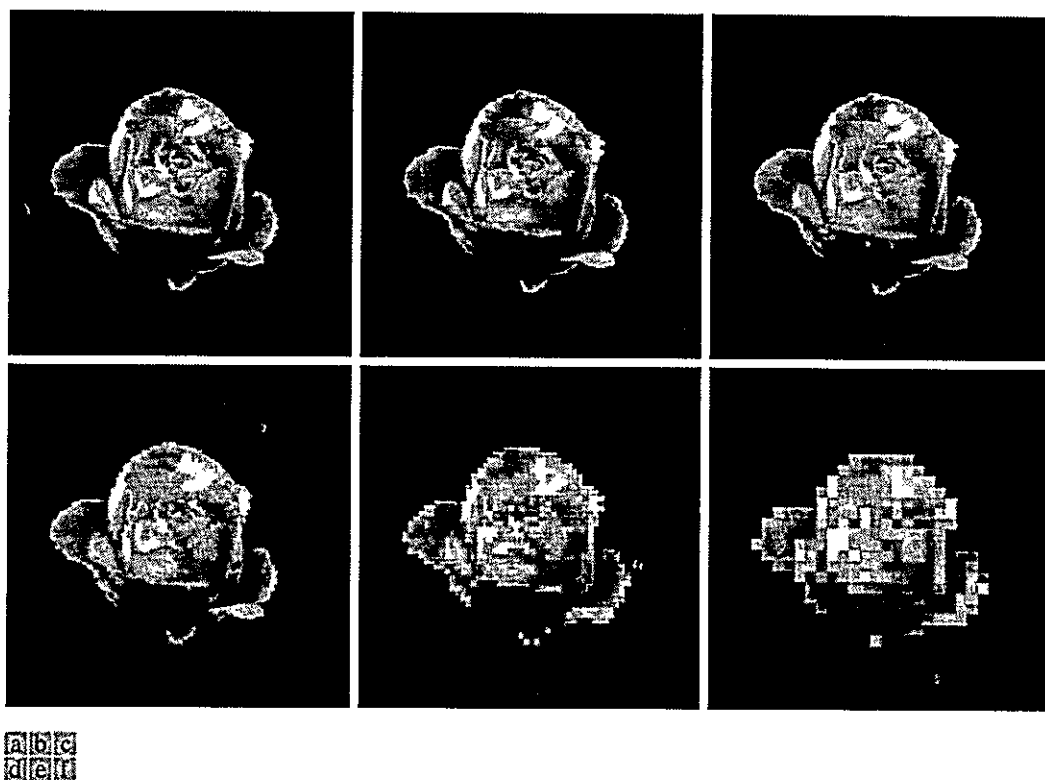


Fig.7.1. A 1024\*1024, 8-bit image subsampled down to size 32\*32 pixels The number of allowable gray levels was kept at 256.

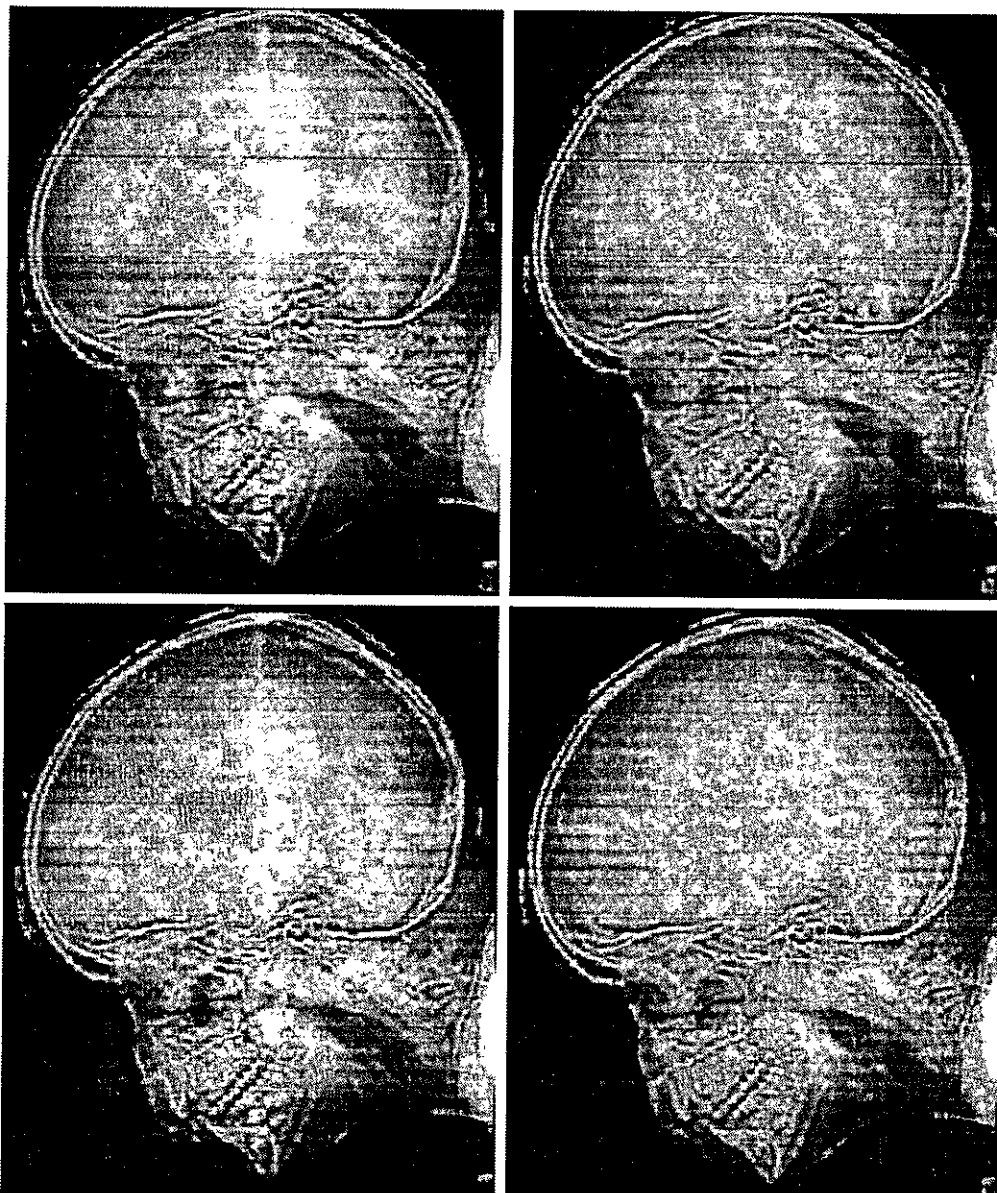
The subsampling was accomplished by deleting the appropriate number of rows and columns from the original image. For example, the 512\*512 image was obtained by deleting every other row and column from the 1024\*1024 image. The 256\*256 image was generated by deleting every other row and column in the 512\*512 image, and so on. The number of allowed gray levels was kept at 256. These images show the dimensional proportions between various sampling densities, but their size differences make it difficult to see the effects resulting from a reduction in the number of samples. The simplest way to compare these effects is to bring all the subsampled images up to size 1024\*1024 by row and column pixel replication. The results are shown in Figs. 7.2 (b) through (f). Figure 7.2 (a) is the same 1024\*1024, 256-level image shown in Fig.7.1; it is repeated to facilitate comparisons.

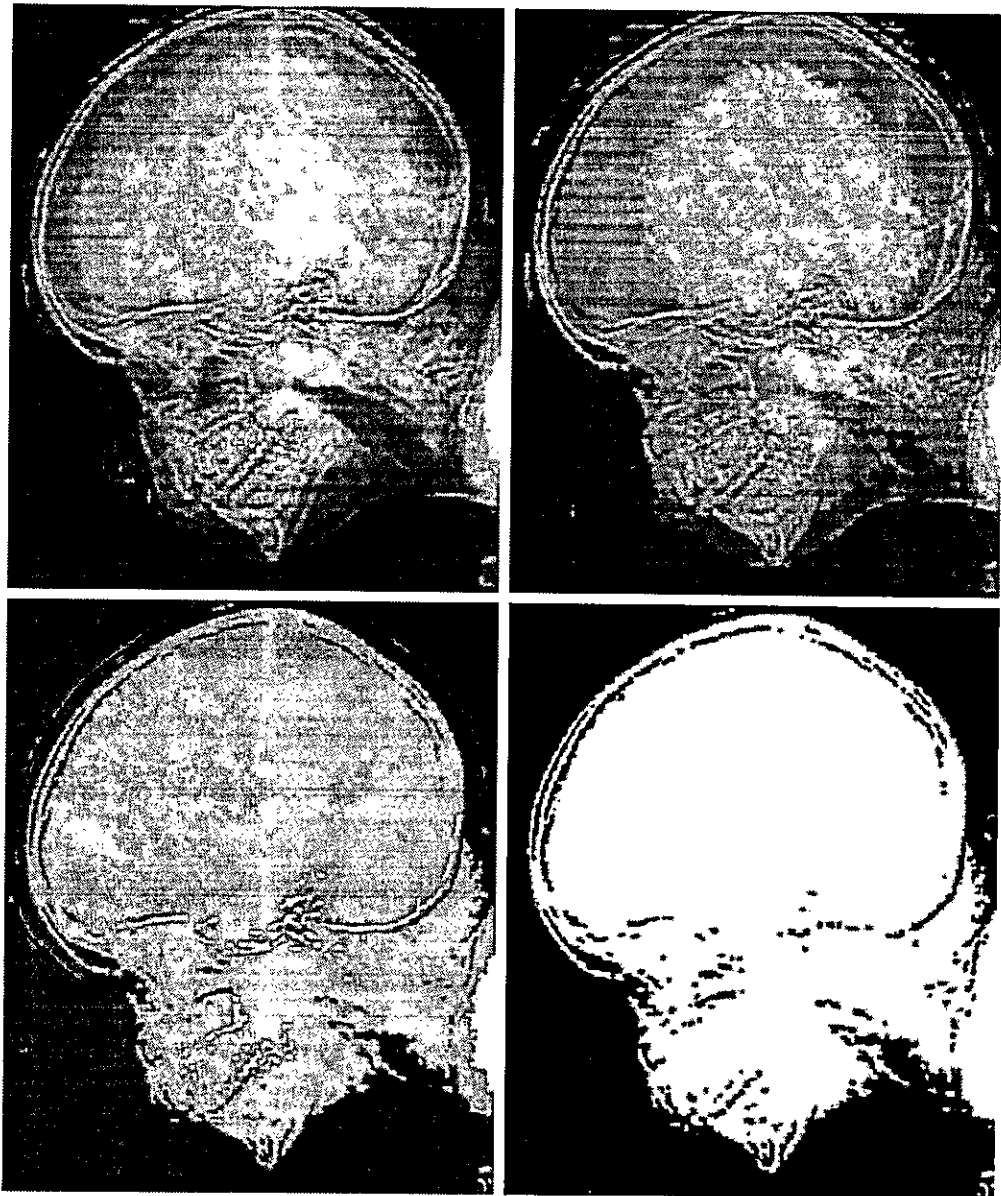


**Fig. 7.2 (a) 1024\*1024, 8-bit image (b) 512\*512 image resampled into 1024\*1024 pixels by row and column duplication (c) through (f) 256\*256, 128\*128, 64\*64, and 32\*32 images resampled into 1024\*1024 pixels**

Compare Fig. 7.2(a) with the 512\*512 image in Fig. 7.2(b) and note that it is virtually impossible to tell these two images apart. The level of detail lost is simply too fine to be seen on the printed page at the scale in which these images are shown. Next, the 256\*256 image in Fig. 7.2(c) shows a very slight fine checkerboard pattern in the borders between flower petals and the black background. A slightly more pronounced graininess throughout the image also is beginning to appear. These effects are much more visible in the 128\*128 image in Fig. 7.2(d), and they become pronounced in the 64\*64 and 32\*32 images in Figs. 7.2 (e) and (f), respectively.

In the next example, we keep the number of samples constant and reduce the number of gray levels from 256 to 2, in integer powers of 2. Figure 7.3(a) is a 452\*374 CAT projection image, displayed with  $k=8$  (256 gray levels). Images such as this are obtained by fixing the X-ray source in one position, thus producing a 2-D image in any desired direction. Projection images are used as guides to set up the parameters for a CAT scanner, including tilt, number of slices, and range. Figures 7.3(b) through (h) were obtained by reducing the number of bits from  $k=7$  to  $k=1$  while keeping the spatial resolution constant at 452\*374 pixels. The 256-, 128-, and 64-level images are visually identical for all practical purposes. The 32-level image shown in Fig. 7.3 (d), however, has an almost imperceptible set of very fine ridge like structures in areas of smooth gray levels (particularly in the skull). This effect, caused by the use of an insufficient number of gray levels in smooth areas of a digital image, is called false contouring, so called because the ridges resemble topographic contours in a map. False contouring generally is quite visible in images displayed using 16 or less uniformly spaced gray levels, as the images in Figs. 7.3(e) through (h) show.





**Fig. 7.3 (a) 452\*374, 256-level image (b)–(d) Image displayed in 128, 64, and 32 gray levels, while keeping the spatial resolution constant (e)–(g) Image displayed in 16, 8, 4, and 2 gray levels.**

As a very rough rule of thumb, and assuming powers of 2 for convenience, images of size  $256 \times 256$  pixels and 64 gray levels are about the smallest images that can be expected to be reasonably free of objectionable sampling checker-boards and false contouring.

The results in Examples 7.2 and 7.3 illustrate the effects produced on image quality by varying  $N$  and  $k$  independently. However, these results only partially answer the question of how varying  $N$  and  $k$  affect images because we have not considered yet any relationships that might exist between these two parameters.

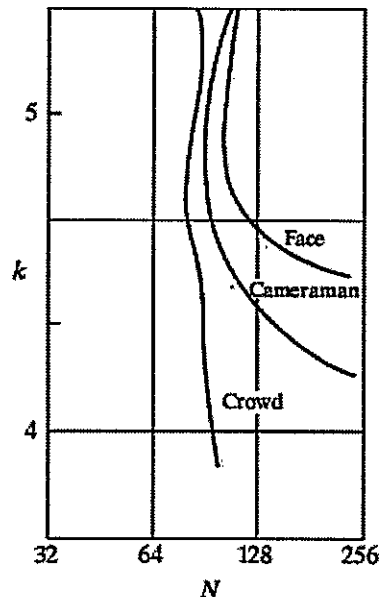
An early study by Huang [1965] attempted to quantify experimentally the effects on image quality produced by varying  $N$  and  $k$  simultaneously. The experiment consisted of a set of subjective tests. Images similar to those shown in Fig.7.4 were used. The woman's face is representative of an image with relatively little detail; the picture of the cameraman contains an intermediate amount of detail; and the crowd picture contains, by comparison, a large amount of detail. Sets of these three types of images were generated by varying  $N$  and  $k$ , and observers were then asked to rank them according to their subjective quality. Results were summarized in the form of so-called isopreference curves in the  $Nk$ -plane (Fig.7.5 shows average isopreference curves representative of curves corresponding to the images shown in Fig.7.4). Each point in the  $Nk$ -plane represents an image having values of  $N$  and  $k$  equal to the coordinates of that point.



**Fig.7.4 (a) Image with a low level of detail (b) Image with a medium level of detail (c) Image with a relatively large amount of detail**

Points lying on an isopreference curve correspond to images of equal subjective quality. It was found in the course of the experiments that the isopreference curves tended to shift right and upward, but their shapes in each of the three image categories were similar to those shown in

Fig. 7.5. This is not unexpected, since a shift up and right in the curves simply means larger values for  $N$  and  $k$ , which implies better picture quality.



**Fig.7.5. Representative isopreference curves for the three types of images in Fig.7.4**

The key point of interest in the context of the present discussion is that isopreference curves tend to become more vertical as the detail in the image increases. This result suggests that for images with a large amount of detail only a few gray levels may be needed. For example, the isopreference curve in Fig.7.5 corresponding to the crowd is nearly vertical. This indicates that, for a fixed value of  $N$ , the perceived quality for this type of image is nearly independent of the number of gray levels used. It is also of interest to note that perceived quality in the other two image categories remained the same in some intervals in which the spatial resolution was increased, but the number of gray levels actually decreased. The most likely reason for this result is that a decrease in  $k$  tends to increase the apparent contrast of an image, a visual effect that humans often perceive as improved quality in an image.

## 8. Explain about Aliasing and Moire patterns.

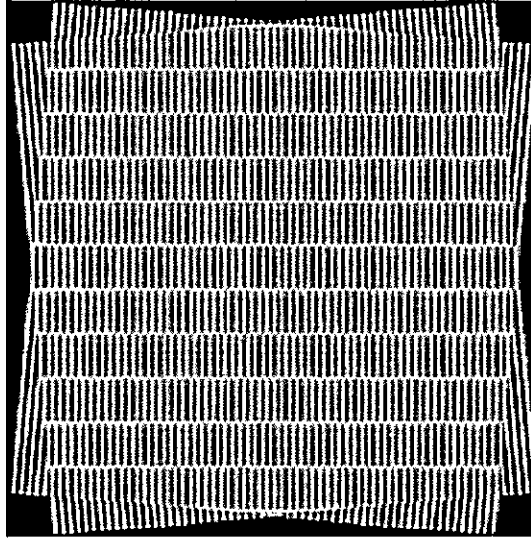
### Aliasing and Moiré Patterns:

Functions whose area under the curve is finite can be represented in terms of sines and cosines of various frequencies. The sine/cosine component with the highest frequency determines the highest "frequency content" of the function. Suppose that this highest frequency is finite and that the function is of unlimited duration (these functions are called band-limited functions). Then, the Shannon sampling theorem [Brace well (1995)] tells us that, if the function is sampled at a rate equal to or greater than twice its highest frequency, it is possible to recover completely the original function from its samples. If the function is undersampled, then a phenomenon called aliasing corrupts the sampled image. The corruption is in the form of additional frequency components being introduced into the sampled function. These are called aliased frequencies. Note that the sampling rate in images is the number of samples taken (in both spatial directions) per unit distance.

As it turns out, except for a special case discussed in the following paragraph, it is impossible to satisfy the sampling theorem in practice. We can only work with sampled data that are finite in duration. We can model the process of converting a function of unlimited duration into a function of finite duration simply by multiplying the unlimited function by a "gating function" that is valued 1 for some interval and 0 elsewhere. Unfortunately, this function itself has frequency components that extend to infinity. Thus, the very act of limiting the duration of a band-limited function causes it to cease being band limited, which causes it to violate the key condition of the sampling theorem. The principal approach for reducing the aliasing effects on an image is to reduce its high-frequency components by blurring the image prior to sampling. However, aliasing is always present in a sampled image. The effect of aliased frequencies can be seen under the right conditions in the form of so called Moiré patterns.

There is one special case of significant importance in which a function of infinite duration can be sampled over a finite interval without violating the sampling theorem. When a function is periodic, it may be sampled at a rate equal to or exceeding twice its highest frequency and it is possible to recover the function from its samples provided that the sampling captures exactly an integer number of periods of the function. This special case allows us to illustrate vividly the Moiré effect. Figure 8 shows two identical periodic patterns of equally spaced vertical bars, rotated in opposite directions and then superimposed on each other by multiplying the two images. A Moiré pattern, caused by a breakup of the periodicity, is seen in Fig.8 as a 2-D sinusoidal (aliased) waveform (which looks like a corrugated tin roof) running in a vertical direction. A similar pattern can appear when images are digitized (e.g., scanned) from a printed page, which consists of periodic ink dots.





**Fig.8. Illustration of the Moiré pattern effect**

**9. Explain about the basic relationships and distance measures between pixels in a digital image.**

**Neighbors of a Pixel:**

A pixel  $p$  at coordinates  $(x, y)$  has four horizontal and vertical neighbors whose coordinates are given by  $(x+1, y)$ ,  $(x-1, y)$ ,  $(x, y+1)$ ,  $(x, y-1)$ . This set of pixels, called the 4-neighbors of  $p$ , is denoted by  $N_4(p)$ . Each pixel is a unit distance from  $(x, y)$ , and some of the neighbors of  $p$  lie outside the digital image if  $(x, y)$  is on the border of the image.

The four diagonal neighbors of  $p$  have coordinates  $(x+1, y+1)$ ,  $(x+1, y-1)$ ,  $(x-1, y+1)$ ,  $(x-1, y-1)$  and are denoted by  $N_D(p)$ . These points, together with the 4-neighbors, are called the 8-neighbors of  $p$ , denoted by  $N_8(p)$ . As before, some of the points in  $N_D(p)$  and  $N_8(p)$  fall outside the image if  $(x, y)$  is on the border of the image.

**Connectivity:**

Connectivity between pixels is a fundamental concept that simplifies the definition of numerous digital image concepts, such as regions and boundaries. To establish if two pixels are connected, it must be determined if they are neighbors and if their gray levels satisfy a specified criterion of similarity (say, if their gray levels are equal). For instance, in a binary image with values 0 and 1, two pixels may be 4-neighbors, but they are said to be connected only if they have the same value.

Let  $V$  be the set of gray-level values used to define adjacency. In a binary image,  $V=\{1\}$  if we are referring to adjacency of pixels with value 1. In a grayscale image, the idea is the same, but set  $V$  typically contains more elements. For example, in the adjacency of pixels with a range of possible gray-level values 0 to 255, set  $V$  could be any subset of these 256 values. We consider three types of adjacency:

- (a) 4-adjacency. Two pixels  $p$  and  $q$  with values from  $V$  are 4-adjacent if  $q$  is in the set  $N_4(p)$ :
- (b) 8-adjacency. Two pixels  $p$  and  $q$  with values from  $V$  are 8-adjacent if  $q$  is in the set  $N_8(p)$ .
- (c) m-adjacency (mixed adjacency). Two pixels  $p$  and  $q$  with values from  $V$  are m-adjacent if
  - (i)  $q$  is in  $N_4(p)$ , or
  - (ii)  $q$  is in  $N_D(p)$  and the set has no pixels whose values are from  $V$ .

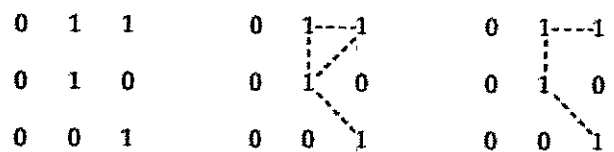
Mixed adjacency is a modification of 8-adjacency. It is introduced to eliminate the ambiguities that often arise when 8-adjacency is used. For example, consider the pixel arrangement shown in Fig.9 (a) for  $V= \{1\}$ . The three pixels at the top of Fig.9 (b) show multiple (ambiguous) 8-adjacency, as indicated by the dashed lines. This ambiguity is removed by using m-adjacency, as shown in Fig. 9 (c). Two image subsets  $S1$  and  $S2$  are adjacent if some pixel in  $S1$  is adjacent to some pixel in  $S2$ . It is understood here and in the following definitions that adjacent means 4-, 8-, or m-adjacent. A (digital) path (or curve) from pixel  $p$  with coordinates  $(x, y)$  to pixel  $q$  with coordinates  $(s, t)$  is a sequence of distinct pixels with coordinates

$$(x_0, y_0), (x_1, y_1), \dots, (x_n, y_n)$$

where  $(x_0, y_0) = (x, y)$ ,  $(x_n, y_n) = (s, t)$ , and pixels  $(x_i, y_i)$  and  $(x_{i-1}, y_{i-1})$  are adjacent for  $1 \leq i \leq n$ . In this case,  $n$  is the length of the path. If  $(x_0, y_0) = (x_n, y_n)$ , the path is a closed path. We can define 4-, 8-, or m-paths depending on the type of adjacency specified. For example, the paths shown in Fig. 9 (b) between the northeast and southeast points are 8-paths, and the path in Fig. 9 (c) is an m-path. Note the absence of ambiguity in the m-path. Let  $S$  represent a subset of pixels in an image. Two pixels  $p$  and  $q$  are said to be connected in  $S$  if there

exists a path between them consisting entirely of pixels in S. For any pixel p in S, the set of pixels that are connected to it in S is called a connected component of S. If it only has one connected component, then set S is called a connected set.

Let R be a subset of pixels in an image. We call R a region of the image if R is a connected set. The boundary (also called border or contour) of a region R is the set of pixels in the region that have one or more neighbors that are not in R. If R happens to be an entire image (which we recall is a rectangular set of pixels), then its boundary is defined as the set of pixels in the first and last rows and columns of the image. This extra definition is required because an image has no neighbors beyond its border. Normally, when we refer to a region, we are referring to a subset



**a b c**

**Fig.9 (a) Arrangement of pixels; (b) pixels that are 8-adjacent (shown dashed) to the center pixel; (c) m-adjacency**

of an image, and any pixels in the boundary of the region that happen to coincide with the border of the image are included implicitly as part of the region boundary.

**Distance Measures:**

For pixels p, q, and z, with coordinates (x, y), (s, t), and (v, w), respectively, D is a distance function or metric if

- (a)  $D(p, q) \geq 0$  ( $D(p, q) = 0$  iff  $p = q$ ),
- (b)  $D(p, q) = D(q, p)$ , and
- (c)  $D(p, z) \leq D(p, q) + D(q, z)$ .

The Euclidean distance between p and q is defined as

$$D_e(p, q) = [(x - s)^2 + (y - t)^2]^{\frac{1}{2}}$$

For this distance measure, the pixels having a distance less than or equal to some value  $r$  from  $(x, y)$  are the points contained in a disk of radius  $r$  centered at  $(x, y)$ .

The  $D_4$  distance (also called city-block distance) between  $p$  and  $q$  is defined as

$$D_4(p, q) = |x - s| + |y - t|.$$

In this case, the pixels having a  $D_4$  distance from  $(x, y)$  less than or equal to some value  $r$  form a diamond centered at  $(x, y)$ . For example, the pixels with  $D_4$  distance  $\leq 2$  from  $(x, y)$  (the center point) form the following contours of constant distance:

$$\begin{array}{ccccc} & & & & 2 \\ & & & & 2 & 1 & 2 \\ & & & 2 & 1 & 0 & 1 & 2 \\ & & & & 2 & 1 & 2 \\ & & & & & & & & 2 \end{array}$$

The pixels with  $D_4=1$  are the 4-neighbors of  $(x, y)$ .

The  $D_8$  distance (also called chessboard distance) between  $p$  and  $q$  is defined as

$$D_8(p, q) = \max(|x - s|, |y - t|).$$

In this case, the pixels with  $D_8$  distance from  $(x, y)$  less than or equal to some value  $r$  form a square centered at  $(x, y)$ . For example, the pixels with  $D_8$  distance  $\leq 2$  from  $(x, y)$  (the center point) form the following contours of constant distance:

$$\begin{array}{cccccc} 2 & 2 & 2 & 2 & 2 \\ 2 & 1 & 1 & 1 & 2 \\ 2 & 1 & 0 & 1 & 2 \\ 2 & 1 & 1 & 1 & 2 \\ 2 & 2 & 2 & 2 & 2 \end{array}$$

The pixels with  $D_8=1$  are the 8-neighbors of  $(x, y)$ . Note that the  $D_4$  and  $D_8$  distances between  $p$  and  $q$  are independent of any paths that might exist between the points because these distances involve only the coordinates of the points. If we elect to consider  $m$ -adjacency, however, the  $D_m$  distance between two points is defined as the shortest  $m$ -path between the points. In this case, the distance between two pixels will depend on the values of the pixels along the path, as well as the values of their neighbors. For instance, consider the following arrangement of pixels and assume that  $p, p_2$ , and  $p_4$  have value 1 and that  $p_1$  and  $p_3$  can have a value of 0 or 1:

$$\begin{array}{cc} & p_3 & p_4 \\ p_1 & & p_2 \\ p & & \end{array}$$

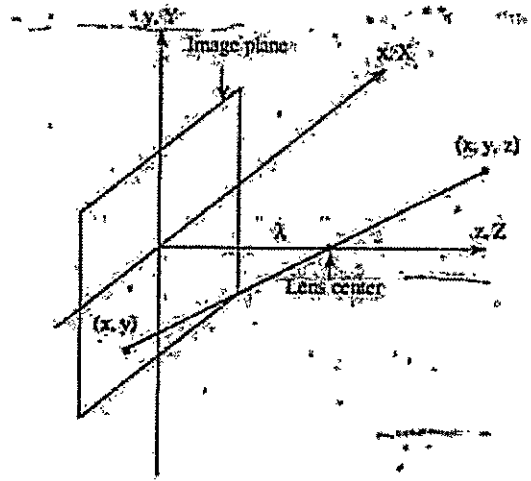
Suppose that we consider adjacency of pixels valued 1 (i.e. = {1}). If  $p_1$  and  $p_3$  are 0, the length of the shortest  $m$ -path (the  $D_m$  distance) between  $p$  and  $p_4$  is 2. If  $p_1$  is 1, then  $p_2$  and  $p$  will no longer be  $m$ -adjacent (see the definition of  $m$ -adjacency) and the length of the shortest  $m$ -path becomes 3 (the path goes through the points  $pp_1p_2p_4$ ). Similar comments apply if  $p_3$  is 1 (and  $p_1$  is 0); in this case, the length of the shortest  $m$ -path also is 3. Finally, if both  $p_1$  and  $p_3$  are 1 the length of the shortest  $m$ -path between  $p$  and  $p_4$  is 4. In this case, the path goes through the sequence of points  $pp_1p_2p_3p_4$ .

## 10. Write about perspective image transformation.

A perspective transformation (also called an imaging transformation) projects 3D points onto a plane. Perspective transformations play a central role in image processing because they provide an approximation to the manner in which an image is formed by viewing a 3D world. These transformations are fundamentally different, because they are nonlinear in that they involve division by coordinate values.

Figure 10 shows a model of the image formation process. The camera coordinate system  $(x, y, z)$  has the image plane coincident with the  $xy$  plane and the optical axis (established by the center of the lens) along the  $z$  axis. Thus the center of the image plane is at the origin, and the centre of the lens is at coordinates  $(0, 0, \lambda)$ . If the camera is in focus for distant objects,  $\lambda$  is the focal length of the lens. Here the assumption is that the camera coordinate system is aligned with the world coordinate system  $(X, Y, Z)$ .

Let  $(X, Y, Z)$  be the world coordinates of any point in a 3-D scene, as shown in the Fig. 10. We assume throughout the following discussion that  $Z > \lambda$ ; that is all points of interest lie in front of the lens. The first step is to obtain a relationship that gives the coordinates  $(x, y)$  of the projection of the point  $(X, Y, Z)$  onto the image plane. This is easily accomplished by the use of similar triangles. With reference to Fig. 10,



**Fig.10 Basic model of the imaging process** The camera coordinate system  $(x, y, z)$  is aligned with the world coordinate system  $(X, Y, Z)$

$$\frac{x}{\lambda} = -\frac{X}{Z - \lambda}$$

$$= \frac{X}{\lambda - Z}$$

$$\frac{y}{\lambda} = -\frac{Y}{Z - \lambda}$$

$$= \frac{Y}{\lambda - Z}$$

Where the negative signs in front of  $X$  and  $Y$  indicate that image points are actually inverted, as the geometry of Fig.10 shows.

The image-plane coordinates of the projected 3-D point follow directly from above equations

$$x = \frac{\lambda X}{\lambda - Z}$$

$$y = \frac{\lambda Y}{\lambda - Z}$$

These equations are nonlinear because they involve division by the variable Z. Although we could use them directly as shown, it is often convenient to express them in linear matrix form, for rotation, translation and scaling. This is easily accomplished by using homogeneous coordinates.

The homogeneous coordinates of a point with Cartesian coordinates (X, Y, Z) are defined as (kX, kY, kZ, k), where k is an arbitrary, nonzero constant. Clearly, conversion of homogeneous coordinates back to Cartesian coordinates is accomplished by dividing the first three homogeneous coordinates by the fourth. A point in the Cartesian world coordinate system may be expressed in vector form as

$$w = \begin{bmatrix} X \\ Y \\ Z \end{bmatrix}$$

and its homogeneous counterpart is

$$w_h = \begin{bmatrix} kX \\ kY \\ kZ \\ k \end{bmatrix}$$

If we define the perspective transformation matrix as

$$P = \begin{bmatrix} 1 & 0 & 0 & 0 \\ 0 & 1 & 0 & 0 \\ 0 & 0 & 1 & 0 \\ 0 & 0 & \frac{-1}{\lambda} & 1 \end{bmatrix}$$

The product  $Pw_h$  yields a vector denoted  $c_h$

$$\begin{aligned}
 c_h &= Pw_h \\
 &= \begin{bmatrix} 1 & 0 & 0 & 0 \\ 0 & 1 & 0 & 0 \\ 0 & 0 & 1 & 0 \\ 0 & 0 & \frac{-1}{\lambda} & 1 \end{bmatrix} \begin{bmatrix} kX \\ kY \\ kZ \\ k \end{bmatrix} \\
 &= \begin{bmatrix} kX \\ kY \\ kZ \\ \frac{-kZ}{\lambda} + k \end{bmatrix}
 \end{aligned}$$

The element of  $c_h$  is the camera coordinates in homogeneous form. As indicated, these coordinates can be converted to Cartesian form by dividing each of the first three components of  $c_h$  by the fourth. Thus the Cartesian of any point in the camera coordinate system are given in vector form by

$$c = \begin{bmatrix} x \\ y \\ z \end{bmatrix} = \begin{bmatrix} \frac{\lambda X}{\lambda - Z} \\ \frac{\lambda Y}{\lambda - Z} \\ \frac{\lambda Z}{\lambda - Z} \end{bmatrix}$$

The first two components of  $c$  are the  $(x, y)$  coordinates in the image plane of a projected 3-D point  $(X, Y, Z)$ . The third component is of no interest in terms of the model in Fig. 10. As shown next, this component acts as a free variable in the inverse perspective transformation

The inverse perspective transformation maps an image point back into 3-D.

$$w_h = P^{-1}c_h$$

Where  $P^{-1}$  is



$$P^{-1} = \begin{bmatrix} 1 & 0 & 0 & 0 \\ 0 & 1 & 0 & 0 \\ 0 & 0 & 1 & 0 \\ 0 & 0 & \frac{1}{\lambda} & 1 \end{bmatrix}$$

Suppose that an image point has coordinates  $(x_0, y_0, 0)$ , where the 0 in the z location simply indicates that the image plane is located at  $z = 0$ . This point may be expressed in homogeneous vector form as

$$c = \begin{bmatrix} kx_0 \\ ky_0 \\ 0 \\ k \end{bmatrix}$$

$$w = \begin{bmatrix} kx_0 \\ ky_0 \\ 0 \\ k \end{bmatrix}$$

or, in Cartesian coordinates

$$w = \begin{bmatrix} X \\ Y \\ Z \end{bmatrix} = \begin{bmatrix} x_0 \\ y_0 \\ 0 \end{bmatrix}$$

This result obviously is unexpected because it gives  $Z = 0$  for any 3-D point. The problem here is caused by mapping a 3-D scene onto the image plane, which is a many-to-one transformation. The image point  $(x_0, y_0)$  corresponds to the set of collinear 3-D points that lie on the line passing through  $(x_0, y_0, 0)$  and  $(0, 0, \lambda)$ . The equation of this line in the world coordinate system; that is,

$$X = \frac{x_0}{\lambda}(\lambda - Z)$$

$$Y = \frac{y_0}{\lambda}(\lambda - Z)$$

Equations above show that unless something is known about the 3-D point that generated an image point (for example, its Z coordinate) it is not possible to completely recover the 3-D point from its image. This observation, which certainly is not unexpected, can be used to formulate the inverse perspective transformation by using the z component of  $c_h$  as a free variable instead of 0. Thus, by letting

$$c_h = \begin{bmatrix} kx_0 \\ ky_0 \\ kz \\ k \end{bmatrix}$$

It thus follows

$$w_k = \begin{bmatrix} kx_0 \\ ky_0 \\ kz \\ \frac{kz}{\lambda} + k \end{bmatrix}$$

which upon conversion to Cartesian coordinate gives

$$w = \begin{bmatrix} X \\ Y \\ Z \end{bmatrix} = \begin{bmatrix} \frac{\lambda x_0}{\lambda + z} \\ \frac{\lambda y_0}{\lambda + z} \\ \frac{\lambda z}{\lambda + z} \end{bmatrix}$$

In other words, treating z as a free variable yields the equations

$$X = \frac{\lambda x_0}{\lambda + z}$$

$$Y = \frac{\lambda y_0}{\lambda + z}$$

$$Z = \frac{\lambda z}{\lambda + z}$$

Solving for  $z$  in terms of  $Z$  in the last equation and substituting in the first two expressions yields

$$X = \frac{x_0}{\lambda} (\lambda - Z)$$

$$Y = \frac{y_0}{\lambda} (\lambda - Z)$$

which agrees with the observation that revering a 3-D point from its image by means of the inverse perspective transformation requires knowledge of at least one of the world coordinates of the point.

1. Define Fourier Transform and its inverse.

Let  $f(x)$  be a continuous function of a real variable  $x$ . The Fourier transform of  $f(x)$  is defined by the equation

$$\mathcal{F}\{f(x)\} = F(u) = \int_{-\infty}^{\infty} f(x) \exp[-j2\pi ux] dx$$

Where  $j = \sqrt{-1}$

Given  $F(u)$ ,  $f(x)$  can be obtained by using the inverse Fourier transform

$$\begin{aligned} \mathcal{F}^{-1}\{F(u)\} &= f(x) \\ &= \int_{-\infty}^{\infty} F(u) \exp[j2\pi ux] du. \end{aligned}$$

The Fourier transform exists if  $f(x)$  is continuous and integrable and  $F(u)$  is integrable.

The Fourier transform of a real function, is generally complex,

$$F(u) = R(u) + jI(u)$$

Where  $R(u)$  and  $I(u)$  are the real and imaginary components of  $F(u)$ .  $F(u)$  can be expressed in exponential form as

$$F(u) = |F(u)| e^{j\phi(u)}$$

where

$$|F(u)| = [R^2(u) + I^2(u)]^{1/2}$$

and

$$\phi(u, v) = \tan^{-1}[I(u, v)/R(u, v)]$$

The magnitude function  $|F(u)|$  is called the Fourier Spectrum of  $f(x)$  and  $\phi(u)$  its phase angle.

The variable  $u$  appearing in the Fourier transform is called the frequency variable.

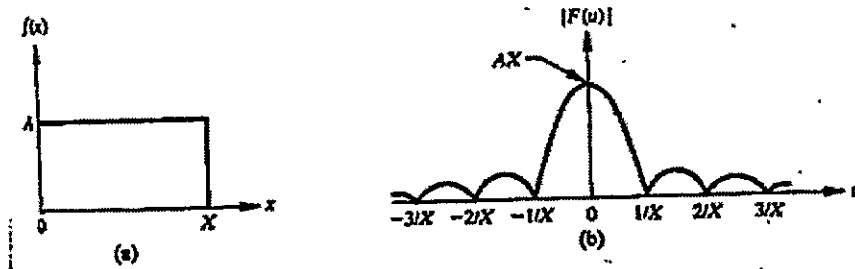


Fig 1 A simple function and its Fourier spectrum

The Fourier transform can be easily extended to a function  $f(x, y)$  of two variables. If  $f(x, y)$  is continuous and integrable and  $F(u, v)$  is integrable, following Fourier transform pair exists

$$\mathcal{F}\{f(x, y)\} = F(u, v) = \iint_{-\infty}^{\infty} f(x, y) \exp[-j2\pi(ux + vy)] dx dy$$

and

$$\mathcal{F}^{-1}\{F(u, v)\} = f(x, y) = \iint_{-\infty}^{\infty} F(u, v) \exp[j2\pi(ux + vy)] du dv$$

Where  $u, v$  are the frequency variables

The Fourier spectrum, phase, are

$$|F(u, v)| = [R^2(u, v) + I^2(u, v)]^{1/2}$$

$$\phi(u, v) = \tan^{-1} [I(u, v)/R(u, v)]$$

## 2. Define discrete Fourier transform and its inverse.

The discrete Fourier transform pair that applies to sampled function is given by,

$$F(u) = \frac{1}{N} \sum_{x=0}^{N-1} f(x) \exp[-j2\pi ux/N] \quad (1)$$

For  $u = 0, 1, 2, \dots, N-1$ , and

GRIET/ECE

$$f(x) = \sum_{u=0}^{N-1} F(u) \exp[j2\pi ux/N] \quad (2)$$

For  $x = 0, 1, 2, \dots, N-1$ .

In the two variable case the discrete Fourier transform pair is

$$F(u, v) = \frac{1}{MN} \sum_{x=0}^{M-1} \sum_{y=0}^{N-1} f(x, y) \exp[-j2\pi(ux/M + vy/N)]$$

For  $u = 0, 1, 2, \dots, M-1, v = 0, 1, 2, \dots, N-1$ , and

$$f(x, y) = \sum_{u=0}^{M-1} \sum_{v=0}^{N-1} F(u, v) \exp[j2\pi(ux/M + vy/N)]$$

For  $x = 0, 1, 2, \dots, M-1, y = 0, 1, 2, \dots, N-1$ .

If  $M = N$ , then discrete Fourier transform pair is

$$F(u, v) = \frac{1}{N} \sum_{x=0}^{N-1} \sum_{y=0}^{N-1} f(x, y) \exp[-j2\pi(ux + vy)/N]$$

For  $u, v = 0, 1, 2, \dots, N-1$ , and

$$f(x, y) = \frac{1}{N} \sum_{u=0}^{N-1} \sum_{v=0}^{N-1} F(u, v) \exp[j2\pi(ux + vy)/N]$$

For  $x, y = 0, 1, 2, \dots, N-1$

### 3. State and prove separability property of 2D-DFT.

The separability property of 2D-DFT states that, the discrete Fourier transform pair can be expressed in the separable forms. i.e. ,

$$F(u, v) = \frac{1}{N} \sum_{x=0}^{N-1} \exp[-j2\pi ux/N] \sum_{y=0}^{N-1} f(x, y) \exp[-j2\pi vy/N] \quad (1)$$

For  $u, v = 0, 1, 2, \dots, N-1$ , and

$$f(x, y) = \frac{1}{N} \sum_{u=0}^{N-1} \exp[j2\pi ux/N] \sum_{v=0}^{N-1} F(u, v) \exp[j2\pi vy/N] \quad (2)$$

For  $x, y = 0, 1, 2, \dots, N-1$

The principal advantage of the separability property is that  $F(u, v)$  or  $f(x, y)$  can be obtained in two steps by successive applications of the 1-D Fourier transform or its inverse. This advantage becomes evident if equation (1) is expressed in the form

$$F(u, v) = \frac{1}{N} \sum_{x=0}^{N-1} F(x, v) \exp[-j2\pi ux/N] \quad (3)$$

Where,

$$F(x, v) = N \left[ \frac{1}{N} \sum_{y=0}^{N-1} f(x, y) \exp[-j2\pi vy/N] \right] \quad (4)$$

For each value of  $x$ , the expression inside the brackets in eq(4) is a 1-D transform, with frequency values  $v = 0, 1, \dots, N-1$ . Therefore the 2-D function  $f(x, v)$  is obtained by taking a transform along each row of  $f(x, y)$  and multiplying the result by  $N$ . The desired result,  $F(u, v)$ , is then obtained by taking a transform along each column of  $F(x, v)$ , as indicated by eq(3)

#### 4. State and prove the translation property.

The translation properties of the Fourier transform pair are

$$f(x, y) \exp[j2\pi(u_0x + v_0y)/N] \Leftrightarrow F(u - u_0, v - v_0) \quad (1)$$

and





$$f(x - x_0, y - y_0) \Leftrightarrow F(u, v) \exp[-j2\pi(ux_0 + vy_0)/N] \quad (2)$$

Where the double arrow indicates the correspondence between a function and its Fourier Transform,

Equation (1) shows that multiplying  $f(x, y)$  by the indicated exponential term and taking the transform of the product results in a shift of the origin of the frequency plane to the point  $(u_0, v_0)$ .

Consider the equation (1) with  $u_0 = v_0 = N/2$  or

$$\begin{aligned} \exp[j2\pi(u_0x + v_0y)/N] &= e^{j\pi(x+y)} \\ &= (-1)^{x+y} \end{aligned}$$

and

$$f(x, y)(-1)^{x+y} \Leftrightarrow F(u - N/2, v - N/2)$$

Thus the origin of the Fourier transform of  $f(x, y)$  can be moved to the center of its corresponding  $N \times N$  frequency square simply by multiplying  $f(x, y)$  by  $(-1)^{x+y}$ . In the one variable case this shift reduces to multiplication of  $f(x)$  by the term  $(-1)^x$ . Note from equation (2) that a shift in  $f(x, y)$  does not affect the magnitude of its Fourier transform as,

$$|F(u, v) \exp[-j2\pi(ux_0 + vy_0)/N]| = |F(u, v)|;$$

#### 4. State distributivity and scaling property.

##### Distributivity:

From the definition of the continuous or discrete transform pair,

$$\mathcal{F}\{f_1(x, y) + f_2(x, y)\} = \mathcal{F}\{f_1(x, y)\} + \mathcal{F}\{f_2(x, y)\}$$

and, in general,

$$\mathcal{F}\{f_1(x, y) \cdot f_2(x, y)\} \neq \mathcal{F}\{f_1(x, y)\} \cdot \mathcal{F}\{f_2(x, y)\}.$$

In other words, the Fourier transform and its inverse are distributive over addition but not over multiplication.

**Scaling:**

For two scalars a and b,

$$af(x, y) \Leftrightarrow aF(u, v)$$

$$f(ax, by) \Leftrightarrow \frac{1}{|ab|} F(ua, vb).$$

**5. Explain the basic principle of Hotelling transform.**

**Hotelling transform:**

The basic principle of hotelling transform is the statistical properties of vector representation. Consider a population of random vectors of the form,

$$x = \begin{bmatrix} x_1 \\ x_2 \\ \vdots \\ x_n \end{bmatrix}$$

And the mean vector of the population is defined as the expected value of x i.e.,

$$m_x = E\{x\}$$

The suffix m represents that the mean is associated with the population of x vectors. The expected value of a vector or matrix is obtained by taking the expected value of each element. The covariance matrix  $C_x$  in terms of x and  $m_x$  is given as

$$C_x = E\{(x-m_x)(x-m_x)^T\}$$

T denotes the transpose operation. Since, x is n dimensional,  $\{(x-m_x)(x-m_x)^T\}$  will be of n x n dimension. The covariance matrix is real and symmetric. If elements  $x_i$  and  $x_j$  are uncorrelated, their covariance is zero and, therefore,  $c_{ij} = c_{ji} = 0$ .

For M vector samples from a random population, the mean vector and covariance matrix can be approximated from the samples by

$$m_x = \frac{1}{M} \sum_{i=1}^M x_i$$

and

$$C_x = \frac{1}{M} \sum_{i=1}^M x_i x_i^T - m_x m_x^T$$

6. Write about Slant transform.

The Slant transform matrix of order  $N \times N$  is the recursive expression  $S_N$  is given by

$$S_N = \frac{1}{\sqrt{2}} \begin{bmatrix} 1 & 0 & 0 & 1 & 0 & 0 \\ a_N & b_N & 0 & -a_N & b_N & 0 \\ 0 & I_{(N/2)-2} & 0 & I_{(N/2)-2} & 0 & 0 \\ 0 & 1 & 0 & 0 & -1 & 0 \\ -b_N & a_N & 0 & b_N & a_N & 0 \\ 0 & I_{(N/2)-2} & 0 & -I_{(N/2)-2} & 0 & 0 \end{bmatrix} \begin{bmatrix} S_{N/2} & 0 \\ 0 & S_{N/2} \end{bmatrix}$$

Where  $I_m$  is the identity matrix of order  $M \times M$ , and

$$S_2 = \frac{1}{\sqrt{2}} \begin{bmatrix} 1 & 1 \\ 1 & -1 \end{bmatrix}$$

The coefficients are

$$a_N = \left[ \frac{3N^2}{4(N^2 - 1)} \right]^{1/2}$$

and

GRIET/ECE

$$b_N = \left[ \frac{N^2 - 4}{4(N^2 - 1)} \right]^{1/2}$$

The slant transform for  $N = 4$  will be

$$S_4 = \frac{1}{\sqrt{4}} \begin{bmatrix} 1 & 1 & 1 & 1 \\ \frac{3}{\sqrt{5}} & \frac{1}{\sqrt{5}} & \frac{-1}{\sqrt{5}} & \frac{-3}{\sqrt{5}} \\ 1 & -1 & -1 & 1 \\ \frac{1}{\sqrt{5}} & \frac{-3}{\sqrt{5}} & \frac{3}{\sqrt{5}} & \frac{-1}{\sqrt{5}} \end{bmatrix}$$

7. What are the properties of Slant transform?

Properties of Slant transform

(i) The slant transform is real and orthogonal.

$$S = S^*$$

$$S^{-1} = S^T$$

(ii) The slant transform is fast, it can be implemented in  $(N \log_2 N)$  operations on an  $N \times 1$  vector.

(iii) The energy deal for images in this transform is rated in very good to excellent range.

(iv) The mean vectors for slant transform matrix  $S$  are not sequentially ordered for  $n \geq 3$ .

8. Define discrete cosine transform.

The 1-D discrete cosine transform is defined as

$$C(u) = \alpha(u) \sum_{x=0}^{N-1} f(x) \cos \left[ \frac{(2x+1)u\pi}{2N} \right]$$

For  $u = 0, 1, 2, \dots, N-1$ . Similarly the inverse DCT is defined as

GRIET/ECE

$$f(x) = \sum_{u=0}^{N-1} \alpha(u)G(y)\cos\left[\frac{(2x+1)u\pi}{2N}\right]$$

For  $u = 0, 1, 2, \dots, N-1$

Where  $\alpha$  is

$$\alpha(u) = \begin{cases} \sqrt{\frac{1}{N}} & \text{for } u = 0 \\ \sqrt{\frac{2}{N}} & \text{for } u = 1, 2, \dots, N-1. \end{cases}$$

The corresponding 2-D DCT pair is

$$C(u, v) = \alpha(u)\alpha(v) \sum_{x=0}^{N-1} \sum_{y=0}^{N-1} f(x, y) \cos\left[\frac{(2x+1)u\pi}{2N}\right] \cos\left[\frac{(2y+1)v\pi}{2N}\right]$$

For  $u, v = 0, 1, 2, \dots, N-1$ , and

$$f(x, y) = \sum_{u=0}^{N-1} \sum_{v=0}^{N-1} \alpha(u)\alpha(v)C(u, v) \cos\left[\frac{(2x+1)u\pi}{2N}\right] \cos\left[\frac{(2y+1)v\pi}{2N}\right]$$

For  $x, y = 0, 1, 2, \dots, N-1$

### 9. Explain about Haar transform.

The Haar transform is based on the Haar functions,  $h_k(z)$ , which are defined over the continuous, closed interval  $z \in [0, 1]$ , and for  $k = 0, 1, 2, \dots, N-1$ , where  $N = 2^n$ . The first step in generating the Haar transform is to note that the integer  $k$  can be decomposed uniquely as

$$k = 2^p + q - 1$$

where  $0 \leq p \leq n-1$ ,  $q = 0$  or  $1$  for  $p = 0$ , and  $1 \leq q \leq 2^p$  for  $p \neq 0$ . For example, if  $N = 4$ ,  $k, q, p$  have following values

k	p	q
0	0	0
1	0	1
2	1	1
3	1	2

The Haar functions are defined as

$$h_0(z) \triangleq h_{00}(z) = \frac{1}{\sqrt{N}} \text{ for } z \in [0, 1] \dots\dots (1)$$

and

$$h_1(z) \triangleq h_{11}(z) = \frac{1}{\sqrt{N}} \begin{cases} 2^{m/2} & \frac{q-1}{2^p} \leq z < \frac{q-1/2}{2^p} \\ -2^{m/2} & \frac{q-1/2}{2^p} \leq z < \frac{q}{2^p} \\ 0 & \text{otherwise for } z \in [0, 1] \end{cases}$$

These results allow derivation of Haar transformation matrices of order N x N by formation of the *i*th row of a Haar matrix from elements of  $h_i(z)$  for  $z = 0/N, 1/N, \dots, (N-1)/N$ . For instance, when N = 2, the first row of the 2 x 2 Haar matrix is computed by using  $h_0(z)$  with  $z = 0/2, 1/2$ . From equation (1),  $h_0(z)$  is equal to  $1/\sqrt{2}$ , independent of z, so the first row of the matrix has two identical  $1/\sqrt{2}$  elements. Similarly row is computed. The 2 x 2 Haar matrix is

$$A_2 = \frac{1}{\sqrt{2}} \begin{bmatrix} 1 & 1 \\ 1 & -1 \end{bmatrix}$$

Similarly matrix for N = 4 is

$$A_4 = \frac{1}{\sqrt{4}} \begin{bmatrix} 1 & 1 & 1 & 1 \\ 1 & 1 & -1 & -1 \\ \sqrt{2} & -\sqrt{2} & 0 & 0 \\ 0 & 0 & \sqrt{2} & -\sqrt{2} \end{bmatrix}$$

10. What are the properties of Haar transform.

**Properties of Haar transform:**

1. The Haar transform is real and orthogonal.
2. The Haar transform is very fast. It can implement  $O(n)$  operations on an  $N \times 1$  vector.
3. The mean vectors of the Haar matrix are sequentially ordered.
4. It has a poor energy deal for images.

**11. Write a short notes on Hadamard transform.**

1-D forward kernel for hadamard transform is

$$g(x, u) = \frac{1}{N} (-1)^{\sum_{i=0}^{n-1} b_i(x)b_i(u)}$$

Expression for the 1-D forward Hadamard transform is

$$H(u) = \frac{1}{N} \sum_{x=0}^{N-1} f(x) (-1)^{\sum_{i=0}^{n-1} b_i(x)b_i(u)}$$

Where  $N = 2^n$  and  $u$  has values in the range  $0, 1, \dots, N-1$ .

1-D inverse kernel for hadamard transform is

$$h(x, u) = (-1)^{\sum_{i=0}^{n-1} b_i(x)b_i(u)}$$

Expression for the 1-D inverse Hadamard transform is

$$f(x) = \sum_{u=0}^{N-1} H(u) (-1)^{\sum_{i=0}^{n-1} b_i(x)b_i(u)}$$

The 2-D kernels are given by the relations

$$g(x, y, u, v) = \frac{1}{N} (-1)^{\sum_{i=0}^{u-1} [b_1(x)b_1(u) + b_1(y)b_1(v)]}$$

and

$$h(x, y, u, v) = \frac{1}{N} (-1)^{\sum_{i=0}^{v-1} [b_1(x)b_1(u) + b_1(y)b_1(v)]}$$

2-D Hadamard transform pair is given by following equations

$$H(u, v) = \frac{1}{N} \sum_{x=0}^{N-1} \sum_{y=0}^{N-1} f(x, y) (-1)^{\sum_{i=0}^{u-1} [b_1(x)b_1(u) + b_1(y)b_1(v)]}$$

$$f(x, y) = \frac{1}{N} \sum_{u=0}^{N-1} \sum_{v=0}^{N-1} H(u, v) (-1)^{\sum_{i=0}^{v-1} [b_1(x)b_1(u) + b_1(y)b_1(v)]}$$

Values of the 1-D hadamard transform kernel for N = 8 is

$u \backslash x$	0	1	2	3	4	5	6	7
0	+	+	+	+	+	+	+	+
1	+	-	+	-	+	-	+	-
2	+	+	-	-	+	+	-	-
3	+	-	-	+	+	-	-	+
4	+	+	+	+	-	-	-	-
5	+	-	+	-	-	+	-	+
6	+	+	-	-	-	-	+	+
7	+	-	-	+	-	+	+	-

The Hadamard matrix of lowest order N = 2 is

$$H_2 = \begin{bmatrix} 1 & 1 \\ 1 & -1 \end{bmatrix}$$

If  $H_N$  represents the matrix of order N, the recursive relationship is given by

GRIET/ECE



$$H_{2N} = \begin{bmatrix} H_N & H_N \\ H_N & -H_N \end{bmatrix}$$

Where  $H_{2N}$  is the Hadamard matrix of order  $2N$  and  $N = 2^n$

12. Write about Walsh transform.

The discrete Walsh transform of a function  $f(x)$ , denoted  $W(u)$ , is given by

$$W(u) = \frac{1}{N} \sum_{x=0}^{N-1} f(x) \prod_{i=0}^{n-1} (-1)^{b_i(x)u_{i-1}-f_i(x)}$$

Walsh transform kernel is symmetric matrix having orthogonal rows and columns. These properties, which hold in general, lead to an inverse kernel given by

$$h(x, u) = \prod_{i=0}^{n-1} (-1)^{b_i(x)u_{i-1}-f_i(x)}$$

Thus the inverse Walsh transform is given by

$$f(x) = \sum_{u=0}^{N-1} W(u) \prod_{i=0}^{n-1} (-1)^{b_i(x)u_{i-1}-f_i(x)}$$

The 2-D forward and inverse Walsh kernels are given by

$$g(x, y, u, v) = \frac{1}{N} \prod_{i=0}^{n-1} (-1)^{[b_i(x)u_{i-1}-f_i(x) + b_i(y)v_{i-1}-f_i(y)]}$$

and

$$h(x, y, u, v) = \frac{1}{N} \prod_{i=0}^{n-1} (-1)^{[b_i(x)u_{i-1}-f_i(x) + b_i(y)v_{i-1}-f_i(y)]}$$

Thus the forward and inverse Walsh transforms for 2-D are given by

$$W(u, v) = \frac{1}{N} \sum_{x=0}^{N-1} \sum_{y=0}^{N-1} f(x, y) \prod_{i=0}^{n-1} (-1)^{[b_i(x)u_{i-1}-f_i(x) + b_i(y)v_{i-1}-f_i(y)]}$$

and

$$f(x, y) = \frac{1}{N} \sum_{u=0}^{N-1} \sum_{v=0}^{N-1} W(u, v) \prod_{i=0}^{N-1} (-1)^{b_i(x) \oplus_{i-1} \dots \oplus_{i-1} b_i(y) \oplus_{i-1} \dots \oplus_{i-1} b_i(x)}$$

The Walsh Transform kernels are separable and symmetric, because

$$\begin{aligned} g(x, y, u, v) &= g_1(x, u)g_2(y, v) \\ &= h_1(x, u)h_2(y, v) \\ &= \left[ \frac{1}{\sqrt{N}} \prod_{i=0}^{N-1} (-1)^{b_i(x) \oplus_{i-1} \dots \oplus_{i-1} b_i(u)} \right] \left[ \frac{1}{\sqrt{N}} \prod_{i=0}^{N-1} (-1)^{b_i(y) \oplus_{i-1} \dots \oplus_{i-1} b_i(v)} \right] \end{aligned}$$

Values of the 1-D walsh transform kernel for N = 8 is

u \ x	0	1	2	3	4	5	6	7
0	+	+	+	+	+	+	+	+
1	+	+	+	+	-	-	-	-
2	+	+	-	-	+	+	+	+
3	+	+	-	-	-	-	+	+
4	+	-	+	-	+	-	+	-
5	+	-	+	-	-	+	-	+
6	+	-	-	+	+	-	-	+
7	+	-	-	+	-	+	+	-

**1. What is meant by image enhancement by point processing? Discuss any two methods in it.**

**Basic Gray Level Transformations:**

The study of image enhancement techniques is done by discussing gray-level transformation functions. These are among the simplest of all image enhancement techniques. The values of pixels, before and after processing, will be denoted by  $r$  and  $s$ , respectively. As indicated in the previous section, these values are related by an expression of the form  $s=T(r)$ , where  $T$  is a transformation that maps a pixel value  $r$  into a pixel value  $s$ . Since we are dealing with digital quantities, values of the transformation function typically are stored in a one-dimensional array and the mappings from  $r$  to  $s$  are implemented via table lookups. For an 8-bit environment, a lookup table containing the values of  $T$  will have 256 entries. As an introduction to gray-level transformations, consider Fig. 1.1, which shows three basic types of functions used frequently for image enhancement: linear (negative and identity transformations), logarithmic (log and inverse-log transformations), and power-law ( $n$ th power and  $n$ th root transformations). The identity function is the trivial case in which output intensities are identical to input intensities. It is included in the graph only for completeness.

**Image Negatives:**

The negative of an image with gray levels in the range  $[0, L-1]$  is obtained by using the negative transformation shown in Fig. 1.1, which is given by the expression

$$s = L - 1 - r.$$

Reversing the intensity levels of an image in this manner produces the equivalent of a photographic negative. This type of processing is particularly suited for enhancing white or gray detail embedded in dark regions of an image, especially when the black areas are dominant in size.

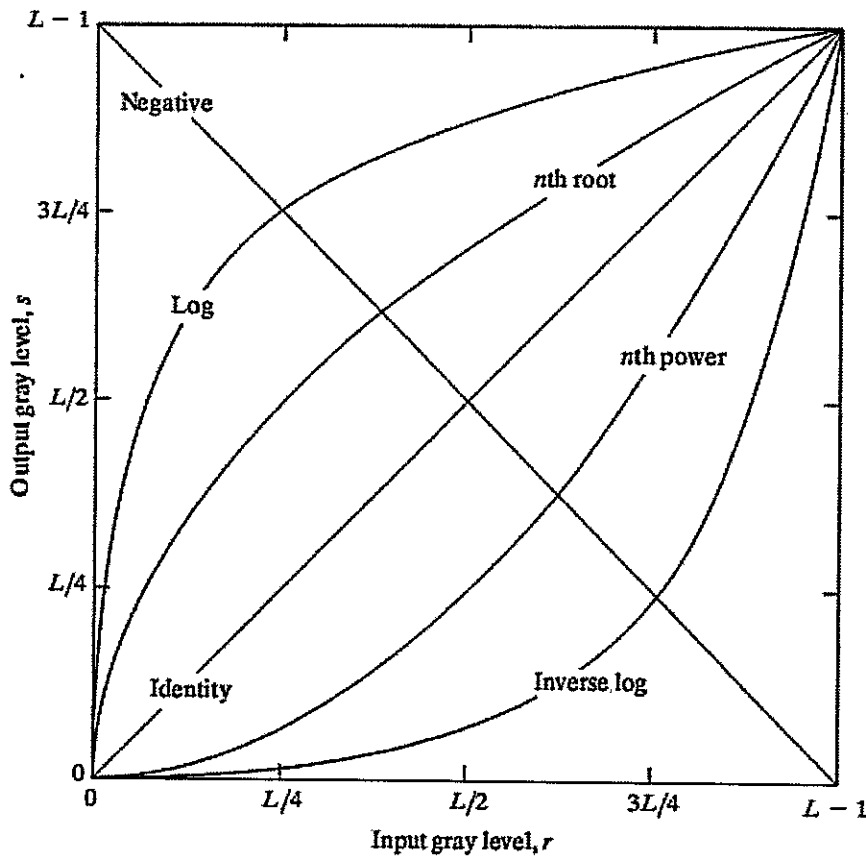


Fig.1.1 Some basic gray-level transformation functions used for image enhancement

**Log Transformations:**

The general form of the log transformation shown in Fig.1.1 is

$$s = c \log(1 + r)$$

where  $c$  is a constant, and it is assumed that  $r \geq 0$ . The shape of the log curve in Fig. 1.1 shows that this transformation maps a narrow range of low gray-level values in the input image into a wider range of output levels. The opposite is true of higher values of input levels. We would use a transformation of this type to expand the values of dark pixels in an image while compressing the higher-level values. The opposite is true of the inverse log transformation.

Any curve having the general shape of the log functions shown in Fig. 1.1 would accomplish this spreading/compressing of gray levels in an image. In fact, the power-law transformations discussed in the next section are much more versatile for this purpose than the log transformation. However, the log function has the important characteristic that it compresses the dynamic range of images with large variations in pixel values. A classic illustration of an application in which pixel values have a large dynamic range is the Fourier spectrum. At the moment, we are concerned only with the image characteristics of spectra. It is not unusual to encounter spectrum values that range from 0 to or higher. While processing numbers such as these presents no problems for a computer, image display systems generally will not be able to reproduce faithfully such a wide range of intensity values. The net effect is that a significant degree of detail will be lost in the display of a typical Fourier spectrum.

### Power-Law Transformations:

Power-law transformations have the basic form

$$s = cr^\gamma$$

where  $c$  and  $g$  are positive constants. Sometimes Eq. is written as  $s = c(r + \epsilon)^\gamma$

to account for an offset (that is, a measurable output when the input is zero). However, offsets typically are an issue of display calibration and as a result they are normally ignored in Eq. Plots of  $s$  versus  $r$  for various values of  $g$  are shown in Fig. 1.2. As in the case of the log transformation, power-law curves with fractional values of  $g$  map a narrow range of dark input values into a wider range of output values, with the opposite being true for higher values of input levels. Unlike the log function, however, we notice here a family of possible transformation curves obtained simply by varying  $\gamma$ . As expected, we see in Fig. 1.2 that curves generated with values of  $g > 1$  have exactly the opposite effect as those generated with values of  $g < 1$ . Finally, we note that Eq. reduces to the identity transformation when  $c = \gamma = 1$ . A variety of devices used for image capture, printing, and display respond according to a power law. By convention, the exponent in the power-law equation is referred to as gamma. The process used to correct this power-law response phenomena is called gamma correction. For example, cathode ray tube (CRT) devices have an intensity-to-voltage response that is a power function, with exponents varying from approximately 1.8 to 2.5. With reference to the curve for  $g=2.5$  in Fig. 1.2, we see that such display systems would tend to produce images that are darker than intended.

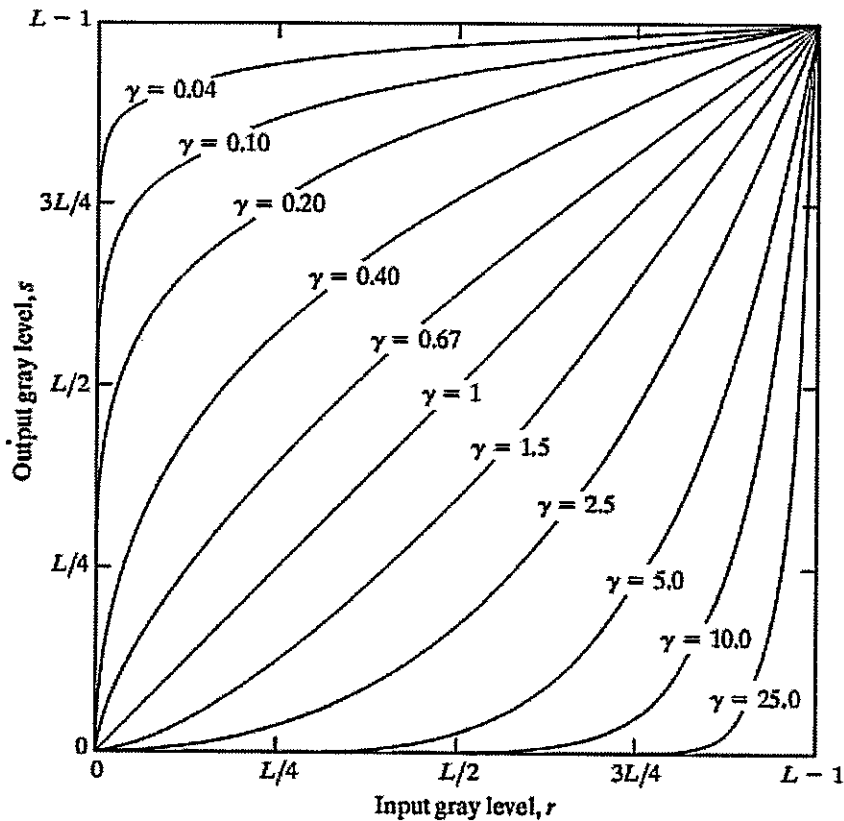


Fig.1.2 Plots of the equation  $s = cr^\gamma$  for various values of  $\gamma$  ( $c=1$  in all cases).

#### Piecewise-Linear Transformation Functions:

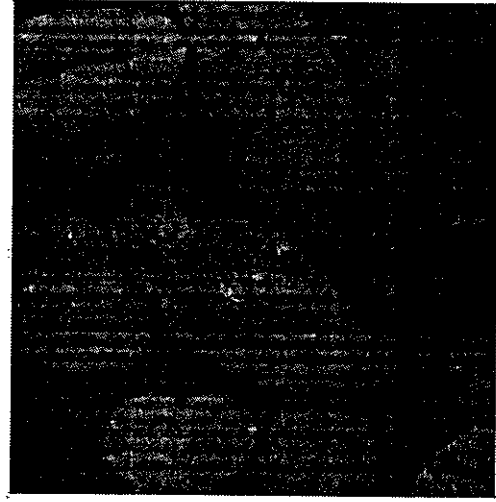
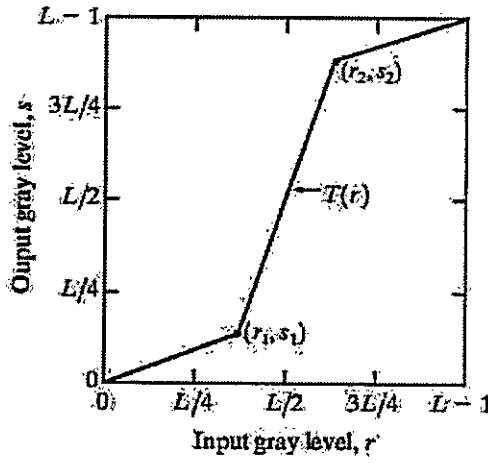
The principal advantage of piecewise linear functions over the types of functions we have discussed above is that the form of piecewise functions can be arbitrarily complex. In fact, as we will see shortly, a practical implementation of some important transformations can be formulated only as piecewise functions. The principal disadvantage of piecewise functions is that their specification requires considerably more user input.

**Contrast stretching:**

One of the simplest piecewise linear functions is a contrast-stretching transformation. Low-contrast images can result from poor illumination, lack of dynamic range in the imaging sensor, or even wrong setting of a lens aperture during image acquisition. The idea behind contrast stretching is to increase the dynamic range of the gray levels in the image being processed.

Figure 1.3 (a) shows a typical transformation used for contrast stretching.

The locations of points  $(r_1, s_1)$  and  $(r_2, s_2)$  control the shape of the transformation



**Fig.1.3 Contrast Stretching (a) Form of Transformation function (b) A low-contrast image (c) Result of contrast stretching (d) Result of thresholding.**

function. If  $r_1=s_1$  and  $r_2=s_2$ , the transformation is a linear function that produces no changes in gray levels. If  $r_1=r_2, s_1=0$  and  $s_2=L-1$ , the transformation becomes a thresholding function that creates a binary image, as illustrated in Fig. 1.3 (b). Intermediate values of  $(r_1, s_1)$  and  $(r_2, s_2)$  produce various degrees of spread in the gray levels of the output image, thus affecting its contrast. In general,  $r_1 \leq r_2$  and  $s_1 \leq s_2$  is assumed so that the function is single valued and monotonically increasing. This condition preserves the order of gray levels, thus preventing the creation of intensity artifacts in the processed image.

Figure 1.3 (b) shows an 8-bit image with low contrast. Fig. 1.3(c) shows the result of contrast stretching, obtained by setting  $(r_1, s_1) = (r_{\min}, 0)$  and  $(r_2, s_2) = (r_{\max}, L-1)$  where  $r_{\min}$  and  $r_{\max}$  denote the minimum and maximum gray levels in the image, respectively. Thus, the transformation function stretched the levels linearly from their original range to the full range  $[0, L-1]$ . Finally, Fig. 1.3 (d) shows the result of using the thresholding function defined previously, with  $r_1 = r_2 = m$ , the mean gray level in the image. The original image on which these results are based is a scanning electron microscope image of pollen, magnified approximately 700 times.

**Gray-level slicing:**

Highlighting a specific range of gray levels in an image often is desired. Applications include enhancing features such as masses of water in satellite imagery and enhancing flaws in X-ray images. There are several ways of doing level slicing, but most of them are variations of two basic themes. One approach is to display a high value for all gray levels in the range of interest and a low value for all other gray levels. This transformation, shown in Fig. 1.4 (a), produces a binary image. The second approach, based on the transformation shown in Fig. 1.4 (b), brightens the desired range of gray levels but preserves the background and gray-level tonalities in the image. Figure 1.4(c) shows a gray-scale image, and Fig. 1.4 (d) shows the result of using the transformation in Fig. 1.4 (a). Variations of the two transformations shown in Fig. 1.4 are easy to formulate.



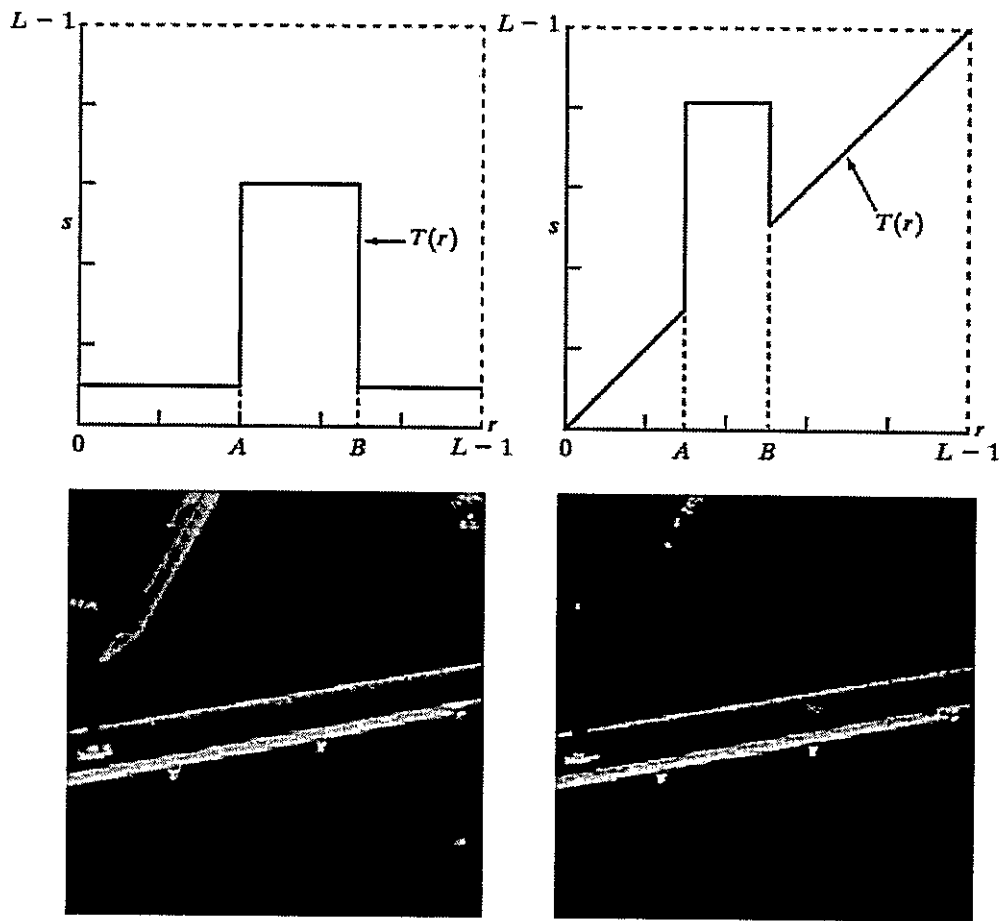


Fig.1.4 (a) This transformation highlights range [A, B] of gray levels and reduce all others to a constant level (b) This transformation highlights range [A, B] but preserves all other levels (c) An image (d) Result of using the transformation in (a).

**Bit-plane slicing:**

Instead of highlighting gray-level ranges, highlighting the contribution made to total image appearance by specific bits might be desired. Suppose that each pixel in an image is represented by 8 bits. Imagine that the image is composed of eight 1-bit planes, ranging from bit-plane 0 for the least significant bit to bit plane 7 for the most significant bit. In terms of 8-bit bytes, plane 0

contains all the lowest order bits in the bytes comprising the pixels in the image and plane 7 contains all the high-order bits. Figure 1.5 illustrates these ideas, and Fig. 1.7 shows the various bit planes for the image shown in Fig.1.6 . Note that the higher-order bits (especially the top four) contain the majority of the visually significant data. The other bit planes contribute to more subtle details in the image. Separating a digital image into its bit planes is useful for analyzing the relative importance played by each bit of the image, a process that aids in determining the adequacy of the number of bits used to quantize each pixel.

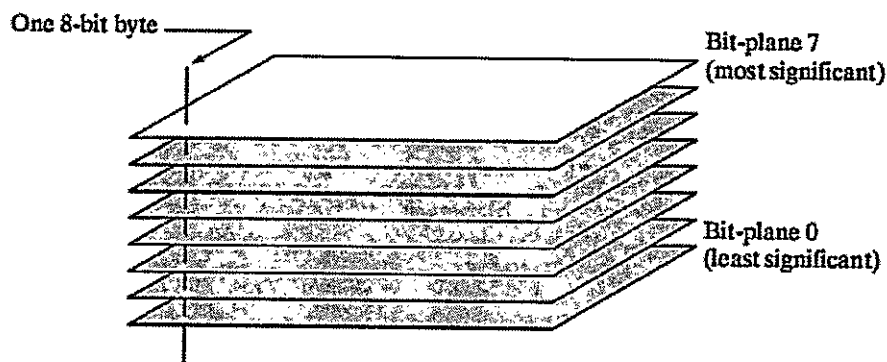
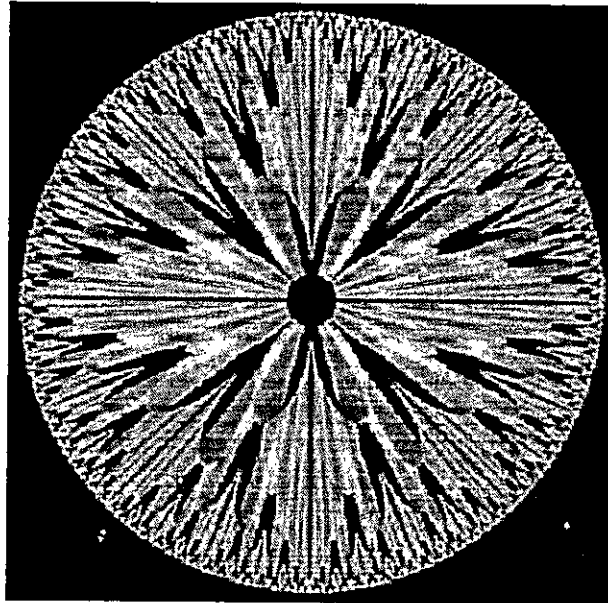


Fig.1.5 Bit-plane representation of an 8-bit image.

In terms of bit-plane extraction for an 8-bit image, it is not difficult to show that the (binary) image for bit-plane 7 can be obtained by processing the input image with a thresholding gray-level transformation function that (1) maps all levels in the image between 0 and 127 to one level (for example, 0); and (2) maps all levels between 129 and 255 to another (for example, 255).



**Fig.1.6 An 8-bit fractal image**

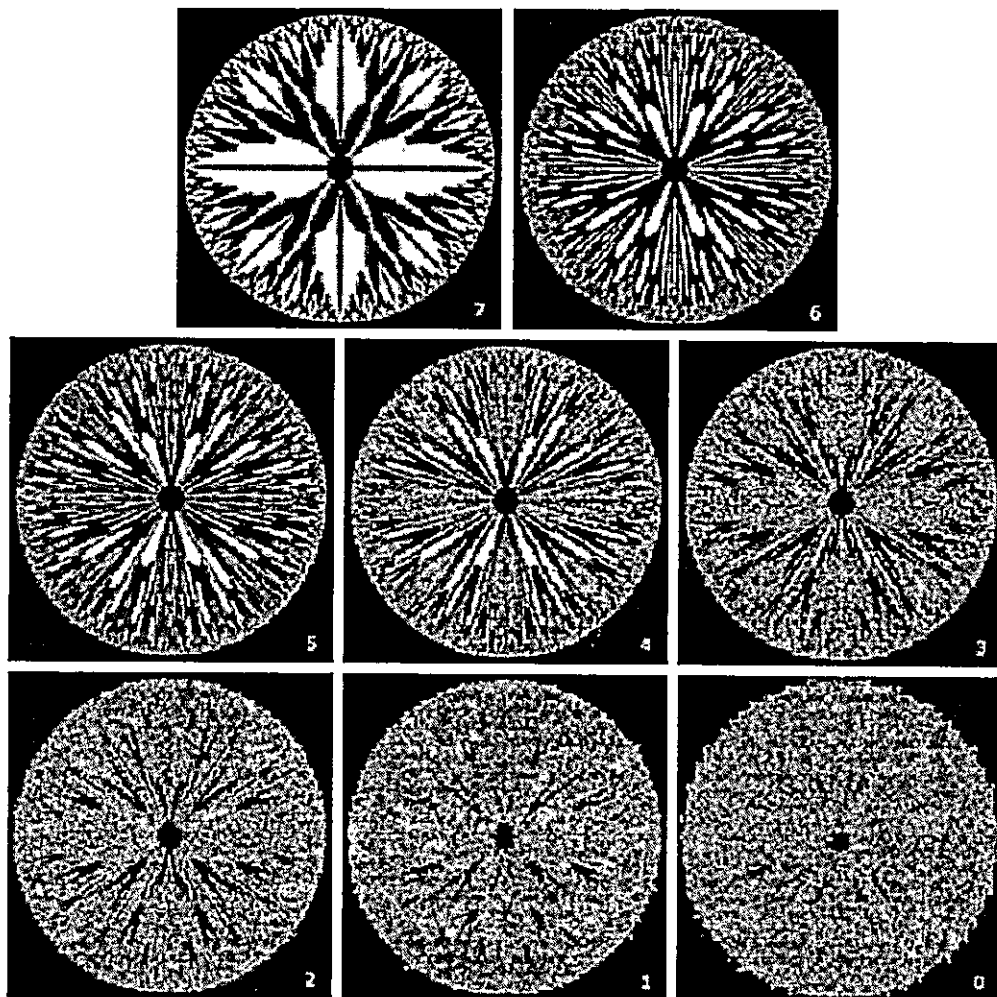


Fig.1.7 The eight bit planes of the image in Fig.1.6. The number at the bottom, right of each image identifies the bit plane.

**2. What is the objective of image enhancement. Define spatial domain. Define point processing.**

The term spatial domain refers to the aggregate of pixels composing an image. Spatial domain methods are procedures that operate directly on these pixels. Spatial domain processes will be denoted by the expression

$$g(x, y) = T[f(x, y)]$$

where  $f(x, y)$  is the input image,  $g(x, y)$  is the processed image, and  $T$  is an operator on  $f$ , defined over some neighborhood of  $(x, y)$ . In addition,  $T$  can operate on a set of input images, such as performing the pixel-by-pixel sum of  $K$  images for noise reduction.

The principal approach in defining a neighborhood about a point  $(x, y)$  is to use a square or rectangular subimage area centered at  $(x, y)$ , as Fig.2.1 shows. The center of the subimage is moved from pixel to pixel starting, say, at the top left corner. The operator  $T$  is applied at each location  $(x, y)$  to yield the output,  $g$ , at that location. The process utilizes only the pixels in the area of the image spanned by the neighborhood.

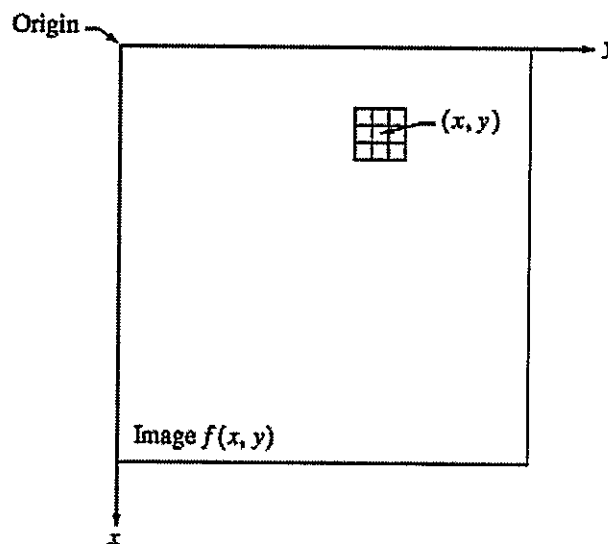


Fig.2.1 A 3\*3 neighborhood about a point  $(x, y)$  in an image.

Although other neighborhood shapes, such as approximations to a circle, sometimes are used, square and rectangular arrays are by far the most predominant because of their ease of implementation. The simplest form of  $T$  is when the neighborhood is of size  $1 \times 1$  (that is, a single pixel). In this case,  $g$  depends only on the value of  $f$  at  $(x, y)$ , and  $T$  becomes a gray-level (also called an intensity or mapping) transformation function of the form

$$s = T(r)$$

where, for simplicity in notation,  $r$  and  $s$  are variables denoting, respectively, the gray level of  $f(x, y)$  and  $g(x, y)$  at any point  $(x, y)$ . For example, if  $T(r)$  has the form shown in Fig. 2.2(a), the effect of this transformation would be to produce an image of higher contrast than the original by darkening the levels below  $m$  and brightening the levels above  $m$  in the original image. In this technique, known as contrast stretching, the values of  $r$  below  $m$  are compressed by the transformation function into a narrow range of  $s$ , toward black. The opposite effect takes place for values of  $r$  above  $m$ . In the limiting case shown in Fig. 2.2(b),  $T(r)$  produces a two-level (binary) image. A mapping of this form is called a thresholding function. Some fairly simple, yet powerful, processing approaches can be formulated with gray-level transformations. Because enhancement at any point in an image depends only on the gray level at that point, techniques in this category often are referred to as point processing.

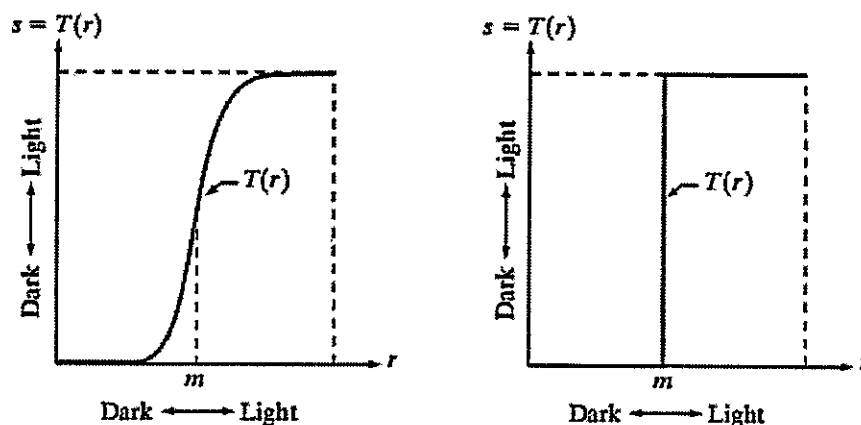


Fig.2.2 Graylevel transformation functions for contrast enhancement.

Larger neighborhoods allow considerably more flexibility. The general approach is to use a function of the values of  $f$  in a predefined neighborhood of  $(x, y)$  to determine the value of  $g$  at  $(x, y)$ . One of the principal approaches in this formulation is based on the use of so-called masks

(also referred to as filters, kernels, templates, or windows). Basically, a mask is a small (say, 3\*3) 2-D array, such as the one shown in Fig. 2.1, in which the values of the mask coefficients determine the nature of the process, such as image sharpening.

### 3. Define histogram of a digital image. Explain how histogram is useful in image enhancement?

#### Histogram Processing:

The histogram of a digital image with gray levels in the range  $[0, L-1]$  is a discrete function  $h(r_k) = n_k$ , where  $r_k$  is the  $k$ th gray level and  $n_k$  is the number of pixels in the image having gray level  $r_k$ . It is common practice to normalize a histogram by dividing each of its values by the total number of pixels in the image, denoted by  $n$ . Thus, a normalized histogram is given by

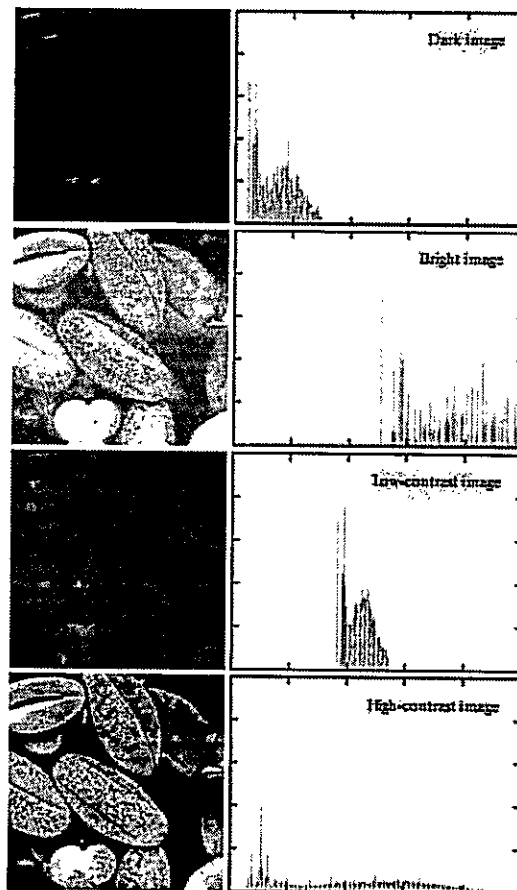
$$p(r_k) = n_k/n$$

for  $k=0,1,\dots,L-1$ . Loosely speaking,  $p(r_k)$  gives an estimate of the probability of occurrence of gray level  $r_k$ . Note that the sum of all components of a normalized histogram is equal to 1.

Histograms are the basis for numerous spatial domain processing techniques. Histogram manipulation can be used effectively for image enhancement. Histograms are simple to calculate in software and also lend themselves to economic hardware implementations, thus making them a popular tool for real-time image processing.

As an introduction to the role of histogram processing in image enhancement, consider Fig. 3, which is the pollen image shown in four basic gray-level characteristics: dark, light, low contrast, and high contrast. The right side of the figure shows the histograms corresponding to these images. The horizontal axis of each histogram plot corresponds to gray level values,  $r_k$ .

The vertical axis corresponds to values of  $h(r_k) = n_k$  or  $p(r_k) = n_k/n$  if the values are normalized. Thus, as indicated previously, these histogram plots are simply plots of  $h(r_k) = n_k$  versus  $r_k$  or  $p(r_k) = n_k/n$  versus  $r_k$ .



**Fig.3 Four basic image types: dark, light, low contrast, high contrast, and their corresponding histograms.**

We note in the dark image that the components of the histogram are concentrated on the low (dark) side of the gray scale. Similarly, the components of the histogram of the bright image are biased toward the high side of the gray scale. An image with low contrast has a histogram that will be narrow and will be centered toward the middle of the gray scale. For a monochrome image this implies a dull, washed-out gray look. Finally, we see that the components of the histogram in the high-contrast image cover a broad range of the gray scale and, further, that the distribution of pixels is not too far from uniform, with very few vertical lines being much higher than the others. Intuitively, it is reasonable to conclude that an image whose pixels tend to occupy the entire range of possible gray levels and, in addition, tend to be distributed uniformly, will have an appearance of high contrast and will exhibit a large variety of gray tones. The net effect will be an image that shows a great deal of gray-level detail and has high dynamic



range. It will be shown shortly that it is possible to develop a transformation function that can automatically achieve this effect, based only on information available in the histogram of the input image.

#### 4. Write about histogram equalization.

##### Histogram Equalization:

Consider for a moment continuous functions, and let the variable  $r$  represent the gray levels of the image to be enhanced. We assume that  $r$  has been normalized to the interval  $[0, 1]$ , with  $r=0$  representing black and  $r=1$  representing white. Later, we consider a discrete formulation and allow pixel values to be in the interval  $[0, L-1]$ . For any  $r$  satisfying the aforementioned conditions, we focus attention on transformations of the form

$$s = T(r) \quad 0 \leq r \leq 1$$

that produce a level  $s$  for every pixel value  $r$  in the original image. For reasons that will become obvious shortly, we assume that the transformation function  $T(r)$  satisfies the following conditions:

- (a)  $T(r)$  is single-valued and monotonically increasing in the interval  $0 \leq r \leq 1$ ; and
- (b)  $0 \leq T(r) \leq 1$  for  $0 \leq r \leq 1$ .

The requirement in (a) that  $T(r)$  be single valued is needed to guarantee that the inverse transformation will exist, and the monotonicity condition preserves the increasing order from black to white in the output image. A transformation function that is not monotonically increasing could result in at least a section of the intensity range being inverted, thus producing some inverted gray levels in the output image. Finally, condition (b) guarantees that the output gray levels will be in the same range as the input levels. Figure 4.1 gives an example of a transformation function that satisfies these two conditions. The inverse transformation from  $s$  back to  $r$  is denoted

$$r = T^{-1}(s) \quad 0 \leq s \leq 1.$$

It can be shown by example that even if  $T(r)$  satisfies conditions (a) and (b), it is possible that the corresponding inverse  $T^{-1}(s)$  may fail to be single valued.

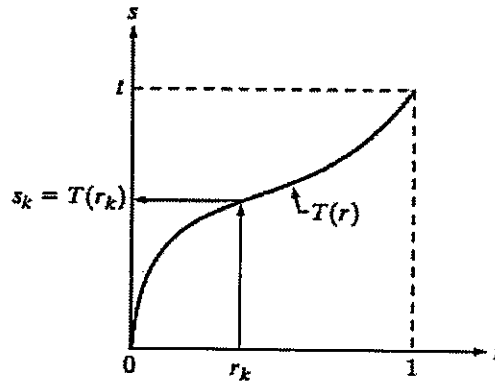


Fig.4.1 A gray-level transformation function that is both single valued and monotonically increasing.

The gray levels in an image may be viewed as random variables in the interval  $[0, 1]$ . One of the most fundamental descriptors of a random variable is its probability density function (PDF). Let  $p_r(r)$  and  $p_s(s)$  denote the probability density functions of random variables  $r$  and  $s$ , respectively, where the subscripts on  $p$  are used to denote that  $p_r$  and  $p_s$  are different functions. A basic result from an elementary probability theory is that, if  $p_r(r)$  and  $T(r)$  are known and  $T^{-1}(s)$  satisfies condition (a), then the probability density function  $p_s(s)$  of the transformed variable  $s$  can be obtained using a rather simple formula:

$$p_s(s) = p_r(r) \left| \frac{dr}{ds} \right|.$$

Thus, the probability density function of the transformed variable,  $s$ , is determined by the gray-level PDF of the input image and by the chosen transformation function. A transformation function of particular importance in image processing has the form

$$s = T(r) = \int_0^r p_r(w) dw$$

where  $w$  is a dummy variable of integration. The right side of Eq. above is recognized as the cumulative distribution function (CDF) of random variable  $r$ . Since probability density functions are always positive, and recalling that the integral of a function is the area under the function, it follows that this transformation function is single valued and monotonically increasing, and, therefore, satisfies condition (a). Similarly, the integral of a probability density function for variables in the range  $[0, 1]$  also is in the range  $[0, 1]$ , so condition (b) is satisfied as well.

Given transformation function  $T(r)$ , we find  $p_s(s)$  by applying Eq. We know from basic calculus (Leibniz's rule) that the derivative of a definite integral with respect to its upper limit is simply the integrand evaluated at that limit. In other words,

$$\begin{aligned}\frac{ds}{dr} &= \frac{dT(r)}{dr} \\ &= \frac{d}{dr} \left[ \int_0^r p_r(w) dw \right] \\ &= p_r(r).\end{aligned}$$

Substituting this result for  $dr/ds$ , and keeping in mind that all probability values are positive, yields

$$\begin{aligned}p_s(s) &= p_r(r) \left| \frac{dr}{ds} \right| \\ &= p_r(r) \left| \frac{1}{p_r(r)} \right| \\ &= 1 \quad 0 \leq s \leq 1.\end{aligned}$$

Because  $p_s(s)$  is a probability density function, it follows that it must be zero outside the interval  $[0, 1]$  in this case because its integral over all values of  $s$  must equal 1. We recognize the form of  $p_s(s)$  as a uniform probability density function. Simply stated, we have demonstrated that performing the transformation function yields a random variable  $s$  characterized by a uniform probability density function. It is important to note from Eq. discussed above that  $T(r)$  depends on  $p_r(r)$ , but, as indicated by Eq. after it, the resulting  $p_s(s)$  always is uniform, independent of the form of  $p_r(r)$ . For discrete values we deal with probabilities and summations instead of probability density functions and integrals. The probability of occurrence of gray level  $r$  in an image is approximated by

$$p_r(r_k) = \frac{n_k}{n} \quad k = 0, 1, 2, \dots, L - 1$$

where, as noted at the beginning of this section,  $n$  is the total number of pixels in the image,  $n_k$  is the number of pixels that have gray level  $r_k$ , and  $L$  is the total number of possible gray levels in the image. The discrete version of the transformation function given in Eq. is

$$\begin{aligned}s_k &= T(r_k) = \sum_{j=0}^k p_r(r_j) \\ &= \sum_{j=0}^k \frac{n_j}{n} \quad k = 0, 1, 2, \dots, L - 1.\end{aligned}$$

Thus, a processed (output) image is obtained by mapping each pixel with level  $r_k$  in the input image into a corresponding pixel with level  $s_k$  in the output image. As indicated earlier, a plot of  $p_r(r_k)$  versus  $r_k$  is called a histogram. The transformation (mapping) is called histogram equalization or histogram linearization. It is not difficult to show that the transformation in Eq. satisfies conditions (a) and (b) stated previously. Unlike its continuous counterpart, it cannot be proved in general that this discrete transformation will produce the discrete equivalent of a uniform probability density function, which would be a uniform histogram.

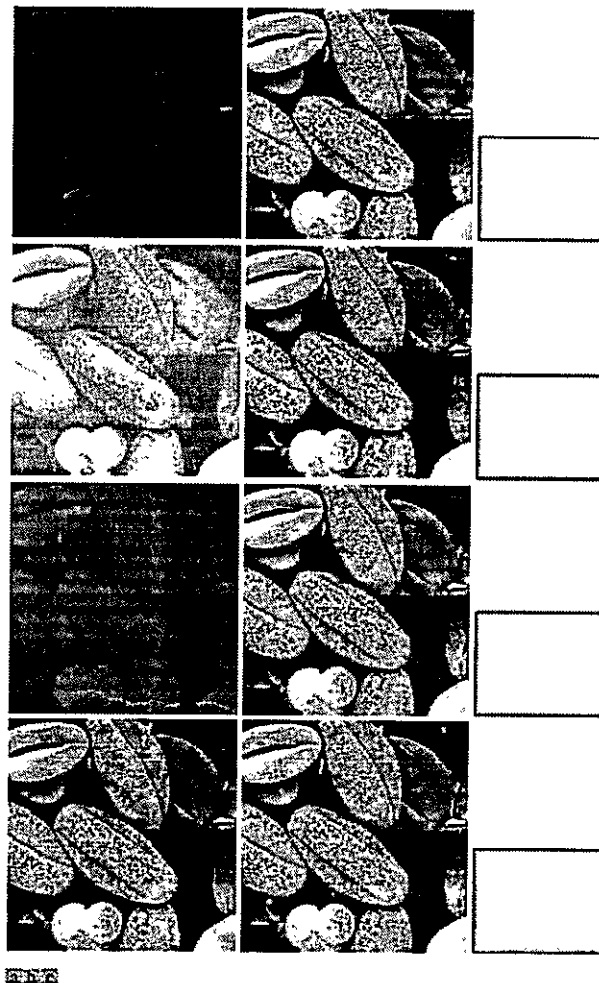


Fig.4.2 (a) Images from Fig.3 (b) Results of histogram equalization. (c) Corresponding histograms.

The inverse transformation from  $s$  back to  $r$  is denoted by

$$r_k = T^{-1}(s_k) \quad k = 0, 1, 2, \dots, L - 1$$

### 5. Write about histogram specification.

#### Histogram Matching (Specification):

Histogram equalization automatically determines a transformation function that seeks to produce an output image that has a uniform histogram. When automatic enhancement is desired, this is a good approach because the results from this technique are predictable and the method is simple to implement. In particular, it is useful sometimes to be able to specify the shape of the histogram that we wish the processed image to have. The method used to generate a processed image that has a specified histogram is called histogram matching or histogram specification.

#### Development of the method:

Let us return for a moment to continuous gray levels  $r$  and  $z$  (considered continuous random variables), and let  $p_r(r)$  and  $p_z(z)$  denote their corresponding continuous probability density functions. In this notation,  $r$  and  $z$  denote the gray levels of the input and output (processed) images, respectively. We can estimate  $p_r(r)$  from the given input image, while  $p_z(z)$  is the specified probability density function that we wish the output image to have.

Let  $s$  be a random variable with the property

$$s = T(r) = \int_0^r p_r(w) dw$$

$r \rightarrow s$   
map

where  $w$  is a dummy variable of integration. We recognize this expression as the continuous version of histogram equalization. Suppose next that we define a random variable  $z$  with the property

$$G(z) = \int_0^z p_z(t) dt = s$$

$z \rightarrow s$   
map

where  $t$  is a dummy variable of integration. It then follows from these two equations that  $G(z)=T(r)$  and, therefore, that  $z$  must satisfy the condition

$$z = G^{-1}(s) = G^{-1}[T(r)].$$

The transformation  $T(r)$  can be obtained once  $p_r(r)$  has been estimated from the input image. Similarly, the transformation function  $G(z)$  can be obtained because  $p_z(z)$  is given. Assuming that  $G^{-1}$  exists and that it satisfies conditions (a) and (b) in the histogram equalization process, the above three equations show that an image with a specified probability density function can be obtained from an input image by using the following procedure:

- (1) Obtain the transformation function  $T(r)$ .
- (2) To obtain the transformation function  $G(z)$ .
- (3) Obtain the inverse transformation function  $G^{-1}$ .
- (4) Obtain the output image by applying above Eq. to all the pixels in the input image.

The result of this procedure will be an image whose gray levels,  $z$ , have the specified probability density function  $p_z(z)$ . Although the procedure just described is straightforward in principle, it is seldom possible in practice to obtain analytical expressions for  $T(r)$  and for  $G^{-1}$ . Fortunately, this problem is simplified considerably in the case of discrete values. The price we pay is the same as in histogram equalization, where only an approximation to the desired histogram is achievable. In spite of this, however, some very useful results can be obtained even with crude approximations.

$$\begin{aligned} s_k &= T(r_k) = \sum_{j=0}^k p_r(r_j) \\ &= \sum_{j=0}^k \frac{n_j}{n} \quad k = 0, 1, 2, \dots, L - 1 \end{aligned}$$

where  $n$  is the total number of pixels in the image,  $n_j$  is the number of pixels with gray level  $r_j$ , and  $L$  is the number of discrete gray levels. Similarly, the discrete formulation is obtained from the given histogram  $p_z(z_i)$ ,  $i=0, 1, 2, \dots, L-1$ , and has the form

$$v_k = G(z_k) = \sum_{i=0}^k p_z(z_i) = s_k \quad k = 0, 1, 2, \dots, L - 1.$$

As in the continuous case, we are seeking values of  $z$  that satisfy this equation. The variable  $v_k$  was added here for clarity in the discussion that follows. Finally, the discrete version of the above Eqn. is given by

$$z_k = G^{-1}[T(r_k)] \quad k = 0, 1, 2, \dots, L - 1$$

Or

$$z_k = G^{-1}(s_k) \quad k = 0, 1, 2, \dots, L - 1.$$

**Implementation:**

We start by noting the following: (1) Each set of gray levels  $\{r_j\}$ ,  $\{s_j\}$ , and  $\{z_j\}$ ,  $j=0, 1, 2, \dots, L-1$ , is a one-dimensional array of dimension  $L \times 1$ . (2) All mappings from  $r$  to  $s$  and from  $s$  to  $z$  are simple table lookups between a given pixel value and these arrays. (3) Each of the elements of these arrays, for example,  $s_k$ , contains two important pieces of information: The subscript  $k$  denotes the location of the element in the array, and  $s$  denotes the value at that location. (4) We need to be concerned only with integer pixel values. For example, in the case of an 8-bit image,  $L=256$  and the elements of each of the arrays just mentioned are integers between 0 and 255. This implies that we now work with gray level values in the interval  $[0, L-1]$  instead of the normalized interval  $[0, 1]$  that we used before to simplify the development of histogram processing techniques.

In order to see how histogram matching actually can be implemented, consider Fig. 5(a), ignoring for a moment the connection shown between this figure and Fig. 5(c). Figure 5(a) shows a hypothetical discrete transformation function  $s=T(r)$  obtained from a given image. The first gray level in the image,  $r_1$ , maps to  $s_1$ ; the second gray level,  $r_2$ , maps to  $s_2$ ; the  $k$ th level  $r_k$  maps to  $s_k$ ; and so on (the important point here is the ordered correspondence between these values). Each value  $s_j$  in the array is precomputed, so the process of mapping simply uses the actual value of a pixel as an index in an array to determine the corresponding value of  $s$ . This process is particularly easy because we are dealing with integers. For example, the  $s$  mapping for an 8-bit pixel with value 127 would be found in the 128th position in array  $\{s_j\}$  (recall that we start at 0) out of the possible 256 positions. If we stopped here and mapped the value of each pixel of an input image by the

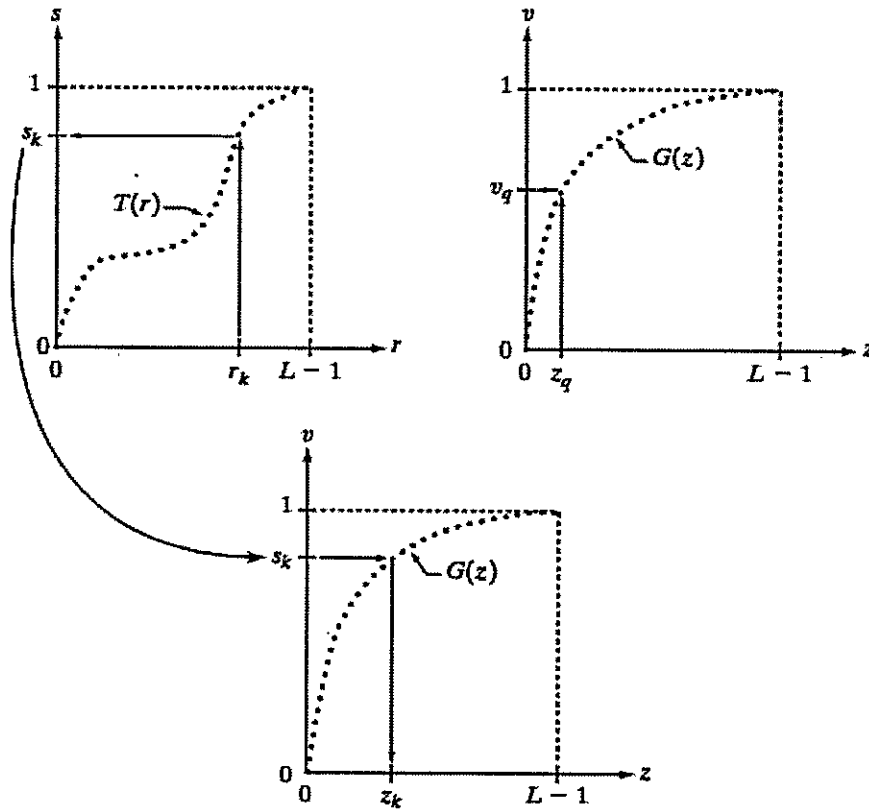


Fig.5. (a) Graphical interpretation of mapping from  $r_k$  to  $s_k$  via  $T(r)$ . (b) Mapping of  $z_q$  to its corresponding value  $v_q$  via  $G(z)$  (c) Inverse mapping from  $s_k$  to its corresponding value of  $z_k$ .

method just described, the output would be a histogram-equalized image. In order to implement histogram matching we have to go one step further. Figure 5(b) is a hypothetical transformation function  $G$  obtained from a given histogram  $p_z(z)$ . For any  $z_q$ , this transformation function yields a corresponding value  $v_q$ . This mapping is shown by the arrows in Fig. 5(b). Conversely, given any value  $v_q$ , we would find the corresponding value  $z_q$  from  $G^{-1}$ . In terms of the figure, all this means graphically is that we would reverse the direction of the arrows to map  $v_q$  into its corresponding  $z_q$ . However, we know from the definition that  $v=s$  for corresponding subscripts, so we can use exactly this process to find the  $z_k$  corresponding to any value  $s_k$  that we computed previously from the equation  $s_k = T(r_k)$ . This idea is shown in Fig.5(c).



Since we really do not have the  $z$ 's (recall that finding these values is precisely the objective of histogram matching), we must resort to some sort of iterative scheme to find  $z$  from  $s$ . The fact that we are dealing with integers makes this a particularly simple process. Basically, because  $v_k = s_k$ , we have that the  $z$ 's for which we are looking must satisfy the equation  $G(z_k) = s_k$ , or  $(G(z_k) - s_k) = 0$ . Thus, all we have to do to find the value of  $z_k$  corresponding to  $s_k$  is to iterate on values of  $z$  such that this equation is satisfied for  $k=0, 1, 2, \dots, L-1$ . We do not have to find the inverse of  $G$  because we are going to iterate on  $z$ . Since we are dealing with integers, the closest we can get to satisfying the equation  $(G(z_k) - s_k) = 0$  is to let  $z_k = \hat{z}$  for each value of  $k$ , where  $\hat{z}$  is the smallest integer in the interval  $[0, L-1]$  such that

$$(G(\hat{z}) - s_k) \geq 0 \quad k = 0, 1, 2, \dots, L - 1.$$

Given a value  $s_k$ , all this means conceptually in terms of Fig. 5(c) is that we would start with and increase it in integer steps until Eq. is satisfied, at which point we let repeating this process for all values of  $k$  would yield all the required mappings from  $s$  to  $z$ , which constitutes the implementation of Eq. In practice, we would not have to start with each time because the values of  $s_k$  are known to increase monotonically. Thus, for  $k=k+1$ , we would start with  $\hat{z} = z_k$  and increment in integer values from there.

## 6. Write about Local enhancement.

### Local Enhancement:

The histogram processing methods discussed in the previous two sections are global, in the sense that pixels are modified by a transformation function based on the gray-level content of an entire image. Although this global approach is suitable for overall enhancement, there are cases in which it is necessary to enhance details over small areas in an image. The number of pixels in these areas may have negligible influence on the computation of a global transformation whose shape does not necessarily guarantee the desired local enhancement. The solution is to devise transformation functions based on the gray-level distribution—or other properties—in the neighborhood of every pixel in the image.

The histogram processing techniques are easily adaptable to local enhancement. The procedure is to define a square or rectangular neighborhood and move the center of this area from pixel to pixel. At each location, the histogram of the points in the neighborhood is computed and either a histogram equalization or histogram specification transformation function is obtained. This function is finally used to map the gray level of the

pixel centered in the neighborhood. The center of the neighborhood region is then moved to an adjacent pixel location and the procedure is repeated. Since only one new row or column of the neighborhood changes during a pixel-to-pixel translation of the region, updating the histogram obtained in the previous location with the new data introduced at each motion step is possible. This approach has obvious advantages over repeatedly computing the histogram over all pixels in the neighborhood region each time the region is moved one pixel location. Another approach used some times to reduce computation is to utilize nonoverlapping regions, but this method usually produces an undesirable checkerboard effect.

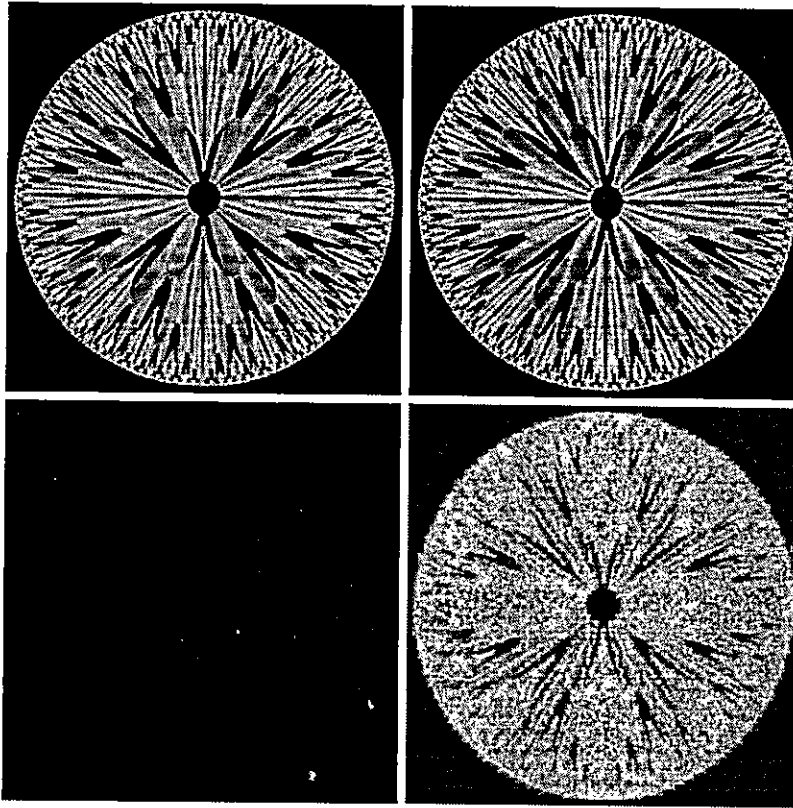
### 7. What is meant by image subtraction? Discuss various areas of application of image subtraction.

#### Image Subtraction:

The difference between two images  $f(x, y)$  and  $h(x, y)$ , expressed as

$$g(x, y) = f(x, y) - h(x, y),$$

is obtained by computing the difference between all pairs of corresponding pixels from  $f$  and  $h$ . The key usefulness of subtraction is the enhancement of differences between images. The higher-order bit planes of an image carry a significant amount of visually relevant detail, while the lower planes contribute more to fine (often imperceptible) detail. Figure 7(a) shows the fractal image used earlier to illustrate the concept of bit planes. Figure 7(b) shows the result of discarding (setting to zero) the four least significant bit planes of the original image. The images are nearly identical visually, with the exception of a very slight drop in overall contrast due to less variability of the graylevel values in the image of Fig. 7(b). The pixel-by-pixel difference between these two images is shown in Fig. 7(c). The differences in pixel values are so small that the difference image appears nearly black when displayed on an 8-bit display. In order to bring out more detail, we can perform a contrast stretching transformation. We chose histogram equalization, but an appropriate power-law transformation would have done the job also. The result is shown in Fig. 7(d). This is a very useful image for evaluating the effect of setting to zero the lower-order planes.



**Fig.7 (a) Original fractal image (b) Result of setting the four lower-order bit planes to zero (c) Difference between (a) and(b) (d) Histogram equalized difference image.**

One of the most commercially successful and beneficial uses of image subtraction is in the area of medical imaging called mask mode radiography. In this case  $h(x, y)$ , the mask, is an X-ray image of a region of a patient's body captured by an intensified TV camera (instead of traditional X-ray film) located opposite an X-ray source. The procedure consists of injecting a contrast medium into the patient's bloodstream, taking a series of images of the same anatomical region as  $h(x, y)$ , and subtracting this mask from the series of incoming images after injection of the contrast medium. The net effect of subtracting the mask from each sample in the incoming stream of TV images is that the areas that are different between  $f(x, y)$  and  $h(x, y)$  appear in the output image as enhanced detail. Because images can be captured at TV rates, this procedure in essence gives a movie showing how the contrast medium propagates through the various arteries in the area being observed.

**8. Explain about image averaging process.****Image Averaging:**

Consider a noisy image  $g(x, y)$  formed by the addition of noise  $h(x, y)$  to an original image  $f(x, y)$ ; that is,

$$g(x, y) = f(x, y) + \eta(x, y)$$

where the assumption is that at every pair of coordinates  $(x, y)$  the noise is uncorrelated and has zero average value. The objective of the following procedure is to reduce the noise content by adding a set of noisy images,  $\{g_i(x, y)\}$ . If the noise satisfies the constraints just stated, it can be shown that if an image  $\bar{g}(x, y)$  is formed by averaging  $K$  different noisy images,

$$\bar{g}(x, y) = \frac{1}{K} \sum_{i=1}^K g_i(x, y)$$

Then it follows that

$$E\{\bar{g}(x, y)\} = f(x, y)$$

and

$$\sigma_{\bar{g}(x, y)}^2 = \frac{1}{K} \sigma_{\eta(x, y)}^2$$

Where  $E\{\bar{g}(x, y)\}$  is the expected value of  $\bar{g}$  and  $\sigma_{\bar{g}(x, y)}^2$  and  $\sigma_{\eta(x, y)}^2$  are the variances of  $\bar{g}$  and  $\eta$ , all at coordinates  $(x, y)$ . The standard deviation at any point in the average image is

$$\sigma_{\bar{g}(x, y)} = \frac{1}{\sqrt{K}} \sigma_{\eta(x, y)}$$

As  $K$  increases, the above equations indicate that the variability (noise) of the pixel values at each location  $(x, y)$  decreases. Because  $E\{\bar{g}(x, y)\} = f(x, y)$ , this means that  $\bar{g}(x, y)$  approaches  $f(x, y)$  as the number of noisy images used in the averaging process increases. In practice, the images  $g_i(x, y)$  must be registered (aligned) in order to avoid the introduction of blurring and other artifacts in the output image.

**9. Discuss about the mechanics of filtering in spatial domain. Mention the points to be considered in implementation neighbourhood operations for spatial filtering.**

#### Basics of Spatial Filtering:

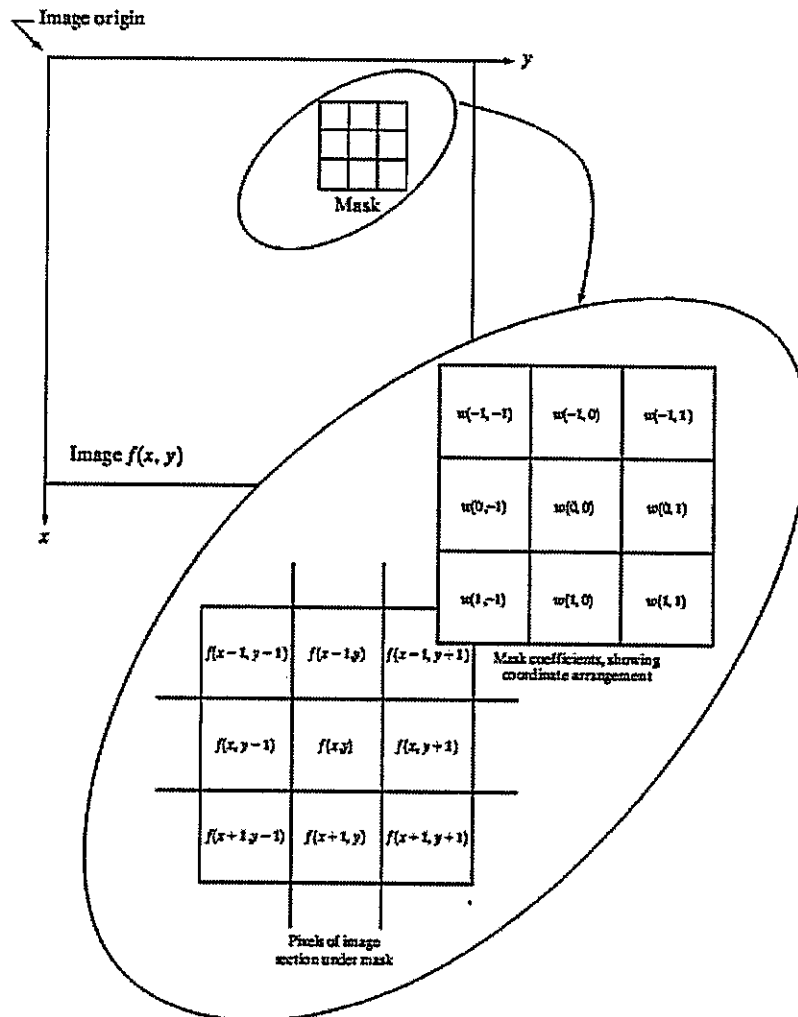
Some neighborhood operations work with the values of the image pixels in the neighborhood and the corresponding values of a subimage that has the same dimensions as the neighborhood. The subimage is called a filter, mask, kernel, template, or window, with the first three terms being the most prevalent terminology. The values in a filter subimage are referred to as coefficients, rather than pixels. The concept of filtering has its roots in the use of the Fourier transform for signal processing in the so-called frequency domain. We use the term spatial filtering to differentiate this type of process from the more traditional frequency domain filtering.

The mechanics of spatial filtering are illustrated in Fig.9.1. The process consists simply of moving the filter mask from point to point in an image. At each point  $(x, y)$ , the response of the filter at that point is calculated using a predefined relationship. The response is given by a sum of products of the filter coefficients and the corresponding image pixels in the area spanned by the filter mask. For the  $3 \times 3$  mask shown in Fig. 9.1, the result (or response),  $R$ , of linear filtering with the filter mask at a point  $(x, y)$  in the image is

$$R = w(-1, -1)f(x - 1, y - 1) + w(-1, 0)f(x - 1, y) + \dots \\ + w(0, 0)f(x, y) + \dots + w(1, 0)f(x + 1, y) + w(1, 1)f(x + 1, y + 1),$$

which we see is the sum of products of the mask coefficients with the corresponding pixels directly under the mask. Note in particular that the coefficient  $w(0, 0)$  coincides with image

value  $f(x, y)$ , indicating that the mask is centered at  $(x, y)$  when the computation of the sum of products takes place. For a mask of size  $m \times n$ , we assume that  $m=2a+1$  and  $n=2b+1$ , where  $a$  and  $b$  are nonnegative integers.



**Fig.9.1** The mechanics of spatial filtering. The magnified drawing shows a 3X3 mask and the image section directly under it; the image section is shown displaced out from under the mask for ease of readability.

In general, linear filtering of an image  $f$  of size  $M \times N$  with a filter mask of size  $m \times n$  is given by the expression:

$$g(x, y) = \sum_{s=-a}^a \sum_{t=-b}^b w(s, t) f(x + s, y + t)$$

where, from the previous paragraph,  $a=(m-1)/2$  and  $b=(n-1)/2$ . To generate a complete filtered image this equation must be applied for  $x=0,1,2,\dots,M-1$  and  $y=0,1,2,\dots,N-1$ . In this way, we are assured that the mask processes all pixels in the image. It is easily verified when  $m=n=3$  that this expression reduces to the example given in the previous paragraph.

The process of linear filtering is similar to a frequency domain concept called convolution. For this reason, linear spatial filtering often is referred to as "convolving a mask with an image." Similarly, filter masks are sometimes called convolution masks. The term convolution kernel also is in common use. When interest lies on the response,  $R$ , of an  $m \times n$  mask at any point  $(x,y)$ , and not on the mechanics of implementing mask convolution, it is common practice to simplify the notation by using the following expression:

$$\begin{aligned} R &= w_1 z_1 + w_2 z_2 + \dots + w_{mn} z_{mn} \\ &= \sum_{i=1}^{mn} w_i z_i \end{aligned}$$

where the  $w$ 's are mask coefficients, the  $z$ 's are the values of the image graylevels corresponding to those coefficients, and  $mn$  is the total number of coefficients in the mask. For the  $3 \times 3$  general mask shown in Fig.9.2 the response at any point  $(x, y)$  in the image is given by

$$\begin{aligned} R &= w_1 z_1 + w_2 z_2 + \dots + w_9 z_9 \\ &= \sum_{i=1}^9 w_i z_i \end{aligned}$$

$w_1$	$w_2$	$w_3$
$w_4$	$w_5$	$w_6$
$w_7$	$w_8$	$w_9$

**Fig.9.2 Another representation of a general 3 x 3 spatial filter mask.**

An important consideration in implementing neighborhood operations for spatial filtering is the issue of what happens when the center of the filter approaches the border of the image. Consider for simplicity a square mask of size  $n \times n$ . At least one edge of such a mask will coincide with the border of the image when the center of the mask is at a distance of  $(n-1)/2$  pixels away from the border of the image. If the center of the mask moves any closer to the border, one or more rows or columns of the mask will be located outside the image plane. There are several ways to handle this situation. The simplest is to limit the excursions of the center of the mask to be at a distance no less than  $(n-1)/2$  pixels from the border. The resulting filtered image will be smaller than the original, but all the pixels in the filtered image will have been processed with the full mask. If the result is required to be the same size as the original, then the approach typically employed is to filter all pixels only with the section of the mask that is fully contained in the image. With this approach, there will be bands of pixels near the border that will have been processed with a partial filter mask. Other approaches include "padding" the image by adding rows and columns of 0's (or other constant gray level), or padding by replicating rows or columns. The padding is then stripped off at the end of the process.

This keeps the size of the filtered image the same as the original, but the values of the padding will have an effect near the edges that becomes more prevalent as the size of the mask increases. The only way to obtain a perfectly filtered result is to accept a somewhat smaller filtered image by limiting the excursions of the center of the filter mask to a distance no less than  $(n-1)/2$  pixels from the border of the original image.

## 10. Write about Smoothing Spatial filters.

### Smoothing Spatial Filters:

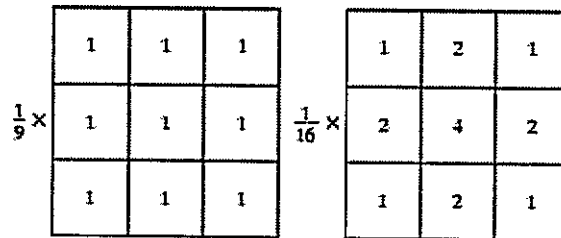
Smoothing filters are used for blurring and for noise reduction. Blurring is used in preprocessing steps, such as removal of small details from an image prior to (large) object extraction, and bridging of small gaps in lines or curves. Noise reduction can be accomplished by blurring with a linear filter and also by non-linear filtering.

#### (1) Smoothing Linear Filters:

The output (response) of a smoothing, linear spatial filter is simply the average of the pixels contained in the neighborhood of the filter mask. These filters sometimes are called averaging filters. The idea behind smoothing filters is straightforward. By replacing the value of every pixel



in an image by the average of the gray levels in the neighborhood defined by the filter mask, this process results in an image with reduced "sharp" transitions in gray levels. Because random noise typically consists of sharp transitions in gray levels, the most obvious application of smoothing is noise reduction. However, edges (which almost always are desirable features of an image) also are characterized by sharp transitions in gray levels, so averaging filters have the undesirable side effect that they blur edges. Another application of this type of process includes the smoothing of false contours that result from using an insufficient number of gray levels.



**Fig.10.1 Two 3 x 3 smoothing (averaging) filter masks. The constant multiplier in front of each mask is equal to the sum of the values of its coefficients, as is required to compute an average.**

A major use of averaging filters is in the reduction of "irrelevant" detail in an image. By "irrelevant" we mean pixel regions that are small with respect to the size of the filter mask.

Figure 10.1 shows two 3 x 3 smoothing filters. Use of the first filter yields the standard average of the pixels under the mask. This can best be seen by substituting the coefficients of the mask in

$$R = \frac{1}{9} \sum_{i=1}^9 z_i,$$

which is the average of the gray levels of the pixels in the 3 x 3 neighborhood defined by the mask. Note that, instead of being 1/9, the coefficients of the filter are all 1's. The idea here is that it is computationally more efficient to have coefficients valued 1. At the end of the filtering process the entire image is divided by 9. An m x n mask would have a normalizing constant equal to 1/mn.

A spatial averaging filter in which all coefficients are equal is sometimes called a box filter.

The second mask shown in Fig.10.1 is a little more interesting. This mask yields a so-called weighted average, terminology used to indicate that pixels are multiplied by different coefficients, thus giving more importance (weight) to some pixels at the expense of others. In the mask shown in Fig. 10.1(b) the pixel at the center of the mask is multiplied by a higher value than any other, thus giving this pixel more importance in the calculation of the average. The other pixels are inversely weighted as a function of their distance from the center of the mask. The diagonal terms are further away from the center than the orthogonal neighbors (by a factor of  $\sqrt{2}$ ) and, thus, are weighed less than these immediate neighbors of the center pixel. The basic strategy behind weighing the center point the highest and then reducing the value of the coefficients as a function of increasing distance from the origin is simply an attempt to reduce blurring in the smoothing process. We could have picked other weights to accomplish the same general objective. However, the sum of all the coefficients in the mask of Fig. 10.1(b) is equal to 16, an attractive feature for computer implementation because it has an integer power of 2. In practice, it is difficult in general to see differences between images smoothed by using either of the masks in Fig. 10.1, or similar arrangements, because the area these masks span at any one location in an image is so small.

The general implementation for filtering an  $M \times N$  image with a weighted averaging filter of size  $m \times n$  ( $m$  and  $n$  odd) is given by the expression

$$g(x, y) = \frac{\sum_{s=-a}^a \sum_{t=-b}^b w(s, t) f(x + s, y + t)}{\sum_{s=-a}^a \sum_{t=-b}^b w(s, t)}$$

## (2) Order-Statistics Filters:

Order-statistics filters are nonlinear spatial filters whose response is based on ordering (ranking) the pixels contained in the image area encompassed by the filter, and then replacing the value of the center pixel with the value determined by the ranking result. The best-known example in this category is the median filter, which, as its name implies, replaces the value of a pixel by the median of the gray levels in the neighborhood of that pixel (the original value of the pixel is included in the computation of the median). Median filters are quite popular because, for certain types of random noise, they provide excellent noise-reduction capabilities, with considerably less blurring than linear smoothing filters of similar size. Median filters are particularly effective in the presence of impulse noise, also called salt-and-pepper noise because of its appearance as white and black dots superimposed on an image.

The median,  $\epsilon$ , of a set of values is such that half the values in the set are less than or equal to  $\epsilon$ , and half are greater than or equal to  $\epsilon$ . In order to perform median filtering at a point in an image, we first sort the values of the pixel in question and its neighbors, determine their median, and

assign this value to that pixel. For example, in a 3 x 3 neighborhood the median is the 5th largest value, in a 5 x 5 neighborhood the 13th largest value, and so on. When several values in a neighborhood are the same, all equal values are grouped. For example, suppose that a 3 x 3 neighborhood has values (10, 20, 20, 20, 15, 20, 20, 25, 100). These values are sorted as (10, 15, 20, 20, 20, 20, 20, 25, 100), which results in a median of 20. Thus, the principal function of median filters is to force points with distinct gray levels to be more like their neighbors. In fact, isolated clusters of pixels that are light or dark with respect to their neighbors, and whose area is less than  $n^2/2$  (one-half the filter area), are eliminated by an  $n \times n$  median filter. In this case "eliminated" means forced to the median intensity of the neighbors. Larger clusters are affected considerably less.

**11. What is meant by the Gradient and the Laplacian? Discuss their role in image enhancement.**

**Use of Second Derivatives for Enhancement—The Laplacian:**

The approach basically consists of defining a discrete formulation of the second-order derivative and then constructing a filter mask based on that formulation. We are interested in isotropic filters, whose response is independent of the direction of the discontinuities in the image to which the filter is applied. In other words, isotropic filters are rotation invariant, in the sense that rotating the image and then applying the filter gives the same result as applying the filter to the image first and then rotating the result.

**Development of the method:**

It can be shown (Rosenfeld and Kak [1982]) that the simplest isotropic derivative operator is the Laplacian, which, for a function (image)  $f(x, y)$  of two variables, is defined as

$$\nabla^2 f = \frac{\partial^2 f}{\partial x^2} + \frac{\partial^2 f}{\partial y^2}.$$

Because derivatives of any order are linear operations, the Laplacian is a linear operator. In order to be useful for digital image processing, this equation needs to be expressed in discrete form. There are several ways to define a digital Laplacian using neighborhoods. digital second. Taking into account that we now have two variables, we use the following notation for the partial second-order derivative in the x-direction:

$$\frac{\partial^2 f}{\partial x^2} = f(x + 1, y) + f(x - 1, y) - 2f(x, y)$$

and, similarly in the y-direction, as

$$\frac{\partial^2 f}{\partial y^2} = f(x, y + 1) + f(x, y - 1) - 2f(x, y)$$

The digital implementation of the two-dimensional Laplacian in Eq. is obtained by summing these two components

$$\nabla^2 f = [f(x + 1, y) + f(x - 1, y) + f(x, y + 1) + f(x, y - 1)] - 4f(x, y). \quad ($$

This equation can be implemented using the mask shown in Fig.11.1(a), which gives an isotropic result for rotations in increments of 90°.

The diagonal directions can be incorporated in the definition of the digital Laplacian by adding two more terms to Eq., one for each of the two diagonal directions. The form of each new term is the same as either Eq.

0	1	0	1	1	1
1	-4	1	1	-8	1
0	1	0	1	1	1
0	-1	0	-1	-1	-1
-1	4	-1	-1	8	-1
0	-1	0	-1	-1	-1

a	b
c	d

**Fig.11.1. (a) Filter mask used to implement the digital Laplacian (b) Mask used to implement an extension of this equation that includes the diagonal neighbors. (c) and (d) Two other implementations of the Laplacian.**

but the coordinates are along the diagonals. Since each diagonal term also contains a  $-2f(x, y)$  term, the total subtracted from the difference terms now would be  $-8f(x, y)$ . The mask used to implement this new definition is shown in Fig.11.1(b). This mask yields isotropic results for increments of  $45^\circ$ . The other two masks shown in Fig. 11 also are used frequently in practice.

They are based on a definition of the Laplacian that is the negative of the one we used here. As such, they yield equivalent results, but the difference in sign must be kept in mind when combining (by addition or subtraction) a Laplacian-filtered image with another image.

Because the Laplacian is a derivative operator, its use highlights gray-level discontinuities in an image and deemphasizes regions with slowly varying gray levels. This will tend to produce images that have grayish edge lines and other discontinuities, all superimposed on a dark, featureless background. Background features can be "recovered" while still preserving the sharpening effect of the Laplacian operation simply by adding the original and Laplacian images. As noted in the previous paragraph, it is important to keep in mind which definition of the Laplacian is used. If the definition used has a negative center coefficient, then we subtract, rather

than add, the Laplacian image to obtain a sharpened result. Thus, the basic way in which we use the Laplacian for image enhancement is as follows:

$$g(x, y) = \begin{cases} f(x, y) - \nabla^2 f(x, y) & \text{if the center coefficient of the} \\ & \text{Laplacian mask is negative} \\ f(x, y) + \nabla^2 f(x, y) & \text{if the center coefficient of the} \\ & \text{Laplacian mask is positive.} \end{cases}$$

#### Use of First Derivatives for Enhancement—The Gradient:

First derivatives in image processing are implemented using the magnitude of the gradient. For a function  $f(x, y)$ , the gradient of  $f$  at coordinates  $(x, y)$  is defined as the two-dimensional column vector

$$\nabla f = \begin{bmatrix} G_x \\ G_y \end{bmatrix} = \begin{bmatrix} \frac{\partial f}{\partial x} \\ \frac{\partial f}{\partial y} \end{bmatrix}.$$

The magnitude of this vector is given by

$$\begin{aligned} \nabla f &= \text{mag}(\nabla f) \\ &= [G_x^2 + G_y^2]^{1/2} \\ &= \left[ \left( \frac{\partial f}{\partial x} \right)^2 + \left( \frac{\partial f}{\partial y} \right)^2 \right]^{1/2}. \end{aligned}$$

The components of the gradient vector itself are linear operators, but the magnitude of this vector obviously is not because of the squaring and square root operations. On the other hand, the partial derivatives are not rotation invariant (isotropic), but the magnitude of the gradient vector is. Although it is not strictly correct, the magnitude of the gradient vector often is referred to as the gradient.

The computational burden of implementing over an entire image is not trivial, and it is common practice to approximate the magnitude of the gradient by using absolute values instead of squares and square roots:

$$\nabla f \approx |G_x| + |G_y|.$$

This equation is simpler to compute and it still preserves relative changes in gray levels, but the isotropic feature property is lost in general. However, as in the case of the Laplacian, the isotropic properties of the digital gradient defined in the following paragraph are preserved only for a limited number of rotational increments that depend on the masks used to approximate the derivatives. As it turns out, the most popular masks used to approximate the gradient give the same result only for vertical and horizontal edges and thus the isotropic properties of the gradient are preserved only for multiples of  $90^\circ$ .

As in the case of the Laplacian, we now define digital approximations to the preceding equations, and from there formulate the appropriate filter masks. In order to simplify the discussion that follows, we will use the notation in Fig. 11.2 (a) to denote image points in a  $3 \times 3$  region. For example, the center point,  $z_5$ , denotes  $f(x, y)$ ,  $z_1$  denotes  $f(x-1, y-1)$ , and so on. The simplest approximations to a first-order derivative that satisfy the conditions stated in that section are  $G_x = (z_8 - z_5)$  and  $G_y = (z_6 - z_5)$ . Two other definitions proposed by Roberts [1965] in the early development of digital image processing use cross differences:

$$G_x = (z_9 - z_5) \quad \text{and} \quad G_y = (z_8 - z_6).$$

we compute the gradient as

$$\nabla f = [(z_9 - z_5)^2 + (z_8 - z_6)^2]^{1/2}$$

If we use absolute values, then substituting the quantities in the equations gives us the following approximation to the gradient:

$$\nabla f \approx |z_9 - z_5| + |z_8 - z_6|.$$

This equation can be implemented with the two masks shown in Figs. 11.2 (b) and (c). These masks are referred to as the Roberts cross-gradient operators. Masks of even size are awkward to implement. The smallest filter mask in which we are interested is of size  $3 \times 3$ . An approximation using absolute values, still at point  $z_5$ , but using a  $3 \times 3$  mask, is

$$\nabla f \approx |(z_7 + 2z_8 + z_9) - (z_1 + 2z_2 + z_3)| \\ + |(z_3 + 2z_6 + z_9) - (z_1 + 2z_4 + z_7)|.$$

The difference between the third and first rows of the 3 x 3 image region approximates the derivative in the x-direction, and the difference between the third and first columns approximates the derivative in the y-direction. The masks shown in Figs. 11.2 (d) and (e), called the Sobel operators. The idea behind using a weight value of 2 is to achieve some smoothing by giving more importance to the center point. Note that the coefficients in all the masks shown in Fig. 11.2 sum to 0, indicating that they would give a response of 0 in an area of constant gray level, as expected of a derivative operator.

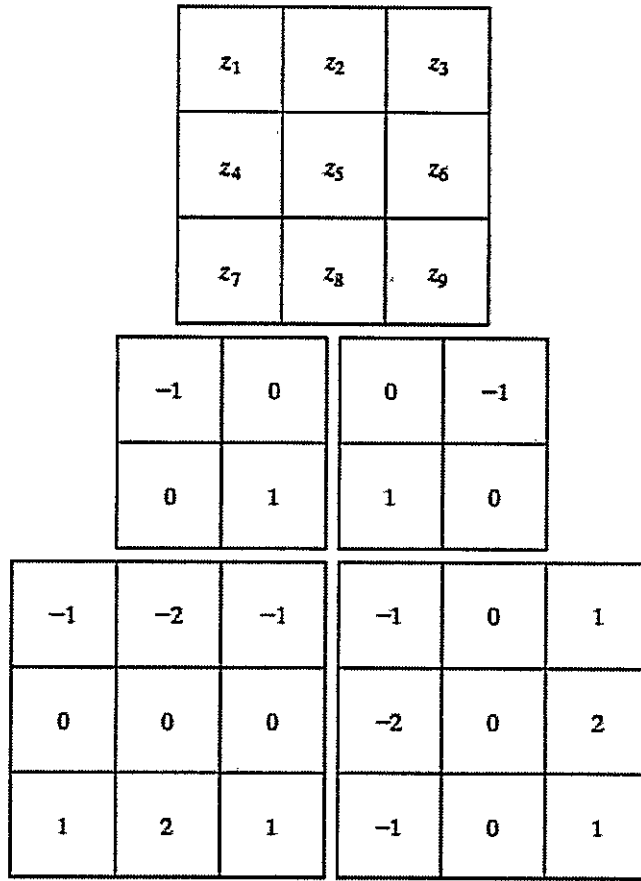


Fig.11.2 A 3 x 3 region of an image (the z's are gray-level values) and masks used to compute the gradient at point labeled  $z_5$ . All masks coefficients sum to zero, as expected of a derivative operator.



for more :- <http://www.UandiStar.org>

**Digital Image Processing**

**Question & Answers**

**GRIET/ECE**

**39**

100% free SMS:- ON<space>UandiStar to 9870807070 for JNTU, Job Alerts, Tech News , GK News directly to ur Mobile

**1. Discuss the frequency domain techniques of image enhancement in detail.**

Enhancement In Frequency Domain:

The frequency domain methods of image enhancement are based on convolution theorem. This is represented as,

$$g(x, y) = h(x, y) * f(x, y)$$

Where.

$g(x, y)$  = Resultant image

$h(x, y)$  = Position invariant operator

$f(x, y)$  = Input image

The Fourier transform representation of equation above is,

$$G(u, v) = H(u, v) F(u, v)$$

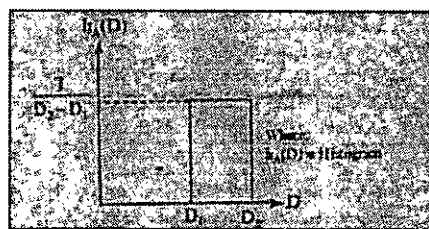
The function  $H(u, v)$  in equation is called transfer function. It is used to boost the edges of input image  $f(x, y)$  to emphasize the high frequency components.

The different frequency domain methods for image enhancement are as follows.

1. Contrast stretching.
2. Clipping and thresholding.
3. Digital negative.
4. Intensity level slicing and
5. Bit extraction.

**1. Contrast Stretching:**

Due to non-uniform lighting conditions, there may be poor contrast between the background and the feature of interest. Figure 1.1 (a) shows the contrast stretching transformations.



**Fig.1.1 (a) Histogram of input image**

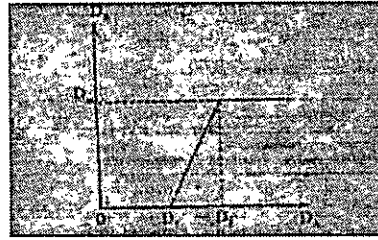


Fig.1.1 (b) Linear Law

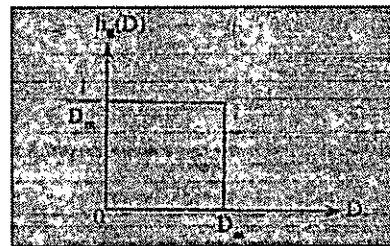


Fig.1.1 (c) Histogram of the transformed image

These stretching transformations are expressed as

In the area of stretching the slope of transformation is considered to be greater than unity. The parameters of stretching transformations i.e.,  $a$  and  $b$  can be determined by examining the histogram of the image.

## 2. Clipping and Thresholding:

Clipping is considered as the special scenario of contrast stretching. It is the case in which the parameters are  $\alpha = \gamma = 0$ . Clipping is more advantageous for reduction of noise in input signals of range  $[a, b]$ .

Threshold of an image is selected by means of its histogram. Let us take the image shown in the following figure 1.2.

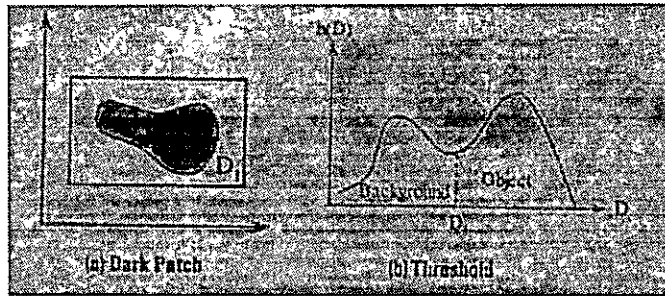


Fig. 1.2

The figure 1.2 (b) consists of two peaks i.e., background and object. At the abscissa of histogram minimum ( $D_1$ ) the threshold is selected. This selected threshold ( $D_1$ ) can separate background and object to convert the image into its respective binary form. The thresholding transformations are shown in figure 1.3.

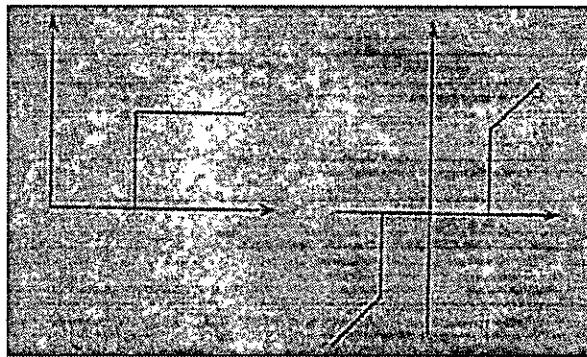


Fig.1.3

### 3. Digital Negative:

The digital negative of an image is achieved by reverse scaling of its grey levels to the transformation. They are much essential in displaying of medical images.

A digital negative transformation of an image is shown in figure 1.4.

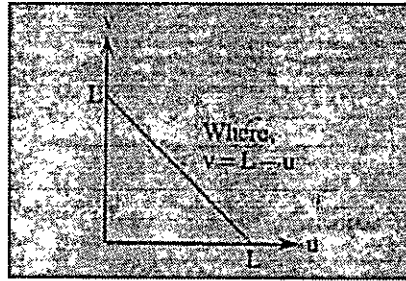


Fig.1.4

**4. Intensity Level Slicing:**

The images which consist of grey levels in between intensity at background and other objects require to reduce the intensity of the object. This process of changing intensity level is done with the help of intensity level slicing. They are expressed as

$$V = \begin{cases} L & a \leq u \leq b \\ 0 & \text{elsewhere} \end{cases} \quad \text{without background}$$

And

$$V = \begin{cases} L & a \leq u \leq b \\ u & \text{elsewhere} \end{cases} \quad \text{with background}$$

The histogram of input image and its respective intensity level slicing is shown in the figure 1.5.

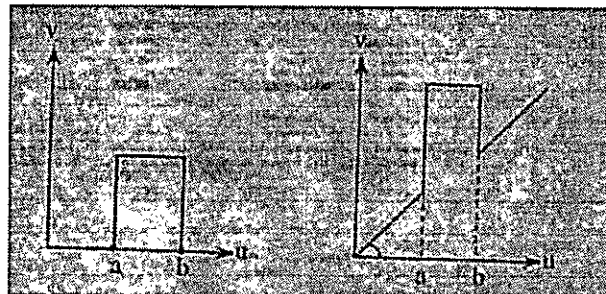


Fig.1.5

When an image is uniformly quantized then, the  $n^{\text{th}}$  most significant bit can be extracted and displayed.

$$\text{Let, } u = k_1 2^{B-1} + k_2 2^{B-2} + \dots + k_{B-1} 2 + k_B$$

Then, the output is expressed as

$$V = \begin{cases} L, & \text{for } k_n = 1 \\ 0, & \text{elsewhere} \end{cases}$$

## 2. Distinguish between spatial domain and frequency domain enhancement techniques.

The spatial domain refers to the image plane itself, and approaches in this category are based on direct manipulation of pixels in an image. Frequency domain processing techniques are based on modifying the Fourier transform of an image.

The term spatial domain refers to the aggregate of pixels composing an image and spatial domain methods are procedures that operate directly on these pixels. Image processing function in the spatial domain may be expressed as.

$$g(x, y) = T[f(x, y)]$$

Where

$f(x, y)$  is the input image  
 $g(x, y)$  is the processed image and  
 $T$  is the operator on  $f$  defined over some neighborhood values of

$(x, y)$ .

Frequency domain techniques are based on convolution theorem. Let  $g(x, y)$  be the image formed by the convolution of an image  $f(x, y)$  and linear position invariant operation  $h(x, y)$  i.e.,

$$g(x, y) = h(x, y) * f(x, y)$$

Applying convolution theorem

$$G(u, v) = H(u, v) F(u, v)$$

Where G, H and F are the Fourier transforms of g, h and f respectively. In the terminology of linear system the transform H (u, v) is called the transfer function of the process. The edges in f(x, y) can be boosted by using H (u, v) to emphasize the high frequency components of F (u, v).

### 3. Explain about Ideal Low Pass Filter (ILPF) in frequency domain.

#### Lowpass Filter:

The edges and other sharp transitions (such as noise) in the gray levels of an image contribute significantly to the high-frequency content of its Fourier transform. Hence blurring (smoothing) is achieved in the frequency domain by attenuating us the transform of a given image.

$$G(u, v) = H(u, v) F(u, v)$$

where F (u, v) is the Fourier transform of an image to be smoothed. The problem is to select a filter transfer function H (u, v) that yields G (u, v) by attenuating the high-frequency components of F (u, v). The inverse transform then will yield the desired smoothed image g (x, y).

#### Ideal Filter:

A 2-D ideal lowpass filter (ILPF) is one whose transfer function satisfies the relation

$$H(u, v) = \begin{cases} 1 & \text{if } D(u, v) \leq D_0 \\ 0 & \text{if } D(u, v) > D_0 \end{cases}$$

where D is a specified nonnegative quantity, and D(u, v) is the distance from point (u, v) to the origin of the frequency plane; that is,

$$D(u, v) = (u^2 + v^2)^{1/2}.$$

Figure 3 (a) shows a 3-D perspective plot of H (u, v) u a function of u and v. The name ideal filter indicates that oil frequencies inside a circle of radius

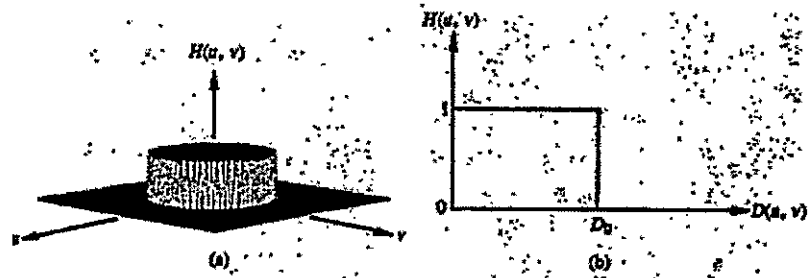


Fig.3 (a) Perspective plot of an ideal lowpass filter transfer function; (b) filter cross section.

Do are passed with no attenuation, whereas all frequencies outside this circle are completely attenuated.

The lowpass filters are radially symmetric about the origin. For this type of filter, specifying a cross section extending as a function of distance from the origin along a radial line is sufficient, as Fig. 3 (b) shows. The complete filter transfer function can then be generated by rotating the cross section 360 about the origin. Specification of radially symmetric filters centered on the  $N \times N$  frequency square is based on the assumption that the origin of the Fourier transform has been centered on the square.

For an ideal lowpass filter cross section, the point of transition between  $H(u, v) = 1$  and  $H(u, v) = 0$  is often called the cutoff frequency. In the case of Fig.3 (b), for example, the cutoff frequency is  $D_0$ . As the cross section is rotated about the origin, the point  $D_0$  traces a circle giving a locus of cutoff frequencies, all of which are a distance  $D_0$  from the origin. The cutoff frequency concept is quite useful in specifying filter characteristics. It also serves as a common base for comparing the behavior of different types of filters.

The sharp cutoff frequencies of an ideal lowpass filter cannot be realized with electronic components, although they can certainly be simulated in a computer.



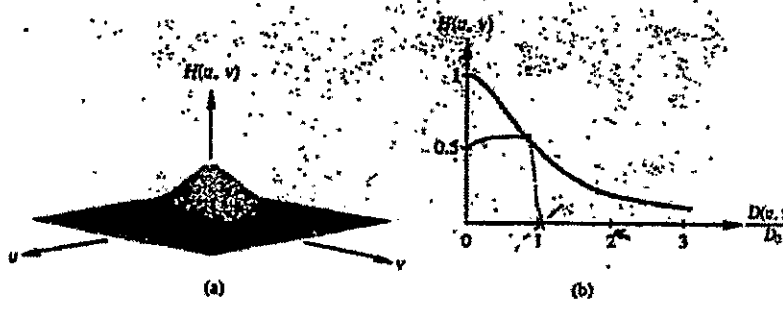
**4. Discuss about Butterworth lowpass filter with a suitable example.**

**Butterworth filter:**

The transfer function of the Butterworth lowpass (BLPF) of order n and with cutoff frequency locus at a distance  $D_0$ , from the origin is defined by the relation

$$H(u, v) = \frac{1}{1 + [D(u, v)/D_0]^2}$$

A perspective plot and cross section of the BLPF function are shown in figure 4.



**Fig.4 (a) A Butterworth lowpass filter (b) radial cross section for n = 1.**

Unlike the ILPF, the BLPF transfer function does not have a sharp discontinuity that establishes a clear cutoff between passed and filtered frequencies. For filters with smooth transfer functions, defining a cutoff frequency locus at points for which  $H(u, v)$  is down to a certain fraction of its maximum value is customary. In the case of above Eq.  $H(u, v) = 0.5$  (down 50 percent from its maximum value of 1) when  $D(u, v) = D_0$ . Another value commonly used is  $1/\sqrt{2}$  of the maximum value of  $H(u, v)$ . The following simple modification yields the desired value when  $D(u, v) = D_0$ :

$$H(u, v) = \frac{1}{1 + [\sqrt{2} - 1][D(u, v)/D_0]^2}$$

$$= \frac{1}{1 + 0.414[D(u, v)/D_0]^2}$$

### 5. Discuss about Ideal High Pass Filter and Butterworth High Pass filter.

#### High pass Filtering:

An image can be blurred by attenuating the high-frequency components of its Fourier transform. Because edges and other abrupt changes in gray levels are associated with high-frequency components, image sharpening can be achieved in the frequency domain by a high pass filtering process, which attenuates the low-frequency components without disturbing high-frequency information in the Fourier transform.

#### Ideal filter:

2-D ideal high pass filter (IHPF) is one whose transfer function satisfies the relation

$$H(u, v) = \begin{cases} 0 & \text{if } D(u, v) \leq D_0 \\ 1 & \text{if } D(u, v) > D_0 \end{cases}$$

where  $D_0$  is the cutoff distance measured from the origin of the frequency plane. Figure 5.1 shows a perspective plot and cross section of the IHPF function. This filter is the opposite of the ideal lowpass filter, because it completely attenuates all frequencies inside a circle of radius  $D_0$  while passing, without attenuation, all frequencies outside the circle. As in the case of the ideal lowpass filter, the IHPF is not physically realizable.

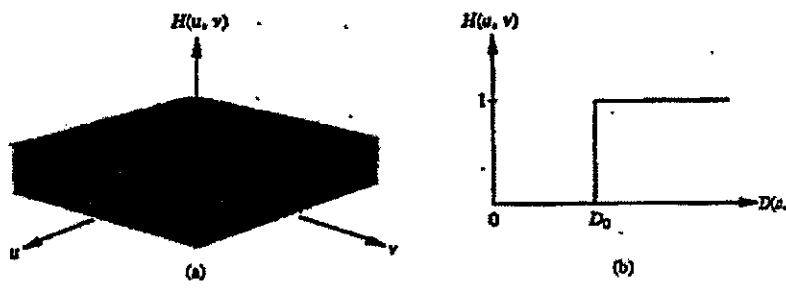


Fig.5.1 Perspective plot and radial cross section of ideal high pass filter

**Butterworth filter:**

The transfer function of the Butterworth high pass filter (BHPF) of order  $n$  and with cutoff frequency locus at a distance  $D_0$  from the origin is defined by the relation

$$H(u, v) = \frac{1}{1 + [D_0/D(u, v)]^{2n}}$$

Figure 5.2 shows a perspective plot and cross section of the BHPF function. Note that when  $D(u, v) = D_0$ ,  $H(u, v)$  is down to  $1/2$  of its maximum value. As in the case of the Butterworth lowpass filter, common practice is to select the cutoff frequency locus at points for which  $H(u, v)$  is down to  $1/\sqrt{2}$  of its maximum value.

$$\begin{aligned} H(u, v) &= \frac{1}{1 + [\sqrt{2} - 1][D_0/D(u, v)]^{2n}} \\ &= \frac{1}{1 + 0.414[D_0/D(u, v)]^{2n}} \end{aligned}$$

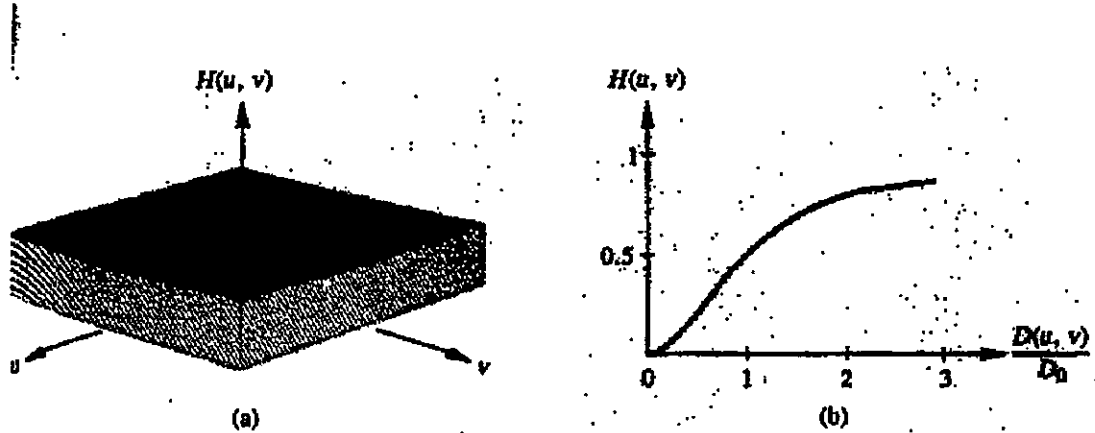


Fig.5.2 Perspective plot and radial cross section for Butterworth High Pass Filter with  $n = 1$

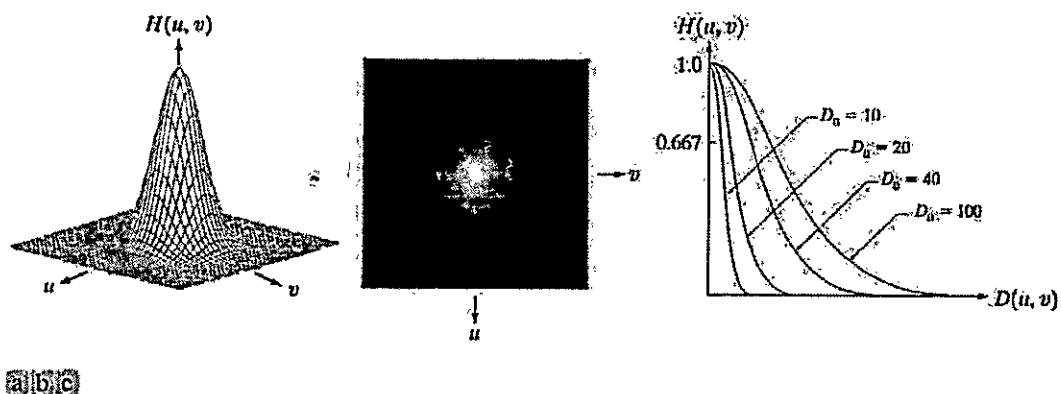
**6. Discuss about Gaussian High Pass and Gaussian Low Pass Filter.**

**Gaussian Lowpass Filters:**

The form of these filters in two dimensions is given by

$$H(u, v) = e^{-D^2(u, v)/2\sigma^2}$$

where,  $D(u, v)$  is the distance from the origin of the Fourier transform.



**Fig.6.1 (a) Perspective plot of a GLPF transfer function, (b) Filter displayed as an image, (c) Filter radial cross sections for various values of  $D_0$ .**

$\sigma$  is a measure of the spread of the Gaussian curve. By letting  $\sigma = D_0$ , we can express the filter in a more familiar form in terms of the notation:

$$H(u, v) = e^{-D^2(u, v)/2D_0^2}$$

where  $D_0$  is the cutoff frequency. When  $D(u, v) = D_0$ , the filter is down to 0.607 of its maximum value.

**Gaussian Highpass Filters:**

The transfer function of the Gaussian highpass filter (GHPF) with cutoff frequency locus at a distance  $D_0$  from the origin is given by

$$H(u, v) = 1 - e^{-D^2(u, v)/2D_0^2}$$

The figure 6.2 shows a perspective plot, image, and cross section of the GHPF function.

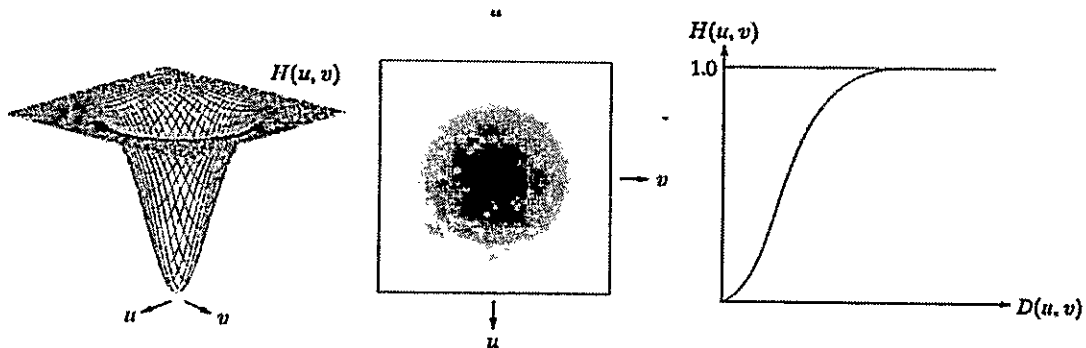


Fig.6.2. Perspective plot, image representation, and cross section of a typical Gaussian high pass filter

Even the filtering of the smaller objects and thin bars is cleaner with the Gaussian filter.

### 7. Explain how Laplacian is implemented in frequency domain.

**The Laplacian in the Frequency Domain:**

It can be shown that

$$\mathfrak{F}\left[\frac{d^n f(x)}{dx^n}\right] = (ju)^n F(u)$$

From this simple expression, it follows that

$$\begin{aligned} \mathfrak{F}\left[\frac{\partial^2 f(x, y)}{\partial x^2} + \frac{\partial^2 f(x, y)}{\partial y^2}\right] &= (ju)^2 F(u, v) + (jv)^2 F(u, v) \\ &= -(u^2 + v^2)F(u, v). \end{aligned}$$

The expression inside the brackets on the left side of the above Eq. is recognized as the Laplacian of  $f(x, y)$ . Thus, we have the important result

$$\mathfrak{S}[\nabla^2 f(x,y)] = -(u^2 + v^2)F(u,v),$$

which simply says that the Laplacian can be implemented in the frequency domain by using the filter

$$H(u,v) = -(u^2 + v^2).$$

As in all filtering operations, the assumption is that the origin of  $F(u, v)$  has been centered by performing the operation  $f(x, y) (-1)^{x+y}$  prior to taking the transform of the image. If  $f$  (and  $F$ ) are of size  $M \times N$ , this operation shifts the center transform so that  $(u, v) = (0, 0)$  is at point  $(M/2, N/2)$  in the frequency rectangle. As before, the center of the filter function also needs to be shifted:

$$H(u,v) = -[(u - M/2)^2 + (v - N/2)^2].$$

The Laplacian-filtered image in the spatial domain is obtained by computing the inverse Fourier transform of  $H(u, v) F(u, v)$ :

$$\nabla^2 f(x,y) = \mathfrak{S}^{-1}\{ -[(u - M/2)^2 + (v - N/2)^2] F(u,v) \}.$$

Conversely, computing the Laplacian in the spatial domain and computing the Fourier transform of the result is equivalent to multiplying  $F(u, v)$  by  $H(u, v)$ . We express this dual relationship in the familiar Fourier-transform-pair notation

$$\nabla^2 f(x,y) \Leftrightarrow -[(u - M/2)^2 + (v - N/2)^2] F(u,v).$$

The spatial domain Laplacian filter function obtained by taking the inverse Fourier transform of Eq. has some interesting properties, as Fig.7 shows. Figure 7(a) is a 3-D perspective plot. The function is centered at  $(M/2, N/2)$ , and its value at the top of the dome is zero. All other values are negative. Figure 7(b) shows  $H(u, v)$  as an image, also centered. Figure 7(c) is the Laplacian in the spatial domain, obtained by multiplying by  $H(u, v)$  by  $(-1)^{u+v}$ , taking the inverse Fourier transform, and multiplying the real part of the result by  $(-1)^{x+y}$ . Figure 7(d) is a zoomed section at about the origin of Fig.7(c). Figure 7(e) is a horizontal gray-level profile passing through the center of the zoomed section. Finally, Fig.7 (f) shows the mask to implement the definition of the discrete Laplacian in the spatial domain.

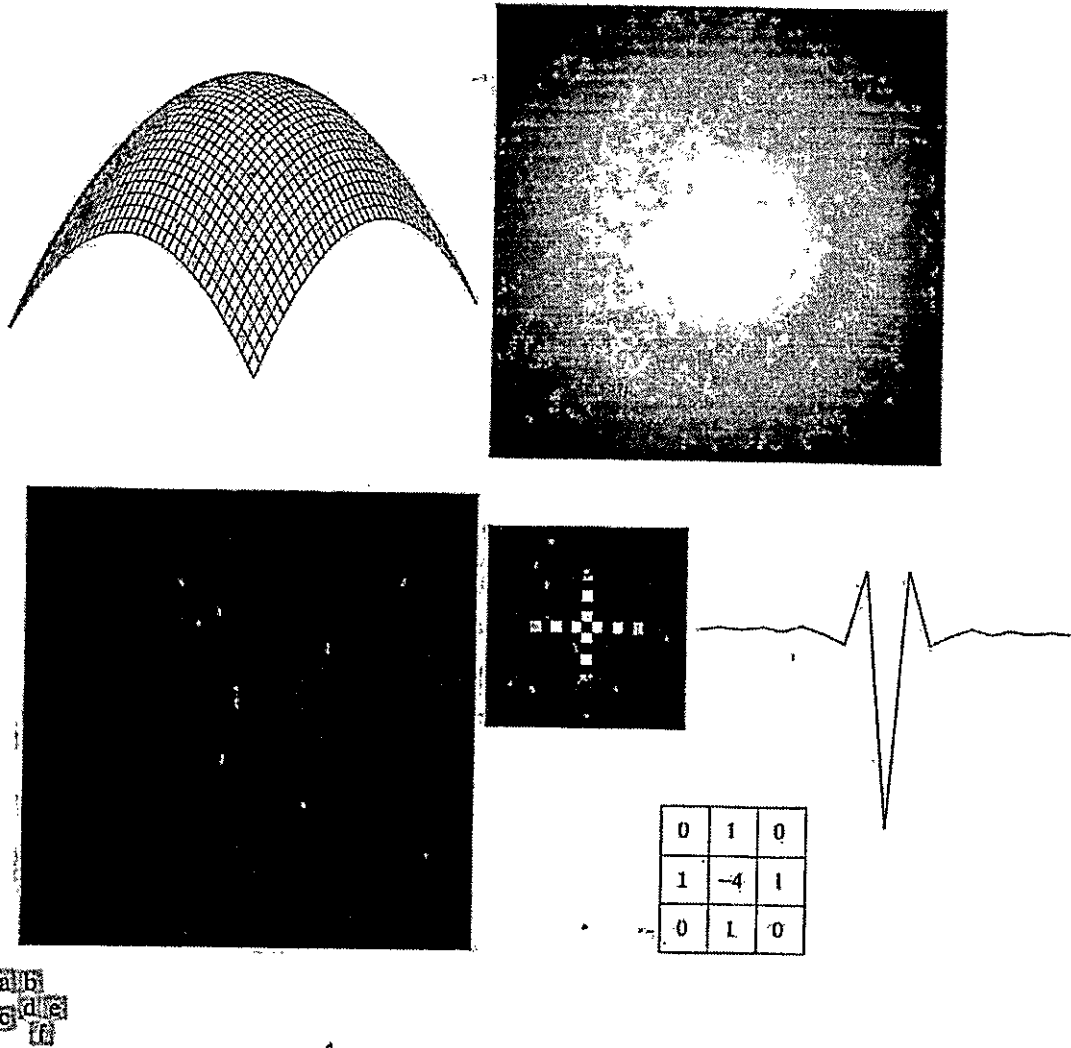


Fig.7 (a) 3-D plot of Laplacian in the frequency domain, (b) Image representation of (a), (c) Laplacian in the spatial domain obtained from the inverse DFT of (b) (d) Zoomed section of the origin of (c). (e) Gray-level profile through the center of (d). (f) Laplacian mask

A horizontal profile through the center of this mask has the same basic shape as the profile in Fig. 7(e) (that is, a negative value between two smaller positive values). We form an enhanced image  $g(x, y)$  by subtracting the Laplacian from the original image:

$$g(x, y) = f(x, y) - \nabla^2 f(x, y).$$

### 8. Write about high boost and high frequency filtering.

#### High-Boost Filtering and High-Frequency Emphasis Filtering:

All the filtered images have one thing in common: Their average background intensity has been reduced to near black. This is due to the fact that the highpass filters we applied to those images eliminate the zero-frequency component of their Fourier transforms. In fact, enhancement using the Laplacian does precisely this, by adding back the entire image to the filtered result. Sometimes it is advantageous to increase the contribution made by the original image to the overall filtered result. This approach, called high-boost filtering, is a generalization of unsharp masking. Unsharp masking consists simply of generating a sharp image by subtracting from an image a blurred version of itself. Using frequency domain terminology, this means obtaining a highpass-filtered image by subtracting from the image a lowpass-filtered version of itself. That is

$$f_{hp}(x, y) = f(x, y) - f_{lp}(x, y).$$

High-boost filtering generalizes this by multiplying  $f(x, y)$  by a constant  $A > 1$ :

$$f_{hb} = Af(x, y) - f_{lp}(x, y).$$

Thus, high-boost filtering gives us the flexibility to increase the contribution made by the image to the overall enhanced result. This equation may be written as

$$f_{hb}(x, y) = (A - 1)f(x, y) + f_{hp}(x, y).$$

Then, using above Eq. we obtain

$$f_{hb}(x, y) = (A - 1)f(x, y) + f_{hp}(x, y).$$

This result is based on a highpass rather than a lowpass image. When  $A = 1$ , high-boost filtering reduces to regular highpass filtering. As  $A$  increases past 1, the contribution made by the image itself becomes more dominant.



We have  $F_{hp}(u,v) = F(u,v) - F_{lp}(u,v)$ . But  $F_{lp}(u,v) = H_{lp}(u,v)F(u,v)$ , where  $H_{lp}$  is the transfer function of a lowpass filter. Therefore, unsharp masking can be implemented directly in the frequency domain by using the composite filter

$$H_{hp}(u,v) = 1 - H_{lp}(u,v)$$

Similarly, high-boost filtering can be implemented with the composite filter

$$H_{hb}(u,v) = (A - 1) + H_{lp}(u,v)$$

with  $A > 1$ . The process consists of multiplying this filter by the (centered) transform of the input image and then taking the inverse transform of the product. Multiplication of the real part of this result by  $(-1)^{x+y}$  gives us the high-boost filtered image  $f_{hb}(x, y)$  in the spatial domain.

## 9. Explain the concept of homomorphic filtering.

### Homomorphic filtering:

The illumination-reflectance model can be used to develop a frequency domain procedure for improving the appearance of an image by simultaneous gray-level range compression and contrast enhancement. An image  $f(x, y)$  can be expressed as the product of illumination and reflectance components:

$$f(x, y) = i(x, y)r(x, y).$$

Equation above cannot be used directly to operate separately on the frequency components of illumination and reflectance because the Fourier transform of the product of two functions is not separable; in other words,

$$\mathcal{F}\{f(x, y)\} \neq \mathcal{F}\{i(x, y)\}\mathcal{F}\{r(x, y)\}.$$

Suppose, however, that we define

$$\begin{aligned} z(x, y) &= \ln f(x, y) \\ &= \ln i(x, y) + \ln r(x, y). \end{aligned}$$

Then

$$\begin{aligned} \mathcal{F}\{z(x, y)\} &= \mathcal{F}\{\ln f(x, y)\} \\ &= \mathcal{F}\{\ln i(x, y)\} + \mathcal{F}\{\ln r(x, y)\} \end{aligned}$$

or

$$Z(u, v) = F_i(u, v) + F_r(u, v)$$

where  $F_i(u, v)$  and  $F_r(u, v)$  are the Fourier transforms of  $\ln i(x, y)$  and  $\ln r(x, y)$ , respectively. If we process  $Z(u, v)$  by means of a filter function  $H(u, v)$  then, from

$$\begin{aligned} S(u, v) &= H(u, v)Z(u, v) \\ &= H(u, v)F_i(u, v) + H(u, v)F_r(u, v) \end{aligned}$$

where  $S(u, v)$  is the Fourier transform of the result. In the spatial domain,

$$\begin{aligned} s(x, y) &= \mathcal{F}^{-1}\{S(u, v)\} \\ &= \mathcal{F}^{-1}\{H(u, v)F_i(u, v)\} + \mathcal{F}^{-1}\{H(u, v)F_r(u, v)\}. \end{aligned}$$

By letting

$$i'(x, y) = \mathcal{F}^{-1}\{H(u, v)F_i(u, v)\}$$

and

$$r'(x, y) = \mathcal{F}^{-1}\{H(u, v)F_r(u, v)\},$$

Now we have

$$s(x, y) = i'(x, y) + r'(x, y).$$

Finally, as  $z(x, y)$  was formed by taking the logarithm of the original image  $f(x, y)$ , the inverse (exponential) operation yields the desired enhanced image, denoted by  $g(x, y)$ ; that is,

$$\begin{aligned} g(x, y) &= e^{s(x, y)} \\ &= e^{i'(x, y)} \cdot e^{r'(x, y)} \\ &= i_0(x, y)r_0(x, y) \end{aligned}$$

where:

$$\begin{aligned} i_0(x, y) &= e^{i'(x, y)} \\ r_0(x, y) &= e^{r'(x, y)} \end{aligned}$$

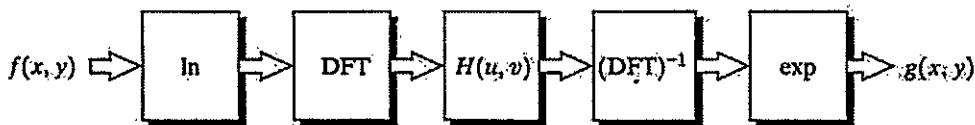


Fig.9.1 Homomorphic filtering approach for image enhancement

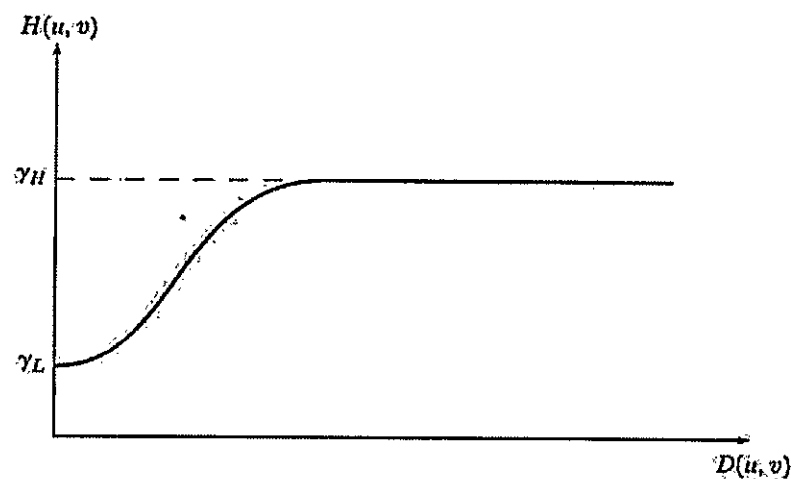
and

$$r_0(x, y) = e^{f(x, y)}$$

are the illumination and reflectance components of the output image. The enhancement approach using the foregoing concepts is summarized in Fig. 9.1. This method is based on a special case of a class of systems known as homomorphic systems. In this particular application, the key to the approach is the separation of the illumination and reflectance components achieved. The homomorphic filter function  $H(u, v)$  can then operate on these components separately.

The illumination component of an image generally is characterized by slow spatial variations, while the reflectance component tends to vary abruptly, particularly at the junctions of dissimilar objects. These characteristics lead to associating the low frequencies of the Fourier transform of the logarithm of an image with illumination and the high frequencies with reflectance. Although these associations are rough approximations, they can be used to advantage in image enhancement.

A good deal of control can be gained over the illumination and reflectance components with a homomorphic filter. This control requires specification of a filter function  $H(u, v)$  that affects the low- and high-frequency components of the Fourier transform in different ways. Figure 9.2 shows a cross section of such a filter. If the parameters  $\gamma_L$  and  $\gamma_H$  are chosen so that  $\gamma_L < 1$  and  $\gamma_H > 1$ , the filter function shown in Fig. 9.2 tends to decrease the contribution made by the low frequencies (illumination) and amplify the contribution made by high frequencies (reflectance). The net result is simultaneous dynamic range compression and contrast enhancement.



**Fig.9.2** Cross section of a circularly symmetric filter function  $D(u, v)$  is the distance from the origin of the centered transform.



## 1. Explain about gray level interpolation.

The distortion correction equations yield non integer values for  $x'$  and  $y'$ . Because the distorted image  $g$  is digital, its pixel values are defined only at integer coordinates. Thus using non integer values for  $x'$  and  $y'$  causes a mapping into locations of  $g$  for which no gray levels are defined. Inferring what the gray-level values at those locations should be, based only on the pixel values at integer coordinate locations, then becomes necessary. The technique used to accomplish this is called gray-level interpolation.

The simplest scheme for gray-level interpolation is based on a nearest neighbor approach. This method, also called zero-order interpolation, is illustrated in Fig. 6.1. This figure shows

(A) The mapping of integer  $(x, y)$  coordinates into fractional coordinates  $(x', y')$  by means of following equations

$$x' = c_1x + c_2y + c_3xy + c_4$$

and

$$y' = c_5x + c_6y + c_7xy + c_8$$

(B) The selection of the closest integer coordinate neighbor to  $(x', y')$ ;

and

(C) The assignment of the gray level of this nearest neighbor to the pixel located at  $(x, y)$ .

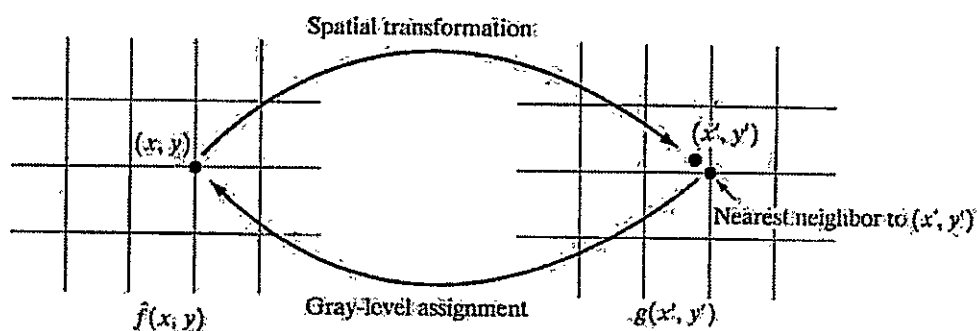


Fig. 6.1 Gray-level interpolation based on the nearest neighbor concept.

Although nearest neighbor interpolation is simple to implement, this method often has the drawback of producing undesirable artifacts, such as distortion of straight edges in images of high resolution. Smoother results can be obtained by using more sophisticated techniques, such as cubic convolution interpolation, which fits a surface of the  $\sin(z)/z$  type through a much larger number of neighbors (say, 16) in order to obtain a smooth estimate of the gray level at any

GRIET/ECE1

desired point. Typical areas in which smoother approximations generally are required include 3-D graphics and medical imaging. The price paid for smoother approximations is additional computational burden. For general-purpose image processing a bilinear interpolation approach that uses the gray levels of the four nearest neighbors usually is adequate. This approach is straightforward. Because the gray level of each of the four integral nearest neighbors of a non integral pair of coordinates  $(x', y')$  is known, the gray-level value at these coordinates, denoted  $v(x', y')$ , can be interpolated from the values of its neighbors by using the relationship

$$v(x', y') = ax' + by' + c x' y' + d$$

where the four coefficients are easily determined from the four equations in four unknowns that can be written using the four known neighbors of  $(x', y')$ . When these coefficients have been determined,  $v(x', y')$  is computed and this value is assigned to the location in  $f(x, y)$  that yielded the spatial mapping into location  $(x', y')$ . It is easy to visualize this procedure with the aid of Fig. 6.1. The exception is that, instead of using the gray-level value of the nearest neighbor to  $(x', y')$ , we actually interpolate a value at location  $(x', y')$  and use this value for the gray-level assignment at  $(x, y)$ .

## 2. Explain about Wiener filter used for image restoration.

The inverse filtering approach makes no explicit provision for handling noise. This approach incorporates both the degradation function and statistical characteristics of noise into the restoration process. The method is founded on considering images and noise as random processes, and the objective is to find an estimate  $f$  of the uncorrupted image  $f$  such that the mean square error between them is minimized. This error measure is given by

$$e^2 = E \{(f - \hat{f})^2\}$$

where  $E\{\cdot\}$  is the expected value of the argument. It is assumed that the noise and the image are uncorrelated; that one or the other has zero mean; and that the gray levels in the estimate are a linear function of the levels in the degraded image. Based on these conditions, the minimum of the error function is given in the frequency domain by the expression

$$\begin{aligned}\hat{F}(u, v) &= \left[ \frac{H^*(u, v)S_f(u, v)}{S_f(u, v)|H(u, v)|^2 + S_n(u, v)} \right] G(u, v) \\ &= \left[ \frac{H^*(u, v)}{|H(u, v)|^2 + S_n(u, v)/S_f(u, v)} \right] G(u, v) \\ &= \left[ \frac{1}{|H(u, v)|^2 + S_n(u, v)/S_f(u, v)} \right] G(u, v)\end{aligned}$$

where we used the fact that the product of a complex quantity with its conjugate is equal to the magnitude of the complex quantity squared. This result is known as the Wiener filter, after N. Wiener [1942], who first proposed the concept in the year shown. The filter, which consists of the terms inside the brackets, also is commonly referred to as the minimum mean square error filter or the least square error filter. The Wiener filter does not have the same problem as the inverse filter with zeros in the degradation function, unless both  $H(u, v)$  and  $S_n(u, v)$  are zero for the same value(s) of  $u$  and  $v$ .

The terms in above equation are as follows:

$H(u, v)$  = degradation function

$H^*(u, v)$  = complex conjugate of  $H(u, v)$

$|H(u, v)|^2 = H^*(u, v) \cdot H(u, v)$

$S_n(u, v) = |N(u, v)|^2$  = power spectrum of the noise

$S_f(u, v) = |F(u, v)|^2$  = power spectrum of the undegraded image.

$$\hat{F}(u, v) = \left[ \frac{1}{|H(u, v)|^2 + \frac{S_n(u, v)}{S_f(u, v)}} \right] G(u, v)$$

As before,  $H(u, v)$  is the transform of the degradation function and  $G(u, v)$  is the transform of the degraded image. The restored image in the spatial domain is given by the inverse Fourier transform of the frequency-domain estimate  $F(u, v)$ . Note that if the noise is zero, then the noise power spectrum vanishes and the Wiener filter reduces to the inverse filter.

When we are dealing with spectrally white noise, the spectrum  $|N(u, v)|^2$  is a constant, which simplifies things considerably. However, the power spectrum of the undegraded image seldom is known. An approach used frequently when these quantities are not known or cannot be estimated is to approximate the equation as

GRIET/ECE3

$$\hat{F}(u, v) = \left[ \frac{1}{H(u, v) |H(u, v)|^2 + K} \right] G(u, v)$$

where K is a specified constant.

### 3. Explain a Model of the Image Degradation/Restoration Process.

The Fig. 6.3 shows, the degradation process is modeled as a degradation function that, together with an additive noise term, operates on an input image  $f(x, y)$  to produce a degraded image  $g(x, y)$ . Given  $g(x, y)$ , some knowledge about the degradation function  $H$ , and some knowledge about the additive noise term  $\eta(x, y)$ , the objective of restoration is to obtain an estimate  $\hat{f}(x, y)$  of the original image. the estimate should be as close as possible to the original input image and, in general, the more we know about  $H$  and  $\eta$ , the closer  $\hat{f}(x, y)$  will be to  $f(x, y)$ .

The degraded image is given in the spatial domain by

$$g(x, y) = h(x, y) * f(x, y) + \eta(x, y)$$

where  $h(x, y)$  is the spatial representation of the degradation function and, the symbol  $*$  indicates convolution. Convolution in the spatial domain is equal to multiplication in the frequency domain, hence

$$G(u, v) = H(u, v) F(u, v) + N(u, v)$$

where the terms in capital letters are the Fourier transforms of the corresponding terms in above equation.

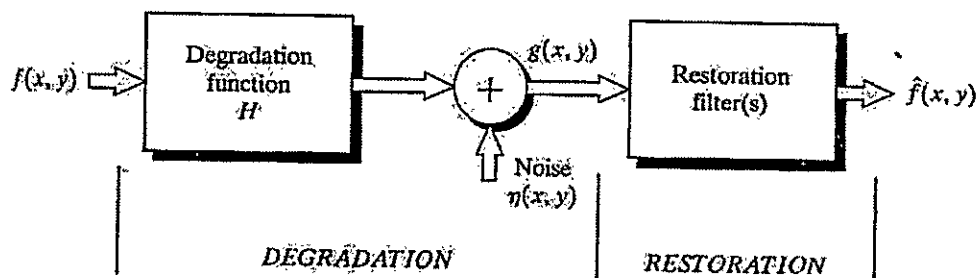


Fig. 6.3 model of the image degradation/restoration process.



4. Explain about the restoration filters used when the image degradation is due to noise only.

If the degradation present in an image is only due to noise, then,

$$g(x, y) = f(x, y) + \eta(x, y)$$

$$G(u, v) = F(u, v) + N(u, v)$$

The restoration filters used in this case are,

1. Mean filters
2. Order static filters and
3. Adaptive filters

Also read 5, 6, 7 answers.

5. Explain Mean filters.

There are four types of mean filters. They are

(i) Arithmetic mean filter

This is the simplest of the mean filters. Let  $S_{xy}$  represent the set of coordinates in a rectangular subimage window of size  $m \times n$ , centered at point  $(x, y)$ . The arithmetic mean filtering process computes the average value of the corrupted image  $g(x, y)$  in the area defined by  $S_{xy}$ . The value of the restored image  $f$  at any point  $(x, y)$  is simply the arithmetic mean computed using the pixels in the region defined by  $S_{xy}$ . In other words

$$\hat{f}(x, y) = \frac{1}{mn} \sum_{(s,t) \in S_{xy}} g(s, t).$$

This operation can be implemented using a convolution mask in which all coefficients have value  $1/mn$

(ii) Geometric mean filter

An image restored using a geometric mean filter is given by the expression

GRIET/ECE5

$$\hat{f}(x, y) = \left[ \prod_{(s,t) \in S_{xy}} g(s, t) \right]^{\frac{1}{mn}}$$

Here, each restored pixel is given by the product of the pixels in the subimage window, raised to the power  $1/mn$ . A geometric mean filter achieves smoothing comparable to the arithmetic mean filter, but it tends to lose less image detail in the process.

**(iii) Harmonic mean filter**

The harmonic mean filtering operation is given by the expression

$$\hat{f}(x, y) = \frac{mn}{\sum_{(s,t) \in S_{xy}} \frac{1}{g(s, t)}}$$

The harmonic mean filter works well for salt noise, but fails for pepper noise. It does well also with other types of noise like Gaussian noise.

**(iv) Contra harmonic mean filter**

The contra harmonic mean filtering operation yields a restored image based on the expression

$$\hat{f}(x, y) = \frac{\sum_{(s,t) \in S_{xy}} g(s, t)^{Q+1}}{\sum_{(s,t) \in S_{xy}} g(s, t)^Q}$$

$\frac{mn}{\sum_{(s,t) \in S_{xy}} \frac{1}{g(s, t)}}$

where  $Q$  is called the order of the filter. This filter is well suited for reducing or virtually eliminating the effects of salt-and-pepper noise. For positive values of  $Q$ , the filter eliminates pepper noise. For negative values of  $Q$  it eliminates salt noise. It cannot do both simultaneously. Note that the contra harmonic filter reduces to the arithmetic mean filter if  $Q = 0$ , and to the harmonic mean filter if  $Q = -1$ .

**6. Explain the Order-Statistic Filters.**

There are four types of Order-Statistic filters. They are

**(i) Median filter**

The best-known order-statistics filter is the median filter, which, as its name implies, replaces the value of a pixel by the median of the gray levels in the neighborhood of that pixel:

$$\hat{f}(x, y) = \text{median}_{(s,t) \in S_{xy}} \{g(s, t)\}.$$

The original value of the pixel is included in the computation of the median. Median filters are quite popular because, for certain types of random noise, they provide excellent noise-reduction capabilities, with considerably less blurring than linear smoothing filters of similar size. Median filters are particularly effective in the presence of both bipolar and unipolar impulse noise.

**(ii) Max and min filters**

Although the median filter is by far the order-statistics filter most used in image processing, it is by no means the only one. The median represents the 50th percentile of a ranked set of numbers, but the reader will recall from basic statistics that ranking lends itself to many other possibilities. For example, using the 100<sup>th</sup> percentile results in the so-called max filter, given by

$$\hat{f}(x, y) = \max_{(s,t) \in S_{xy}} \{g(s, t)\}.$$

This filter is useful for finding the brightest points in an image. Also, because pepper noise has very low values, it is reduced by this filter as a result of the max selection process in the subimage area  $S_{xy}$ .

The 0<sup>th</sup> percentile filter is the min filter.

$$\hat{f}(x, y) = \min_{(s,t) \in S_{xy}} \{g(s, t)\}.$$

This filter is useful for finding the darkest points in an image. Also, it reduces salt noise as a result of the min operation.

**(iii) Midpoint filter**

The midpoint filter simply computes the midpoint between the maximum and minimum values in the area encompassed by the filter:

$$\hat{f}(x, y) = \frac{1}{2} \left[ \max_{(s,t) \in S_{xy}} \{g(s, t)\} + \min_{(s,t) \in S_{xy}} \{g(s, t)\} \right].$$

Note that this filter combines order statistics and averaging. This filter works best for randomly distributed noise, like Gaussian or uniform noise.

**(iv) Alpha - trimmed mean filter**

It is a filter formed by deleting the  $d/2$  lowest and the  $d/2$  highest gray-level values of  $g(s, t)$  in the neighborhood  $S_{xy}$ . Let  $g_r(s, t)$  represent the remaining  $mn - d$  pixels. A filter formed by averaging these remaining pixels is called an alpha-trimmed mean filter:

$$\hat{f}(x, y) = \frac{1}{mn - d} \sum_{(s,t) \in S_{xy}} g_r(s, t)$$

where the value of  $d$  can range from 0 to  $mn - 1$ . When  $d = 0$ , the alpha-trimmed filter reduces to the arithmetic mean filter. If  $d = (mn - 1)/2$ , the filter becomes a median filter. For other values of  $d$ , the alpha-trimmed filter is useful in situations involving multiple types of noise, such as a combination of salt-and-pepper and Gaussian noise.

**7. Explain the Adaptive Filters.**

Adaptive filters are filters whose behavior changes based on statistical characteristics of the image inside the filter region defined by the  $m \times n$  rectangular window  $S_{xy}$ .

**Adaptive, local noise reduction filter:**

The simplest statistical measures of a random variable are its mean and variance. These are reasonable parameters on which to base an adaptive filter because they are quantities closely related to the appearance of an image. The mean gives a measure of average gray level in the region over which the mean is computed, and the variance gives a measure of average contrast in that region.

This filter is to operate on a local region,  $S_{xy}$ . The response of the filter at any point  $(x, y)$  on which the region is centered is to be based on four quantities: (a)  $g(x, y)$ , the value of the noisy image at  $(x, y)$ ; (b)  $\sigma^2$ , the variance of the noise corrupting  $g(x, y)$ ; (c)  $\mu$ , the local mean of the pixels in  $S_{xy}$ ; and (d)  $\sigma^2_L$ , the local variance of the pixels in  $S_{xy}$ .

The behavior of the filter to be as follows:

**GRIET/ECE8**

1. If  $\sigma_n^2$  is zero, the filter should return simply the value of  $g(x, y)$ . This is the trivial, zero-noise case in which  $g(x, y)$  is equal to  $f(x, y)$ .
2. If the local variance is high relative to  $\sigma_n^2$  the filter should return a value close to  $g(x, y)$ . A high local variance typically is associated with edges, and these should be preserved.
3. If the two variances are equal, we want the filter to return the arithmetic mean value of the pixels in  $S_{xy}$ . This condition occurs when the local area has the same properties as the overall image, and local noise is to be reduced simply by averaging.

Adaptive local noise filter is given by,

$$\hat{f}(x, y) = g(x, y) - \frac{\sigma_n^2}{\sigma_L^2} [g(x, y) - m_L].$$

The only quantity that needs to be known or estimated is the variance of the overall noise,  $\sigma_n^2$ . The other parameters are computed from the pixels in  $S_{xy}$  at each location  $(x, y)$  on which the filter window is centered.

#### Adaptive median filter:

The median filter performs well as long as the spatial density of the impulse noise is not large (as a rule of thumb,  $P_a$  and  $P_b$  less than 0.2). The adaptive median filtering can handle impulse noise with probabilities even larger than these. An additional benefit of the adaptive median filter is that it seeks to preserve detail while smoothing nonimpulse noise, something that the "traditional" median filter does not do. The adaptive median filter also works in a rectangular window area  $S_{xy}$ . Unlike those filters, however, the adaptive median filter changes (increases) the size of  $S_{xy}$  during filter operation, depending on certain conditions. The output of the filter is a single value used to replace the value of the pixel at  $(x, y)$ , the particular point on which the window  $S_{xy}$  is centered at a given time.

Consider the following notation:

$z_{\min}$  = minimum gray level value in  $S_{xy}$

$z_{\max}$  = maximum gray level value in  $S_{xy}$

$z_{\text{med}}$  = median of gray levels in  $S_{xy}$

$z_{xy}$  = gray level at coordinates  $(x, y)$

$S_{\max}$  = maximum allowed size of  $S_{xy}$ .

GRIET/ECE9

The adaptive median filtering algorithm works in two levels, denoted level A and level B, as follows:

**Level A:**       $A1 = Z_{med} - Z_{min}$

$$A2 = Z_{med} - Z_{max}$$

If  $A1 > 0$  AND  $A2 < 0$ , Go to level B

Else increase the window size

If window size  $\leq S_{max}$  repeat level A

Else output  $z_{xy}$

**Level B:**       $B1 = Z_{xy} - Z_{min}$

$$B2 = Z_{xy} - Z_{max}$$

If  $B1 > 0$  AND  $B2 < 0$ , output  $z_{xy}$

Else output  $z_{med}$

### 8. Explain a simple Image Formation Model.

An image is represented by two-dimensional functions of the form  $f(x, y)$ . The value or amplitude of  $f$  at spatial coordinates  $(x, y)$  is a positive scalar quantity whose physical meaning is determined by the source of the image. When an image is generated from a physical process, its values are proportional to energy radiated by a physical source (e.g., electromagnetic waves). As a consequence,  $f(x, y)$  must be nonzero and finite; that is,

$$0 < f(x, y) < \infty \quad \dots (1)$$

The function  $f(x, y)$  may be characterized by two components:

A) The amount of source illumination incident on the scene being viewed.

B) The amount of illumination reflected by the objects in the scene.

Appropriately, these are called the illumination and reflectance components and are denoted by  $i(x, y)$  and  $r(x, y)$ , respectively. The two functions combine as a product to form  $f(x, y)$ .

$$f(x, y) = i(x, y) r(x, y) \quad \dots (2)$$

where

GRIET/ECE10

$$0 < i(x, y) < \infty \quad \dots (3)$$

and

$$0 < r(x, y) < 1 \quad \dots (4)$$

Equation (4) indicates that reflectance is bounded by 0 (total absorption) and 1 (total reflectance). The nature of  $i(x, y)$  is determined by the illumination source, and  $r(x, y)$  is determined by the characteristics of the imaged objects. It is noted that these expressions also are applicable to images formed via transmission of the illumination through a medium, such as a chest X-ray.

**9. Write brief notes on inverse filtering.**

The simplest approach to restoration is direct inverse filtering, where  $F(u, v)$ , the transform of the original image is computed simply by dividing the transform of the degraded image,  $G(u, v)$ , by the degradation function

$$\hat{F}(u, v) = \frac{G(u, v)}{H(u, v)}$$

The divisions are between individual elements of the functions.

But  $G(u, v)$  is given by

$$G(u, v) = F(u, v) + N(u, v)$$

Hence

$$\hat{F}(u, v) = F(u, v) + \frac{N(u, v)}{H(u, v)}$$

It tells that even if the degradation function is known the undegraded image cannot be recovered [the inverse Fourier transform of  $F(u, v)$ ] exactly because  $N(u, v)$  is a random function whose Fourier transform is not known.

If the degradation has zero or very small values, then the ratio  $N(u, v)/H(u, v)$  could easily dominate the estimate  $F(u, v)$ .

One approach to get around the zero or small-value problem is to limit the filter frequencies to values near the origin.  $H(0, 0)$  is equal to the average value of  $h(x, y)$  and that this

GRIET/ECE11

is usually the highest value of  $H(u, v)$  in the frequency domain. Thus, by limiting the analysis to frequencies near the origin, the probability of encountering zero values is reduced.

**10. Write about Noise Probability Density Functions.**

The following are among the most common PDFs found in image processing applications.

**Gaussian noise**

Because of its mathematical tractability in both the spatial and frequency domains, Gaussian (also called normal) noise models are used frequently in practice. In fact, this tractability is so convenient that it often results in Gaussian models being used in situations in which they are marginally applicable at best.

The PDF of a Gaussian random variable,  $z$ , is given by

$$p(z) = \frac{1}{\sqrt{2\pi}\sigma} e^{-(z-\mu)^2/2\sigma^2} \quad \dots (1)$$

where  $z$  represents gray level,  $\mu$  is the mean of average value of  $z$ , and  $\sigma$  is its standard deviation. The standard deviation squared,  $\sigma^2$ , is called the variance of  $z$ . A plot of this function is shown in Fig. 5.10. When  $z$  is described by Eq. (1), approximately 70% of its values will be in the range  $[(\mu - \sigma), (\mu + \sigma)]$ , and about 95% will be in the range  $[(\mu - 2\sigma), (\mu + 2\sigma)]$ .

**Rayleigh noise**

The PDF of Rayleigh noise is given by

$$p(z) = \begin{cases} \frac{2}{b} (z - a) e^{-(z-a)^2/b} & \text{for } z \geq a \\ 0 & \text{for } z < a. \end{cases}$$

The mean and variance of this density are given by

$$\mu = a + \sqrt{\pi b/4}$$

$$\sigma^2 = b(4 - \pi)/4$$



Figure 5.10 shows a plot of the Rayleigh density. Note the displacement from the origin and the fact that the basic shape of this density is skewed to the right. The Rayleigh density can be quite useful for approximating skewed histograms.

**Erlang (Gamma) noise**

The PDF of Erlang noise is given by

$$p(z) = \begin{cases} \frac{a^b z^{b-1}}{(b-1)!} e^{-az} & \text{for } z \geq 0 \\ 0 & \text{for } z < 0 \end{cases}$$

where the parameters are such that  $a > 0$ ,  $b$  is a positive integer, and "!" indicates factorial. The mean and variance of this density are given by

$$\mu = b / a$$

$$\sigma^2 = b / a^2$$

**Exponential noise**

The PDF of exponential noise is given by

$$p(z) = \begin{cases} ae^{-az} & \text{for } z \geq 0 \\ 0 & \text{for } z < 0 \end{cases}$$

The mean of this density function is given by

$$\mu = 1 / a$$

$$\sigma^2 = 1 / a^2$$

This PDF is a special case of the Erlang PDF, with  $b = 1$ .

**Uniform noise**

The PDF of uniform noise is given by

$$p(z) = \begin{cases} \frac{1}{b-a} & \text{if } a \leq z \leq b \\ 0 & \text{otherwise.} \end{cases}$$

The mean of this density function is given by

$$\mu = a + b / 2$$
$$\sigma^2 = (b - a)^2 / 12$$

**Impulse (salt-and-pepper) noise**

The PDF of (bipolar) impulse noise is given by

$$p(z) = \begin{cases} P_a & \text{for } z = a \\ P_b & \text{for } z = b \\ 0 & \text{otherwise} \end{cases}$$

If  $b > a$ , gray-level  $b$  will appear as a light dot in the image. Conversely, level  $a$  will appear like a dark dot. If either  $P_a$  or  $P_b$  is zero, the impulse noise is called unipolar. If neither probability is zero, and especially if they are approximately equal, impulse noise values will resemble salt-and-pepper granules randomly distributed over the image. For this reason, bipolar impulse noise also is called salt-and-pepper noise. Shot and spike noise also are terms used to refer to this type of noise.

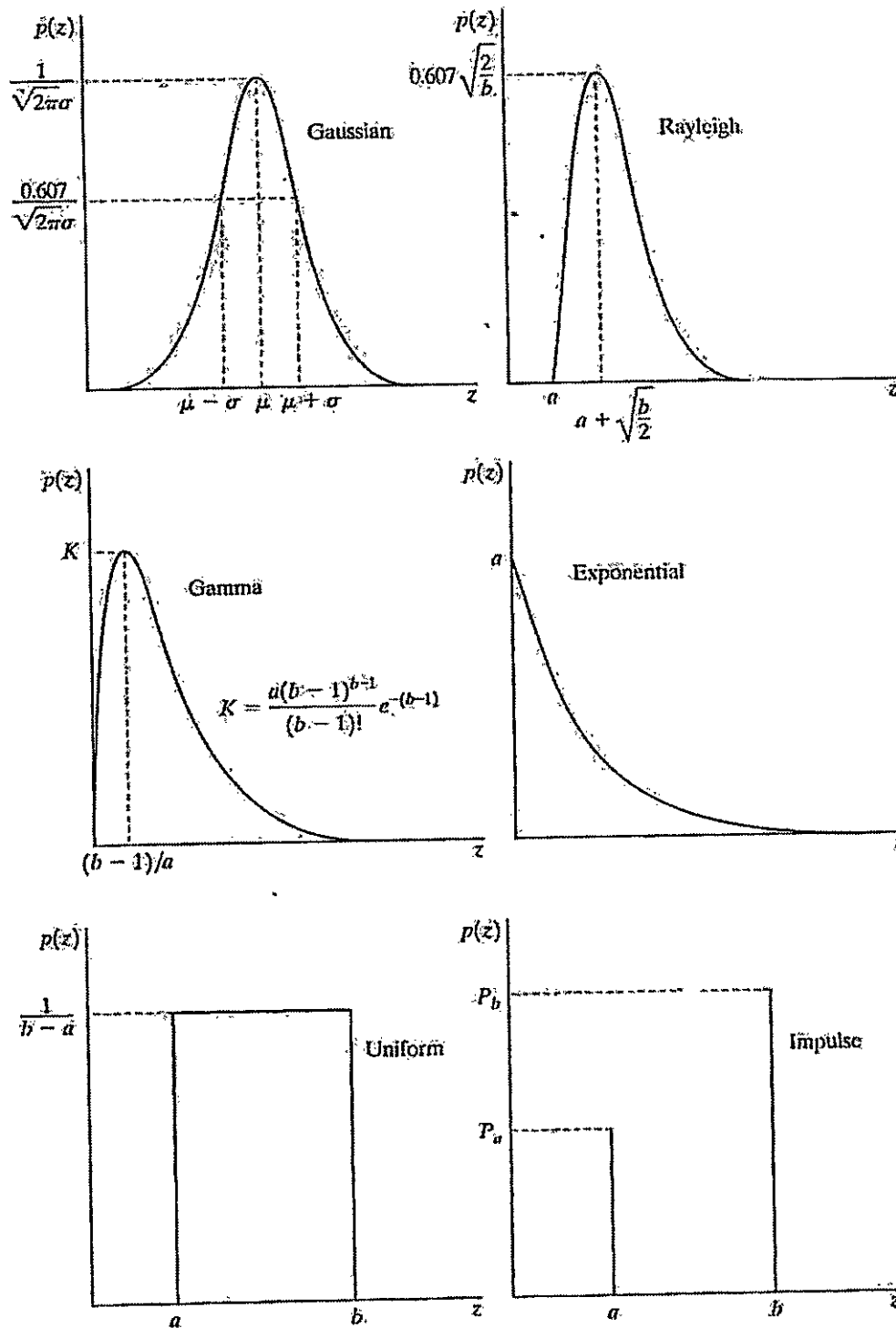


Fig.5.10 Some important probability density functions

GRIET/ECE15

**11. Enumerate the differences between the image enhancement and image restoration.**

(i) Image enhancement techniques are heuristic procedures designed to manipulate an image in order to take advantage of the psychophysical aspects of the human system. Whereas image restoration techniques are basically reconstruction techniques by which a degraded image is reconstructed by using some of the prior knowledge of the degradation phenomenon.

(ii) Image enhancement can be implemented by spatial and frequency domain technique, whereas image restoration can be implement by frequency domain and algebraic techniques.

(iii) The computational complexity for image enhancement is relatively less when compared to the computational complexity for image restoration, since algebraic methods requires manipulation of large number of simultaneous equation. But, under some condition computational complexity can be reduced to the same level as that required by traditional frequency domain technique.

(iv) Image enhancement techniques are problem oriented, whereas image restoration techniques are general and are oriented towards modeling the degradation and applying the reverse process in order to reconstruct the original image.

(v) Masks are used in spatial domain methods for image enhancement, whereas masks are not used for image restoration techniques.

(vi) Contrast stretching is considered as image enhancement technique because it is based on the pleasing aspects of the review, whereas removal of image blur by applying a deblurring function is considered as a image restoration technique.

**12. Explain about iterative nonlinear restoration using the Lucy-Richardson algorithm.**

Lucy-Richardson algorithm is a nonlinear restoration method used to recover a latent image which is blurred by a Point Spread Function (psf). It is also known as Richardson-Lucy deconvolution.

With as the point spread function, the pixels in observed image are expressed as,

$$c_i = \sum_j u_j h_{ij}$$

Here,

$u_j$  = Pixel value at location  $j$  in the image

$c_i$  = Observed value at  $i^{\text{th}}$  pixel location

GRIET/ECE16

## Digital Image Processing

## Question & Answers

The L-R algorithm cannot be used in application in which the psf ( $P_{ij}$ ) is dependent on one or more unknown variables.

The L-R algorithm is based on maximum-likelihood formulation, in this formulation Poisson statistics are used to model the image. If the likelihood of model is increased, then the result is an equation which satisfies when the following iteration converges.

$$\hat{f}_{k+1}(x, y) = \hat{f}_k(x, y) \left[ \frac{H(x, y) \times \frac{g(x, y)}{H(x, y) \times \hat{f}_k(x, y)}}{H(x, y) \times \hat{f}_k(x, y)} \right]$$

Here,

$f$  = Estimation of undegraded image.

The factor  $f$  which is present in the right side denominator leads to non-linearity. Since, the algorithm is a type of nonlinear restorations; hence it is stopped when satisfactory result is obtained.

The basic syntax of function deconvlucy with the L-R algorithm is implemented is given below.

$f_r$  = Deconvlucy (g, psf, NUMIT, DAMPAR, WEIGHT)

Here the parameters are,

$g$  = Degraded image

$f_r$  = Restored image

psf = Point spread function

NUMIT = Total number of iterations.

The remaining two parameters are,

### DAMPAR

The DAMPAR parameter is a scalar parameter which is used to determine the deviation of resultant image with the degraded image ( $g$ ). The pixels which get deviated from their original value within the DAMPAR, for these pixels iterations are cancelled so as to reduce noise generation and present essential image information.

GRIET/ECE17

**WEIGHT**

WEIGHT parameter gives a weight to each and every pixel. It is array of size similar to that of degraded image ( $g$ ). In applications where a pixel leads to improper image is removed by assigning it to a weight as 0'. The pixels may also be given weights depending upon the flat-field correction, which is essential according to image array. Weights are used in applications such as blurring with specified psf. They are used to remove the pixels which are present at the boundary of the image and are blurred separately by psf.

If the array size of psf is  $n \times n$  then the width of weight of border of zeroes being used is  $\text{ceil}(n/2)$

**GRIET/ECE18**

1. Explain about color fundamentals.

Color of an object is determined by the nature of the light reflected from it. When a beam of sunlight passes through a glass prism, the emerging beam of light is not white but consists instead of a continuous spectrum of colors ranging from violet at one end to red at the other. As Fig. 5.1.1 shows, the color spectrum may be divided into six broad regions: violet, blue, green, yellow, orange, and red. When viewed in full color (Fig. 5.1.2), no color in the spectrum ends abruptly, but rather each color blends smoothly into the next.

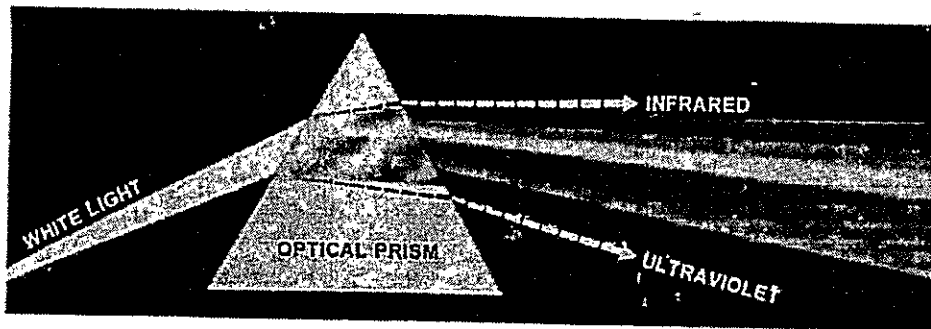


Fig. 5.1.1 Color spectrum seen by passing white light through a prism.

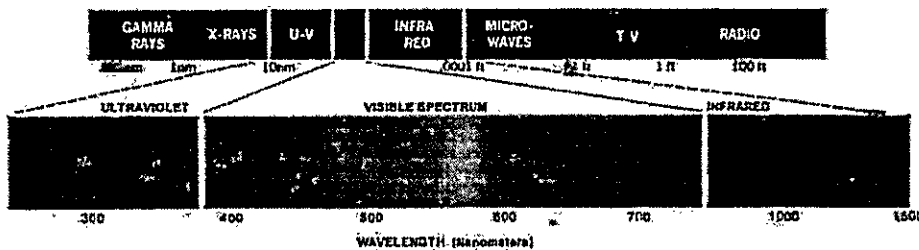


Fig. 5.1.2 Wavelengths comprising the visible range of the electromagnetic spectrum.

As illustrated in Fig. 5.1.2, visible light is composed of a relatively narrow band of frequencies in the electromagnetic spectrum. A body that reflects light that is balanced in all visible wavelengths appears white to the observer. However, a body that favors reflectance in a limited range of the visible spectrum exhibits some shades of color. For example, green objects reflect light with wavelengths primarily in the 500 to 570 nm range while absorbing most of the energy at other wavelengths.

Characterization of light is central to the science of color. If the light is achromatic (void of color), its only attribute is its intensity, or amount. Achromatic light is what viewers see on a black and white television set.

Three basic quantities are used to describe the quality of a chromatic light source: radiance, luminance, and brightness.

**Radiance:**

Radiance is the total amount of energy that flows from the light source, and it is usually measured in watts (W).

**Luminance:**

Luminance, measured in lumens (lm), gives a measure of the amount of energy an observer perceives from a light source. For example, light emitted from a source operating in the far infrared region of the spectrum could have significant energy (radiance), but an observer would hardly perceive it; its luminance would be almost zero.

**Brightness:**

Brightness is a subjective descriptor that is practically impossible to measure. It embodies the achromatic notion of intensity and is one of the key factors in describing color sensation.

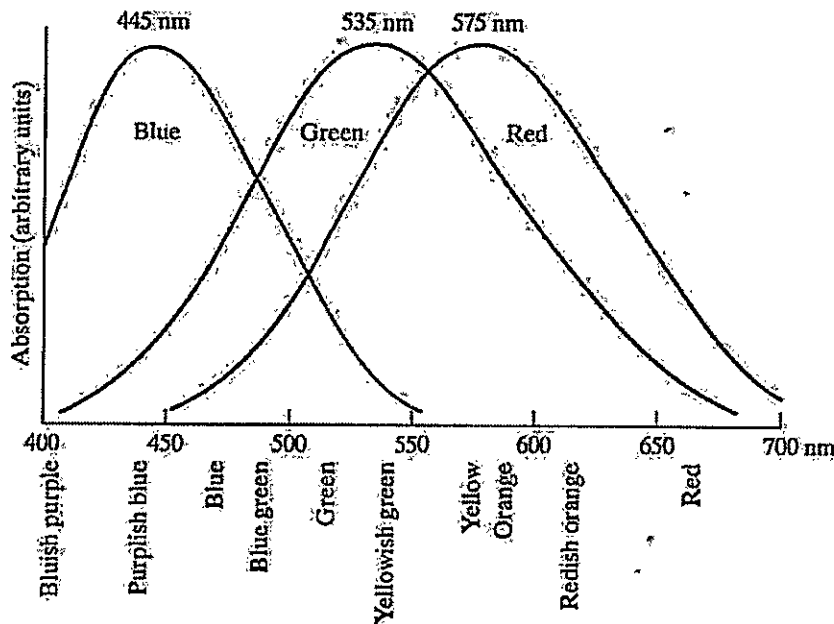


Fig. 5.1.3 Absorption of light by the red, green, and blue cones in the human eye as a function of wavelength.

Cones are the sensors in the eye responsible for color vision. Detailed experimental evidence has established that the 6 to 7 million cones in the human eye can be divided into three principal sensing categories, corresponding roughly to red, green, and blue. Approximately 65%



of all cones are sensitive to red light, 33% are sensitive to green light, and only about 2% are sensitive to blue (but the blue cones are the most sensitive). Figure 5.1.3 shows average experimental curves detailing the absorption of light by the red, green, and blue cones in the eye. Due to these absorption characteristics of the human eye, colors are seen as variable combinations of the so-called primary colors red (R), green (G), and blue (B).

The primary colors can be added to produce the secondary colors of light --magenta (red plus blue), cyan (green plus blue), and yellow (red plus green). Mixing the three primaries, or a secondary with its opposite primary color, in the right intensities produces white light.

The characteristics generally used to distinguish one color from another are brightness, hue, and saturation. Brightness embodies the chromatic notion of intensity. Hue is an attribute associated with the dominant wavelength in a mixture of light waves. Hue represents dominant color as perceived by an observer. Saturation refers to the relative purity or the amount of white light mixed with a hue. The pure spectrum colors are fully saturated. Colors such as pink (red and white) and lavender (violet and white) are less saturated, with the degree of saturation being inversely proportional to the amount of white light-added.

Hue and saturation taken together are called chromaticity, and, therefore, a color may be characterized by its brightness and chromaticity.

## **2. Explain RGB color model.**

The purpose of a color model (also called color space or color system) is to facilitate the specification of colors in some standard, generally accepted way. In essence, a color model is a specification of a coordinate system and a subspace within that system where each color is represented by a single point.

### **The RGB Color Model:**

In the RGB model, each color appears in its primary spectral components of red, green, and blue. This model is based on a Cartesian coordinate system. The color subspace of interest is the cube shown in Fig. 5.2, in which RGB values are at three corners; cyan, magenta, and yellow are at three other corners; black is at the origin; and white is at the corner farthest from the origin. In this model, the gray scale (points of equal RGB values) extends from black to white along the line joining these two points. The different colors in this model are points on or inside the cube, and are defined by vectors extending from the origin. For convenience, the assumption is that all color values have been normalized so that the cube shown in Fig. 5.2 is the unit cube. That is, all values of R, G, and B are assumed to be in the range [0, 1].

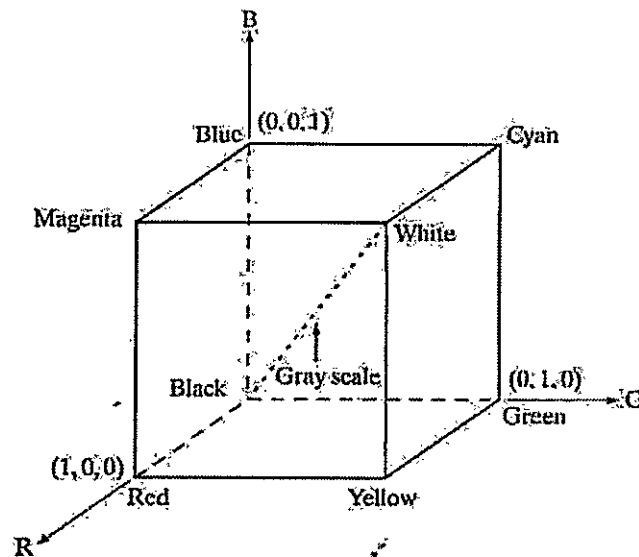


Fig. 5.2 Schematic of the RGB color cube.

Images represented in the RGB color model consist of three component images, one for each primary color. When fed into an RGB monitor, these three images combine on the phosphor screen to produce a composite color image. The number of bits used to represent each pixel in RGB space is called the pixel depth.

Consider an RGB image in which each of the red, green, and blue images is an 8-bit image. Under these conditions each RGB color pixel [that is, a triplet of values (R, G, B)] is said to have a depth of 24 bits (3 image planes times the number of bits per plane). The term full-color image is used often to denote a 24-bit RGB color image. The total number of colors in a 24-bit RGB image is  $(2^8)^3 = 16,777,216$ .

RGB is ideal for image color generation (as in image capture by a color camera or image display in a monitor screen), but its use for color description is much more limited.

### 3. Explain CMY color model.

Cyan, magenta, and yellow are the secondary colors of light or, alternatively, the primary colors of pigments. For example, when a surface coated with cyan pigment is illuminated with white light, no red light is reflected from the surface. That is, cyan subtracts red light from reflected white light, which itself is composed of equal amounts of red, green, and blue light.

Most devices that deposit colored pigments on paper, such as color printers and copiers, require CMY data input or perform an RGB to CMY conversion internally. This conversion is performed using the simple operation (1) where, again, the assumption is that all color values

have been normalized to the range [0, 1]. Equation (1) demonstrates that light reflected from a surface coated with pure cyan does not contain red (that is,  $C = 1 - R$  in the equation).

$$\begin{bmatrix} C \\ M \\ Y \end{bmatrix} = \begin{bmatrix} 1 \\ 1 \\ 1 \end{bmatrix} - \begin{bmatrix} R \\ G \\ B \end{bmatrix} \quad (1)$$

Similarly, pure magenta does not reflect green, and pure yellow does not reflect blue. Equation (1) also reveals that RGB values can be obtained easily from a set of CMY values by subtracting the individual CMY values from 1. As indicated earlier, in image processing this color model is used in connection with generating hardcopy output, so the inverse operation from CMY to RGB generally is of little practical interest.

Equal amounts of the pigment primaries, cyan, magenta, and yellow should produce black. In practice, combining these colors for printing produces a muddy-looking black.

#### 4. Explain HSI color model.

When humans view a color object, we describe it by its hue, saturation, and brightness. Hue is a color attribute that describes a pure color (pure yellow, orange, or red), whereas saturation gives a measure of the degree to which a pure color is diluted by white light. Brightness is a subjective descriptor that is practically impossible to measure. It embodies the achromatic notion of intensity and is one of the key factors in describing color sensation.

Intensity (gray level) is a most useful descriptor of monochromatic images. This quantity definitely is measurable and easily interpretable. The HSI (hue, saturation, intensity) color model, decouples the intensity component from the color-carrying information (hue and saturation) in a color image. As a result, the HSI model is an ideal tool for developing image processing algorithms based on color descriptions that are natural and intuitive to humans.

In Fig 5.4 the primary colors are separated by  $120^\circ$ . The secondary colors are  $60^\circ$  from the primaries, which means that the angle between secondaries is also  $120^\circ$ . Figure 5.4(b) shows the same hexagonal shape and an arbitrary color point (shown as a dot). The hue of the point is determined by an angle from some reference point. Usually (but not always) an angle of  $0^\circ$  from the red axis designates 0 hue, and the hue increases counterclockwise from there. The saturation (distance from the vertical axis) is the length of the vector from the origin to the point. Note that the origin is defined by the intersection of the color plane with the vertical intensity axis. The important components of the HSI color space are the vertical intensity axis, the length of the vector to a color point, and the angle this vector makes with the red axis.

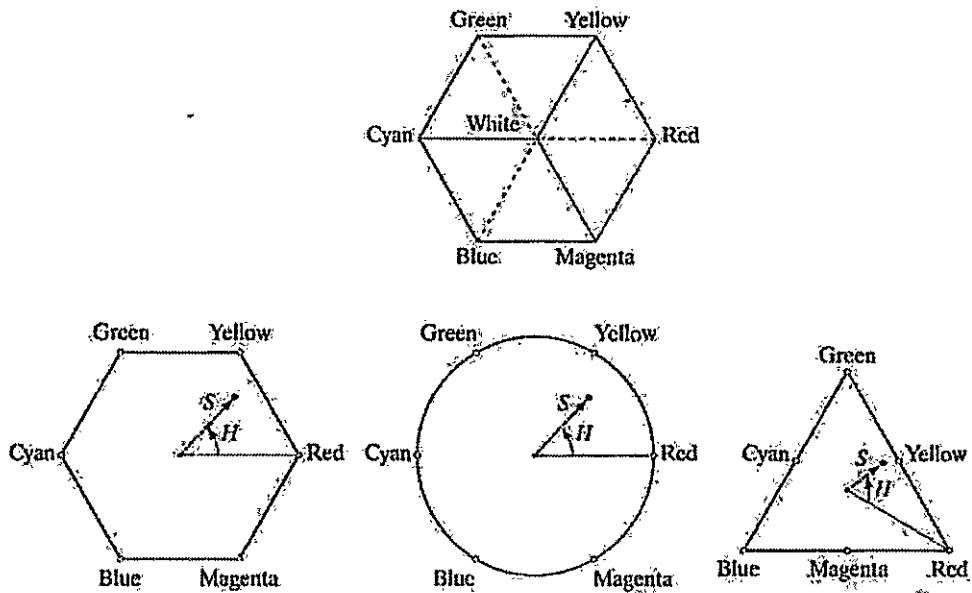


Fig 5.4 Hue and saturation in the HSI color model.

**6. Discuss procedure for conversion from RGB color model to HSI color model.**

Given an image in RGB color format, the H component of each RGB pixel is obtained using the equation

$$H = \begin{cases} \theta & \text{if } B \leq G \\ 360 - \theta & \text{if } B > G \end{cases} \quad (1)$$

With

$$\theta = \cos^{-1} \left\{ \frac{\frac{1}{2}[(R - G) + (R - B)]}{[(R - G)^2 + (R - B)(G - B)]^{1/2}} \right\} \quad (2)$$

The saturation component is given by

$$S = 1 - \frac{3}{(R + G + B)} [\min(R, G, B)]. \quad (3)$$

Finally, the intensity component is given by

$$I = \frac{1}{3}(R + G + B). \quad (4)$$

It is assumed that the RGB values have been normalized to the range [0, 1] and that angle  $\theta$  is measured with respect to the red axis of the HST space. Hue can be normalized to the range [0, 1] by dividing by  $360^\circ$  all values resulting from Eq. (1). The other two HSI components already are in this range if the given RGB values are in the interval [0, 1].

**7. Discuss procedure for conversion from HSI color model to RGB color model.**

Given values of HSI in the interval [0,1 ], one can find the corresponding RGB values in the same range. The applicable equations depend on the values of H. There are three sectors of interest, corresponding to the  $120^\circ$  intervals in the separation of primaries.\

**RG sector ( $0^\circ \leq H < 120^\circ$ ):**

When H is in this sector, the RGB components are given by the equations

$$B = I(1 - S)$$

$$G = 3I - (R + B)$$

$$R = I[1 + (S * \cos H / \cos(60^\circ - H))]$$

**GB sector ( $120^\circ \leq H < 240^\circ$ ):**

If the given value of H is in this sector, first subtract  $120^\circ$  from it.

$$H = H - 120^\circ$$

Then the RGB components are

$$R = I(1 - S)$$

$$B = 3I - (R + G)$$

$$G = I[1 + (S * \cos H / \cos(60^\circ - H))]$$

**BR sector ( $240^\circ \leq H \leq 360^\circ$ ):**

If H is in this range, subtract  $240^\circ$  from it

$$H = H - 240^\circ$$

Then the RGB components are

$$G = I(1 - S)$$

$$R = 3I - (B + G)$$

$$B = I [1 + (S * \cos H / \cos(60^\circ - H))]$$

### 8. Explain about pseudocolor image processing.

Pseudocolor (also called false color) image processing consists of assigning colors to gray values based on a specified criterion. The term pseudo or false color is used to differentiate the process of assigning colors to monochrome images from the processes associated with true color images. The process of gray level to color transformations is known as pseudocolor image processing.

The two techniques used for pseudocolor image processing are,

(i) Intensity Slicing

(ii) Gray Level to Color Transformation

(i) Intensity Slicing:

The technique of intensity (sometimes called density) slicing and color coding is one of the simplest examples of pseudocolor image processing. If an image is interpreted as a 3-D function (intensity versus spatial coordinates), the method can be viewed as one of placing planes parallel to the coordinate plane of the image; each plane then "slices" the function in the area of intersection. Figure 5.8 shows an example of using a plane at  $f(x, y) = l_1$  to slice the image function into two levels.

If a different color is assigned to each side of the plane shown in Fig. 5.8, any pixel whose gray level is above the plane will be coded with one color, and any pixel below the plane will be coded with the other. Levels that lie on the plane itself may be arbitrarily assigned one of the two colors. The result is a two-color image whose relative appearance can be controlled by moving the slicing plane up and down the gray-level axis.

In general, the technique may be summarized as follows. Let  $[0, L - 1]$  represent the gray scale, let level  $l_0$  represent black [ $f(x, y) = 0$ ], and level  $l_{L-1}$  represent white [ $f(x, y) = L - 1$ ]. Suppose that  $P$  planes perpendicular to the intensity axis are defined at levels  $l_1, l_2, \dots, l_p$ . Then, assuming that  $0 < P < L - 1$ , the  $P$  planes partition the gray scale into  $P + 1$  intervals,  $V_1, V_2, \dots, V_{P+1}$ . Gray-level to color assignments are made according to the relation

$$f(x, y) = C_k \quad \text{if } f(x, y) \in V_k$$

where  $C_k$  is the color associated with the  $k$ th intensity interval  $V_k$  defined by the partitioning planes at  $l = k - 1$  and  $l = k$ .

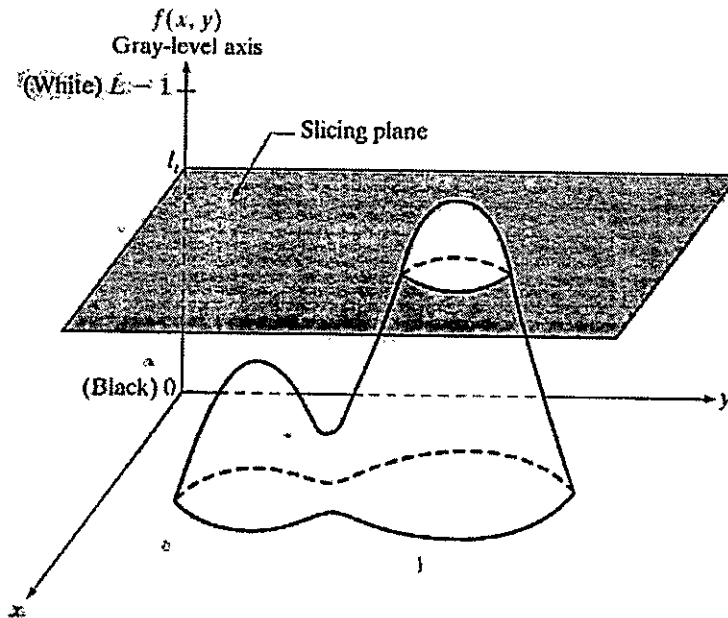


Fig 5.8.1 Geometric interpretation of the intensity-slicing technique.

The idea of planes is useful primarily for a geometric interpretation of the intensity-slicing technique. Figure 5.8.2 shows an alternative representation that defines the same mapping as in Fig. 5.8.1. According to the mapping function shown in Fig. 5.8.2, any input gray level is assigned one of two colors, depending on whether it is above or below the value of  $l_i$ . When more levels are used, the mapping function takes on a staircase form.

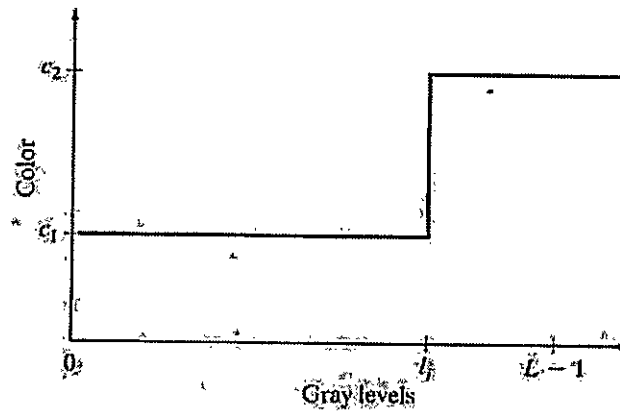


Fig 5.8.2 An alternative representation of the intensity-slicing technique.

**(ii) Gray Level to Color Transformation:**

The idea underlying this approach is to perform three independent transformations on the gray level of any input pixel. The three results are then fed separately into the red, green, and blue channels of a color television monitor. This method produces a composite image whose color content is modulated by the nature of the transformation functions. Note that these are transformations on the gray-level values of an image and are not functions of position.

In intensity slicing, piecewise linear functions of the gray levels are used to generate colors. On the other hand, this method can be based on smooth, nonlinear functions, which, as might be expected, gives the technique considerable flexibility.

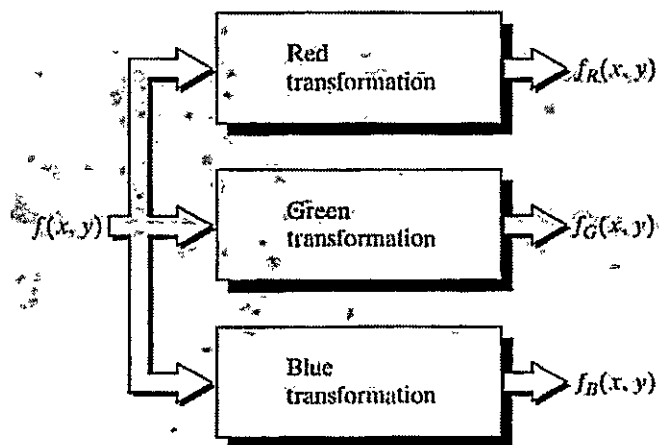


Fig. 5.8.3 Functional block diagram for pseudocolor image processing.

The output of each transformation is a composite image.

**9. Write about the basics of full color image processing.**

Full-color image processing approaches fall into two major categories. In the first category, each component image is processed individually and then form a composite processed color image from the individually processed components. In the second category, one works with color pixels directly. Because full-color images have at least three components, color pixels really are vectors. For example, in the RGB system, each color point can be interpreted as a vector extending from the origin to that point in the RGB coordinate system.

Let  $c$  represent an arbitrary vector in RGB color space:



$$c = \begin{bmatrix} c_R \\ c_G \\ c_B \end{bmatrix} = \begin{bmatrix} R \\ G \\ B \end{bmatrix} \quad (1)$$

This equation indicates that the components of  $c$  are simply the RGB components of a color image at a point. If the color components are a function of coordinates  $(x, y)$  by using the notation

$$c(x, y) = \begin{bmatrix} c_R(x, y) \\ c_G(x, y) \\ c_B(x, y) \end{bmatrix} = \begin{bmatrix} R(x, y) \\ G(x, y) \\ B(x, y) \end{bmatrix} \quad (2)$$

For an image of size  $M \times N$ , there are  $MN$  such vectors,  $c(x, y)$ , for  $x = 0, 1, 2, \dots, M-1$ ;  $y = 0, 1, 2, \dots, N-1$ .

It is important to keep clearly in mind that Eq. (2) depicts a vector whose components are spatial variables in  $x$  and  $y$ .

In order for per-color-component and vector-based processing to be equivalent, two conditions have to be satisfied: First, the process has to be applicable to both vectors and scalars. Second, the operation on each component of a vector must be independent of the other components.

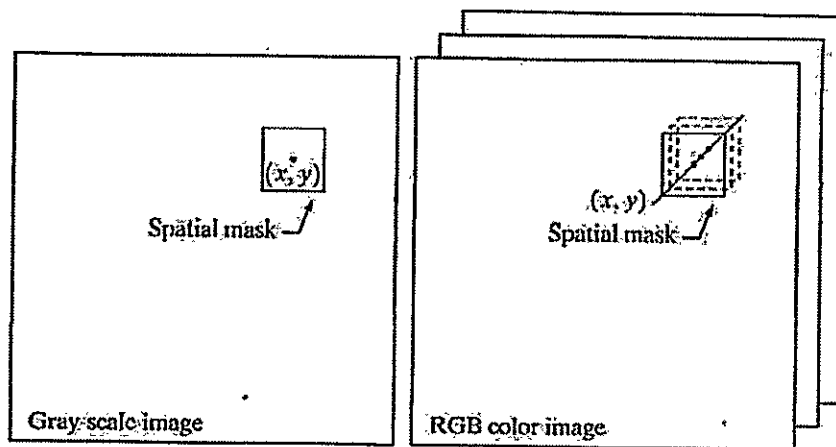


Fig 9 Spatial masks for gray-scale and RGB color images.

Fig 9 shows neighborhood spatial processing of gray-scale and full-color images. Suppose that the process is neighborhood averaging. In Fig. 9(a), averaging would be

accomplished by summing the gray levels of all the pixels in the neighborhood and dividing by the total number of pixels in the neighborhood. In Fig. 9(b), averaging would be done by summing all the vectors in the neighborhood and dividing each component by the total number of vectors in the neighborhood. But each component of the average vector is the sum of the pixels in the image corresponding to that component, which is the same as the result that would be obtained if the averaging were done on a per-color-component basis and then the vector was formed.

**10. Explain about color segmentation process.**

Segmentation is a process that partitions an image into regions and partitioning an image into regions based on color is known as color segmentation.

**Segmentation in HSI Color Space:**

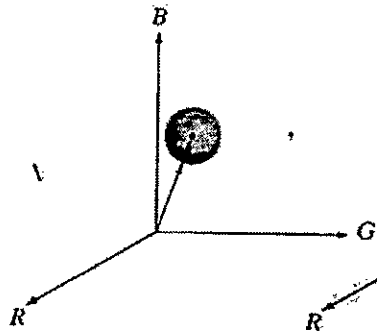
If anybody want to segment an image based on color, and in addition, to carry out the process on individual planes, it is natural to think first of the HSI space because color is conveniently represented in the hue image. Typically, saturation is used as a masking image in order to isolate further regions of interest in the hue image. The intensity image is used less frequently for segmentation of color images because it carries no color information.

**Segmentation in RGB Vector Space:**

Although, working in HSI space is more intuitive, segmentation is one area in which better results generally are obtained by using RGB color vectors. The approach is straightforward. Suppose that the objective is to segment objects of a specified color range in an RGB image. Given a set of sample color points representative of the colors of interest, we obtain an estimate of the "average" color that we wish to segment. Let this average color be denoted by the RGB vector  $\mathbf{a}$ . The objective of segmentation is to classify each RGB pixel in a given image as having a color in the specified range or not. In order to perform this comparison, it is necessary to have a measure of similarity. One of the simplest measures is the Euclidean distance. Let  $\mathbf{z}$  denote an arbitrary point in RGB space.  $\mathbf{z}$  is similar to  $\mathbf{a}$  if the distance between them is less than a specified threshold,  $D_0$ . The Euclidean distance between  $\mathbf{z}$  and  $\mathbf{a}$  is given by

$$\begin{aligned} D(\mathbf{z}, \mathbf{a}) &= \|\mathbf{z} - \mathbf{a}\| \\ &= [(\mathbf{z} - \mathbf{a})^T(\mathbf{z} - \mathbf{a})]^{1/2} \\ &= [(z_R - a_R)^2 + (z_G - a_G)^2 + (z_B - a_B)^2]^{1/2} \end{aligned}$$

where the subscripts R, G, and B, denote the RGB components of vectors  $\mathbf{a}$  and  $\mathbf{z}$ . The locus of points such that  $D(\mathbf{z}, \mathbf{a}) \leq D_0$  is a solid sphere of radius  $D_0$ .



Points contained within or on the surface of the sphere satisfy the specified color criterion; points outside the sphere do not. Coding these two sets of points in the image with, say, black and white, produces a binary segmented image.

A useful generalization of previous equation is a distance measure of the form

$$D(\mathbf{z}, \mathbf{a}) = [(\mathbf{z}-\mathbf{a})^T \mathbf{C}^{-1} (\mathbf{z}-\mathbf{a})]^{1/2}$$

where  $\mathbf{C}$  is the covariance matrix of the samples representative of the color to be segmented.

The above equation represents an ellipse with color points such that  $D(\mathbf{z}, \mathbf{a}) \leq D_0$ .

**1. Define image compression. Explain about the redundancies in a digital image.**

The term data compression refers to the process of reducing the amount of data required to represent a given quantity of information. A clear distinction must be made between data and information. They are not synonymous. In fact, data are the means by which information is conveyed. Various amounts of data may be used to represent the same amount of information. Such might be the case, for example, if a long-winded individual and someone who is short and to the point were to relate the same story. Here, the information of interest is the story; words are the data used to relate the information. If the two individuals use a different number of words to tell the same basic story, two different versions of the story are created, and at least one includes nonessential data. That is, it contains data (or words) that either provide no relevant information or simply restate that which is already known. It is thus said to contain data redundancy.

Data redundancy is a central issue in digital image compression. It is not an abstract concept but a mathematically quantifiable entity. If  $n_1$  and  $n_2$  denote the number of information-carrying units in two data sets that represent the same information, the relative data redundancy  $R_D$  of the first data set (the one characterized by  $n_1$ ) can be defined as

$$R_D = 1 - \frac{1}{C_R}$$

where  $C_R$ , commonly called the compression ratio, is

$$C_R = \frac{n_1}{n_2}$$

For the case  $n_2 = n_1$ ,  $C_R = 1$  and  $R_D = 0$ , indicating that (relative to the second data set) the first representation of the information contains no redundant data. When  $n_2 \ll n_1$ ,  $C_R \rightarrow \infty$  and  $R_D \rightarrow 1$ , implying significant compression and highly redundant data. Finally, when  $n_2 \gg n_1$ ,  $C_R \rightarrow 0$  and  $R_D \rightarrow \infty$ , indicating that the second data set contains much more data than the original representation. This, of course, is the normally undesirable case of data expansion. In general,  $C_R$  and  $R_D$  lie in the open intervals  $(0, \infty)$  and  $(-\infty, 1)$ , respectively. A practical compression ratio, such as 10 (or 10:1), means that the first data set has 10 information carrying units (say, bits) for every 1 unit in the second or compressed data set. The corresponding redundancy of 0.9 implies that 90% of the data in the first data set is redundant.

In digital image compression, three basic data redundancies can be identified and exploited: **coding redundancy**, **interpixel redundancy**, and **psychovisual redundancy**. Data compression is achieved when one or more of these redundancies are reduced or eliminated.

**Coding Redundancy:**

In this, we utilize formulation to show how the gray-level histogram of an image also can provide a great deal of insight into the construction of codes to reduce the amount of data used to represent it.

Let us assume, once again, that a discrete random variable  $r_k$  in the interval  $[0, 1]$  represents the gray levels of an image and that each  $r_k$  occurs with probability  $p_r(r_k)$ .

$$p_r(r_k) = \frac{n_k}{n} \quad k = 0, 1, 2, \dots, L - 1$$

where  $L$  is the number of gray levels,  $n_k$  is the number of times that the  $k$ th gray level appears in the image, and  $n$  is the total number of pixels in the image. If the number of bits used to represent each value of  $r_k$  is  $l(r_k)$ , then the average number of bits required to represent each pixel is

$$L_{avg} = \sum_{k=0}^{L-1} l(r_k) p_r(r_k).$$

That is, the average length of the code words assigned to the various gray-level values is found by summing the product of the number of bits used to represent each gray level and the probability that the gray level occurs. Thus the total number of bits required to code an  $M \times N$  image is  $MNL_{avg}$ .

**Interpixel Redundancy:**

Consider the images shown in Figs. 1.1(a) and (b). As Figs. 1.1(c) and (d) show, these images have virtually identical histograms. Note also that both histograms are trimodal, indicating the presence of three dominant ranges of gray-level values. Because the gray levels in these images are not equally probable, variable-length coding can be used to reduce the coding redundancy that would result from a straight or natural binary encoding of their pixels. The coding process, however, would not alter the level of correlation between the pixels within the images. In other words, the codes used to represent the gray levels of each image have nothing to do with the correlation between pixels. These correlations result from the structural or geometric relationships between the objects in the image.

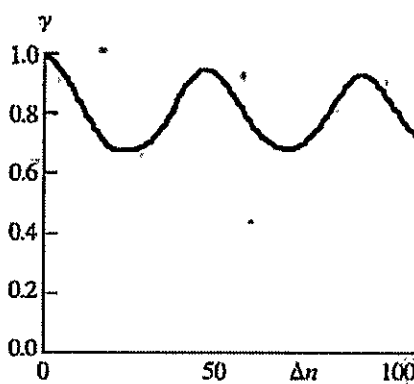
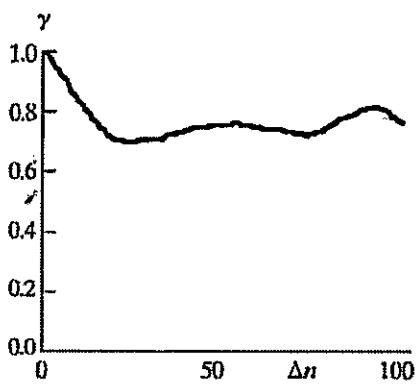
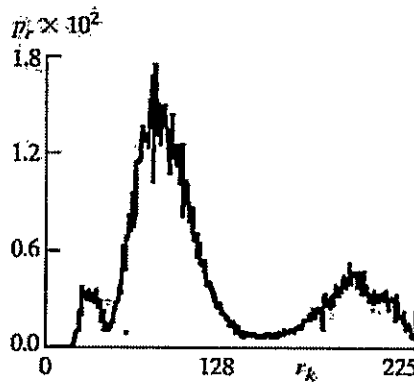
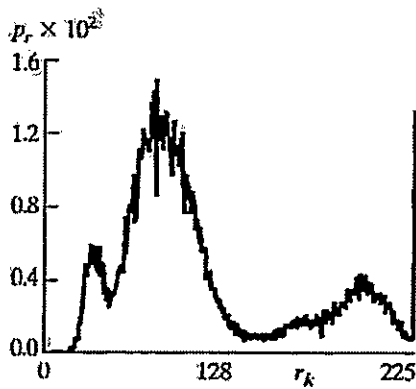
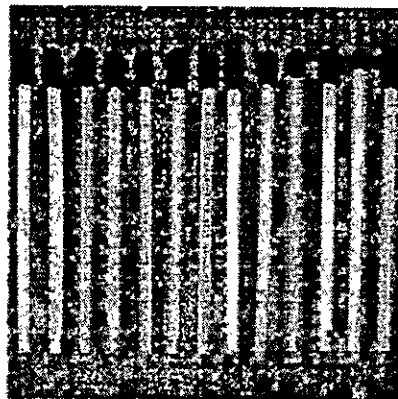
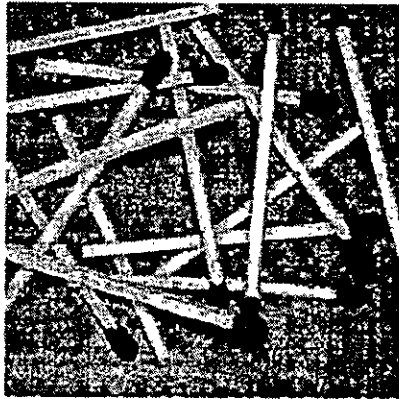


Fig.1.1 Two images and their gray-level histograms and normalized autocorrelation coefficients along one line.

Figures 1.1(e) and (f) show the respective autocorrelation coefficients computed along one line of each image.

$$\gamma(\Delta n) = \frac{A(\Delta n)}{A(0)}$$

where

$$A(\Delta n) = \frac{1}{N - \Delta n} \sum_{y=0}^{N-1-\Delta n} f(x, y)f(x, y + \Delta n).$$

The scaling factor in Eq. above accounts for the varying number of sum terms that arise for each integer value of  $\Delta n$ . Of course,  $\Delta n$  must be strictly less than  $N$ , the number of pixels on a line. The variable  $x$  is the coordinate of the line used in the computation. Note the dramatic difference between the shape of the functions shown in Figs. 1.1(e) and (f). Their shapes can be qualitatively related to the structure in the images in Figs. 1.1(a) and (b). This relationship is particularly noticeable in Fig. 1.1 (f), where the high correlation between pixels separated by 45 and 90 samples can be directly related to the spacing between the vertically oriented matches of Fig. 1.1(b). In addition, the adjacent pixels of both images are highly correlated. When  $\Delta n$  is 1,  $\gamma$  is 0.9922 and 0.9928 for the images of Figs. 1.1 (a) and (b), respectively. These values are typical of most properly sampled television images.

These illustrations reflect another important form of data redundancy—one directly related to the interpixel correlations within an image. Because the value of any given pixel can be reasonably predicted from the value of its neighbors, the information carried by individual pixels is relatively small. Much of the visual contribution of a single pixel to an image is redundant; it could have been guessed on the basis of the values of its neighbors. A variety of names, including spatial redundancy, geometric redundancy, and interframe redundancy, have been coined to refer to these interpixel dependencies. We use the term interpixel redundancy to encompass them all.

In order to reduce the interpixel redundancies in an image, the 2-D pixel array normally used for human viewing and interpretation must be transformed into a more efficient (but usually "nonvisual") format. For example, the differences between adjacent pixels can be used to represent an image. Transformations of this type (that is, those that remove interpixel redundancy) are referred to as mappings. They are called reversible mappings if the original image elements can be reconstructed from the transformed data set.

**Psychovisual Redundancy:**

The brightness of a region, as perceived by the eye, depends on factors other than simply the light reflected by the region. For example, intensity variations (Mach bands) can be perceived in an area of constant intensity. Such phenomena result from the fact that the eye does not respond with equal sensitivity to all visual information. Certain information simply has less relative importance than other information in normal visual processing. This information is said to be psychovisually redundant. It can be eliminated without significantly impairing the quality of image perception.

That psychovisual redundancies exist should not come as a surprise, because human perception of the information in an image normally does not involve quantitative analysis of every pixel value in the image. In general, an observer searches for distinguishing features such as edges or textural regions and mentally combines them into recognizable groupings. The brain then correlates these groupings with prior knowledge in order to complete the image interpretation process. Psychovisual redundancy is fundamentally different from the redundancies discussed earlier. Unlike coding and interpixel redundancy, psychovisual redundancy is associated with real or quantifiable visual information. Its elimination is possible only because the information itself is not essential for normal visual processing. Since the elimination of psychovisually redundant data results in a loss of quantitative information, it is commonly referred to as quantization.

This terminology is consistent with normal usage of the word, which generally means the mapping of a broad range of input values to a limited number of output values. As it is an irreversible operation (visual information is lost), quantization results in lossy data compression.

**2. Explain about fidelity criterion.**

The removal of psychovisually redundant data results in a loss of real or quantitative visual information. Because information of interest may be lost, a repeatable or reproducible means of quantifying the nature and extent of information loss is highly desirable. Two general classes of criteria are used as the basis for such an assessment:

- A) Objective fidelity criteria and
- B) Subjective fidelity criteria.



When the level of information loss can be expressed as a function of the original or input image and the compressed and subsequently decompressed output image, it is said to be based on an objective fidelity criterion. A good example is the root-mean-square (rms) error between an input and output image. Let  $f(x, y)$  represent an input image and let  $\hat{f}(x, y)$  denote an estimate or approximation of  $f(x, y)$  that results from compressing and subsequently decompressing the input. For any value of  $x$  and  $y$ , the error  $e(x, y)$  between  $f(x, y)$  and  $\hat{f}(x, y)$  can be defined as

$$e(x, y) = \hat{f}(x, y) - f(x, y)$$

so that the total error between the two images is

$$\sum_{x=0}^{M-1} \sum_{y=0}^{N-1} [\hat{f}(x, y) - f(x, y)]$$

where the images are of size  $M \times N$ . The root-mean-square error,  $e_{\text{rms}}$ , between  $\hat{f}(x, y)$  and  $f(x, y)$  then is the square root of the squared error averaged over the  $M \times N$  array, or

$$e_{\text{rms}} = \left[ \frac{1}{MN} \sum_{x=0}^{M-1} \sum_{y=0}^{N-1} [\hat{f}(x, y) - f(x, y)]^2 \right]^{1/2}$$

A closely related objective fidelity criterion is the mean-square signal-to-noise ratio of the compressed-decompressed image. If  $\hat{f}(x, y)$  is considered to be the sum of the original image  $f(x, y)$  and a noise signal  $e(x, y)$ , the mean-square signal-to-noise ratio of the output image, denoted  $\text{SNR}_{\text{rms}}$ , is

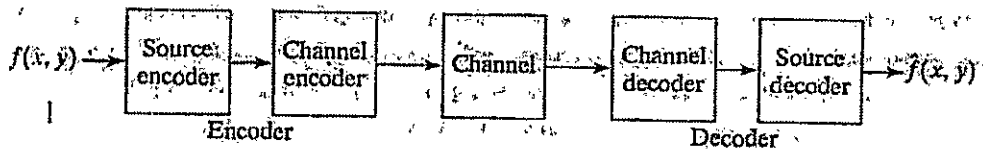
$$\text{SNR}_{\text{rms}} = \frac{\sum_{x=0}^{M-1} \sum_{y=0}^{N-1} f(x, y)^2}{\sum_{x=0}^{M-1} \sum_{y=0}^{N-1} [\hat{f}(x, y) - f(x, y)]^2}$$

The rms value of the signal-to-noise ratio, denoted  $\text{SNR}_{\text{rms}}$ , is obtained by taking the square root of Eq. above.

Although objective fidelity criteria offer a simple and convenient mechanism for evaluating information loss, most decompressed images ultimately are viewed by humans. Consequently, measuring image quality by the subjective evaluations of a human observer often is more appropriate. This can be accomplished by showing a "typical" decompressed image to an appropriate cross section of viewers and averaging their evaluations. The evaluations may be made using an absolute rating scale or by means of side-by-side comparisons of  $f(x, y)$  and  $\hat{f}(x, y)$ .

**3. Explain about image compression models.**

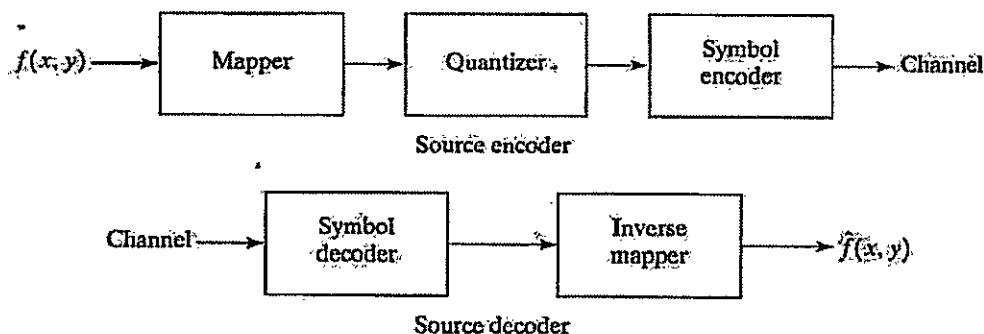
Fig. 3.1 shows, a compression system consists of two distinct structural blocks: an encoder and a decoder. An input image  $f(x, y)$  is fed into the encoder, which creates a set of symbols from the input data. After transmission over the channel, the encoded representation is fed to the decoder, where a reconstructed output image  $\hat{f}(x, y)$  is generated. In general,  $\hat{f}(x, y)$  may or may not be an exact replica of  $f(x, y)$ . If it is, the system is error free or information preserving; if not, some level of distortion is present in the reconstructed image. Both the encoder and decoder shown in Fig. 3.1 consist of two relatively independent functions or subblocks. The encoder is made up of a source encoder, which removes input redundancies, and a channel encoder, which increases the noise immunity of the source encoder's output. As would be expected, the decoder includes a channel decoder followed by a source decoder. If the channel between the encoder and decoder is noise free (not prone to error), the channel encoder and decoder are omitted, and the general encoder and decoder become the source encoder and decoder, respectively.



**Fig.3.1 A general compression system model**

**The Source Encoder and Decoder:**

The source encoder is responsible for reducing or eliminating any coding, interpixel, or psychovisual redundancies in the input image. The specific application and associated fidelity requirements dictate the best encoding approach to use in any given situation. Normally, the approach can be modeled by a series of three independent operations. As Fig. 3.2 (a) shows, each operation is designed to reduce one of the three redundancies. Figure 3.2 (b) depicts the corresponding source decoder. In the first stage of the source encoding process, the mapper transforms the input data into a (usually nonvisual) format designed to reduce interpixel redundancies in the input image. This operation generally is reversible and may or may not reduce directly the amount of data required to represent the image.



(a)  
(b)

Fig.3.2 (a) Source encoder and (b) source decoder model

Run-length coding is an example of a mapping that directly results in data compression in this initial stage of the overall source encoding process. The representation of an image by a set of transform coefficients is an example of the opposite case. Here, the mapper transforms the image into an array of coefficients, making its interpixel redundancies more accessible for compression in later stages of the encoding process.

The second stage, or quantizer block in Fig. 3.2 (a), reduces the accuracy of the mapper's output in accordance with some preestablished fidelity criterion. This stage reduces the psychovisual redundancies of the input image. This operation is irreversible. Thus it must be omitted when error-free compression is desired.

In the third and final stage of the source encoding process, the symbol coder creates a fixed- or variable-length code to represent the quantizer output and maps the output in accordance with the code. The term symbol coder distinguishes this coding operation from the overall source encoding process. In most cases, a variable-length code is used to represent the mapped and quantized data set. It assigns the shortest code words to the most frequently occurring output values and thus reduces coding redundancy. The operation, of course, is reversible. Upon completion of the symbol coding step, the input image has been processed to remove each of the three redundancies.

Figure 3.2(a) shows the source encoding process as three successive operations, but all three operations are not necessarily included in every compression system. Recall, for example, that the quantizer must be omitted when error-free compression is desired. In addition, some compression techniques normally are modeled by merging blocks that are physically separate in

Fig. 3.2(a). In the predictive compression systems, for instance, the mapper and quantizer are often represented by a single block, which simultaneously performs both operations.

The source decoder shown in Fig. 3.2(b) contains only two components: a symbol decoder and an inverse mapper. These blocks perform, in reverse order, the inverse operations of the source encoder's symbol encoder and mapper blocks. Because quantization results in irreversible information loss, an inverse quantizer block is not included in the general source decoder model shown in Fig. 3.2(b).

#### The Channel Encoder and Decoder:

The channel encoder and decoder play an important role in the overall encoding-decoding process when the channel of Fig. 3.1 is noisy or prone to error. They are designed to reduce the impact of channel noise by inserting a controlled form of redundancy into the source encoded data. As the output of the source encoder contains little redundancy, it would be highly sensitive to transmission noise without the addition of this "controlled redundancy." One of the most useful channel encoding techniques was devised by R. W. Hamming (Hamming [1950]). It is based on appending enough bits to the data being encoded to ensure that some minimum number of bits must change between valid code words. Hamming showed, for example, that if 3 bits of redundancy are added to a 4-bit word, so that the distance between any two valid code words is 3, all single-bit errors can be detected and corrected. (By appending additional bits of redundancy, multiple-bit errors can be detected and corrected.) The 7-bit Hamming (7, 4) code word  $h_1, h_2, h_3, \dots, h_6, h_7$  associated with a 4-bit binary number  $b_3b_2b_1b_0$  is

$$\begin{aligned} h_1 &= b_3 \oplus b_2 \oplus b_0 & h_3 &= b_3 \\ h_2 &= b_3 \oplus b_1 \oplus b_0 & h_5 &= b_2 \\ h_4 &= b_2 \oplus b_1 \oplus b_0 & h_6 &= b_1 \\ & & h_7 &= b_0 \end{aligned}$$

where  $\oplus$  denotes the exclusive OR operation. Note that bits  $h_1, h_2,$  and  $h_4$  are even-parity bits for the bit fields  $b_3 b_2 b_0, b_3 b_1 b_0,$  and  $b_2 b_1 b_0,$  respectively. (Recall that a string of binary bits has even parity if the number of bits with a value of 1 is even.) To decode a Hamming encoded result, the channel decoder must check the encoded value for odd parity over the bit fields in which even parity was previously established. A single-bit error is indicated by a nonzero parity word  $c_4c_2c_1,$  where

$$c_1 = h_1 \oplus h_3 \oplus h_5 \oplus h_7$$

$$c_2 = h_2 \oplus h_3 \oplus h_6 \oplus h_7$$

$$c_4 = h_4 \oplus h_5 \oplus h_6 \oplus h_7.$$

If a nonzero value is found, the decoder simply complements the code word bit position indicated by the parity word. The decoded binary value is then extracted from the corrected code word as  $h_3h_5h_6h_7$ .

#### 4. Explain a method of generating variable length codes with an example.

##### Variable-Length Coding:

The simplest approach to error-free image compression is to reduce only coding redundancy. Coding redundancy normally is present in any natural binary encoding of the gray levels in an image. It can be eliminated by coding the gray levels. To do so requires construction of a variable-length code that assigns the shortest possible code words to the most probable gray levels. Here, we examine several optimal and near optimal techniques for constructing such a code. These techniques are formulated in the language of information theory. In practice, the source symbols may be either the gray levels of an image or the output of a gray-level mapping operation (pixel differences, run lengths, and so on).

##### Huffman coding:

The most popular technique for removing coding redundancy is due to Huffman (Huffman [1952]). When coding the symbols of an information source individually, Huffman coding yields the smallest possible number of code symbols per source symbol. In terms of the noiseless coding theorem, the resulting code is optimal for a fixed value of  $n$ , subject to the constraint that the source symbols be coded one at a time.

The first step in Huffman's approach is to create a series of source reductions by ordering the probabilities of the symbols under consideration and combining the lowest probability symbols into a single symbol that replaces them in the next source reduction. Figure 4.1 illustrates this process for binary coding ( $K$ -ary Huffman codes can also be constructed). At the far left, a hypothetical set of source symbols and their probabilities are ordered from top to bottom in terms of decreasing probability values. To form the first source reduction, the bottom two probabilities, 0.06 and 0.04, are combined to form a "compound symbol" with probability 0.1. This compound symbol and its associated probability are placed in the first source reduction column so that the

probabilities of the reduced source are also ordered from the most to the least probable. This process is then repeated until a reduced source with two symbols (at the far right) is reached.

The second step in Huffman's procedure is to code each reduced source, starting with the smallest source and working back to the original source. The minimal length binary code for a two-symbol source, of course, is the symbols 0 and 1. As Fig. 4.2 shows, these symbols are assigned to the two symbols on the right (the assignment is arbitrary; reversing the order of the 0 and 1 would work just as well). As the reduced source symbol with probability 0.6 was generated by combining two symbols in the reduced source to its left, the 0 used to code it is now assigned to both of these symbols, and a 0 and 1 are arbitrarily

Original source		Source reduction			
Symbol	Probability	1	2	3	4
$a_2$	0.4	0.4	0.4	0.4	0.6
$a_6$	0.3	0.3	0.3	0.3	0.4
$a_1$	0.1	0.1	0.2	0.3	
$a_4$	0.1	0.1	0.1		
$a_3$	0.06	0.1			
$a_5$	0.04				

Fig.4.1 Huffman source reductions.

Original source			Source reduction			
Sym.	Prob.	Code	1	2	3	4
$a_2$	0.4	1	0.4	1	0.4	1
$a_6$	0.3	00	0.3	00	0.3	00
$a_1$	0.1	011	0.1	011	0.2	010
$a_4$	0.1	0100	0.1	0100	0.1	011
$a_3$	0.06	01010	0.1	0101		
$a_5$	0.04	01011				

Fig.4.2 Huffman code assignment procedure.

appended to each to distinguish them from each other. This operation is then repeated for each reduced source until the original source is reached. The final code appears at the far left in Fig. 4.2. The average length of this code is

$$L_{avg} = (0.4)(1) + (0.3)(2) + (0.1)(3) + (0.1)(4) + (0.06)(5) + (0.04)(5) \\ = 2.2 \text{ bits/symbol}$$

and the entropy of the source is 2.14 bits/symbol. The resulting Huffman code efficiency is 0.973.

Huffman's procedure creates the optimal code for a set of symbols and probabilities subject to the constraint that the symbols be coded one at a time. After the code has been created, coding and/or decoding is accomplished in a simple lookup table manner. The code itself is an instantaneous uniquely decodable block code. It is called a block code because each source symbol is mapped into a fixed sequence of code symbols. It is instantaneous, because each code word in a string of code symbols can be decoded without referencing succeeding symbols. It is uniquely decodable, because any string of code symbols can be decoded in only one way. Thus, any string of Huffman encoded symbols can be decoded by examining the individual symbols of the string in a left to right manner. For the binary code of Fig. 4.2, a left-to-right scan of the encoded string 010100111100 reveals that the first valid code word is 01010, which is the code for symbol  $a_3$ . The next valid code is 011, which corresponds to symbol  $a_1$ . Continuing in this manner reveals the completely decoded message to be  $a_3a_1a_2a_2a_6$ .

### 5. Explain arithmetic encoding process with an example.

Arithmetic coding:

Unlike the variable-length codes described previously, arithmetic coding generates nonblock codes. In arithmetic coding, which can be traced to the work of Elias, a one-to-one correspondence between source symbols and code words does not exist. Instead, an entire sequence of source symbols (or message) is assigned a single arithmetic code word. The code word itself defines an interval of real numbers between 0 and 1. As the number of symbols in the message increases, the interval used to represent it becomes smaller and the number of information units (say, bits) required to represent the interval becomes larger. Each symbol of the message reduces the size of the interval in accordance with its probability of occurrence. Because the technique does not require, as does Huffman's approach, that each source symbol translate into an integral number of code symbols (that is, that the symbols be coded one at a time), it achieves (but only in theory) the bound established by the noiseless coding theorem.

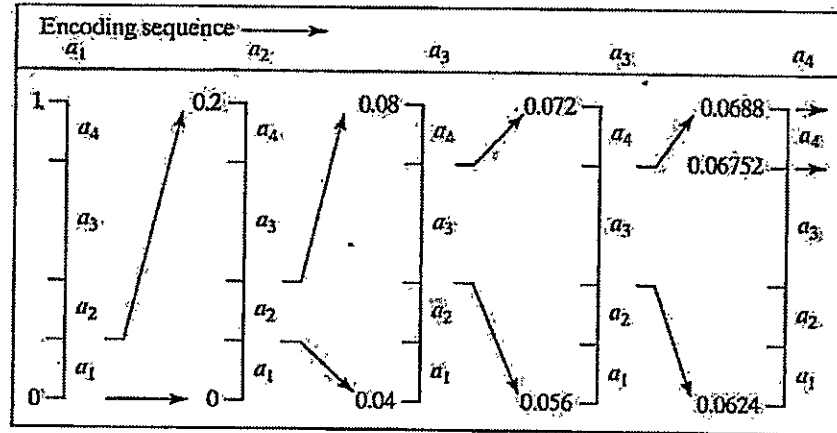


Fig.5.1 Arithmetic coding procedure

Figure 5.1 illustrates the basic arithmetic coding process. Here, a five-symbol sequence or message,  $a_1a_2a_3a_4$ , from a four-symbol source is coded. At the start of the coding process, the message is assumed to occupy the entire half-open interval  $[0, 1)$ . As Table 5.2 shows, this interval is initially subdivided into four regions based on the probabilities of each source symbol. Symbol  $a_x$ , for example, is associated with subinterval  $[0, 0.2)$ . Because it is the first symbol of the message being coded, the message interval is initially narrowed to  $[0, 0.2)$ . Thus in Fig. 5.1  $[0, 0.2)$  is expanded to the full height of the figure and its end points labeled by the values of the narrowed range. The narrowed range is then subdivided in accordance with the original source symbol probabilities and the process continues with the next message symbol.

Source Symbol	Probability	Initial Subinterval
$a_1$	0.2	$[0.0, 0.2)$
$a_2$	0.2	$[0.2, 0.4)$
$a_3$	0.4	$[0.4, 0.8)$
$a_4$	0.2	$[0.8, 1.0)$

Table 5.1 Arithmetic coding example

In this manner, symbol  $a_2$  narrows the subinterval to  $[0.04, 0.08)$ ,  $a_3$  further narrows it to  $[0.056, 0.072)$ , and so on. The final message symbol, which must be reserved as a special end-of-



message indicator, narrows the range to [0.06752, 0.0688). Of course, any number within this subinterval—for example, 0.068—can be used to represent the message.

In the arithmetically coded message of Fig. 5.1, three decimal digits are used to represent the five-symbol message. This translates into  $3/5$  or 0.6 decimal digits per source symbol and compares favorably with the entropy of the source, which is 0.58 decimal digits or 10-ary units/symbol. As the length of the sequence being coded increases, the resulting arithmetic code approaches the bound established by the noiseless coding theorem.

In practice, two factors cause coding performance to fall short of the bound: (1) the addition of the end-of-message indicator that is needed to separate one message from another; and (2) the use of finite precision arithmetic. Practical implementations of arithmetic coding address the latter problem by introducing a scaling strategy and a rounding strategy (Langdon and Rissanen [1981]). The scaling strategy renormalizes each subinterval to the [0, 1) range before subdividing it in accordance with the symbol probabilities. The rounding strategy guarantees that the truncations associated with finite precision arithmetic do not prevent the coding subintervals from being represented accurately.

## 6. Explain LZW coding with an example.

### LZW Coding:

The technique, called Lempel-Ziv-Welch (LZW) coding, assigns fixed-length code words to variable length sequences of source symbols but requires no a priori knowledge of the probability of occurrence of the symbols to be encoded. LZW compression has been integrated into a variety of mainstream imaging file formats, including the graphic interchange format (GIF), tagged image file format (TIFF), and the portable document format (PDF).

LZW coding is conceptually very simple (Welch [1984]). At the onset of the coding process, a codebook or "dictionary" containing the source symbols to be coded is constructed. For 8-bit monochrome images, the first 256 words of the dictionary are assigned to the gray values 0, 1, 2, ..., and 255. As the encoder sequentially examines the image's pixels, gray-level sequences that are not in the dictionary are placed in algorithmically determined (e.g., the next unused) locations. If the first two pixels of the image are white, for instance, sequence "255-255" might be assigned to location 256, the address following the locations reserved for gray levels 0 through 255. The next time that two consecutive white pixels are encountered, code word 256, the address of the location containing sequence 255-255, is used to represent them. If a 9-bit, 512-word dictionary is employed in the coding process, the original (8 + 8) bits that were used to represent the two pixels are replaced by a single 9-bit code word. Clearly, the size of the

**Digital Image Processing**

**Question & Answers**

dictionary is an important system parameter. If it is too small, the detection of matching gray-level sequences will be less likely; if it is too large, the size of the code words will adversely affect compression performance.

Consider the following 4 x 4, 8-bit image of a vertical edge:

39	39	126	126
39	39	126	126
39	39	126	126
39	39	126	126

Table 6.1 details the steps involved in coding its 16 pixels. A 512-word dictionary with the following starting content is assumed:

Dictionary Location	Entry
0	0
1	1
⋮	⋮
255	255
256	—
⋮	⋮
511	—

Locations 256 through 511 are initially unused. The image is encoded by processing its pixels in a left-to-right, top-to-bottom manner. Each successive gray-level value is concatenated with a variable—column 1 of Table 6.1—called the "currently recognized sequence." As can be seen, this variable is initially null or empty. The dictionary is searched for each concatenated sequence and if found, as was the case in the first row of the table, is replaced by the newly concatenated and recognized (i.e., located in the dictionary) sequence. This was done in column 1 of row 2.

Currently Recognized Sequence	Pixel Being Processed	Encoded Output	Dictionary Location (Code Word)	Dictionary Entry
	39			
39	39	39	256	39-39
39	126	39	257	39-126
126	126	126	258	126-126
126	39	126	259	126-39
39	39			
39-39	126	256	260	39-39-126
126	126			
126-126	39	258	261	126-126-39
39	39			
39-39	126			
39-39-126	126	260	262	39-39-126-126
126	39			
126-39	39	259	263	126-39-39
39	126			
39-126	126	257	264	39-126-126
126		126		

Table 6.1 LZW coding example

No output codes are generated, nor is the dictionary altered. If the concatenated sequence is not found, however, the address of the currently recognized sequence is output as the next encoded value, the concatenated but unrecognized sequence is added to the dictionary, and the currently recognized sequence is initialized to the current pixel value. This occurred in row 2 of the table. The last two columns detail the gray-level sequences that are added to the dictionary when scanning the entire 4 x 4 image. Nine additional code words are defined. At the conclusion of coding, the dictionary contains 265 code words and the LZW algorithm has successfully identified several repeating gray-level sequences—leveraging them to reduce the original 128-bit image to 90 bits (i.e., 10 9-bit codes). The encoded output is obtained by reading the third column from top to bottom. The resulting compression ratio is 1.42:1.

A unique feature of the LZW coding just demonstrated is that the coding dictionary or code book is created while the data are being encoded. Remarkably, an LZW decoder builds an identical decompression dictionary as it decodes simultaneously the encoded data stream. Although not needed in this example, most practical applications require a strategy for handling dictionary overflow. A simple solution is to flush or reinitialize the dictionary when it becomes full and continue coding with a new initialized dictionary. A more complex option is

to monitor compression performance and flush the dictionary when it becomes poor or unacceptable. Alternately, the least used dictionary entries can be tracked and replaced when necessary.

### 7. Explain the concept of bit plane coding method.

#### Bit-Plane Coding:

An effective technique for reducing an image's interpixel redundancies is to process the image's bit planes individually. The technique, called bit-plane coding, is based on the concept of decomposing a multilevel (monochrome or color) image into a series of binary images and compressing each binary image via one of several well-known binary compression methods.

#### Bit-plane decomposition:

The gray levels of an  $m$ -bit gray-scale image can be represented in the form of the base 2 polynomial

$$a_{m-1}2^{m-1} + a_{m-2}2^{m-2} + \dots + a_12^1 + a_02^0.$$

Based on this property, a simple method of decomposing the image into a collection of binary images is to separate the  $m$  coefficients of the polynomial into  $m$  1-bit bit planes. The zeroth-order bit plane is generated by collecting the  $a_0$  bits of each pixel, while the  $(m - 1)$  st-order bit plane contains the  $a_{m-1}$  bits or coefficients. In general, each bit plane is numbered from 0 to  $m-1$  and is constructed by setting its pixels equal to the values of the appropriate bits or polynomial coefficients from each pixel in the original image. The inherent disadvantage of this approach is that small changes in gray level can have a significant impact on the complexity of the bit planes. If a pixel of intensity 127 (01111111) is adjacent to a pixel of intensity 128 (10000000), for instance, every bit plane will contain a corresponding 0 to 1 (or 1 to 0) transition. For example, as the most significant bits of the two binary codes for 127 and 128 are different, bit plane 7 will contain a zero-valued pixel next to a pixel of value 1, creating a 0 to 1 (or 1 to 0) transition at that point.

An alternative decomposition approach (which reduces the effect of small gray-level variations) is to first represent the image by an  $m$ -bit Gray code. The  $m$ -bit Gray code  $g_{m-1} \dots g_2 g_1 g_0$  that corresponds to the polynomial in Eq. above can be computed from

$$g_i = a_i \oplus a_{i+1} \quad 0 \leq i \leq m-2$$

$$g_{m-1} = a_{m-1}$$

Here,  $\oplus$  denotes the exclusive OR operation. This code has the unique property that successive code words differ in only one bit position. Thus, small changes in gray level are less likely to affect all  $m$  bit planes. For instance, when gray levels 127 and 128 are adjacent, only the 7th bit plane will contain a 0 to 1 transition, because the Gray codes that correspond to 127 and 128 are 11000000 and 01000000, respectively.

## 8. Explain about lossless predictive coding.

### Lossless Predictive Coding:

The error-free compression approach does not require decomposition of an image into a collection of bit planes. The approach, commonly referred to as lossless predictive coding, is based on eliminating the interpixel redundancies of closely spaced pixels by extracting and coding only the new information in each pixel. The new information of a pixel is defined as the difference between the actual and predicted value of that pixel.

Figure 8.1 shows the basic components of a lossless predictive coding system. The system consists of an encoder and a decoder, each containing an identical predictor. As each successive pixel of the input image, denoted  $f_n$ , is introduced to the encoder, the predictor generates the anticipated value of that pixel based on some number of past inputs. The output of the predictor is then rounded to the nearest integer, denoted  $\hat{f}_n$  and used to form the difference or prediction error which is coded using a variable-length code (by the symbol encoder) to generate the next element of the compressed data stream.

$$e_n = f_n - \hat{f}_n$$

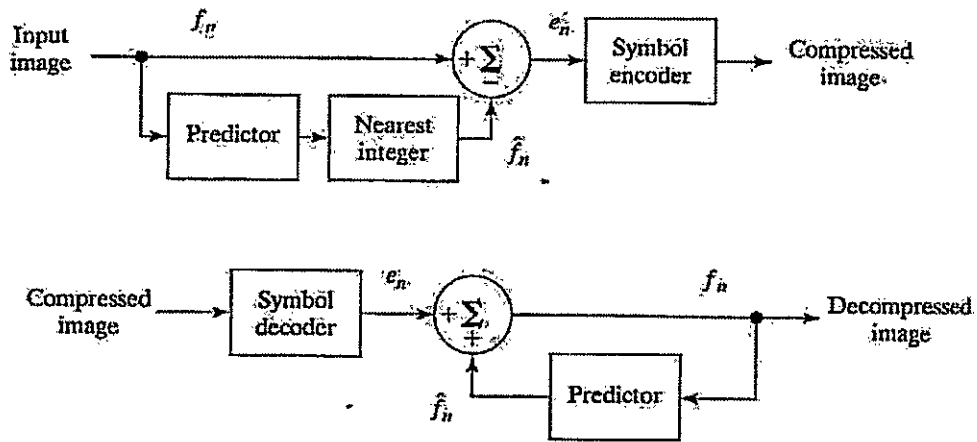


Fig.8.1 A lossless predictive coding model: (a) encoder; (b) decoder

The decoder of Fig. 8.1 (b) reconstructs  $e_n$  from the received variable-length code words and performs the inverse operation

$$\hat{f}_n = e_n + \hat{f}_n$$

Various local, global, and adaptive methods can be used to generate  $\hat{f}_n$ . In most cases, however, the prediction is formed by a linear combination of  $m$  previous pixels. That is,

$$\hat{f}_n = \text{round} \left[ \sum_{i=1}^m \alpha_i f_{n-i} \right]$$

where  $m$  is the order of the linear predictor,  $\text{round}$  is a function used to denote the rounding or nearest integer operation, and the  $\alpha_i$  for  $i = 1, 2, \dots, m$  are prediction coefficients. In raster scan applications, the subscript  $n$  indexes the predictor outputs in accordance with their time of occurrence. That is,  $f_n$ ,  $\hat{f}_n$  and  $e_n$  in Eqns. above could be replaced with the more explicit notation  $f(t)$ ,  $\hat{f}(t)$ , and  $e(t)$ , where  $t$  represents time. In other cases,  $n$  is used as an index on the spatial coordinates and/or frame number (in a time sequence of images) of an image. In 1-D linear predictive coding, for example, Eq. above can be written as

$$\hat{f}_n(x; y) = \text{round} \left[ \sum_{i=1}^m \alpha_i f(x, y - i) \right]$$

where each subscripted variable is now expressed explicitly as a function of spatial coordinates  $x$  and  $y$ . The Eq. indicates that the 1-D linear prediction  $f(x, y)$  is a function of the previous pixels on the current line alone. In 2-D predictive coding, the prediction is a function of the previous pixels in a left-to-right, top-to-bottom scan of an image. In the 3-D case, it is based on these pixels and the previous pixels of preceding frames. Equation above cannot be evaluated for the first  $m$  pixels of each line, so these pixels must be coded by using other means (such as a Huffman code) and considered as an overhead of the predictive coding process. A similar comment applies to the higher-dimensional cases.

**9. Explain about lossy predictive coding.**

**Lossy Predictive Coding:**

In this type of coding, we add a quantizer to the lossless predictive model and examine the resulting trade-off between reconstruction accuracy and compression performance. As Fig.9 shows, the quantizer, which absorbs the nearest integer function of the error-free encoder, is inserted between the symbol encoder and the point at which the prediction error is formed. It maps the prediction error into a limited range of outputs, denoted  $\hat{e}_n$  which establish the amount of compression and distortion associated with lossy predictive coding.

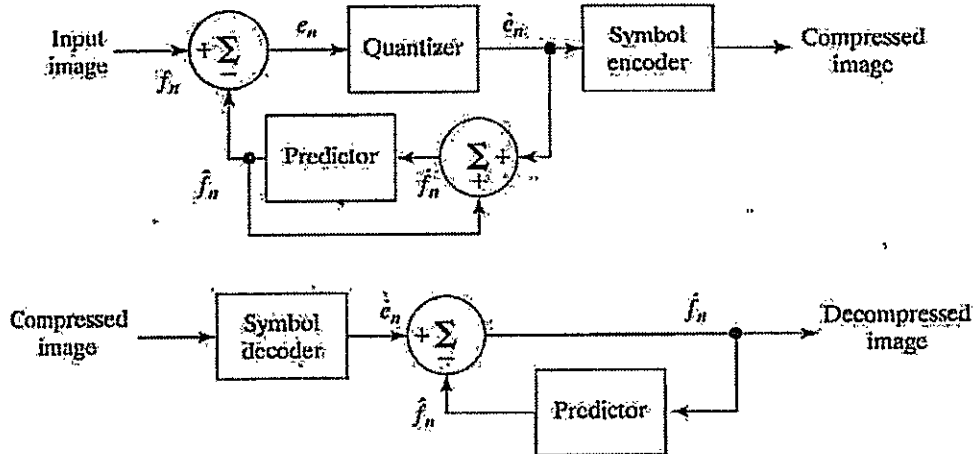


Fig. 9 A lossy predictive coding model: (a) encoder and (b) decoder.

In order to accommodate the insertion of the quantization step, the error-free encoder of figure must be altered so that the predictions generated by the encoder and decoder are equivalent. As Fig.9 (a) shows, this is accomplished by placing the lossy encoder's predictor within a feedback loop, where its input, denoted  $f_n$ , is generated as a function of past predictions and the corresponding quantized errors. That is,

$$\hat{f}_n = \hat{e}_n + \hat{f}_n$$

This closed loop configuration prevents error buildup at the decoder's output. Note from Fig. 9 (b) that the output of the decoder also is given by the above Eqn.

#### Optimal predictors:

The optimal predictor used in most predictive coding applications minimizes the encoder's mean-square prediction error

$$E\{e_n^2\} = E\{[f_n - \hat{f}_n]^2\}$$

subject to the constraint that

$$\hat{f}_n = \hat{e}_n + \hat{f}_n \approx e_n + \hat{f}_n = f_n$$

and

$$\hat{f}_n = \sum_{i=1}^m a_i f_{n-i}$$

That is, the optimization criterion is chosen to minimize the mean-square prediction error, the quantization error is assumed to be negligible ( $\hat{e}_n \approx e_n$ ), and the prediction is constrained to a linear combination of  $m$  previous pixels. These restrictions are not essential, but they simplify the analysis considerably and, at the same time, decrease the computational complexity of the predictor. The resulting predictive coding approach is referred to as differential pulse code modulation (DPCM).



**10. Explain with a block diagram about transform coding system.****Transform Coding:**

All the predictive coding techniques operate directly on the pixels of an image and thus are spatial domain methods. In this coding, we consider compression techniques that are based on modifying the transform of an image. In transform coding, a reversible, linear transform (such as the Fourier transform) is used to map the image into a set of transform coefficients, which are then quantized and coded. For most natural images, a significant number of the coefficients have small magnitudes and can be coarsely quantized (or discarded entirely) with little image distortion. A variety of transformations, including the discrete Fourier transform (DFT), can be used to transform the image data.

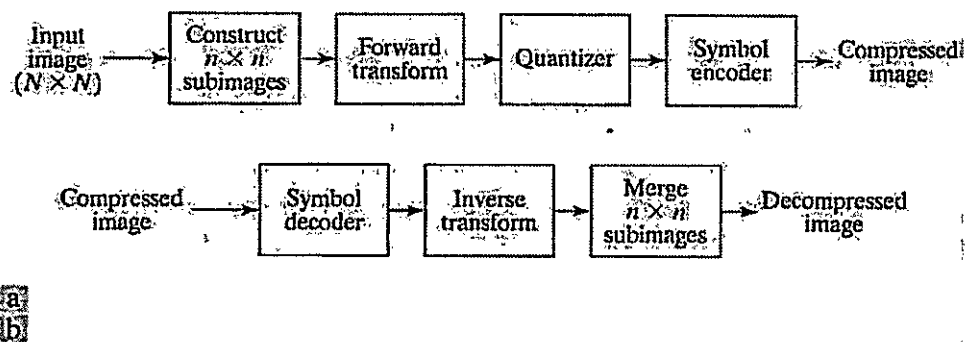


Fig. 10 A transform coding system: (a) encoder; (b) decoder.

Figure 10 shows a typical transform coding system. The decoder implements the inverse sequence of steps (with the exception of the quantization function) of the encoder, which performs four relatively straightforward operations: subimage decomposition, transformation, quantization, and coding. An  $N \times N$  input image first is subdivided into subimages of size  $n \times n$ , which are then transformed to generate  $(N/n)^2$  subimage transform arrays, each of size  $n \times n$ . The goal of the transformation process is to decorrelate the pixels of each subimage, or to pack as much information as possible into the smallest number of transform coefficients. The quantization stage then selectively eliminates or more coarsely quantizes the coefficients that carry the least information. These coefficients have the smallest impact on reconstructed subimage quality. The encoding process terminates by coding (normally using a variable-length code) the quantized coefficients. Any or all of the transform encoding steps can be adapted to

local image content, called adaptive transform coding, or fixed for all subimages, called nonadaptive transform coding.

### 11. Explain about wavelet coding.

#### Wavelet Coding:

The wavelet coding is based on the idea that the coefficients of a transform that decorrelates the pixels of an image can be coded more efficiently than the original pixels themselves. If the transform's basis functions—in this case wavelets—pack most of the important visual information into a small number of coefficients, the remaining coefficients can be quantized coarsely or truncated to zero with little image distortion.

Figure 11 shows a typical wavelet coding system. To encode a  $2^J \times 2^J$  image, an analyzing wavelet,  $\Psi$ , and minimum decomposition level,  $J - P$ , are selected and used to compute the image's discrete wavelet transform. If the wavelet has a complimentary scaling function  $\phi$ , the fast wavelet transform can be used. In either case, the computed transform converts a large portion of the original image to horizontal, vertical, and diagonal decomposition coefficients with zero mean and Laplacian-like distributions.

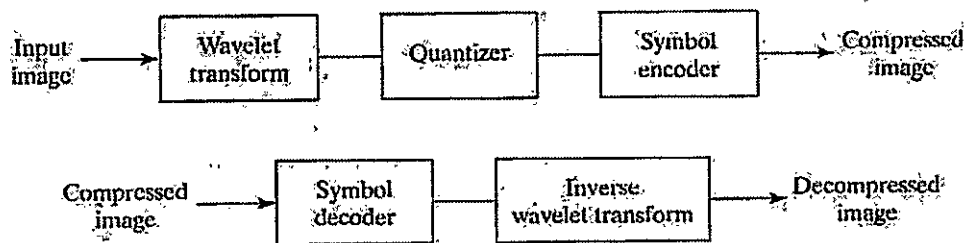


Fig.11 A wavelet coding system: (a) encoder; (b) decoder.

Since many of the computed coefficients carry little visual information, they can be quantized and coded to minimize intercoefficient and coding redundancy. Moreover, the quantization can be adapted to exploit any positional correlation across the  $P$  decomposition levels. One or more of the lossless coding methods, including run-length, Huffman, arithmetic, and bit-plane coding, can be incorporated into the final symbol coding step. Decoding is accomplished by inverting the encoding operations—with the exception of quantization, which cannot be reversed exactly.

The principal difference between the wavelet-based system and the transform coding system is the omission of the transform coder's subimage processing stages.

**Digital Image Processing**

**Question & Answers**

Because wavelet transforms are both computationally efficient and inherently local (i.e., their basis functions are limited in duration), subdivision of the original image is unnecessary.

### 1. What are the derivative operators useful in image segmentation? Explain their role in segmentation.

#### Gradient operators:

First-order derivatives of a digital image are based on various approximations of the 2-D gradient. The gradient of an image  $f(x, y)$  at location  $(x, y)$  is defined as the vector

$$\nabla f = \begin{bmatrix} G_x \\ G_y \end{bmatrix} = \begin{bmatrix} \frac{\partial f}{\partial x} \\ \frac{\partial f}{\partial y} \end{bmatrix}$$

It is well known from vector analysis that the gradient vector points in the direction of maximum rate of change of  $f$  at coordinates  $(x, y)$ . An important quantity in edge detection is the magnitude of this vector, denoted by  $|\nabla f|$ , where

$$|\nabla f| = \text{mag}(\nabla f) = [G_x^2 + G_y^2]^{1/2}$$

This quantity gives the maximum rate of increase of  $f(x, y)$  per unit distance in the direction of  $\nabla f$ . It is a common (although not strictly correct) practice to refer to  $|\nabla f|$  also as the gradient. The direction of the gradient vector also is an important quantity. Let  $\alpha(x, y)$  represent the direction angle of the vector  $\nabla f$  at  $(x, y)$ . Then, from vector analysis,

$$\alpha(x, y) = \tan^{-1} \left( \frac{G_y}{G_x} \right)$$

where the angle is measured with respect to the x-axis. The direction of an edge at  $(x, y)$  is perpendicular to the direction of the gradient vector at that point. Computation of the gradient of an image is based on obtaining the partial derivatives  $\partial f/\partial x$  and  $\partial f/\partial y$  at every pixel location. Let the 3x3 area shown in Fig. 1.1 (a) represent the gray levels in a neighborhood of an image. One of the simplest ways to implement a first-order partial derivative at point  $z_5$  is to use the following Roberts cross-gradient operators:

$$G_x = (z_4 - z_6)$$

and

$$G_y = (z_8 - z_2)$$

These derivatives can be implemented for an entire image by using the masks shown in Fig. 1.1(b). Masks of size 2 X 2 are awkward to implement because they do not have a clear center. An approach using masks of size 3 X 3 is given by

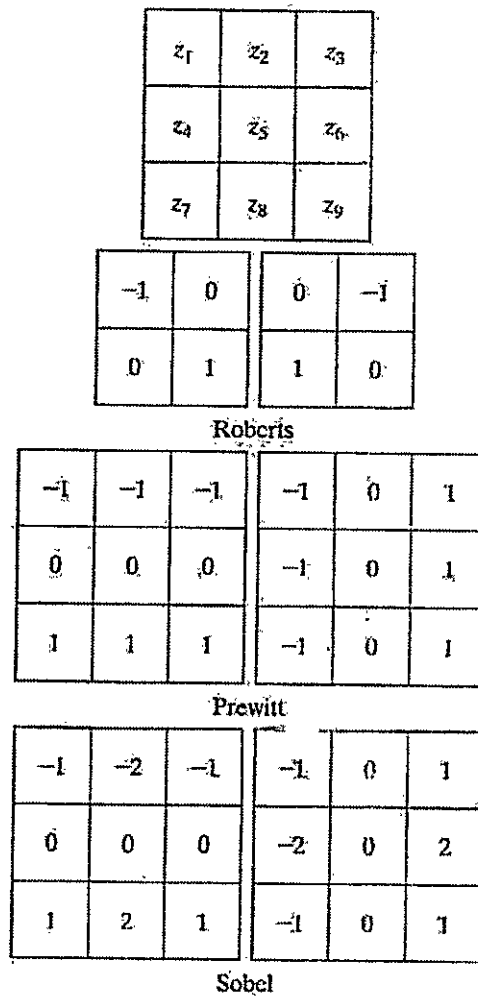


Fig.1.1 A 3 X 3 region of an image (the z's are gray-level values) and various masks used to compute the gradient at point labeled  $z_5$ .

$$\bar{G}_x = (z_7 + z_8 + z_9) - (z_1 + z_2 + z_3)$$

and

$$\bar{G}_y = (z_3 + z_6 + z_9) - (z_1 + z_4 + z_7)$$

A weight value of 2 is used to achieve some smoothing by giving more importance to the center point. Figures 1.1(f) and (g), called the Sobel operators, and are used to implement these two equations. The Prewitt and Sobel operators are among the most used in practice for computing digital gradients. The Prewitt masks are simpler to implement than the Sobel masks, but the latter have slightly superior noise-suppression characteristics, an important issue when dealing with derivatives. Note that the coefficients in all the masks shown in Fig. 1.1 sum to 0, indicating that they give a response of 0 in areas of constant gray level, as expected of a derivative operator.

The masks just discussed are used to obtain the gradient components  $G_x$  and  $G_y$ . Computation of the gradient requires that these two components be combined. However, this implementation is not always desirable because of the computational burden required by squares and square roots. An approach used frequently is to approximate the gradient by absolute values:

$$|\nabla f| \approx |G_x| + |G_y|$$

This equation is much more attractive computationally, and it still preserves relative changes in gray levels. However, this is not an issue when masks such as the Prewitt and Sobel masks are used to compute  $G_x$  and  $G_y$ .

It is possible to modify the 3 X 3 masks in Fig. 1.1 so that they have their strongest responses along the diagonal directions. The two additional Prewitt and Sobel masks for detecting discontinuities in the diagonal directions are shown in Fig. 1.2.

0	1	1	-1	-1	0
-1	0	1	-1	0	1
-1	-1	0	0	1	1

Prewitt

0	1	2	-2	-1	0
-1	0	1	-1	0	1
2	1	0	0	1	2

Sobel

-1	2	-1
0	0	0
1	2	1

Fig.1.2 Prewitt and Sobel masks for detecting diagonal edges

**The Laplacian:**

The Laplacian of a 2-D function  $f(x, y)$  is a second-order derivative defined as

$$\nabla^2 f = \frac{\partial^2 f}{\partial x^2} + \frac{\partial^2 f}{\partial y^2}$$

For a 3 X 3 region, one of the two forms encountered most frequently in practice is

$$\nabla^2 f = 4z_5 - (z_2 + z_4 + z_6 + z_8)$$

0	-1	0	-1	-1	-1
-1	4	-1	-1	8	-1
0	-1	0	-1	-1	-1

Fig.1.3 Laplacian masks used to implement Eqns. above.

where the z's are defined in Fig. 1.1(a). A digital approximation including the diagonal neighbors is given by

$$\nabla^2 f = 8z_5 - (z_1 + z_2 + z_3 + z_4 + z_6 + z_7 + z_8 + z_9)$$

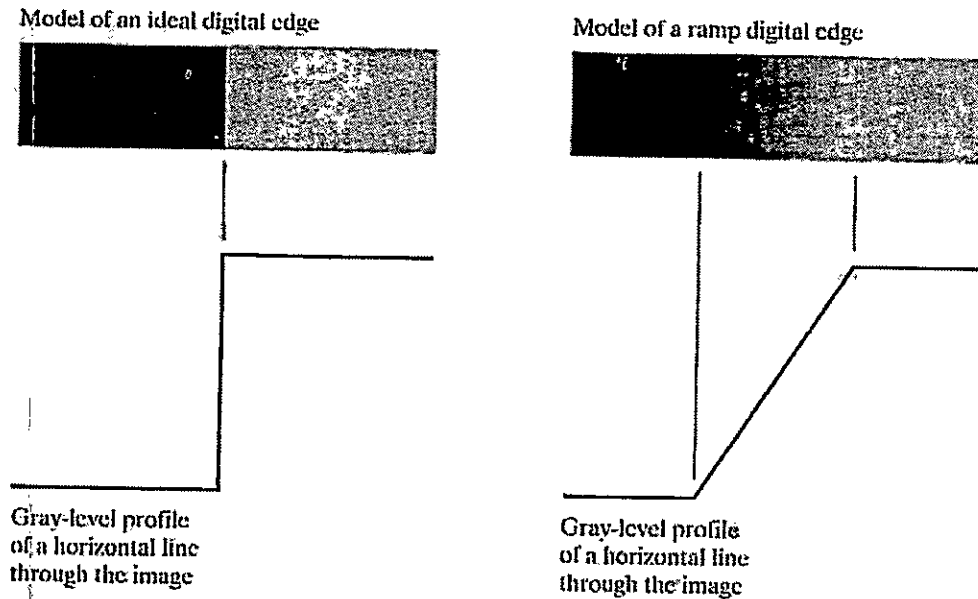
Masks for implementing these two equations are shown in Fig. 1.3. We note from these masks that the implementations of Eqns. are isotropic for rotation increments of 90° and 45°, respectively.

## 2. Write about edge detection.

Intuitively, an edge is a set of connected pixels that lie on the boundary between two regions. Fundamentally, an edge is a "local" concept whereas a region boundary, owing to the way it is defined, is a more global idea. A reasonable definition of "edge" requires the ability to measure gray-level transitions in a meaningful way. We start by modeling an edge intuitively. This will lead us to formalism in which "meaningful" transitions in gray levels can be measured. Intuitively, an ideal edge has the properties of the model shown in Fig. 2.1(a). An ideal edge according to this model is a set of connected pixels (in the vertical direction here), each of which is located at an orthogonal step transition in gray level (as shown by the horizontal profile in the figure).

In practice, optics, sampling, and other image acquisition imperfections yield edges that are blurred, with the degree of blurring being determined by factors such as the quality of the image acquisition system, the sampling rate, and illumination conditions under which the image is acquired. As a result, edges are more closely modeled as having a "ramp like" profile, such as the one shown in Fig.2.1 (b).





**Fig.2.1 (a) Model of an ideal digital edge (b) Model of a ramp edge. The slope of the ramp is proportional to the degree of blurring in the edge.**

The slope of the ramp is inversely proportional to the degree of blurring in the edge. In this model, we no longer have a thin (one pixel thick) path. Instead, an edge point now is any point contained in the ramp, and an edge would then be a set of such points that are connected. The "thickness" of the edge is determined by the length of the ramp, as it transitions from an initial to a final gray level. This length is determined by the slope, which, in turn, is determined by the degree of blurring. This makes sense: Blurred edges tend to be thick and sharp edges tend to be thin. Figure 2.2(a) shows the image from which the close-up in Fig. 2.1(b) was extracted. Figure 2.2(b) shows a horizontal gray-level profile of the edge between the two regions. This figure also shows the first and second derivatives of the gray-level profile. The first derivative is positive at the points of transition into and out of the ramp as we move from left to right along the profile; it is constant for points in the ramp; and is zero in areas of constant gray level. The second derivative is positive at the transition associated with the dark side of the edge, negative at the transition associated with the light side of the edge, and zero along the ramp and in areas of constant gray level. The signs of the derivatives in Fig. 2.2(b) would be reversed for an edge that transitions from light to dark.

We conclude from these observations that the magnitude of the first derivative can be used to detect the presence of an edge at a point in an image (i.e. to determine if a point is on a ramp). Similarly, the sign of the second derivative can be used to determine whether an edge pixel lies

on the dark or light side of an edge. We note two additional properties of the second derivative around an edge: A) It produces two values for every edge in an image (an undesirable feature); and B) an imaginary straight line joining the extreme positive and negative values of the second derivative would cross zero near the midpoint of the edge. This zero-crossing property of the second derivative is quite useful for locating the centers of thick edges.

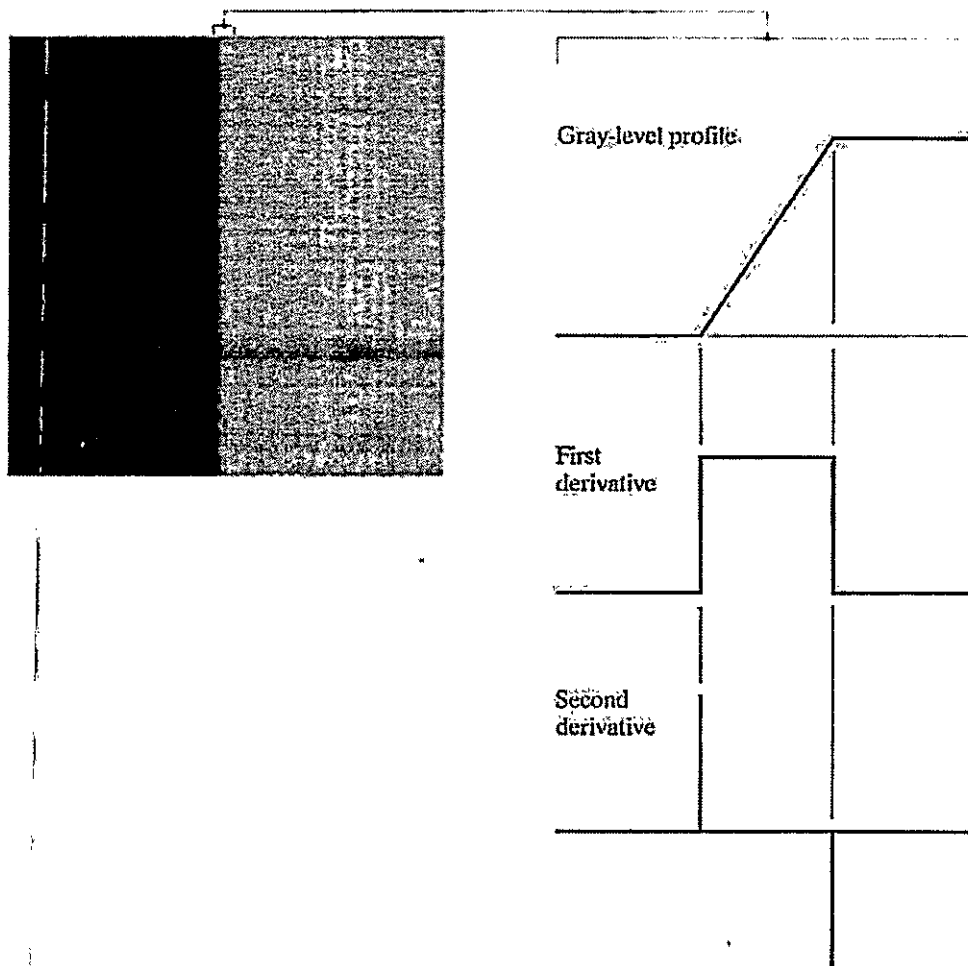


Fig.2.2 (a) Two regions separated by a vertical edge (b) Detail near the edge, showing a gray-level profile, and the first and second derivatives of the profile.

**3. Explain about the edge linking procedures.**

The different methods for edge linking are as follows

- (i) Local processing
- (ii) Global processing via the Hough Transform
- (iii) Global processing via graph-theoretic techniques.

**(i) Local Processing:**

One of the simplest approaches for linking edge points is to analyze the characteristics of pixels in a small neighborhood (say, 3 X 3 or 5 X 5) about every point (x, y) in an image that has been labeled an edge point. All points that are similar according to a set of predefined criteria are linked, forming an edge of pixels that share those criteria.

The two principal properties used for establishing similarity of edge pixels in this kind of analysis are (1) the strength of the response of the gradient operator used to produce the edge pixel; and (2) the direction of the gradient vector. The first property is given by the value of  $\nabla f$ .

Thus an edge pixel with coordinates  $(x_0, y_0)$  in a predefined neighborhood of  $(x, y)$ , is similar in magnitude to the pixel at  $(x, y)$  if

$$|\nabla f(x, y) - \nabla f(x_0, y_0)| \leq E$$

The direction (angle) of the gradient vector is given by Eq. An edge pixel at  $(x_0, y_0)$  in the predefined neighborhood of  $(x, y)$  has an angle similar to the pixel at  $(x, y)$  if

$$|\alpha(x, y) - \alpha(x_0, y_0)| \leq A$$

where A is a nonnegative angle threshold. The direction of the edge at  $(x, y)$  is perpendicular to the direction of the gradient vector at that point.

A point in the predefined neighborhood of  $(x, y)$  is linked to the pixel at  $(x, y)$  if both magnitude and direction criteria are satisfied. This process is repeated at every location in the image. A record must be kept of linked points as the center of the neighborhood is moved from pixel to pixel. A simple bookkeeping procedure is to assign a different gray level to each set of linked edge pixels.

**(ii) Global processing via the Hough Transform:**

In this process, points are linked by determining first if they lie on a curve of specified shape. We now consider global relationships between pixels. Given  $n$  points in an image, suppose that we want to find subsets of these points that lie on straight lines. One possible solution is to first find all lines determined by every pair of points and then find all subsets of points that are close to particular lines. The problem with this procedure is that it involves finding  $n(n-1)/2 \sim n^2$  lines and then performing  $(n)(n(n-1)/2) \sim n^3$  comparisons of every point to all lines. This approach is computationally prohibitive in all but the most trivial applications.

Hough [1962] proposed an alternative approach, commonly referred to as the Hough transform. Consider a point  $(x_i, y_i)$  and the general equation of a straight line in slope-intercept form,  $y_i = a.x_i + b$ . Infinitely many lines pass through  $(x_i, y_i)$  but they all satisfy the equation  $y_i = a.x_i + b$  for varying values of  $a$  and  $b$ . However, writing this equation as  $b = -a.x_i + y_i$ , and considering the  $ab$ -plane (also called parameter space) yields the equation of a single line for a fixed pair  $(x_i, y_i)$ . Furthermore, a second point  $(x_j, y_j)$  also has a line in parameter space associated with it, and this line intersects the line associated with  $(x_i, y_i)$  at  $(a', b')$ , where  $a'$  is the slope and  $b'$  the intercept of the line containing both  $(x_i, y_i)$  and  $(x_j, y_j)$  in the  $xy$ -plane. In fact, all points contained on this line have lines in parameter space that intersect at  $(a', b')$ . Figure 3.1 illustrates these concepts.

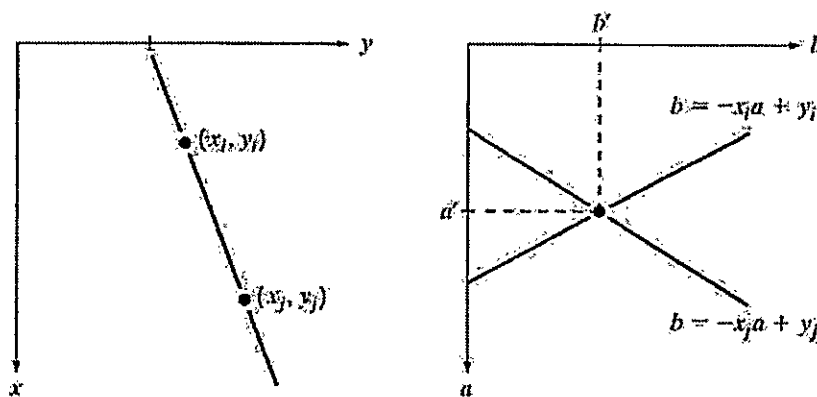


Fig.3.1 (a)  $xy$ -plane (b) Parameter space

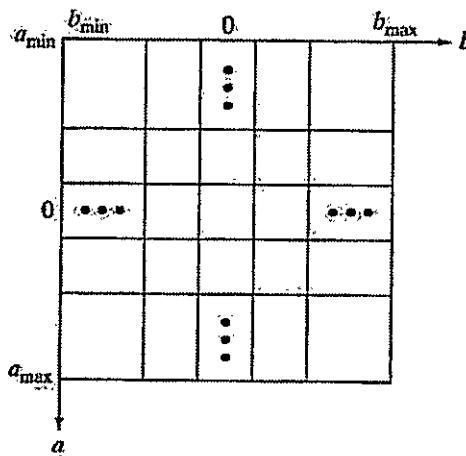


Fig.3.2 Subdivision of the parameter plane for use in the Hough transform

The computational attractiveness of the Hough transform arises from subdividing the parameter space into so-called accumulator cells, as illustrated in Fig. 3.2, where  $(a_{max}, a_{min})$  and  $(b_{max}, b_{min})$ , are the expected ranges of slope and intercept values. The cell at coordinates  $(i, j)$ , with accumulator value  $A(i, j)$ , corresponds to the square associated with parameter space coordinates  $(a_i, b_j)$ .

Initially, these cells are set to zero. Then, for every point  $(x_k, y_k)$  in the image plane, we let the parameter  $a$  equal each of the allowed subdivision values on the  $a$ -axis and solve for the corresponding  $b$  using the equation  $b = -x_k a + y_k$ . The resulting  $b$ 's are then rounded off to the nearest allowed value in the  $b$ -axis. If a choice of  $a_p$  results in solution  $b_q$ , we let  $A(p, q) = A(p, q) + 1$ . At the end of this procedure, a value of  $Q$  in  $A(i, j)$  corresponds to  $Q$  points in the  $xy$ -plane lying on the line  $y = a_i x + b_j$ . The number of subdivisions in the  $ab$ -plane determines the accuracy of the co-linearity of these points. Note that subdividing the  $a$  axis into  $K$  increments gives, for every point  $(x_k, y_k)$ ,  $K$  values of  $b$  corresponding to the  $K$  possible values of  $a$ . With  $n$  image points, this method involves  $nK$  computations. Thus the procedure just discussed is linear in  $n$ , and the product  $nK$  does not approach the number of computations discussed at the beginning unless  $K$  approaches or exceeds  $n$ .

A problem with using the equation  $y = ax + b$  to represent a line is that the slope approaches infinity as the line approaches the vertical. One way around this difficulty is to use the normal representation of a line:

$$x \cos\theta + y \sin\theta = \rho$$

Figure 3.3(a) illustrates the geometrical interpretation of the parameters used. The use of this representation in constructing a table of accumulators is identical to the method discussed for the slope-intercept representation. Instead of straight lines, however, the loci are sinusoidal curves in the  $\rho\theta$ -plane. As before,  $Q$  collinear points lying on a line  $x \cos\theta_j + y \sin\theta_j = \rho$ , yield  $Q$  sinusoidal curves that intersect at  $(\rho_i, \theta_j)$  in the parameter space. Incrementing  $\theta$  and solving for the corresponding  $\rho$  gives  $Q$  entries in accumulator  $A(i, j)$  associated with the cell determined by  $(\rho_i, \theta_j)$ . Figure 3.3 (b) illustrates the subdivision of the parameter space.

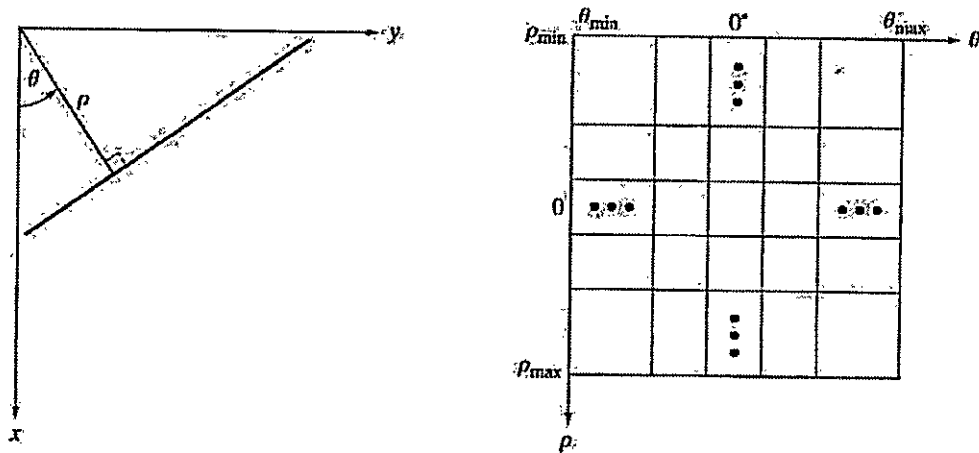


Fig.3.3 (a) Normal representation of a line (b) Subdivision of the  $\rho\theta$ -plane into cells

The range of angle  $\theta$  is  $\pm 90^\circ$ , measured with respect to the x-axis. Thus with reference to Fig. 3.3 (a), a horizontal line has  $\theta = 0^\circ$ , with  $\rho$  being equal to the positive x-intercept. Similarly, a vertical line has  $\theta = 90^\circ$ , with  $\rho$  being equal to the positive y-intercept, or  $\theta = -90^\circ$ , with  $\rho$  being equal to the negative y-intercept.

### (iii) Global processing via graph-theoretic techniques

In this process we have a global approach for edge detection and linking based on representing edge segments in the form of a graph and searching the graph for low-cost paths that correspond to significant edges. This representation provides a rugged approach that performs well in the presence of noise.

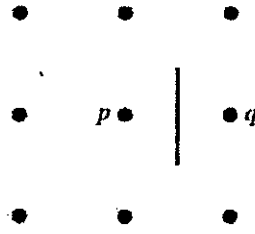


Fig.3.4 Edge element between pixels p and q

We begin the development with some basic definitions. A graph  $G = (N, U)$  is a finite, nonempty set of nodes  $N$ , together with a set  $U$  of unordered pairs of distinct elements of  $N$ . Each pair  $(n_i, n_j)$  of  $U$  is called an arc. A graph in which the arcs are directed is called a directed graph. If an arc is directed from node  $n_i$  to node  $n_j$ , then  $n_j$  is said to be a successor of the parent node  $n_i$ . The process of identifying the successors of a node is called expansion of the node. In each graph we define levels, such that level 0 consists of a single node, called the start or root node, and the nodes in the last level are called goal nodes. A cost  $c(n_i, n_j)$  can be associated with every arc  $(n_i, n_j)$ . A sequence of nodes  $n_1, n_2, \dots, n_k$ , with each node  $n_i$  being a successor of node  $n_{i-1}$  is called a path from  $n_1$  to  $n_k$ . The cost of the entire path is

$$c = \sum_{i=2}^k c(n_{i-1}, n_i).$$

The following discussion is simplified if we define an edge element as the boundary between two pixels  $p$  and  $q$ , such that  $p$  and  $q$  are 4-neighbors, as Fig.3.4 illustrates. Edge elements are identified by the  $xy$ -coordinates of points  $p$  and  $q$ . In other words, the edge element in Fig. 3.4 is defined by the pairs  $(x_p, y_p)$   $(x_q, y_q)$ . Consistent with the definition an edge is a sequence of connected edge elements.

We can illustrate how the concepts just discussed apply to edge detection using the 3 X 3 image shown in Fig. 3.5 (a). The outer numbers are pixel

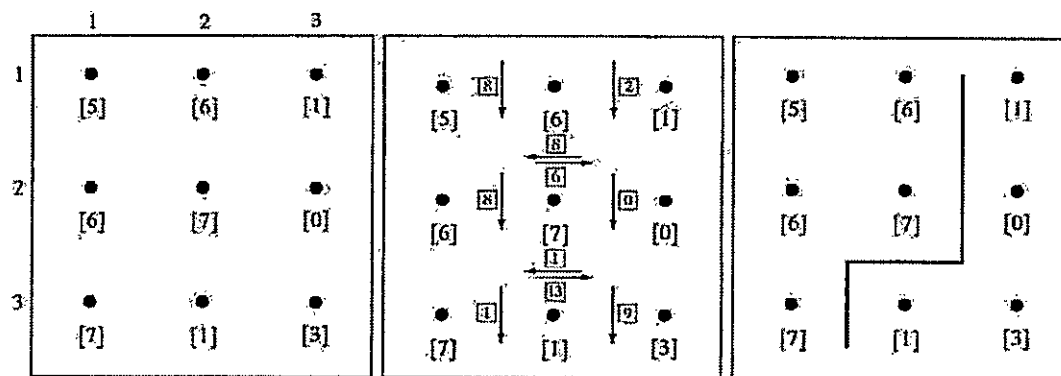


Fig.3.5 (a) A 3 X 3 image region, (b) Edge segments and their costs, (c) Edge corresponding to the lowest-cost path in the graph shown in Fig. 3.6

coordinates and the numbers in brackets represent gray-level values. Each edge element, defined by pixels p and q, has an associated cost, defined as

$$c(p, q) = H - [f(p) - f(q)]$$

where H is the highest gray-level value in the image (7 in this case), and f(p) and f(q) are the gray-level values of p and q, respectively. By convention, the point p is on the right-hand side of the direction of travel along edge elements. For example, the edge segment (1, 2) (2, 2) is between points (1, 2) and (2, 2) in Fig. 3.5 (b). If the direction of travel is to the right, then p is the point with coordinates (2, 2) and q is point with coordinates (1, 2); therefore,  $c(p, q) = 7 - [7 - 6] = 6$ . This cost is shown in the box below the edge segment. If, on the other hand, we are traveling to the left between the same two points, then p is point (1, 2) and q is (2, 2). In this case the cost is 8, as shown above the edge segment in Fig. 3.5(b). To simplify the discussion, we assume that edges start in the top row and terminate in the last row, so that the first element of an edge can be only between points (1, 1), (1, 2) or (1, 2), (1, 3). Similarly, the last edge element has to be between points (3, 1), (3, 2) or (3, 2), (3, 3). Keep in mind that p and q are 4-neighbors, as noted earlier. Figure 3.6 shows the graph for this problem. Each node (rectangle) in the graph corresponds to an edge element from Fig. 3.5. An arc exists between two nodes if the two corresponding edge elements taken in succession can be part of an edge.



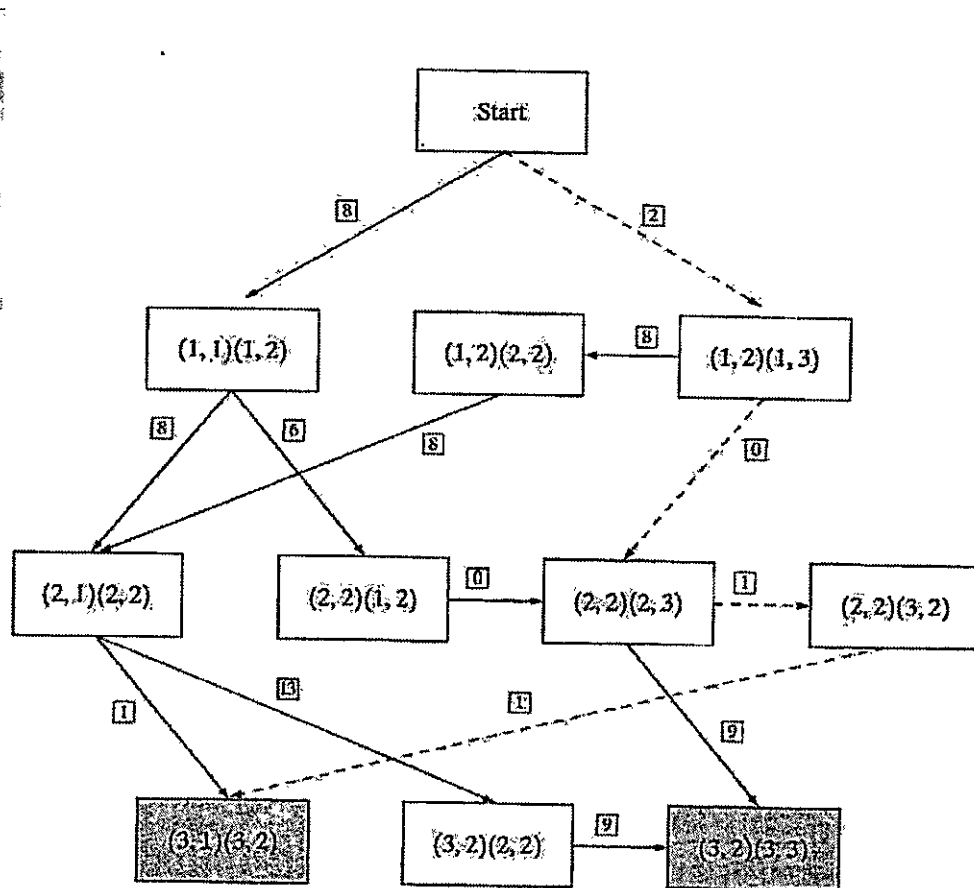


Fig. 3.6 Graph for the image in Fig.3.5 (a). The lowest-cost path is shown dashed.

As in Fig. 3.5 (b), the cost of each edge segment, is shown in a box on the side of the arc leading into the corresponding node. Goal nodes are shown shaded. The minimum cost path is shown dashed, and the edge corresponding to this path is shown in Fig. 3.5 (c).

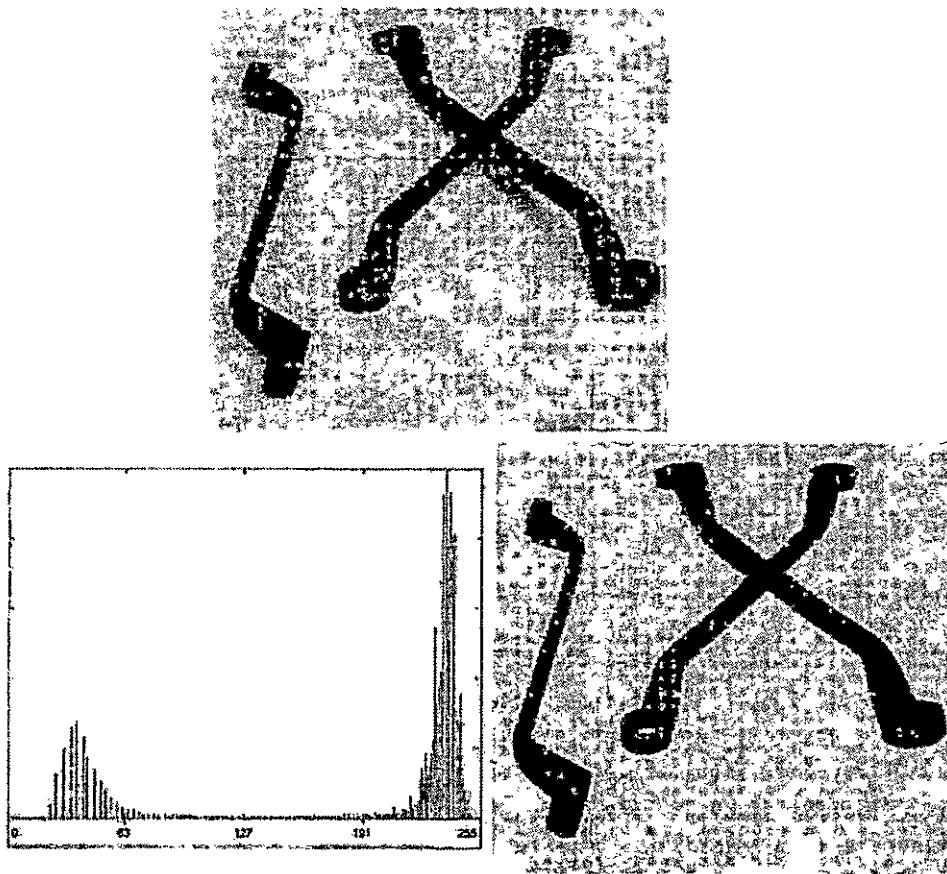
**4. What is thresholding? Explain about global thresholding.**

**Thresholding:**

Because of its intuitive properties and simplicity of implementation, image thresholding enjoys a central position in applications of image segmentation.

**Global Thresholding:**

The simplest of all thresholding techniques is to partition the image histogram by using a single global threshold,  $T$ . Segmentation is then accomplished by scanning the image pixel by pixel and labeling each pixel as object or back-ground, depending on whether the gray level of that pixel is greater or less than the value of  $T$ . As indicated earlier, the success of this method depends entirely on how well the histogram can be partitioned.



**Fig.4.1** FIGURE 10.28 (a) Original image, (b) Image histogram, (c) Result of global thresholding with  $T$  midway between the maximum and minimum gray levels.

Figure 4.1(a) shows a simple image, and Fig. 4.1(b) shows its histogram. Figure 4.1(c) shows the result of segmenting Fig. 4.1(a) by using a threshold  $T$  midway between the maximum and minimum gray levels. This threshold achieved a "clean" segmentation by eliminating the shadows and leaving only the objects themselves. The objects of interest in this case are darker than the background, so any pixel with a gray level  $\leq T$  was labeled black (0), and any pixel with a gray level  $\geq T$  was labeled white (255). The key objective is merely to generate a binary image, so the black-white relationship could be reversed. The type of global thresholding just described can be expected to be successful in highly controlled environments. One of the areas in which this often is possible is in industrial inspection applications, where control of the illumination usually is feasible.

The threshold in the preceding example was specified by using a heuristic approach, based on visual inspection of the histogram. The following algorithm can be used to obtain T automatically:

1. Select an initial estimate for T.
2. Segment the image using T. This will produce two groups of pixels:  $G_1$  consisting of all pixels with gray level values  $>T$  and  $G_2$  consisting of pixels with values  $< T$ .
3. Compute the average gray level values  $\mu_1$  and  $\mu_2$  for the pixels in regions  $G_1$  and  $G_2$ .
4. Compute a new threshold value:

$$T = \frac{1}{2}(\mu_1 + \mu_2),$$

5. Repeat steps 2 through 4 until the difference in T in successive iterations is smaller than a predefined parameter  $T_0$ .

When there is reason to believe that the background and object occupy comparable areas in the image, a good initial value for T is the average gray level of the image. When objects are small compared to the area occupied by the background (or vice versa), then one group of pixels will dominate the histogram and the average gray level is not as good an initial choice. A more appropriate initial value for T in cases such as this is a value midway between the maximum and minimum gray levels. The parameter  $T_0$  is used to stop the algorithm after changes become small in terms of this parameter. This is used when speed of iteration is an important issue.

5. Explain about basic adaptive thresholding process used in image segmentation.

#### **Basic Adaptive Thresholding:**

Imaging factors such as uneven illumination can transform a perfectly segmentable histogram into a histogram that cannot be partitioned effectively by a single global threshold. An approach for handling such a situation is to divide the original image into subimages and then utilize a

different threshold to segment each subimage. The key issues in this approach are how to subdivide the image and how to estimate the threshold for each resulting subimage. Since the threshold used for each pixel depends on the location of the pixel in terms of the subimages, this type of thresholding is adaptive.

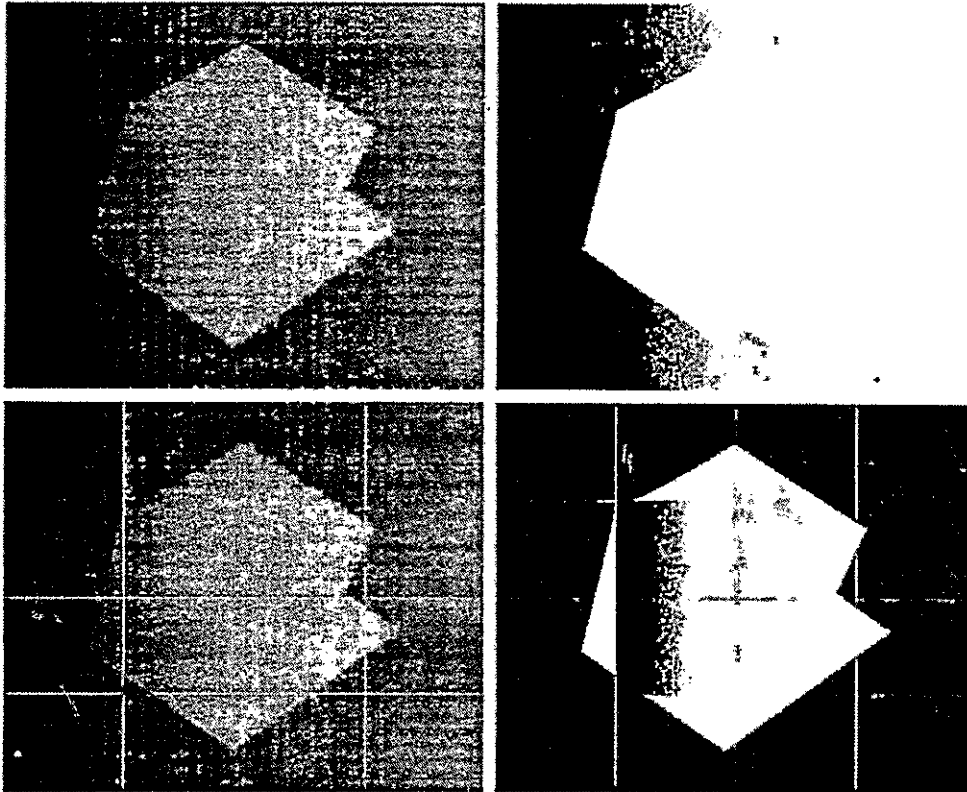


Fig.5 (a) Original image, (b) Result of global thresholding. (c) Image subdivided into individual subimages (d) Result of adaptive thresholding.

We illustrate adaptive thresholding with an example. Figure 5(a) shows the image, which we concluded could not be thresholded effectively with a single global threshold. In fact, Fig. 5(b) shows the result of thresholding the image with a global threshold manually placed in the valley of its histogram. One approach to reduce the effect of nonuniform illumination is to subdivide the image into smaller subimages, such that the illumination of each subimage is approximately uniform. Figure 5(c) shows such a partition, obtained by subdividing the image into four equal parts, and then subdividing each part by four again. All the subimages that did not contain a boundary between object and back-ground had variances of less than 75. All subimages containing boundaries had variances in excess of 100. Each subimage with variance greater than 100 was segmented with a threshold computed for that subimage using the algorithm. The initial

value for T in each case was selected as the point midway between the minimum and maximum gray levels in the subimage. All subimages with variance less than 100 were treated as one composite image, which was segmented using a single threshold estimated using the same algorithm. The result of segmentation using this procedure is shown in Fig. 5(d).

With the exception of two subimages, the improvement over Fig. 5(b) is evident. The boundary between object and background in each of the improperly segmented subimages was small and dark, and the resulting histogram was almost unimodal.

## 6. Explain in detail the threshold selection based on boundary characteristics.

### Use of Boundary Characteristics for Histogram Improvement and Local Thresholding:

It is intuitively evident that the chances of selecting a "good" threshold are enhanced considerably if the histogram peaks are tall, narrow, symmetric, and separated by deep valleys. One approach for improving the shape of histograms is to consider only those pixels that lie on or near the edges between objects and the background. An immediate and obvious improvement is that histograms would be less dependent on the relative sizes of objects and the background. For instance, the histogram of an image composed of a small object on a large background area (or vice versa) would be dominated by a large peak because of the high concentration of one type of pixels.

If only the pixels on or near the edge between object and the background were used, the resulting histogram would have peaks of approximately the same height. In addition, the probability that any of those given pixels lies on an object would be approximately equal to the probability that it lies on the back-ground, thus improving the symmetry of the histogram peaks.

Finally, as indicated in the following paragraph, using pixels that satisfy some simple measures based on gradient and Laplacian operators has a tendency to deepen the valley between histogram peaks.

The principal problem with the approach just discussed is the implicit assumption that the edges between objects and background are known. This information clearly is not available during segmentation, as finding a division between objects and background is precisely what segmentation is all about. However, an indication of whether a pixel is on an edge may be obtained by computing its gradient. In addition, use of the Laplacian can yield information regarding whether a given pixel lies on the dark or light side of an edge. The average value of the Laplacian is 0 at the transition of an edge, so in practice the valleys of histograms formed from

the pixels selected by a gradient/Laplacian criterion can be expected to be sparsely populated. This property produces the highly desirable deep valleys.

The gradient  $\nabla f$  at any point  $(x, y)$  in an image can be found. Similarly, the Laplacian  $\nabla^2 f$  can also be found. These two quantities may be used to form a three-level image, as follows:

$$s(x, y) = \begin{cases} 0 & \text{if } \nabla f < T \\ + & \text{if } \nabla f \geq T \text{ and } \nabla^2 f \geq 0 \\ - & \text{if } \nabla f \geq T \text{ and } \nabla^2 f < 0 \end{cases}$$

where the symbols 0, +, and - represent any three distinct gray levels, T is a threshold, and the gradient and Laplacian are computed at every point  $(x, y)$ . For a dark object on a light background, the use of the Eqn. produces an image  $s(x, y)$  in which (1) all pixels that are not on an edge (as determined by  $\nabla f$  being less than T) are labeled 0; (2) all pixels on the dark side of an edge are labeled +; and (3) all pixels on the light side of an edge are labeled -. The symbols + and - in Eq. above are reversed for a light object on a dark background. Figure 6.1 shows the labeling produced by Eq. for an image of a dark, underlined stroke written on a light background.

The information obtained with this procedure can be used to generate a segmented, binary image in which 1's correspond to objects of interest and 0's correspond to the background. The transition (along a horizontal or vertical scan line) from a light background to a dark object must be characterized by the occurrence of a - followed by a + in  $s(x, y)$ . The interior of the object is composed of pixels that are labeled either 0 or +. Finally, the transition from the object back to the background is characterized by the occurrence of a + followed by a -. Thus a horizontal or vertical scan line containing a section of an object has the following structure:

$$(\dots)(-, +)(0 \text{ or } +)(+, \dots)$$



Fig.6.1 Image of a handwritten stroke coded by using Eq. discussed above

where (...) represents any combination of +, -, and 0. The innermost parentheses contain object points and are labeled 1. All other pixels along the same scan line are labeled 0, with the exception of any other sequence of (- or +) bounded by (-, +) and (+, -).

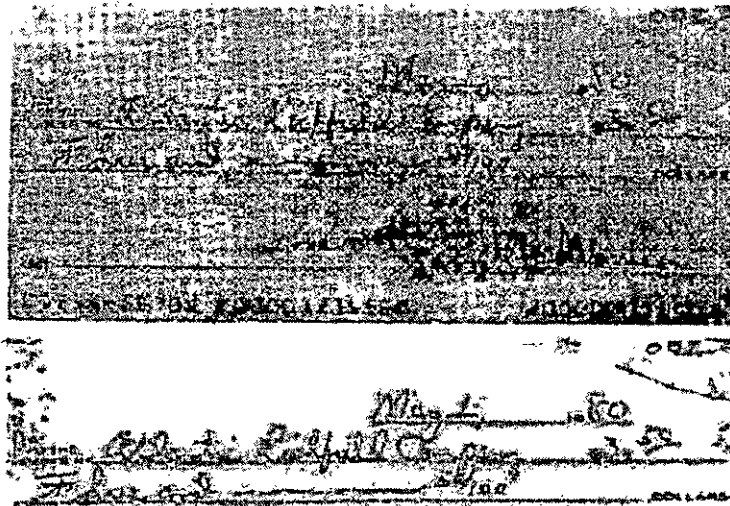


Fig.6.2 (a) Original image, (b) Image segmented by local thresholding.



Figure 6.2 (a) shows an image of an ordinary scenic bank check. Figure 6.3 shows the histogram as a function of gradient values for pixels with gradients greater than 5. Note that this histogram has two dominant modes that are symmetric, nearly of the same height, and are separated by a distinct valley. Finally, Fig. 6.2(b) shows the segmented image obtained by with T at or near the midpoint of the valley. Note that this example is an illustration of local thresholding, because the value of T was determined from a histogram of the gradient and Laplacian, which are local properties.

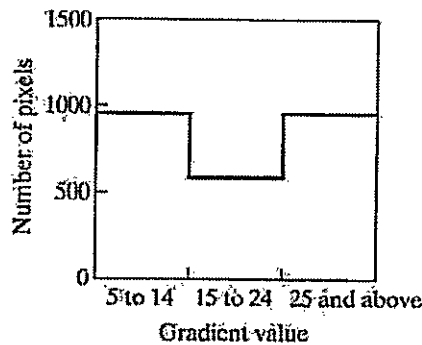


Fig.6.3 Histogram of pixels with gradients greater than 5

## 7. Explain about region based segmentation.

### Region-Based Segmentation:

The objective of segmentation is to partition an image into regions. We approached this problem by finding boundaries between regions based on discontinuities in gray levels, whereas segmentation was accomplished via thresholds based on the distribution of pixel properties, such as gray-level values or color.

### Basic Formulation:

Let R represent the entire image region. We may view segmentation as a process that partitions R into n subregions,  $R_1, R_2, \dots, R_n$ , such that

GRIET/ECE

- (a)  $\bigcup_{i=1}^n R_i = R$ .
- (b)  $R_i$  is a connected region;  $i = 1, 2, \dots, n$ .
- (c)  $R_i \cap R_j = \emptyset$  for all  $i$  and  $j, i \neq j$ .
- (d)  $P(R_i) = \text{TRUE}$  for  $i = 1, 2, \dots, n$ .
- (e)  $P(R_i \cup R_j) = \text{FALSE}$  for  $i \neq j$ .

Here,  $P(R_i)$  is a logical predicate defined over the points in set  $R_i$  and  $\emptyset$  is the null set. Condition (a) indicates that the segmentation must be complete; that is, every pixel must be in a region. Condition (b) requires that points in a region must be connected in some predefined sense. Condition (c) indicates that the regions must be disjoint. Condition (d) deals with the properties that must be satisfied by the pixels in a segmented region—for example  $P(R_i) = \text{TRUE}$  if all pixels in  $R_i$  have the same gray level. Finally, condition (e) indicates that regions  $R_i$  and  $R_j$  are different in the sense of predicate  $P$ .

#### Region Growing:

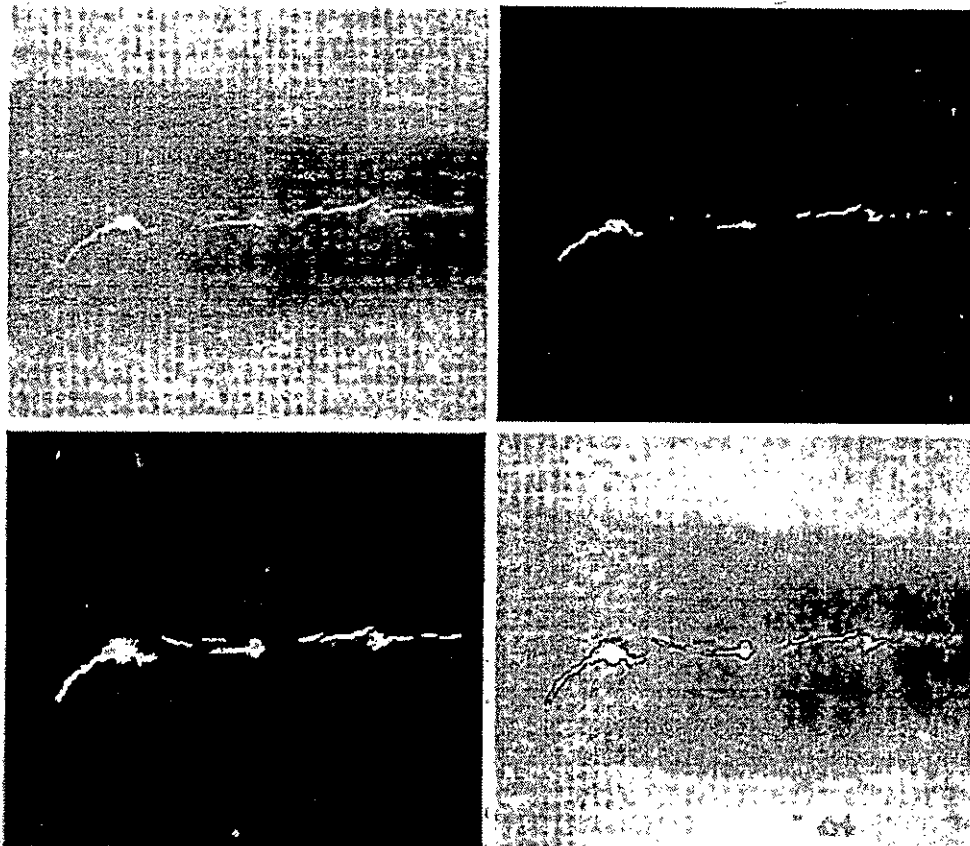
As its name implies, region growing is a procedure that groups pixels or subregions into larger regions based on predefined criteria. The basic approach is to start with a set of "seed" points and from these grow regions by appending to each seed those neighboring pixels that have properties similar to the seed (such as specific ranges of gray level or color). When a priori information is not available, the procedure is to compute at every pixel the same set of properties that ultimately will be used to assign pixels to regions during the growing process. If the result of these computations shows clusters of values, the pixels whose properties place them near the centroid of these clusters can be used as seeds.

The selection of similarity criteria depends not only on the problem under consideration, but also on the type of image data available. For example, the analysis of land-use satellite imagery depends heavily on the use of color. This problem would be significantly more difficult, or even impossible, to handle without the inherent information available in color images. When the images are monochrome, region analysis must be carried out with a set of descriptors based on gray levels and spatial properties (such as moments or texture).

Basically, growing a region should stop when no more pixels satisfy the criteria for inclusion in that region. Criteria such as gray level, texture, and color, are local in nature and do not take into account the "history" of region growth. Additional criteria that increase the power of a region-growing algorithm utilize the concept of size, likeness between a candidate pixel and the pixels grown so far (such as a comparison of the gray level of a candidate and the average gray level of

the grown region), and the shape of the region being grown. The use of these types of descriptors is based on the assumption that a model of expected results is at least partially available.

Figure 7.1 (a) shows an X-ray image of a weld (the horizontal dark region) containing several cracks and porosities (the bright, white streaks running horizontally through the middle of the image). We wish to use region growing to segment the regions of the weld failures. These segmented features could be used for inspection, for inclusion in a database of historical studies, for controlling an automated welding system, and for other numerous applications.



**Fig.7.1 (a) Image showing defective welds, (b) Seed points, (c) Result of region growing, (d) Boundaries of segmented ; defective welds (in black).**

The first order of business is to determine the initial seed points. In this application, it is known that pixels of defective welds tend to have the maximum allowable digital value B55 in this case). Based on this information, we selected as starting points all pixels having values of 255. The points thus extracted from the original image are shown in Fig. 10.40(b). Note that many of the points are clustered into seed regions.

The next step is to choose criteria for region growing. In this particular example we chose two criteria for a pixel to be annexed to a region: (1) The absolute gray-level difference between any pixel and the seed had to be less than 65. This number is based on the histogram shown in Fig. 7.2 and represents the difference between 255 and the location of the first major valley to the left, which is representative of the highest gray level value in the dark weld region. (2) To be included in one of the regions, the pixel had to be 8-connected to at least one pixel in that region.

If a pixel was found to be connected to more than one region, the regions were merged. Figure 7.1 (c) shows the regions that resulted by starting with the seeds in Fig. 7.2 (b) and utilizing the criteria defined in the previous paragraph. Superimposing the boundaries of these regions on the original image [Fig. 7.1(d)] reveals that the region-growing procedure did indeed segment the defective welds with an acceptable degree of accuracy. It is of interest to note that it was not necessary to specify any stopping rules in this case because the criteria for region growing were sufficient to isolate the features of interest.

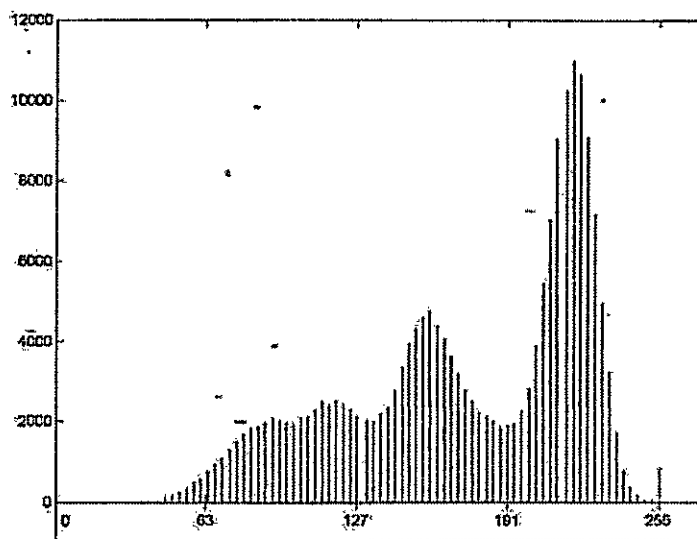


Fig.7.2 Histogram of Fig. 7.1 (a)

**Region Splitting and Merging:**

The procedure just discussed grows regions from a set of seed points. An alternative is to subdivide an image initially into a set of arbitrary, disjoint regions and then merge and/or split the regions in an attempt to satisfy the conditions. A split and merge algorithm that iteratively works toward satisfying these constraints is developed.

Let  $R$  represent the entire image region and select a predicate  $P$ . One approach for segmenting  $R$  is to subdivide it successively into smaller and smaller quadrant regions so that, for any region  $R_i$ ,  $P(R_i) = \text{TRUE}$ . We start with the entire region. If  $P(R) = \text{FALSE}$ , we divide the image into quadrants. If  $P$  is  $\text{FALSE}$  for any quadrant, we subdivide that quadrant into subquadrants, and so on. This particular splitting technique has a convenient representation in the form of a so-called quadtree (that is, a tree in which nodes have exactly four descendants), as illustrated in Fig. 7.3. Note that the root of the tree corresponds to the entire image and that each node corresponds to a subdivision. In this case, only  $R_4$  was subdivided further.

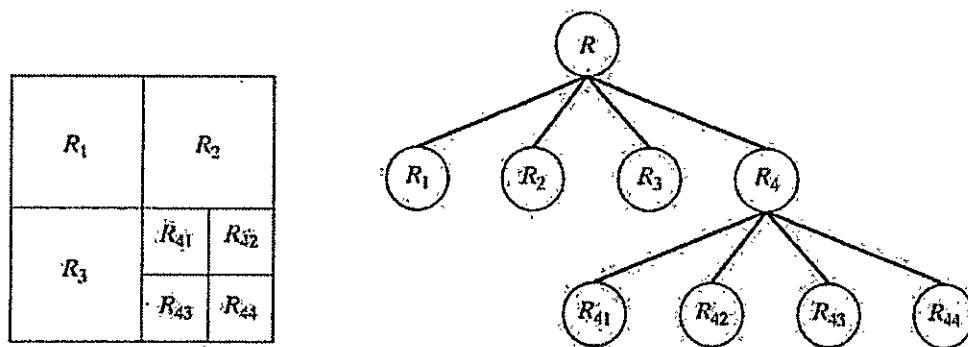


Fig. 7.3 (a) Partitioned image (b) Corresponding quadtree.

If only splitting were used, the final partition likely would contain adjacent regions with identical properties. This drawback may be remedied by allowing merging, as well as splitting. Satisfying the constraints, requires merging only adjacent regions whose combined pixels satisfy the predicate  $P$ . That is, two adjacent regions  $R_j$  and  $R_k$  are merged only if  $P(R_j \cup R_k) = \text{TRUE}$ .

The preceding discussion may be summarized by the following procedure, in which, at any step we

1. Split into four disjoint quadrants any region  $R_i$ , for which  $P(R_i) = \text{FALSE}$ .
2. Merge any adjacent regions  $R_j$  and  $R_k$  for which  $P(R_j \cup R_k) = \text{TRUE}$ .

3. Stop when no further merging or splitting is possible.

Several variations of the preceding basic theme are possible. For example, one possibility is to split the image initially into a set of blocks. Further splitting is carried out as described previously, but merging is initially limited to groups of four blocks that are descendants in the quadtree representation and that satisfy the predicate P. When no further mergings of this type are possible, the procedure is terminated by one final merging of regions satisfying step 2. At this point, the merged regions may be of different sizes. The principal advantage of this approach is that it uses the same quadtree for splitting and merging, until the final merging step.

PPT'S





# DIGITAL IMAGE PROCESSING

## INTRODUCTION

Processing of images which are digital in nature by a digital computer

### Definition:

An image may be defined as a two dimensional function,  $f(x,y)$ , Where  $x$  and  $y$  are spatial(plane ) coordinates and the amplitude of  $f$  at any pair of coordinates  $(x,y)$  is called the intensity or gray level of the image at that point.

*When  $x$ ,  $y$ , and the amplitude values of  $f$  are all finite, discrete quantities, then image is called as a digital image*



### Need of image processing?

*It is motivated by two major applications*

- Improvement of pictorial information for human perception
- Image processing for autonomous machine application
- Efficient storage and transmission

### Human perception

Employ methods of enhancing pictorial information for human interpretation and analysis

Typical applications

- .Noise filtering
- .content enhancement
- .contrast enhancement
- .Deblurring
- .Remote sensing

Filtering

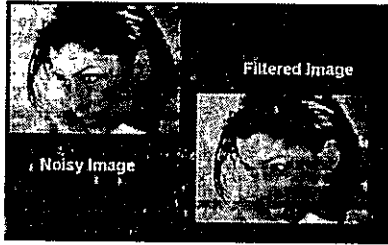


Image deblurring

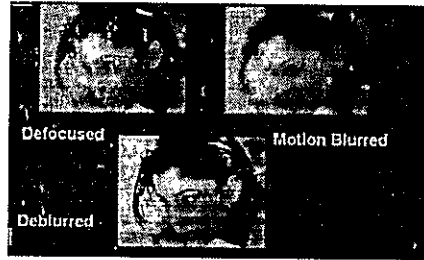


Image enhancement

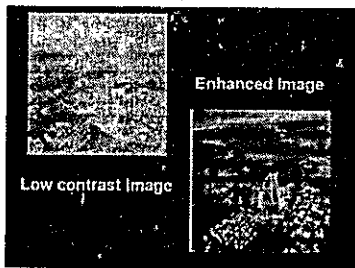
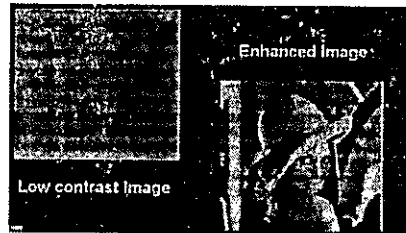
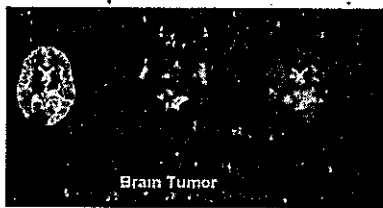


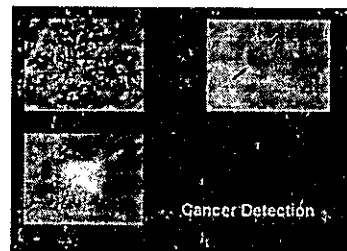
Image enhancement



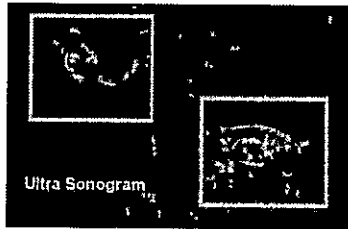
Medical imaging



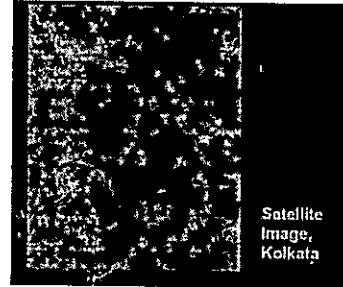
Medical Imaging



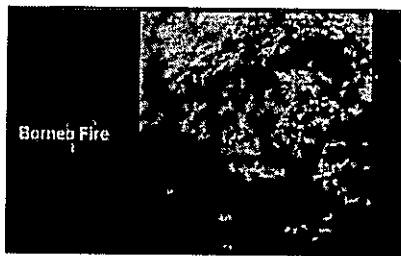
Medical imaging



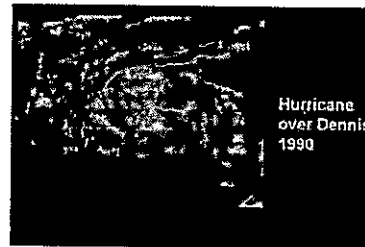
Remote sensing



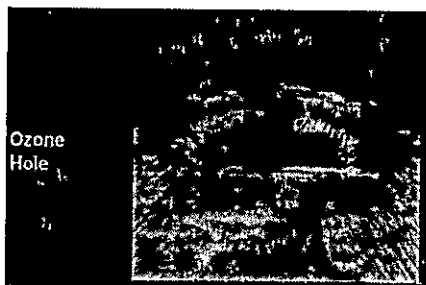
Remote sensing



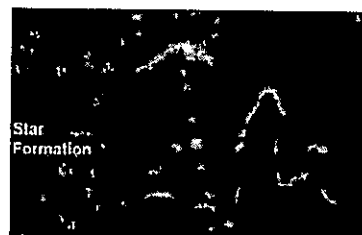
Weather forecasting



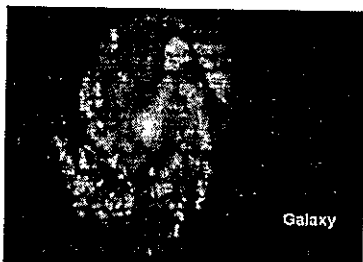
Atmospheric study



Astronomy



## Astronomy



## Origins of DIP

In 1920's submarine cables were used to transmit digitized news paper pictures between London And New york Bartlane systems

Specialized Printing equipments were used to code the pictures for cable transmission and its reproduction on the receiving end



ns picture 412 produced by a telegraphic printer

In 1921,printing procedure was changed to photographic reproduction from tapes performed at telegraph receiving terminals

This improved both tonal quality and resolution



Bartlane system was capable of coding 5 distinct brightness levels

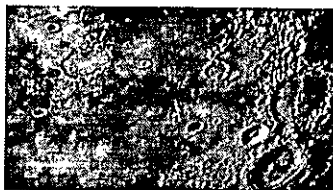
This was increased to 15 levels by 1929



Improvement of processing techniques continued for next 35years

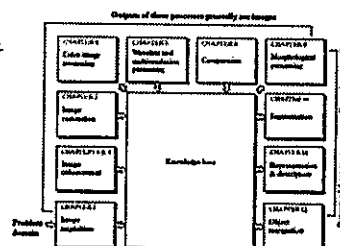
In 1964 computer processing techniques were used to improve the pictures of moon transmitted by Ranger 7 at Jet Propulsion Laboratory

This was the basis of modern Image processing techniques



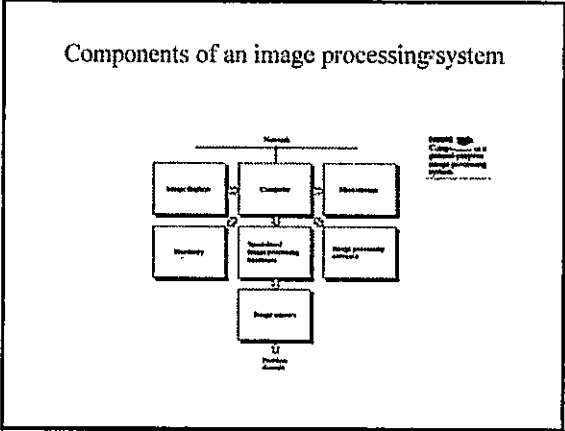
## Fundamental steps in DIP

FIGURE 1.10 Fundamental steps in digital image processing.



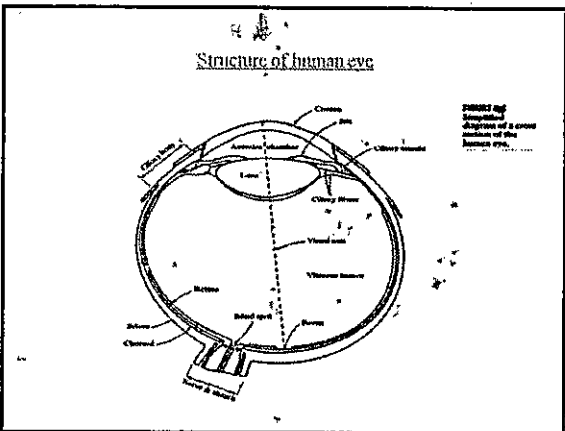
- *Image acquisition* stage involves preprocessing, such as scaling
  - *Image enhancement* is the idea to highlight certain features of interest in an image
  - *Image restoration* is also deals with the improving the appearance of an image
- image restoration is based on mathematical or probabilistic models of image degradation, It is objective  
 image enhancement is human subjective preferences regarding what constitutes a "it looks better", it is subjective.
- *Color image processing* is also concept of extracting features of interest in image

- *Wavelets* are the foundation for representing images in various degrees of resolution
- *Compression* is for reducing the space for storing or reducing the bandwidth for transmission of images
- *Morphological processing* deals with tools extracting image components that are useful representation and description of shape
- *Segmentation* is the process of subdividing the image into its constituent parts or objects  
 It is for "to identify" clearly in an image after the processing
- *Representation and description* is usually a raw pixel data constituting either the boundary or region  
 Description is also called feature selection, for differentiating one class of objects from other
- *Recognition* is the process that assigns a label (e.g., "Vehicle") based on its descriptors



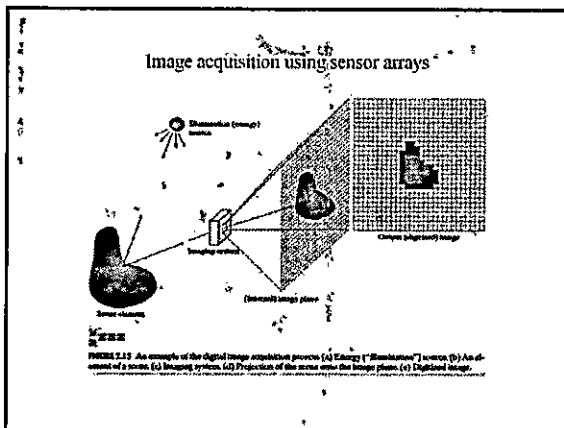
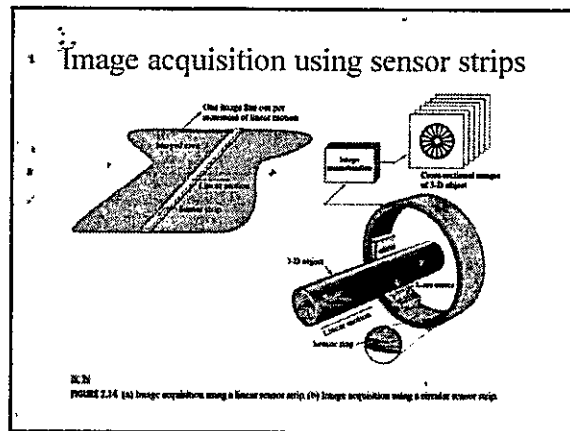
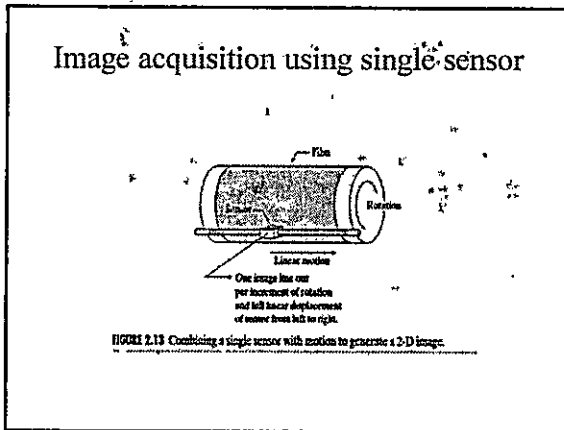
- *Sensors* has the two elements. The first is a physical device that is sensitive to the energy radiated by the object to form an image and then digitizer for converting the output of physical sensing device into digital form.
- *Specialized image processing hardware*, consists of digitizer, plus hardware that performs other primitive operations, like arithmetic logic unit (ALU), this unit performs functions that require fast data throughputs (e.g., digitizing and averaging video images at 30 frames/sec)
- *Software* for image processing consists of specialized modules that perform specific tasks, also includes capability for the user to write code.
- *Mass storage* is for storage space of image processing system.  
 It is categorized as
  - Short term storage (use during processing)
  - On-line storage (for fast recalling)
  - Archival storage (infrequent access)
  - Image displays

- *Image displays* in use today mainly color (flat screen) TV monitors
- *Hard copy devices* for recording images include laser printers, film cameras, ink-jet units,
- *Networking*, in image processing applications the key consideration in image transmission is bandwidth, in dedicated networks it is good




- The eye is nearly sphere with an average diameter of approximately 20mm
- Three membranes encloses the eye Cornea and Sclera outer cover, the choroid and the retina
- The cornea is a tough, transparent tissue that covers the anterior surface of the eye, sclera is an optic membrane that encloses the remainder of the optic globe
- The choroid lies directly below the sclera, this membrane contains a network of blood vessels that serve as the major source of nutrition to the eye.
  - The choroid coat is heavily pigmented and helps to reduce the amount of extraneous light entering the eye
  - At its anterior, the choroid is divided into the ciliary body and iris diaphragm.
  - Iris diaphragm contracts or expands to control the light amount of light that enters the eye.
  - The center of the iris varies in diameter from approximately 2-3mm.

- Lens is made up of concentric circles made-up of fibrous cells and is suspended by fibers that attached to the ciliary body and it contain 60%-70% water, about 6% fat and more protein than any other tissue in the eye
  - Lens is colored by lightly yellow pigmentation that increases with age.
  - In extreme conditions excessive clouding of lens is referred as cataracts, can lead to poor color discrimination
- The innermost membrane of eye is the retina, which lines the inside of the walls entire posterior portion.
  - Pattern vision is afford by distribution of discrete light receptors over the retinal surface: cones and rods
  - Cones gives the color information
  - Rods gives the overall picture of the field view.
  - Cones Vision is called photopic or bright light vision



- ### Image Sampling and Quantization
- Digitizing the coordinate values is called sampling
  - Digitizing the amplitude value is called quantization



## Spatial Filtering

### Background

- Filter term in "Digital image processing" is referred to the subimage
- There are others term to call subimage such as mask, kernel, template, or window
- The value in a filter subimage are referred as coefficients, rather than pixels.

### Basics of Spatial Filtering

- The concept of filtering has its roots in the use of the Fourier transform for signal processing in the so-called frequency domain.
- Spatial filtering term is the filtering operations that are performed directly on the pixels of an image

### Mechanics of spatial filtering

- The process consists simply of moving the filter mask from point to point in an image.
- At each point (x,y) the response of the filter at that point is calculated using a predefined relationship

### Linear spatial filtering

Pixels of image

$w(-1,-1)$	$w(-1,0)$	$w(-1,1)$
$f(x-1,y-1)$	$f(x,y-1)$	$f(x+1,y-1)$
$w(0,-1)$	$w(0,0)$	$w(0,1)$
$f(x,y-1)$	$f(x,y)$	$f(x,y+1)$
$w(1,-1)$	$w(1,0)$	$w(1,1)$
$f(x+1,y-1)$	$f(x+1,y)$	$f(x+1,y+1)$

The result is the sum of products of the mask coefficients with the corresponding pixels directly under the mask

Mask coefficients

$w(-1,-1)$	$w(-1,0)$	$w(-1,1)$
$w(0,-1)$	$w(0,0)$	$w(0,1)$
$w(1,-1)$	$w(1,0)$	$w(1,1)$

$$f(x,y) = w(-1,-1)f(x-1,y-1) + w(-1,0)f(x-1,y) + w(-1,1)f(x-1,y+1) + w(0,-1)f(x,y-1) + w(0,0)f(x,y) + w(0,1)f(x,y+1) + w(1,-1)f(x+1,y-1) + w(1,0)f(x+1,y) + w(1,1)f(x+1,y+1)$$

### Note: Linear filtering

- The coefficient  $w(0,0)$  coincides with image value  $f(x,y)$ , indicating that the mask is centered at (x,y) when the computation of sum of products takes place.
- For a mask of size  $m \times n$ , we assume that  $m=2a+1$  and  $n=2b+1$ , where a and b are nonnegative integer. Then m and n are odd.

### Linear filtering

- In general, linear filtering of an image  $f$  of size  $M \times N$  with a filter mask of size  $m \times n$  is given by the expression:

$$g(x, y) = \sum_{s=-a}^a \sum_{t=-b}^b w(s, t) f(x+s, y+t)$$

### Discussion

- The process of linear filtering similar to a frequency domain concept called "*convolution*"

Simplify expression

$$R = w_1 z_1 + w_2 z_2 + \dots + w_m z_m = \sum_{i=1}^m w_i z_i$$

$w_1$	$w_2$	$w_3$
$w_4$	$w_5$	$w_6$
$w_7$	$w_8$	$w_9$

$$R = w_1 z_1 + w_2 z_2 + \dots + w_9 z_9 = \sum_{i=1}^9 w_i z_i$$

Where the  $w$ 's are mask coefficients, the  $z$ 's are the value of the image gray levels corresponding to those coefficients

### Nonlinear spatial filtering

- Nonlinear spatial filters also operate on neighborhoods, and the mechanics of sliding a mask past an image are the same as was just outlined.
- The filtering operation is based conditionally on the values of the pixels in the neighborhood under consideration

### Smoothing Spatial Filters

- Smoothing filters are used for blurring and for noise reduction.
  - Blurring is used in preprocessing steps, such as removal of small details from an image prior to object extraction, and bridging of small gaps in lines or curves
  - Noise reduction can be accomplished by blurring

### Type of smoothing filtering

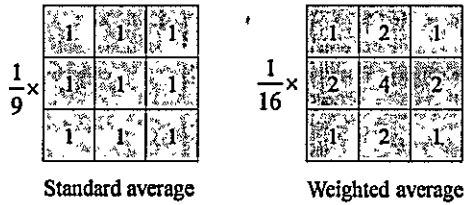
- There are 2 way of smoothing spatial filters
  - ▣ Smoothing Linear Filters
  - ▣ Order-Statistics Filters

### Smoothing Linear Filters

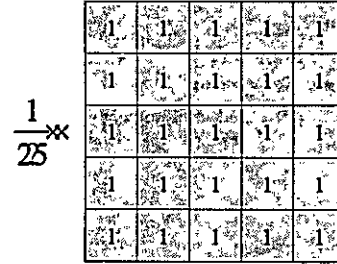
- Linear spatial filter is simply the average of the pixels contained in the neighborhood of the filter mask.
- Sometimes called "averaging filters".
- The idea is replacing the value of every pixel in an image by the average of the gray levels in the neighborhood defined by the filter mask.



### Two 3x3 Smoothing Linear Filters



### 5x5 Smoothing Linear Filters

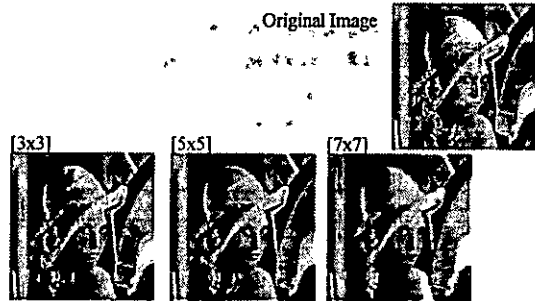


### Smoothing Linear Filters

- The general implementation for filtering an MxN image with a weighted averaging filter of size m x n is given by the expression

$$g(x, y) = \frac{\sum_{s=-a}^a \sum_{t=-b}^b w(s, t) f(x+s, y+t)}{\sum_{s=-a}^a \sum_{t=-b}^b w(s, t)}$$

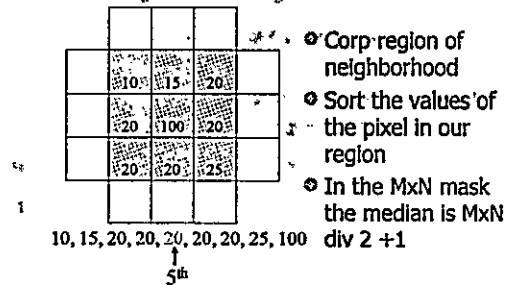
### Result of Smoothing Linear Filters



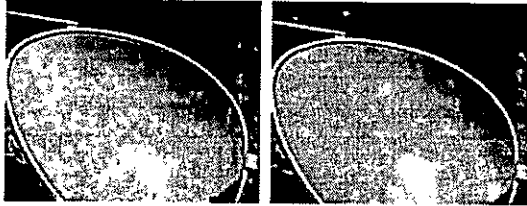
### Order-Statistics Filters

- Order-statistics filters are nonlinear spatial filters whose response is based on ordering (ranking) the pixels contained in the image area encompassed by the filter, and then replacing the value of the center pixel with the value determined by the ranking result.
- Best-known "median filter"

### Process of Median filter



### Result of median filter



Noise from Glass effect    Remove noise by median filter

### Homework

- smoothing filter  
mask standard 3x3, 5x5, 7x7,  
9x9 source code
- median filter mask  
3x3, 5x5, 7x7, 9x9 source  
code
- 100x100

### Sharpening Spatial Filters

- The principal objective of sharpening is to highlight fine detail in an image or to enhance detail that has been blurred, either in error or as a natural effect of a particular method of image acquisition.

### Introduction

- The image blurring is accomplished in the spatial domain by pixel averaging in a neighborhood.
- Since averaging is analogous to integration.
- Sharpening could be accomplished by spatial differentiation.

### Foundation

- We are interested in the behavior of these derivatives in areas of constant gray level (flat segments), at the onset and end of discontinuities (step and ramp discontinuities), and along gray-level ramps.
- These types of discontinuities can be noise points, lines, and edges.

### Definition for a first derivative

- Must be zero in flat segments
- Must be nonzero at the onset of a gray-level step or ramp; and
- Must be nonzero along ramps.

### Definition for a second derivative

- Must be zero in flat areas;
- Must be nonzero at the onset and end of a gray-level step or ramp;
- Must be zero along ramps of constant slope

### Definition of the 1<sup>st</sup>-order derivative

- A basic definition of the first-order derivative of a one-dimensional function  $f(x)$  is

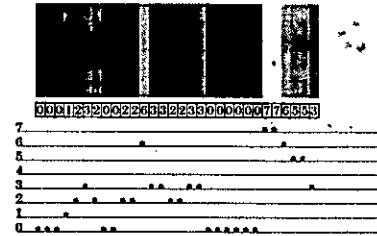
$$\frac{\partial f}{\partial x} = f(x+1) - f(x)$$

### Definition of the 2<sup>nd</sup>-order derivative

- We define a second-order derivative as the difference

$$\frac{\partial^2 f}{\partial x^2} = f(x+1) + f(x-1) - 2f(x)$$

### Gray-level profile



### Derivative of image profile



### Analyze

- The 1<sup>st</sup>-order derivative is nonzero along the entire ramp, while the 2<sup>nd</sup>-order derivative is nonzero only at the onset and end of the ramp.  
1<sup>st</sup> make thick edge and 2<sup>nd</sup> make thin edge
- The response at and around the point is much stronger for the 2<sup>nd</sup>- than for the 1<sup>st</sup>-order derivative

### The Laplacian (2<sup>nd</sup> order derivative)

- Shown by Rosenfeld and Kak[1982] that the simplest isotropic derivative operator is the Laplacian is defined as

$$\nabla^2 f = \frac{\partial^2 f}{\partial x^2} + \frac{\partial^2 f}{\partial y^2}$$

### Discrete form of derivative

$f(x-1,y)$	$f(x,y)$	$f(x+1,y)$
------------	----------	------------

$$\frac{\partial^2 f}{\partial x^2} = f(x+1,y) + f(x-1,y) - 2f(x,y)$$

$f(x,y-1)$
$f(x,y)$
$f(x,y+1)$

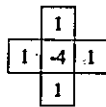
$$\frac{\partial^2 f}{\partial y^2} = f(x,y+1) + f(x,y-1) - 2f(x,y)$$

### 2-Dimensional Laplacian

- The digital implementation of the 2-Dimensional Laplacian is obtained by summing 2 components

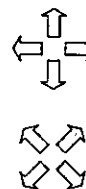
$$\nabla^2 f = \frac{\partial^2 f}{\partial x^2} + \frac{\partial^2 f}{\partial y^2}$$

$$\nabla^2 f = f(x+1,y) + f(x-1,y) + f(x,y+1) + f(x,y-1) - 4f(x,y)$$



### Laplacian

0	1	0
1	-4	1
0	1	0



1	1	1
1	-8	1
1	1	1



### Laplacian

0	-1	0
-1	4	-1
0	-1	0



1	1	1
1	-8	1
1	1	1




### Implementation

$$g(x,y) = \begin{cases} f(x,y) - \nabla^2 f(x,y) & \text{If the center coefficient is negative} \\ f(x,y) + \nabla^2 f(x,y) & \text{If the center coefficient is positive} \end{cases}$$

Where  $f(x,y)$  is the original image  
 $\nabla^2 f(x,y)$  is Laplacian filtered image  
 $g(x,y)$  is the sharpen image

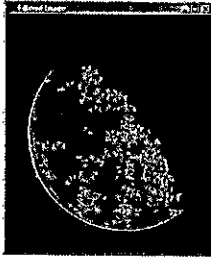
**Implementation**



0	0	0
1	0	0
0	0	0

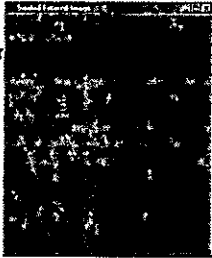
**Implementation**

Filtered = Conv(image,mask)




**Implementation**

filtered = filtered - Min(filtered)  
 filtered = filtered \* (.0/Max(filtered))



**Implementation**

sharpened = image + filtered  
 sharpened = sharpened - Min(sharpened)  
 sharpened = sharpened \* (.0/Max(sharpened))



**Algorithm**

- Using Laplacian filter to original image
- And then add the image result from step 1 and the original image

**Simplification**

- We will apply two step to be one mask

$$g(x,y) = f(x,y) - f(x+1,y) - f(x-1,y) - f(x,y+1) - f(x,y-1) + 4f(x,y)$$

$$g(x,y) = 5f(x,y) - f(x+1,y) - f(x-1,y) - f(x,y+1) - f(x,y-1)$$

0	-1	0
-1	5	-1
0	-1	0

-1	-1	-1
-1	9	-1
-1	-1	-1

## Unsharp masking

- A process to sharpen images consists of subtracting a blurred version of an image from the image itself. This process, called *unsharp masking*, is expressed as

$$f_s(x, y) = f(x, y) - \tilde{f}(x, y)$$

Where  $f_s(x, y)$  denotes the sharpened image obtained by unsharp masking, and  $\tilde{f}(x, y)$  is a blurred version of  $f(x, y)$

## High-boost filtering

- A high-boost filtered image,  $f_{hb}$  is defined at any point  $(x, y)$  as

$$f_{hb}(x, y) = Af(x, y) - \tilde{f}(x, y) \quad \text{where } A \geq 1$$

$$f_{hb}(x, y) = (A-1)f(x, y) + f(x, y) - \tilde{f}(x, y)$$

$$f_{hb}(x, y) = (A-1)f(x, y) + f_s(x, y)$$

This equation is applicable general and does not state explicitly how the sharp image is obtained

## High-boost filtering and Laplacian

- If we choose to use the Laplacian, then we know  $f_s(x, y)$

$$f_{hb} = \begin{cases} Af(x, y) - \nabla^2 f(x, y) & \text{If the center coefficient is negative} \\ Af(x, y) + \nabla^2 f(x, y) & \text{If the center coefficient is positive} \end{cases}$$

0	-1	0
-1	A+4	-1
0	-1	0

1	1	1
1	A+8	1
1	1	1

## The Gradient (1<sup>st</sup> order derivative)

- First Derivatives in Image processing are implemented using the magnitude of the gradient.
- The gradient of function  $f(x, y)$  is

$$\nabla f = \begin{bmatrix} G_x \\ G_y \end{bmatrix} = \begin{bmatrix} \frac{\partial f}{\partial x} \\ \frac{\partial f}{\partial y} \end{bmatrix}$$

## Gradient

- The magnitude of this vector is given by

$$\text{mag}(\nabla f) = \sqrt{G_x^2 + G_y^2} \approx |G_x| + |G_y|$$

$$G_x = \begin{bmatrix} -1 & 1 \end{bmatrix}$$

This mask is simple, and no isotropic. Its result only horizontal and vertical.

$$G_y = \begin{bmatrix} 1 \\ -1 \end{bmatrix}$$

## Robert's Method

- The simplest approximations to a first-order derivative that satisfy the conditions stated in that section are

$z_1$	$z_2$	$z_3$
$z_4$	$z_5$	$z_6$
$z_7$	$z_8$	$z_9$

$$G_x = (z_5 - z_3) \text{ and } G_y = (z_4 - z_6)$$

$$\nabla f = \sqrt{(z_5 - z_3)^2 + (z_4 - z_6)^2}$$

$$\nabla f \approx |z_5 - z_3| + |z_4 - z_6|$$

### Robert's Method

- These mask are referred to as the Roberts cross-gradient operators.

-1	0	0	-1
0	1	1	0

### Sobel's Method

- Mask of even size are awkward to apply.
- The smallest filter mask should be 3x3.
- The difference between the third and first rows of the 3x3 mage region approximate derivative in x-direction, and the difference between the third and first column approximate derivative in y-direction.

### Sobel's Method

- Using this equation

$$\nabla f \approx [(z_7 + 2z_2 + z_9) - (z_1 + 2z_5 + z_3)] + [(z_3 + 2z_6 + z_9) - (z_1 + 2z_4 + z_7)]$$

-1	-2	-1	-1	0	1
0	0	0	-2	0	2
1	2	1	-1	0	1

### Homework

- sharpening filter
  - ▣ Laplacian
  - ▣ High-boost with Laplacian
  - ▣ Gradient
  - ▣ Robert
  - ▣ Sobel
  - ▣ my mask

-	-	-
-	5	-
-	-	-

4 8 16 32

2 4

8

16

32

64

128

256

512

1024

2048

4096

8192

16384

32768

65536

131072

262144

524288

1048576

2097152

4194304

8388608

16777216

33554432

67108864

134217728

268435456

536870912

1073741824

2147483648





## Digital Image Processing

### Image Restoration and Reconstruction (Noise Removal)

Christophoros Nikou  
[cnikou@cs.uoi.gr](mailto:cnikou@cs.uoi.gr)

University of Ioannina - Department of Computer Science

## Image Restoration and Reconstruction

*Things which we see are not by themselves what we see...*

*It remains completely unknown to us what the objects may be by themselves and apart from the receptivity of our senses. We know nothing but our manner of perceiving them.*

Immanuel Kant

© Nikou - Digital Image Processing (E12)

## Contents

In this lecture we will look at image restoration techniques used for noise removal

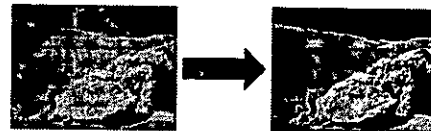
- What is image restoration?
- Noise and images
- Noise models
- Noise removal using spatial domain filtering
- Noise removal using frequency domain filtering

© Nikou - Digital Image Processing (E12)

## What is Image Restoration?

Image restoration attempts to restore images that have been degraded

- Identify the degradation process and attempt to reverse it
- Similar to image enhancement, but more objective

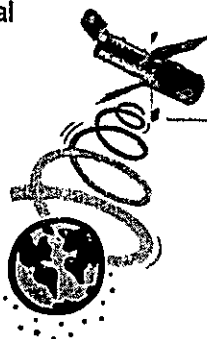


© Nikou - Digital Image Processing (E12)

## Noise and Images

The sources of noise in digital images arise during image acquisition (digitization) and transmission

- Imaging sensors can be affected by ambient conditions
- Interference can be added to an image during transmission



© Nikou - Digital Image Processing (E12)

## Noise Model

We can consider a noisy image to be modelled as follows:

$$g(x, y) = f(x, y) + \eta(x, y)$$

where  $f(x, y)$  is the original image pixel,  $\eta(x, y)$  is the noise term and  $g(x, y)$  is the resulting noisy pixel

If we can estimate the noise model we can figure out how to restore the image

© Nikou - Digital Image Processing (E12)

7 Noise Models (cont...)

There are many different models for the image noise term  $\eta(x, y)$ :

- Gaussian
  - Most common model
- Rayleigh
- Erlang (Gamma)
- Exponential
- Uniform
- Impulse
  - Salt and pepper noise

© Nikou - Digital Image Processing (E12)

8 Noise Example

The test pattern to the right is ideal for demonstrating the addition of noise

The following slides will show the result of adding noise based on various models to this image

Image Histogram

© Nikou - Digital Image Processing (E12)

9 Noise Example (cont...)

Gaussian Rayleigh Erlang

© Nikou - Digital Image Processing (E12)

10 Noise Example (cont...)

Exponential Uniform Impulse

© Nikou - Digital Image Processing (E12)

11 Filtering to Remove Noise

We can use spatial filters of different kinds to remove different kinds of noise

The *arithmetic mean* filter is a very simple one and is calculated as follows:

$$\hat{f}(x, y) = \frac{1}{mn} \sum_{(s,t) \in S_{xy}} g(s, t)$$

This is implemented as the simple smoothing filter

It blurs the image.

1/9	1/9	1/9
1/9	1/9	1/9
1/9	1/9	1/9

© Nikou - Digital Image Processing (E12)

12 Other Means

There are different kinds of mean filters all of which exhibit slightly different behaviour:

- Geometric Mean
- Harmonic Mean
- Contraharmonic Mean

© Nikou - Digital Image Processing (E12)

13 Other Means (cont...)

**Geometric Mean:**

$$\hat{f}(x, y) = \left[ \prod_{(s,t) \in S_{xy}} g(s, t) \right]^{\frac{1}{mn}}$$

Achieves similar smoothing to the arithmetic mean, but tends to lose less image detail.

C. Nikou - Digital Image Processing (E12)

14 Other Means (cont...)

**Harmonic Mean:**

$$\hat{f}(x, y) = \frac{mn}{\sum_{(s,t) \in S_{xy}} \frac{1}{g(s, t)}}$$

Works well for salt noise, but fails for pepper noise.

Also does well for other kinds of noise such as Gaussian noise.

C. Nikou - Digital Image Processing (E12)

15 Other Means (cont...)

**Contra-harmonic Mean:**

$$\hat{f}(x, y) = \frac{\sum_{(s,t) \in S_{xy}} g(s, t)^{Q+1}}{\sum_{(s,t) \in S_{xy}} g(s, t)^Q}$$

$Q$  is the order of the filter.  
 Positive values of  $Q$  eliminate pepper noise.  
 Negative values of  $Q$  eliminate salt noise.  
 It cannot eliminate both simultaneously.

C. Nikou - Digital Image Processing (E12)

16 Noise Removal Examples

Original image		Image corrupted by Gaussian noise	
3x3 Arithmetic Mean Filter		3x3 Geometric Mean Filter (less blurring than AMF, the image is sharper)	

C. Nikou - Digital Image Processing (E12)

17 Noise Removal Examples (cont...)

Image corrupted by pepper noise at 0.1

Filtering with a 3x3 Contra-harmonic Filter with  $Q=1.5$

C. Nikou - Digital Image Processing (E12)

18 Noise Removal Examples (cont...)

Image corrupted by salt noise at 0.1

Filtering with a 3x3 Contra-harmonic Filter with  $Q=-1.5$

C. Nikou - Digital Image Processing (E12)

19 **Contra-harmonic Filter: Here Be Dragons**

Choosing the wrong value for Q when using the contra-harmonic filter can have drastic results

Pepper noise filtered by a 3x3 CF with Q=-1.5      Salt noise filtered by a 3x3 CF with Q=1.5

© Foley - Digital Image Processing (S.12)

20 **Order Statistics Filters**

Spatial filters based on ordering the pixel values that make up the neighbourhood defined by the filter support.

Useful spatial filters include

- Median filter
- Max and min filter
- Midpoint filter
- Alpha trimmed mean filter

© Foley - Digital Image Processing (S.12)

21 **Median Filter**

**Median Filter:**

$$\hat{f}(x, y) = \text{median}\{g(s, t)\}_{(s, t) \in S_{xy}}$$

Excellent at noise removal, without the smoothing effects that can occur with other smoothing filters.

Particularly good when salt and pepper noise is present.

© Foley - Digital Image Processing (S.12)

22 **Max and Min Filter**

**Max Filter:**

$$\hat{f}(x, y) = \max\{g(s, t)\}_{(s, t) \in S_{xy}}$$

**Min Filter:**

$$\hat{f}(x, y) = \min\{g(s, t)\}_{(s, t) \in S_{xy}}$$

Max filter is good for pepper noise and Min filter is good for salt noise.

© Foley - Digital Image Processing (S.12)

23 **Midpoint Filter**

**Midpoint Filter:**

$$\hat{f}(x, y) = \frac{1}{2} \left[ \max\{g(s, t)\}_{(s, t) \in S_{xy}} + \min\{g(s, t)\}_{(s, t) \in S_{xy}} \right]$$

Good for random Gaussian and uniform noise.

© Foley - Digital Image Processing (S.12)

24 **Alpha-Trimmed Mean Filter**

**Alpha-Trimmed Mean Filter:**

$$\hat{f}(x, y) = \frac{1}{mn - d} \sum_{(s, t) \in S_{xy}} g_r(s, t)$$

We can delete the  $d/2$  lowest and  $d/2$  highest grey levels.

So  $g_r(s, t)$  represents the remaining  $mn - d$  pixels.

© Foley - Digital Image Processing (S.12)

25 Noise Removal Examples

Image corrupted by Salt And Pepper noise at 0.2

Result of 1 pass with a 3x3 Median Filter

Result of 2 passes with a 3x3 Median Filter

Result of 3 passes with a 3x3 Median Filter

Repeated passes remove the noise better but also blur the image

© Nikou - Digital Image Processing (E-12)

26 Noise Removal Examples (cont...)

Image corrupted by Pepper noise

Image corrupted by Salt noise

Filtering above with a 3x3 Max Filter

Filtering above with a 3x3 Min Filter

© Nikou - Digital Image Processing (E-12)

27 Noise Removal Examples (cont...)

Image corrupted by uniform noise

Image further corrupted by Salt and Pepper noise

Filtering by a 5x5 Arithmetic Mean Filter

Filtering by a 5x5 Geometric Mean Filter

Filtering by a 5x5 Median Filter

Filtering by a 5x5 Alpha-Trimmed Mean Filter (d=5)

© Nikou - Digital Image Processing (E-12)

28 Adaptive Filters

The filters discussed so far are applied to an entire image without any regard for how image characteristics vary from one point to another.

The behaviour of **adaptive filters** changes depending on the characteristics of the image inside the filter region.

We will take a look at the **adaptive median filter**.

© Nikou - Digital Image Processing (E-12)

29 Adaptive Median Filtering

The median filter performs relatively well on impulse noise as long as the spatial density of the impulse noise is not large.

The adaptive median filter can handle much more spatially dense impulse noise, and also performs some smoothing for non-impulse noise.

© Nikou - Digital Image Processing (E-12)

30 Adaptive Median Filtering (cont...)

The key to understanding the algorithm is to remember that the adaptive median filter has three purposes:

- Remove impulse noise
- Provide smoothing of other noise
- Reduce distortion (excessive thinning or thickening of object boundaries).

© Nikou - Digital Image Processing (E-12)

## Adaptive Median Filtering (cont...)

In the adaptive median filter, the filter size changes depending on the characteristics of the image.

Notation:

- $S_{xy}$  = the support of the filter centered at  $(x, y)$
- $z_{min}$  = minimum grey level in  $S_{xy}$
- $z_{max}$  = maximum grey level in  $S_{xy}$
- $z_{med}$  = median of grey levels in  $S_{xy}$
- $z_{xy}$  = grey level at coordinates  $(x, y)$
- $S_{max}$  = maximum allowed size of  $S_{xy}$

## Adaptive Median Filtering (cont...)

Stage A:  $A1 = z_{med} - z_{min}$   
 $A2 = z_{med} - z_{max}$   
 If  $A1 > 0$  and  $A2 < 0$ , Go to stage B  
 Else increase the window size  
 If window size  $\leq S_{max}$  repeat stage A  
 Else output  $z_{med}$

Stage B:  $B1 = z_{xy} - z_{min}$   
 $B2 = z_{xy} - z_{max}$   
 If  $B1 > 0$  and  $B2 < 0$ , output  $z_{xy}$   
 Else output  $z_{med}$

## Adaptive Median Filtering (cont...)

Stage A:  $A1 = z_{med} - z_{min}$   
 $A2 = z_{med} - z_{max}$   
 If  $A1 > 0$  and  $A2 < 0$ , Go to stage B  
 Else increase the window size  
 If window size  $\leq S_{max}$  repeat stage A  
 Else output  $z_{med}$

Stage A determines if the output of the median filter  $z_{med}$  is an impulse or not (black or white).

If it is not an impulse, we go to stage B.

If it is an impulse the window size is increased until it reaches  $S_{max}$  or  $z_{med}$  is not an impulse.

Note that there is no guarantee that  $z_{med}$  will not be an impulse. The smaller the density of the noise is, and, the larger the support  $S_{max}$ , we expect not to have an impulse.

## Adaptive Median Filtering (cont...)

Stage B:  $B1 = z_{xy} - z_{min}$   
 $B2 = z_{xy} - z_{max}$   
 If  $B1 > 0$  and  $B2 < 0$ , output  $z_{xy}$   
 Else output  $z_{med}$

Stage B determines if the pixel value at  $(x, y)$ , that is  $z_{xy}$ , is an impulse or not (black or white).

If it is not an impulse, the algorithm outputs the unchanged pixel value  $z_{xy}$ .

If it is an impulse the algorithm outputs the median  $z_{med}$ .

## Adaptive Filtering Example

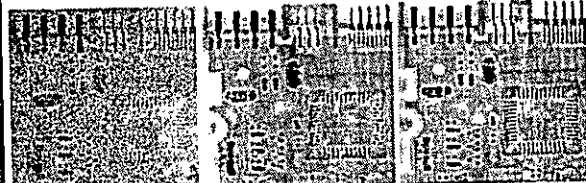


Image corrupted by salt and pepper noise with probabilities  $P_s = P_p = 0.25$

Result of filtering with a 7x7 median filter

Result of adaptive median filtering with  $S_{max} = 7$

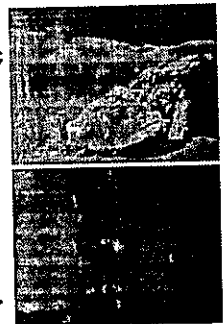
AMF preserves sharpness and details, e.g. the connector fingers.

## Periodic Noise

Typically arises due to electrical or electromagnetic interference.

Gives rise to regular noise patterns in an image.

Frequency domain techniques in the Fourier domain are most effective at removing periodic noise.



## Band Reject Filters

Removing periodic noise from an image involves removing a particular range of frequencies from that image.

*Band reject filters* can be used for this purpose

An ideal band reject filter is given as follows:

$$H(u,v) = \begin{cases} 1 & \text{if } D(u,v) < D_0 - \frac{W}{2} \\ 0 & \text{if } D_0 - \frac{W}{2} \leq D(u,v) \leq D_0 + \frac{W}{2} \\ 1 & \text{if } D(u,v) > D_0 + \frac{W}{2} \end{cases}$$

© Sakry - Digital Image Processing (2012)

## Band Reject Filters (cont...)

The ideal band reject filter is shown below, along with Butterworth and Gaussian versions of the filter



Ideal Band Reject Filter



Butterworth Band Reject Filter (of order 1)

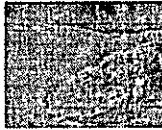


Gaussian Band Reject Filter

© Sakry - Digital Image Processing (2012)

## Band Reject Filter Example

Image corrupted by sinusoidal noise



Fourier spectrum of corrupted image



Butterworth band reject filter



Filtered image

© Sakry - Digital Image Processing (2012)

11  
11  
11

11  
11  
11  
11  
11

11

11





## Chap 4-2. Frequency domain processing

Jen-Chang Liu, 2006

## Review of Fourier transform

- Fourier series: Any function that periodically repeats itself can be expressed as the sum of **sines** and/or **cosines** of different frequencies, each multiplied by a different coefficient
- Fourier transform: Functions that are not periodic can be expressed as the integral of sines and/or cosines multiplied by a weighting functions
- Discrete Fourier transform: extends to discrete samples

## 1-D Discrete Fourier Transform (DFT)

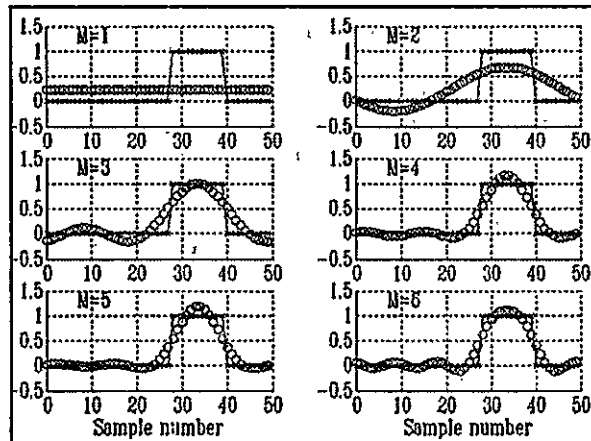
- $f(x)$ ,  $x=0,1,\dots,M-1$  . discrete function
- $F(u)$ ,  $u=0,1,\dots,M-1$ . DFT of  $f(x)$

Inverse transform (reconstruction):

$$f(x) = \sum_{u=0}^{M-1} F(u) e^{j2\pi \frac{u}{M}x}$$

Forward discrete Fourier transform:

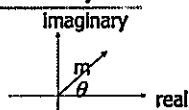
$$F(u) = \frac{1}{M} \sum_{x=0}^{M-1} f(x) e^{-j2\pi \frac{u}{M}x}$$



## $F(u)$ Complex quantity?

- Polar coordinate

$$F(u) = R(u) + jI(u) = |F(u)|e^{-j\theta(u)}$$

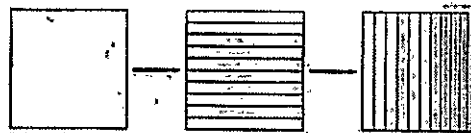


$$\begin{cases} |F(u)| = [R^2(u) + I^2(u)]^{1/2} & \text{magnitude} \\ \theta(u) = \tan^{-1} \left[ \frac{I(u)}{R(u)} \right] & \text{phase} \end{cases}$$

$$P(u) = |F(u)|^2 = R^2(u) + I^2(u) \quad \text{Power spectrum}$$

## Extend to 2-D DFT from 1-D

- 2-D DFT: 1-D DFT in horizontal then vertical



$$f(x, y) = \sum_{u=0}^{M-1} \sum_{v=0}^{N-1} F(u, v) e^{j2\pi \left( \frac{u}{M}x + \frac{v}{N}y \right)}$$

$$F(u, v) = \frac{1}{MN} \sum_{y=0}^{N-1} \sum_{x=0}^{M-1} f(x, y) e^{-j2\pi \left( \frac{u}{M}x + \frac{v}{N}y \right)}$$

### Complex Quantities to Real Quantities

- Useful representation
  - $|F(u,v)| = [R^2(u,v) + I^2(u,v)]^{1/2}$  magnitude
  - $\phi(u,v) = \tan^{-1} \left[ \frac{I(u,v)}{R(u,v)} \right]$  phase
  - Power spectrum  $P(u,v) = [F(u,v)]^2 = R^2(u,v) + I^2(u,v)$

### 2d DFT basis functions

IDFT:  $f(x,y) = \sum_{u=0}^{M-1} \sum_{v=0}^{N-1} F(u,v) e^{j2\pi(\frac{u}{M}x + \frac{v}{N}y)}$

將影像用  $e^{j2\pi(\frac{u}{M}x + \frac{v}{N}y)}$  合成, 其中  $(u,v)$  代表頻率

$c(x,y) = e^{j2\pi(\frac{0}{128}x + \frac{1}{128}y)}$ ,  $x = 0,1,2,\dots,127, y = 0,1,2,\dots,127$

### More DFT basis (real part)

### Example: reconstruction from DFT coefficients

$f(x,y) = \sum_{u=0}^{M-1} \sum_{v=0}^{N-1} F(u,v) e^{j2\pi(\frac{u}{M}x + \frac{v}{N}y)}$

Zigzag scan

### Example: reconstruction from DFT coefficients

<http://www.ncnu.edu.tw/~jcliu/course/dlp2005/lena1dft.m>

### Notes on showing DFT

`imshow(log(abs(F)), [])`

$F(1,1) = 7761921$

$F(1,127) = 334.79 + 10i$

`F = fft2(I);`  
`imshow(abs(F), [])`

Lena 256x256

### Log transformations

- $s = c \log(1+r)$
- Compress the dynamic range of images with large variation in pixel values

### Periodicity and conjugate symmetry property of 2-D DFT

### Outline

- Frequency domain operations
- Smoothing Frequency Domain Filters
- Sharpening Frequency Domain Filters
- Homomorphic Filtering

### Convolution – 2-D case

- 2d convolution 卷积

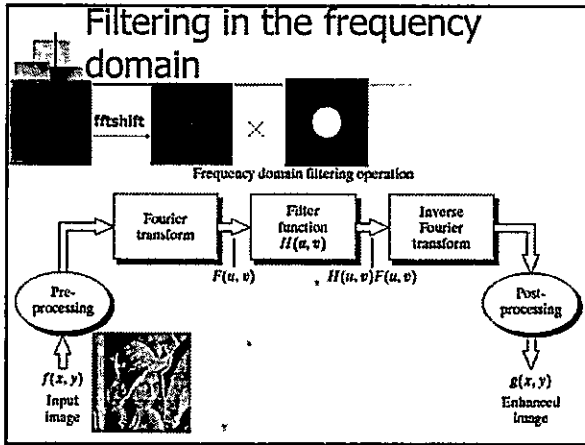
$$g(x, y) = f(x, y) * h(x, y) = \frac{1}{MN} \sum_{m=0}^{M-1} \sum_{n=0}^{N-1} f(m, n) h(x-m, y-n)$$

- Masking operation

$$g(x, y) = \frac{1}{MN} \sum_{m=0}^{M-1} \sum_{n=0}^{N-1} f(m, n) h(m-x, n-y)$$

### Convolution theorem

$$f(x, y) * h(x, y) \Leftrightarrow F(u, v) H(u, v)$$



- ### Outline
- Frequency Domain Operations
  - Smoothing Frequency Domain Filters
  - Sharpening Frequency Domain Filters
  - Homomorphic Filtering

- ### Smoothing frequency-domain filters
- Design issue
    - $G(u,v) = F(u,v) H(u,v)$
    - Remove high freq. component (details, noise, ...)
  - Ideal low-pass filter
  - Butterworth filter
  - Gaussian filter
- More smooth in the edge of cut-off frequency

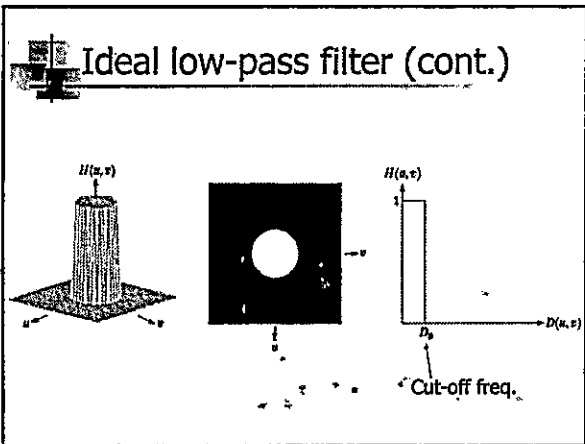
### Ideal low-pass filter

- Sharp cut-off frequency

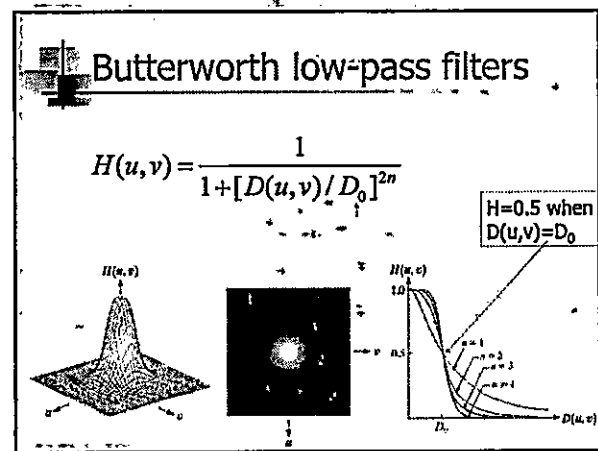
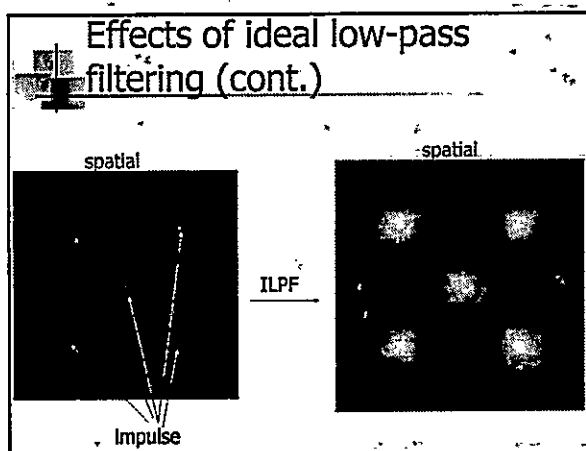
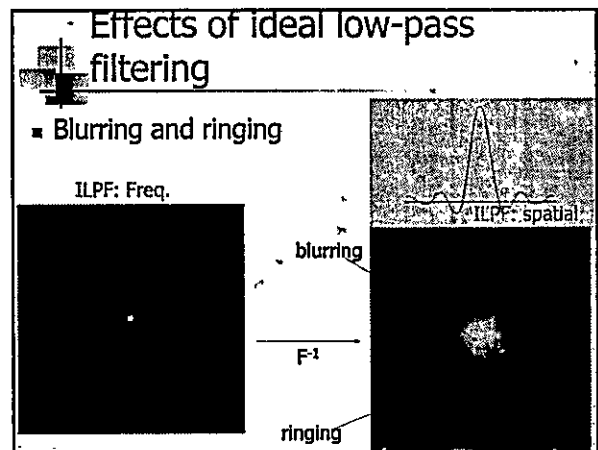
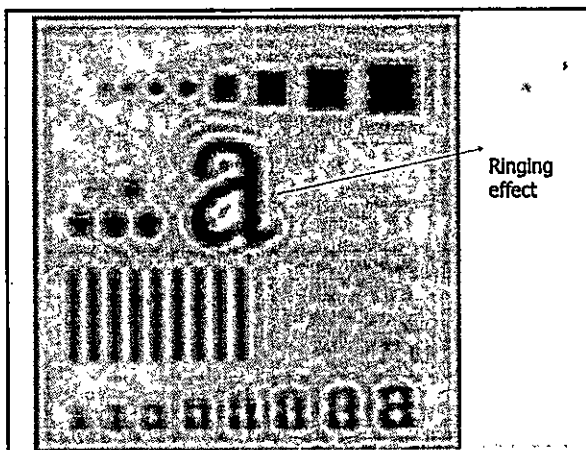
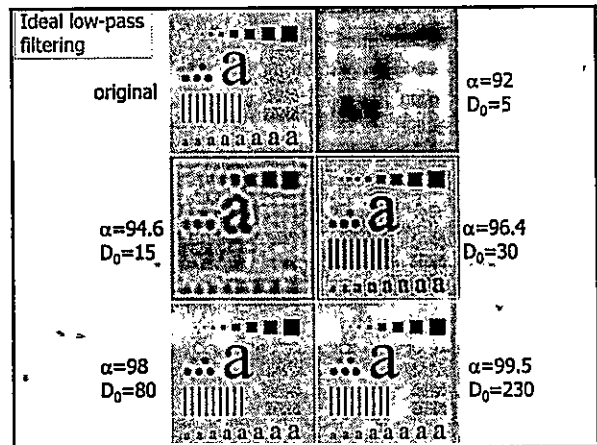
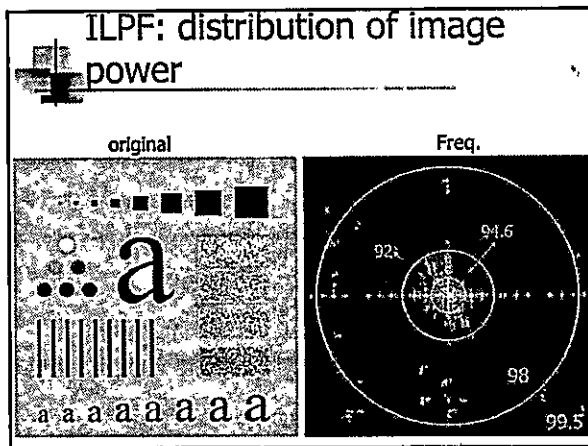
$$H(u,v) = \begin{cases} 1 & \text{if } D(u,v) \leq D_0 \\ 0 & \text{if } D(u,v) \geq D_0 \end{cases}$$

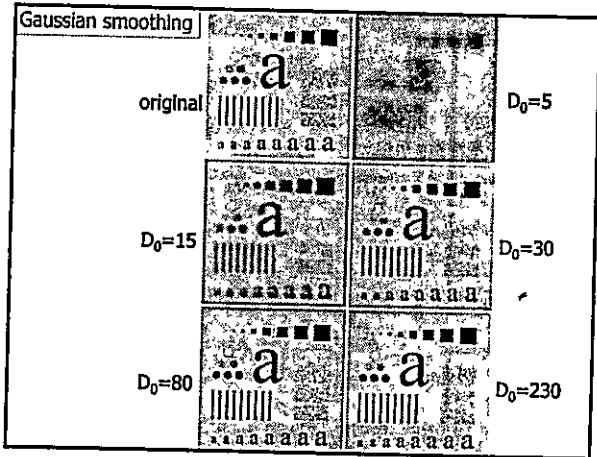
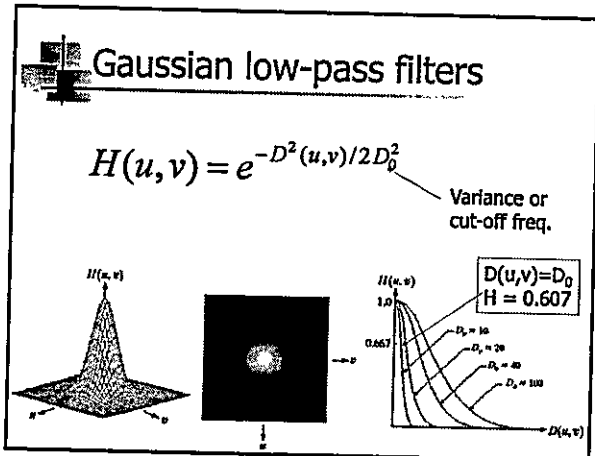
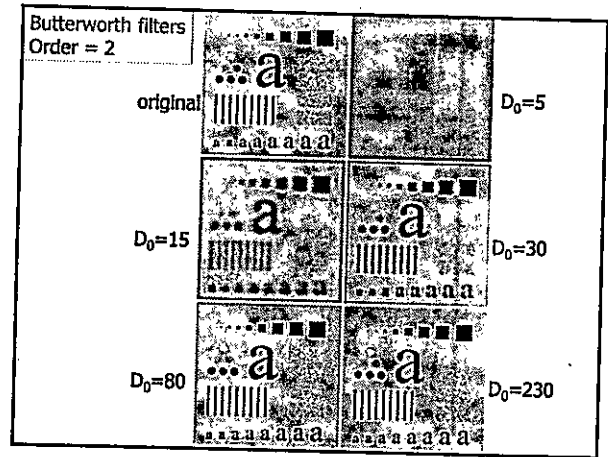
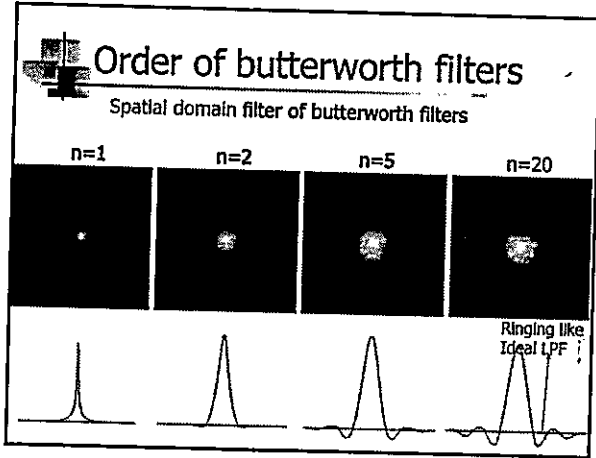
where  $D(u,v)$  is the distance to the center freq.

$$D(u,v) = [(u - M/2)^2 + (v - N/2)^2]^{1/2}$$



- ### Ideal low-pass filter (con.t)
- ILPF can not be realized in electronic components, but can be implemented in a computer
  - Decision of cut-off freq.
    - Measure the percentage of image power within the low freq.
- $$\alpha = 100 \times \left[ \frac{\sum_{(u,v) \text{ cut-off freq}} P(u,v)}{P_T} \right]$$
- $$\text{Total Image power } P_T = \sum_{u=0}^{M-1} \sum_{v=0}^{N-1} P(u,v)$$





### Practical applications: 1

444x508      GLPF,  $D_0=80$

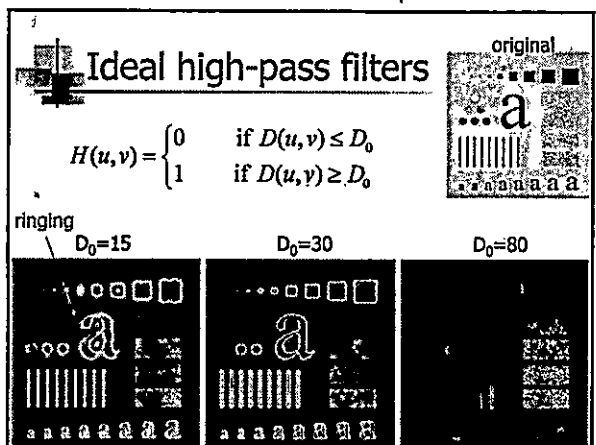
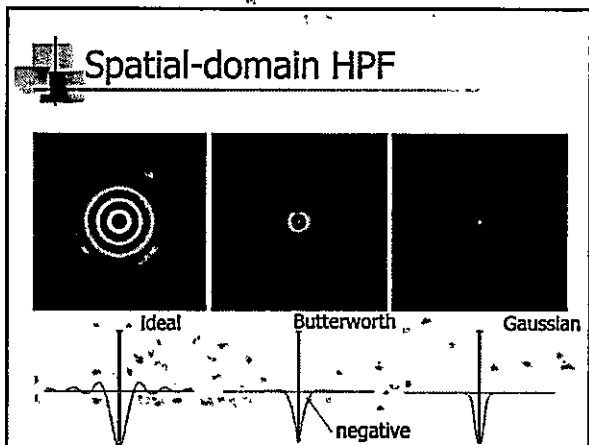
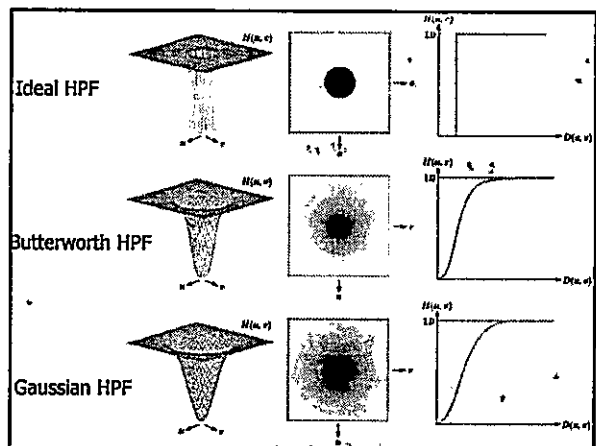
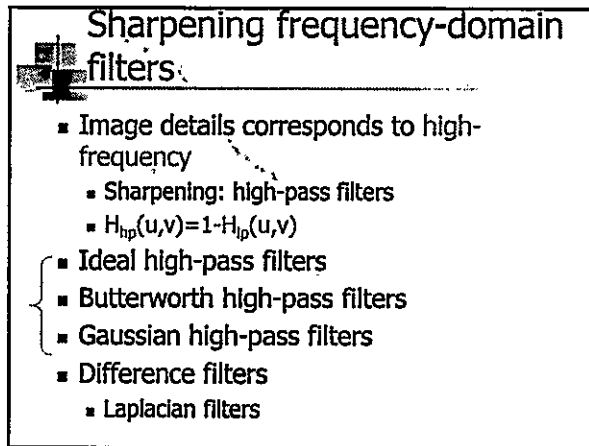
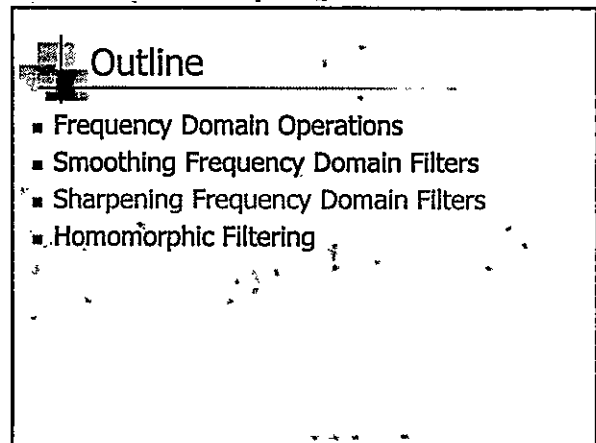
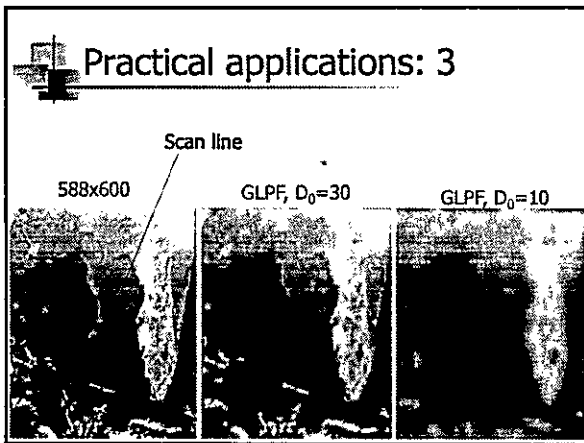
Historically, certain computer programs were written using only two digits rather than four to define the applicable year. Accordingly, the company's software may recognize a date using "00" as 1900 rather than the year 2000.

Historically, certain computer programs were written using only two digits rather than four to define the applicable year. Accordingly, the company's software may recognize a date using "00" as 1900 rather than the year 2000.

### Practical applications: 2

1028x732      GLPF,  $D_0=80$

GLPF,  $D_0=100$



### Butterworth high-pass filters

$$H(u, v) = \frac{1}{1 + [D_0 / D(u, v)]^{2n}}$$

$n=2, D_0=15 \quad D_0=30 \quad D_0=80$

### Gaussian high-pass filters

$$H(u, v) = 1 - e^{-D^2(u, v) / 2D_0^2}$$

$D_0=15 \quad D_0=30 \quad D_0=80$

### Laplacian frequency-domain filters

- Spatial-domain Laplacian (2nd derivative)
 
$$\nabla^2 f = \frac{\partial^2 f}{\partial x^2} + \frac{\partial^2 f}{\partial y^2}$$
- Fourier transform
 
$$\mathcal{F}\left[\frac{\partial^n f(x)}{\partial x^n}\right] = (ju)^n F(u)$$

$$\mathcal{F}\left[\frac{\partial^2 f(x, y)}{\partial x^2} + \frac{\partial^2 f(x, y)}{\partial y^2}\right] = (ju)^2 F(u, v) + (jv)^2 F(u, v)$$

$$= -(u^2 + v^2)F(u, v)$$

### Laplacian frequency-domain filters

The Laplacian filter in the frequency domain is  $H(u, v) = -(u^2 + v^2)$

$H(u, v) = -(u^2 + v^2)$  frequen

spatial

0	1	0
1	-4	1
0	1	0

original      Laplacian

Scaled Laplacian      original + Laplacian



### Outline

- Frequency Domain Operations
- Smoothing Frequency Domain Filters
- Sharpening Frequency Domain Filters
- Homomorphic Filtering

### Image Formation Model

The diagram illustrates the image formation process. An illumination source (represented by a sun) emits light towards a scene (represented by a tree). The light reflects off the scene towards an eye, which observes the scene. The path of the reflected light is labeled 'reflection'.

### Homomorphic filtering

- Image formation model
  - $f(x,y) = i(x,y) r(x,y)$

illumination: Slow spatial variations  
 reflectance: vary abruptly, particularly at the junctions of dissimilar objects

### Homomorphic filtering

- Product term
 
$$\mathfrak{F}\{f(x,y)\} = \mathfrak{F}\{i(x,y)r(x,y)\} \neq \mathfrak{F}\{i(x,y)\}\mathfrak{F}\{r(x,y)\}$$
- Log of product
  - $f(x,y) = i(x,y) r(x,y)$
  - $\Rightarrow \ln f(x,y) = \ln i(x,y) + \ln r(x,y)$
- Separation of signal source:
 
$$\mathfrak{F}\{\ln f(x,y)\} = \mathfrak{F}\{\ln i(x,y) + \ln r(x,y)\}$$

$$= \mathfrak{F}\{\ln i(x,y)\} + \mathfrak{F}\{\ln r(x,y)\}$$

### Homomorphic filtering approach

The flowchart shows the homomorphic filtering process. The input image  $f(x,y)$  is first processed by a natural logarithm ( $\ln$ ) block. The result is then transformed into the frequency domain using the Discrete Fourier Transform (DFT). A filtering block  $H(u,v)$  is applied in the frequency domain. The filtered result is then transformed back to the spatial domain using the inverse DFT ( $(DFT)^{-1}$ ). Finally, an exponential ( $\exp$ ) block is applied to produce the output image  $g(x,y)$ .

A separate diagram illustrates the decomposition of the logarithm of the image into its illumination and reflection components. The input  $\ln f(x,y)$  is split into  $\ln i(x,y)$  (illumination) and  $\ln r(x,y)$  (reflection). These components are then processed by a filter that separates them based on their frequency characteristics.

### How to identify the illumination and reflection?

- Illumination -> low frequency
- Reflection -> high frequency

The graph shows an example filter  $H(u,v)$  for sharpening. The vertical axis is  $H(u,v)$  and the horizontal axis is the radius from the origin. The filter is 1 for low frequencies (illumination) and 0 for high frequencies (reflection). The graph shows a smooth curve that starts at 1 for low frequencies and drops to 0 for high frequencies. The region where  $H(u,v) = 1$  is labeled 'illumination' and the region where  $H(u,v) = 0$  is labeled 'reflection'.




## Color Image Processing

Jen-Chang Liu, Spring 2006

- For a long time I limited myself to one color – as a form of discipline.
  - Pablo Picasso
- It is only after years of preparation that the young artist should touch color – not color used descriptively, that is, but as a means of personal expression.
  - Henri Matisse

## Preview

- Why use color in image processing?
  - Color is a powerful descriptor
    - Object identification and extraction
    - eg. Face detection using skin colors
  - Humans can discern thousands of color shades and intensities
    - c.f. Human discern only two dozen shades of grays



## Preview (cont.)

- Two category of color image processing
  - Full color processing
    - Images are acquired from full-color sensor or equipments
  - Pseudo-color processing
    - In the past decade, color sensors and processing hardware are not available
    - Colors are assigned to a range of monochrome intensities

## Outline

- Color fundamentals
- Color models
- Pseudo-color image processing
- Basics of full-color image processing
- Color transformations
- Smoothing and sharpening

## Color fundamentals

- Physical phenomenon
  - Physical nature of color is known
- Psysio-psychological phenomenon
  - How human brain perceive and interpret color?

### Color fundamentals (cont.)

- 1666, Isaac Newton 三稜鏡

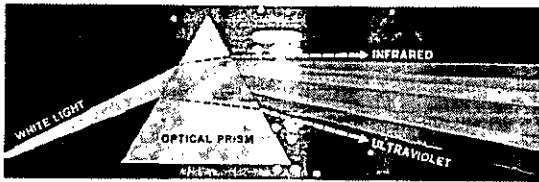


FIGURE 6.1 Color spectrum seen by passing white light through a prism. (Courtesy of the General Electric Co., Lamp Business Division.)

### Visible light

- Chromatic light span the electromagnetic spectrum (EM) from 400 to 700 nm

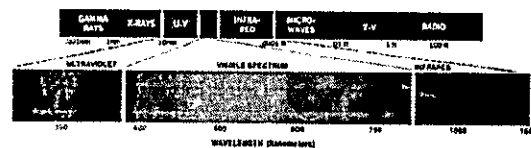
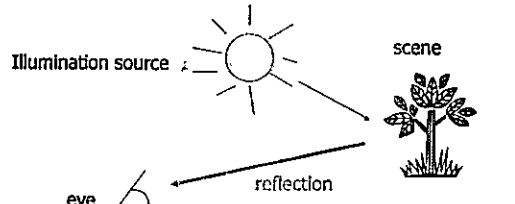


FIGURE 6.2 Wavelengths comprising the visible range of the electromagnetic spectrum. (Courtesy of the General Electric Co., Lamp Business Division.)

### Color fundamentals (cont.)

- The color that human perceive in an object = the light reflected from the object



### Physical quantities to describe a chromatic light source

- Radiance: total amount of energy that flow from the light source, measured in watts (W)
- Luminance: amount of energy an observer perceives from a light source, measured in lumens (lm 流明)
  - Far infrared light: high radiance, but 0 luminance
- Brightness: subjective descriptor that is hard to measure, similar to the achromatic notion of intensity

### How human eyes sense light?

- 6~7M Cones are the sensors in the eye
- 3 principal sensing categories in eyes
  - Red light 65%, green light 33%, and blue light 2%

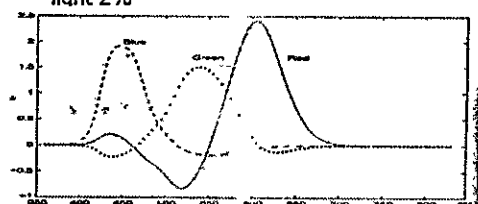
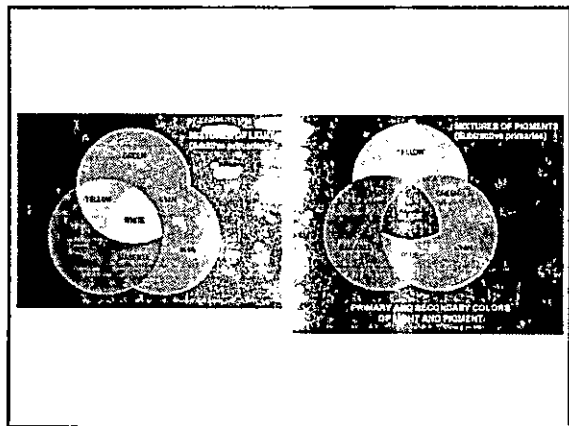


FIGURE 6.3 CIE color-matching functions (CIE, 1931)

### Primary and secondary colors

- In 1931, CIE(International Commission on Illumination) defines specific wavelength values to the primary colors
  - B = 435.8 nm, G = 546.1 nm, R = 700 nm
  - However, we know that no single color may be called red, green, or blue
- Secondary colors: G+B=Cyan, R+G=Yellow, R+B=Magenta



### Primary colors of light v.s. primary colors of pigments

- Primary color of pigments
  - Color that subtracts or absorbs a primary color of light and reflects or transmits the other two

Color of light:            R            G            B

Color of pigments:    absorb R    absorb G    absorb B  
                                 Cyan            Magenta    Yellow

### Application of additive nature of light colors

- Color TV

### CIE XYZ model

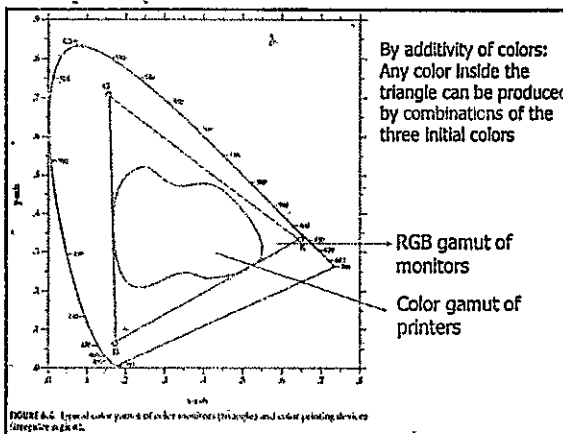
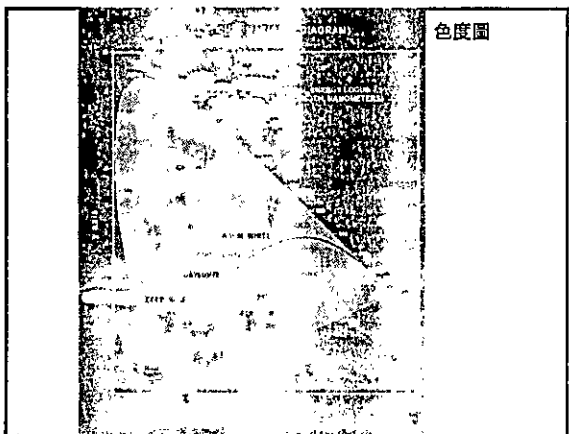
- RGB -> CIE XYZ model

$$\begin{bmatrix} X \\ Y \\ Z \end{bmatrix} = \begin{bmatrix} 0.431 & 0.342 & 0.178 \\ 0.222 & 0.707 & 0.071 \\ 0.020 & 0.130 & 0.939 \end{bmatrix} \begin{bmatrix} R \\ G \\ B \end{bmatrix}$$

- Normalized tristimulus values

$$x = \frac{X}{X+Y+Z} \quad y = \frac{Y}{X+Y+Z} \quad z = \frac{Z}{X+Y+Z}$$

=> x+y+z=1. Thus, x, y (chromaticity coordinate) is enough to describe all colors



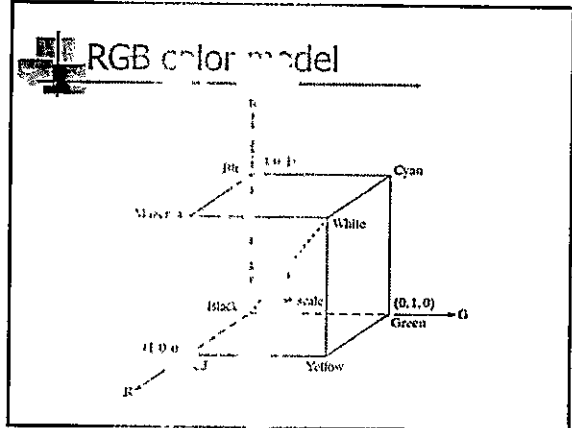
### Outline

- Color fundamentals
- Color models
- Pseudo-color image processing
- Basics of full-color image processing
- Color transformations
- Smoothing and sharpening

### Color models

- Color model, color space, color system
  - Specify colors in a standard way
  - A coordinate system that each color is represented by a single point
- RGB model
- CYM model
- CYMK model
- HSI model

Suitable for hardware or applications  
- match the human description



### Pixel depth

- Pixel depth: the number of bits used to represent each pixel in RGB space
- Full-color image: 24-bit RGB color image
  - (R, G, B) = (8 bits, 8 bits, 8 bits)

### Safe RGB colors

- Subset of colors enough for some applications
- Safe RGB colors (safe Web colors, safe browser colors)

Number System	Color	Hex	Dec	RGB
Hex	000000	00	00	00 00 00
Decimal	000000	00	00	00 00 00

TABLE 6.1 Valid values of each RGB component in a safe color.

### Safe RGB color (cont.)

Full color cube      Safe color cube

10

10

10

10

10

10

10

10

10

10

10

10



10

10

10

10

10

10



10

10

10

10

10

10

10

10

10

10

10

10

10

### Outline

- Color fundamentals
- Color models
- Pseudo-color image processing
- Basics of full-color image processing
- Color transformations
- Smoothing and sharpening

### Color models

- Color model, color space, color system
  - Specify colors in a standard way
  - A coordinate system that each color is represented by a single point
- RGB model
- CYM model
- CYMK model
- HSI model

Suitable for hardware or applications  
- match the human description

### RGB color model

### Pixel depth

- Pixel depth: the number of bits used to represent each pixel in RGB space
- Full-color image: 24-bit RGB color image
  - (R, G, B) = (8 bits, 8 bits, 8 bits)

### Safe RGB colors

- Subset of colors is enough for some application
- Safe RGB colors (safe Web colors, safe browser colors)

Number System	Color Equivalents					
Hex	00	33	66	99	CC	FF
Decimal	0	51	102	153	204	255

$(6)^3 = 216$

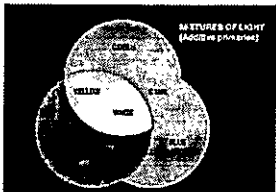
TABLE 6.1  
Valid values of each RGB component in a safe color.

### Safe RGB color (cont.)



### CMY model (+Black = CMYK)

- CMY: secondary colors of light, or primary colors of pigments
- Used to generate hardcopy output

$$\begin{bmatrix} C \\ M \\ Y \end{bmatrix} = \begin{bmatrix} 1 \\ 1 \\ 1 \end{bmatrix} - \begin{bmatrix} R \\ G \\ B \end{bmatrix}$$


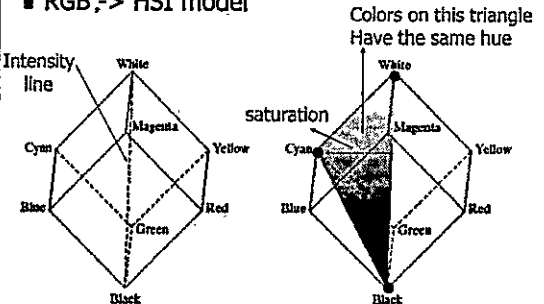
### HSI color model

- Will you describe a color using its R, G, B components?
- Human describe a color by its hue, saturation, and brightness
- Hue 色度: color attribute
- Saturation: purity of color (white->0, primary color->1)
- Brightness: achromatic notion of intensity

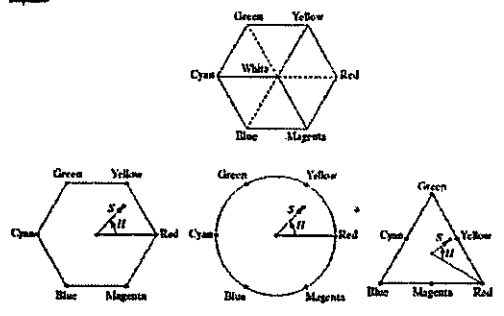
### HSI color model (cont.)

- RGB -> HSI model

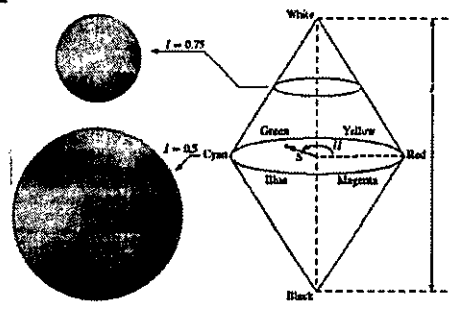
Colors on this triangle Have the same hue



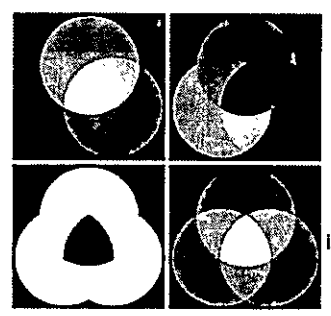
### HSI model: hue and saturation



### HSI model



### HSI component images



### Outline

- Color fundamentals
- Color models
- Pseudo-color image processing
- Basics of full-color image processing
- Color transformations
- Smoothing and sharpening

### Pseudo-color image processing

- Assign colors to gray values based on a specified criterion
- For human visualization and interpretation of gray-scale events
- Intensity slicing
- Gray level to color transformations

### Intensity slicing

- 3-D view of intensity image

### Intensity slicing (cont.)

- Alternative representation of intensity slicing

### Intensity slicing (cont.)

- More slicing plane, more colors

### Application 1

Radiation test pattern — 8 color regions

\* See the gradual gray-level changes

### Application 2

X-ray image of a weld  
焊接物

### Application 3

Rainfall statistics

### Gray level to color transformation

- Intensity slicing: piecewise linear transformation

- General Gray level to color transformation

### Gray level to color transformation

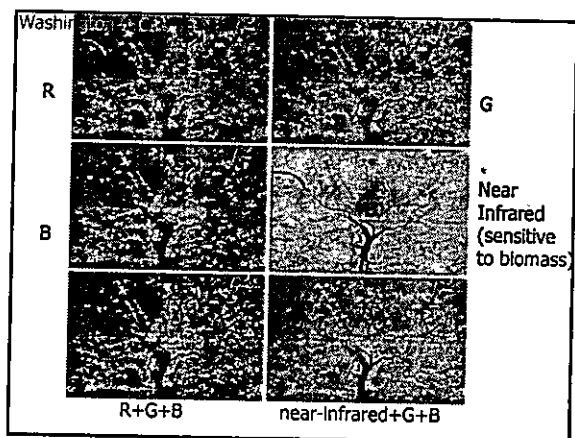
FIGURE 6.23 Functional block diagram for pseudocolor image processing.  $f_R$ ,  $f_G$ , and  $f_B$  are fed into the corresponding red, green, and blue inputs of an RGB color monitor.

### Application 1

Explosive Gunpowder background

### Combine several monochrome images

Example: multi-spectral images



### Outline

- Color fundamentals
- Color models
- Pseudo-color image processing
- Basics of full-color image processing
- Color transformations
- Smoothing and sharpening

### Color pixel

- A pixel at  $(x,y)$  is a vector in the color space
  - RGB color space

$$c(x,y) = \begin{bmatrix} R(x,y) \\ G(x,y) \\ B(x,y) \end{bmatrix}$$

c.f. gray-scale image  
 $f(x,y) = I(x,y)$

### Example: spatial mask

### How to deal with color vector?

- Per-color-component processing
  - Process each color component
- Vector-based processing
  - Process the color vector of each pixel
- When can the above methods be equivalent?
  - Process can be applied to both scalars and vectors
  - Operation on each component of a vector must be independent of the other component

### Two spatial processing categories

- Similar to gray scale processing studied before, we have to major categories
  - Pixel-wise processing
  - Neighborhood processing

### Outline

- Color fundamentals
- Color models
- Pseudo-color image processing
- Basics of full-color image processing
- Color transformations
- Smoothing and sharpening

### Color transformation

- Similar to gray scale transformation
  - $g(x,y) = T[f(x,y)]$
- Color transformation:
  - $s_i = T_i(r_1, r_2, \dots, r_n), i = 1, 2, \dots, n$

$g(x,y)$   
 $s_1$   
 $s_2$   
 $\dots$   
 $s_n$

$f(x,y)$   
 $f_1$   
 $f_2$   
 $\dots$   
 $f_n$

### Use which color model in color transformation?

- RGB  $\Leftrightarrow$  CMY(K)  $\Leftrightarrow$  HSI
- Theoretically, any transformation can be performed in any color model
- Practically, some operations are better suited to specific color model

### Example: modify intensity of a color image

- **Example:**  $g(x,y) = k f(x,y), 0 < k < 1$
- HSI color space
  - Intensity:  $s_3 = k r_3$
  - Note: transform to HSI requires complex operations
- RGB color space
  - For each R,G,B component:  $s_i = k r_i$
- CMY color space
  - For each C,M,Y component:  $s_i = k r_i + (1-k)$

RGB

CMY

I

H,S

### Color image smoothing: averaging mask

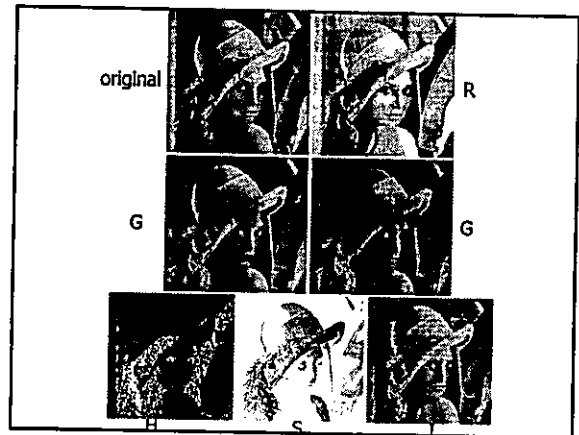
$$\bar{c}(x, y) = \frac{1}{K} \sum_{(x,y) \in S_{xy}} c(x, y)$$

vector processing

↓ Neighborhood Centered at (x,y)

$$\bar{c}(x, y) = \begin{bmatrix} \frac{1}{K} \sum_{(x,y) \in S_{xy}} R(x, y) \\ \frac{1}{K} \sum_{(x,y) \in S_{xy}} G(x, y) \\ \frac{1}{K} \sum_{(x,y) \in S_{xy}} B(x, y) \end{bmatrix}$$

per-component processing



### Example: 5x5 smoothing mask

	Smooth I in HSI model	
RGB model		difference

**FIGURE 4.40** Image smoothing with a 5 × 5 averaging mask. (a) Result of processing each RGB component image. (b) Result of processing the intensity component of the HSI image and converting to RGB. (c) Difference between the two results.

Centre of Excellence for e-Resource Development (COEERD)

Wavelets and Multi-resolution Processing

# Wavelets and Multi-resolution Processing

Centre of Excellence for e-Resource Development (COEERD)

Wavelets and Multi-resolution Processing

## Learning Objectives

At the end of this topic, you will be able to:

- Explain Image Pyramids
- Discuss about Subband Coding & Haar Transform
- Explain Multiresolution Expansions and Wavelet Transforms in One Dimension
- Describe about The Fast Wavelet Transform
- Explain the concept of Wavelet Transforms in Two Dimensions and Wavelet packets

Centre of Excellence for e-Resource Development (COEERD)

Wavelets and Multi-resolution Processing

## Outcomes

By the end of this topic, you will be able to:

- Understand Image Pyramids
- Differentiate the Subband Coding & Haar Transform
- Discuss Multiresolution Expansions and Wavelet Transforms in One Dimension
- Explain about The Fast Wavelet Transform
- Discuss the concept of Wavelet Transforms in Two
- Explain the Dimensions and wavelet packets

Centre of Excellence for e-Resource Development (COEERD)

Wavelets and Multi-resolution Processing

## Outcomes

By the end of this topic, you will be able to:

- Understand Image Pyramids
- Differentiate the Subband Coding & Haar Transform
- Discuss Multiresolution Expansions and Wavelet Transforms in One Dimension
- Explain about The Fast Wavelet Transform
- Discuss the concept of Wavelet Transforms in Two
- Explain the Dimensions and Wavelet packets

Centre of Excellence for e-Resource Development (COEERD)

Wavelets and Multi-resolution Processing

## Image Pyramids

The most simple structure for representing images of more than one resolution found by Sarr and Addison is the image pyramid.

An image pyramid is a collection of decreasing resolution images arranged in the shape of a pyramid.

The base of the pyramid contains a high-resolution representation of the image being processed, the top contains a low-resolution approximation. As moving up the pyramid, both size and resolution decrease.

Base level  $J$  is of size  $2^J \times 2^J$  or  $N \times N$ , where  $J = \log_2 N$ , apex level  $0$  is of size  $1 \times 1$  and

Centre of Excellence for e-Resource Development (COEERD)

Wavelets and Multi-resolution Processing

## Image Pyramids

### Construction of Image Pyramids

The Level  $J - 1$  approximation output provides the images needed to build an approximation pyramid, while the Level  $J$  prediction residual output is used to build a complementary prediction residual pyramid.

- Unlike approximation pyramids, prediction residual pyramids contain only one reduced-resolution approximation of the input image.
- All other levels contain prediction residuals, where the level  $j$  prediction residual is defined as the difference between the level  $j$  approximation and an estimate of the level  $j$  approximation based on the level  $j - 1$  approximation.
- Before the first iteration, the image to be processed in pyramid form is placed

Centre of Excellence for e-Resource Development (COEERD)

Wavelets and Multi-resolution Processing

### Image Pyramids

The diagram illustrates the construction of an image pyramid. It starts with a Level J input image. This image is processed by a Downsampler (rows and columns) and an Approximation filter to produce a Level J-1 approximation. This approximation is then processed by an Approximation operator (rows and columns) to produce a Level J-1 approximation. The Level J-1 approximation is then processed by an Interpolation filter and a Prediction operator to produce a Level J prediction residual.

Centre of Excellence for e-Resource Development (COEERD)

Wavelets and Multi-resolution Processing

### Image Pyramids

Steps for Construction of Image Pyramids

The following three-step procedure is then executed  $P$  times for  $j = J, J-1, \dots, 1$  and  $P > 1$ :

- STEP 1: Compute a reduced-resolution approximation of the Level  $j$  input image. This is done by filtering and downsampling the filtered result by a factor of 2. Place the resulting approximation at level  $j-1$  of the approximation pyramid.
- STEP 2: Create an estimate of the Level  $j$  input image from the reduced-resolution approximation generated at step 1. This is done by upsampling and filtering. The resulting prediction image will have the same dimensions as the Level  $j$  input image.
- STEP 3: Compute the difference between the prediction image of Step 2 and the input to step 1. Place this result in level  $j$  of the prediction residual pyramid.

Centre of Excellence for e-Resource Development (COEERD)

Wavelets and Multi-resolution Processing

### Image Pyramids

Steps for Construction of Image Pyramids

At the conclusion of  $P$  operations, the level  $J-P$  approximation output is placed in the prediction residual pyramid at level  $J-P$ . If a prediction residual pyramid is not needed, this operation along with steps 2 and 3 and the approximation, interpolation filter, and summer can be omitted.

Centre of Excellence for e-Resource Development (COEERD)

Wavelets and Multi-resolution Processing

### Image Pyramids

Expressions for Upsampling and Downsampling

Various approximation filtering methods were used to produce various image pyramids. The following table summarizes the filtering techniques used:

S.No	Filtering Technique	Image Pyramid
1	Neighbor hood averaging	Mean pyramids
2	Low pass Gaussian filtering	Gaussian pyramids
3	No filtering	Subsampling pyramids

Given an integer variable  $n$  and the sequence of samples  $f(n)$ , upsampled sequence  $f(n)$  sampled at factor of 2 is defined as:

$$f_2(n) = \begin{cases} f(n/2) & \text{if } n \text{ is even} \\ 0 & \text{if } n \text{ is odd} \end{cases}$$

The complementary operation of downsampling by 2 is defined as:

$$f_2(n) = f(n/2)$$

Centre of Excellence for e-Resource Development (COEERD)

Wavelets and Multi-resolution Processing

### Subband Coding

In subband coding, an image is decomposed into a set of band limited components, called subbands. The decomposition is performed so that the subbands can be reassembled to reconstruct the original image without error.

$$f(n) = \sum_{k=0}^{K-1} A_k(n) \cos(\frac{\pi k n}{K})$$

$$A_k(n) = \sum_{l=0}^{K-1} a_l(n) \cos(\frac{\pi k l}{K})$$

$$a_l(n) = \sum_{m=0}^{K-1} A_m(n) \cos(\frac{\pi k m}{K})$$

It is constructed from three basic components: unit delays, multipliers, and adders.

Along the top of the filter, unit delays are connected in series to create  $K-1$  delayed

Centre of Excellence for e-Resource Development (COEERD)

Wavelets and Multi-resolution Processing

### Subband Coding

Delayed sequence  $f(n-1)$  is given by:

$$f(n-1) = \sum_{k=0}^{K-1} A_k(n-1) \cos(\frac{\pi k (n-1)}{K})$$

Input sequence  $f(n) = \sum_{k=0}^{K-1} A_k(n) \cos(\frac{\pi k n}{K})$  and the  $K-1$  delayed sequences at the outputs of the unit delays, denoted  $f(n-1), f(n-2), \dots, f(n-K+1)$  are multiplied by constants  $A_0, A_1, \dots, A_{K-1}$ , respectively, and summed to produce the desired output sequence:

$$h(n) = \sum_{k=0}^{K-1} A_k(n) \cos(\frac{\pi k n}{K})$$



Centre of Excellence for e-Resource Development (CoEERD)

Wavelets and Multi-resolution Processing

Subband Coding

A Two-band Sub-band Coding and Decoding System

$$f(n) \xrightarrow{H_0(z)} x_0(n) \xrightarrow{H_1(z)} x_1(n) \xrightarrow{H_2(z)} x_2(n)$$

$$f(n) \xrightarrow{H_1(z)} x_1(n) \xrightarrow{H_0(z)} x_0(n) \xrightarrow{H_2(z)} x_2(n)$$

Low Band High Band

Centre of Excellence for e-Resource Development (CoEERD)

Wavelets and Multi-resolution Processing

Subband Coding

The system is composed of two filter banks, each containing two FIR filters.

- The analysis filter bank, which includes filters  $H_0(z)$  and  $H_1(z)$ , is used to break input sequence  $f(n)$  into two half-length sequences  $x_0(n)$  and  $x_1(n)$ , the subbands that represent the input.
- The filters  $H_0(z)$  and  $H_1(z)$  are half-band filters whose idealized transfer characteristics,  $H_0$  and  $H_1$ ,
- Filter  $h_0(n)$  is a lowpass filter whose output, subband  $x_0(n)$ , is called an approximation of  $f(n)$ ; filter  $H_1(z)$  is a highpass filter whose output, sub-band signal, is called the high frequency part of  $f(n)$ .
- Synthesis filter banks  $G_0(z)$  and  $G_1(z)$  combine  $x_0(n)$  and  $x_1(n)$  to produce  $f(n)$ .
- The goal in subband coding is to select  $h_0(n)$ ,  $H_1(z)$ ,  $G_0(z)$ , and  $G_1(z)$  so that  $f(n) = \hat{f}(n)$ .

Centre of Excellence for e-Resource Development (CoEERD)

Wavelets and Multi-resolution Processing

Perfect Reconstruction Filters

The input and output of the sub-band coding and decoding system are identical. When this is accomplished, the resulting system is said to employ perfect reconstruction filters.

For perfect reconstruction, the impulse responses of the synthesis and analysis filters must be related in one of the following two ways:

$$g_0(n) = (-1)^n h_0(n)$$

$$g_1(n) = (-1)^n h_1(n)$$

$$g_0(n) = (-1)^n h_1(n)$$

$$g_1(n) = (-1)^n h_0(n)$$

Filters  $h_0(z)$ ,  $h_1(z)$ ,  $G_0(z)$ , and  $G_1(z)$  are said to be cross-modulated because:

Centre of Excellence for e-Resource Development (CoEERD)

Wavelets and Multi-resolution Processing

Perfect Reconstruction Filters

The Haar transform

The Haar transform can be expressed in the following matrix form:

$$T = HTT^T$$

Where  $T$  is an  $N \times N$  image matrix,  $H$  is an  $N \times N$  Haar transformation matrix, and  $T$  is the resulting  $N \times N$  transform. The transform is required because  $H$  is not symmetric.

For the Haar transform,  $H$  contains the Haar basis functions,  $h(p, q)$ . They are defined over the continuous, closed interval  $T \in [0, 1]$  for  $1 \leq p, q \leq N$ .

To generate  $H$ , we define the vector  $t$  such that  $t = [t_1, t_2, \dots, t_N]^T$ , where  $t_p = 1$ ,  $t_q = 0$  at  $1 \leq p \leq N$ , and  $t_p = 0$ ,  $t_q = 1$  for  $p \leq N$ . Then the Haar basis functions are:

Centre of Excellence for e-Resource Development (CoEERD)

Wavelets and Multi-resolution Processing

Perfect Reconstruction Filters:

$$x_1(z) = \frac{1}{\sqrt{2}} \begin{bmatrix} 1 & 1 \\ 1 & -1 \end{bmatrix} \begin{bmatrix} x_0(z) \\ x_1(z) \end{bmatrix}$$

The 1<sup>st</sup> row of an  $N \times N$  Haar transformation matrix contains the elements of  $h(p, q)$  for  $p = 0, 1, \dots, N-1$ ,  $q = 0, 1, \dots, N-1$ .

Centre of Excellence for e-Resource Development (CoEERD)

Wavelets and Multi-resolution Processing

Perfect Reconstruction Filters

Example for Haar Transform

$N = 2$ , the first row of the  $2 \times 2$  Haar matrix is computed using  $h(p, q)$  with  $p = 0, 1, 1, 0$ .

From eqn (8)  $h_0(1, 0)$  is equal to  $1/\sqrt{2}$ , independent of  $q$ . In the 2nd row of  $H$ , the two identical  $h(1, 1)$  elements. The second row is obtained by computing  $h_1(1, q)$  for  $q = 0, 1, 1, 0$ .

Because  $h = 2p + q - 1$ , when  $h = 1$ ,  $p = 0$  and  $q = 1$ .

$$h_1(1, 0) = \frac{1}{\sqrt{2}} \begin{bmatrix} 1 & 1 \\ 1 & -1 \end{bmatrix} \begin{bmatrix} 1 \\ 0 \end{bmatrix} = \frac{1}{\sqrt{2}} \begin{bmatrix} 1 \\ 1 \end{bmatrix}$$

$$h_1(1, 1) = \frac{1}{\sqrt{2}} \begin{bmatrix} 1 & 1 \\ 1 & -1 \end{bmatrix} \begin{bmatrix} 0 \\ 1 \end{bmatrix} = \frac{1}{\sqrt{2}} \begin{bmatrix} 1 \\ -1 \end{bmatrix}$$

Centre of Excellence for e-Resource Development (CoEERD)

UR 11, Wavelets and Multi-resolution Processing

### Wavelets and Multi-resolution Processing

#### Perfect Reconstruction Filters

k	p	q
0	0	0
1	0	1
2	1	1
2	1	2

The 4 x 4 transformation matrix,  $H_n$ , is

$$H_n = \frac{1}{\sqrt{4}} \begin{bmatrix} 1 & 1 & 1 & 1 \\ 1 & -1 & 1 & -1 \\ 1 & 1 & -1 & -1 \\ 1 & -1 & -1 & 1 \end{bmatrix}$$

Centre of Excellence for e-Resource Development (CoEERD)

UR 11, Wavelets and Multi-resolution Processing

### Wavelets and Multi-resolution Processing

#### Multiresolution Expansions

- In multiresolution analysis, a scaling function is used to create a series of approximations of a function or image, each differing by a factor of 2 in resolution from its nearest neighboring approximations.
- Additional functions, called wavelets, are then used to encode the difference in information between adjacent approximations.

Centre of Excellence for e-Resource Development (CoEERD)

UR 11, Wavelets and Multi-resolution Processing

### Wavelets and Multi-resolution Processing

#### Wavelet Transforms In One Dimension

Wavelet transforms generally use the Fourier domain like the Fourier series expansion, the discrete Fourier transform, and the integral Fourier transform.

Centre of Excellence for e-Resource Development (CoEERD)

UR 11, Wavelets and Multi-resolution Processing

### Wavelets and Multi-resolution Processing

#### The Fast Wavelet Transform

- The fast wavelet transform (FWT) is a computationally efficient implementation of the discrete wavelet transform (DWT). It is also called as Mallat's heronphone algorithm.
- The multiresolution refinement equation is given by:

$$\phi(x) = \sum_k h_k \phi(2x - k)$$

Scaling  $x$  by 2, translating it by 1, and letting  $n = 2l - k$  gives

$$\phi(2x - k) = \sum_n h_n \phi(x - \frac{n+1}{2})$$

$$\phi(x) = \sum_n h_n \phi(x - \frac{n+1}{2})$$

$$\phi(x) = \sum_n h_n \phi(x - \frac{n+1}{2})$$

Centre of Excellence for e-Resource Development (CoEERD)

UR 11, Wavelets and Multi-resolution Processing

### Wavelets and Multi-resolution Processing

#### The Fast Wavelet Transform

- An analogue result for  $\phi(2x - k)$  that is

$$\phi(2x - k) = \sum_n h_n \phi(x - \frac{n+1}{2})$$

- The wavelet series expansion coefficients of continuous function  $f(x)$ ,

$$d_k(n) = \int f(x) \psi(x - \frac{k+n}{2}) dx$$

- Replacing  $\phi(2x - k)$  in eqn (3) we get:

$$d_k(n) = \int f(x) \sum_n h_n \phi(x - \frac{n+1}{2}) dx$$

- Interchanging the sum and integral and rearranging terms that sum

$$d_k(n) = \sum_n h_n \int f(x) \phi(x - \frac{n+1}{2}) dx$$

Centre of Excellence for e-Resource Development (CoEERD)

UR 11, Wavelets and Multi-resolution Processing

### Wavelets and Multi-resolution Processing

#### The Fast Wavelet Transform

- Therefore, we can write  $d_k(n)$  as

$$d_k(n) = \sum_n h_n \int f(x) \phi(x - \frac{n+1}{2}) dx$$

- Similarly the expression for  $d_k(n)$  also can be derived as

$$d_k(n) = \sum_n h_n \int f(x) \phi(x - \frac{n+1}{2}) dx$$

Centre of Excellence for e-Resource De (COEERD)

Wavelets and Multi-resolution Processing

### Wavelet Transforms in Two Dimensions

$$f(x,y) = \sum_{j_1, j_2} \sum_{k_1, k_2} W_{j_1, j_2, k_1, k_2}(x,y) F_{j_1, j_2, k_1, k_2}$$

$$W_{j_1, j_2, k_1, k_2}(x,y) = \psi_{j_1, k_1}(x) \psi_{j_2, k_2}(y)$$

Centre of Excellence for e-Resource De (COEERD)

Wavelets and Multi-resolution Processing

### Wavelet Transforms in Two Dimensions

- The highest scale coefficients are assumed to be samples of the function itself. That is,  $F_{j_1, j_2, k_1, k_2} = f(x_0, y_0)$  where  $J$  is the highest scale.
- In the first filter bank splits the original function into a (low-pass) approximation component, which corresponds to scaling coefficients  $F_{j_1-1, j_2, k_1, k_2}$  and a (high-pass) detail component, corresponding to coefficients  $F_{j_1, j_2, k_1, k_2}$ .
- The sequence splitting characterizes the scaling space  $V_{j_1}$  is split into wavelet subspaces  $W_{j_1, k_1}$  and scaling subspace  $S_{j_1}$ .
- The spectrum of the original function is split into two half-band components.
- The second filter bank splits the spectrum and subspace  $V_{j_1}$  the lower half-band, into counter-band subspace  $W_{j_1, k_1}$  and  $F_{j_1, j_2, k_1, k_2}$  with corresponding DWT coefficients  $W_{j_1, j_2, k_1, k_2}$  and  $R_{j_1, j_2, k_1, k_2}$  respectively.

Centre of Excellence for e-Resource De (COEERD)

Wavelets and Multi-resolution Processing

### Wavelet Transforms in Two Dimensions

- In two dimensions, a two-dimensional scaling function,  $\psi(x, y)$ , and two one-dimensional wavelets,  $\psi_1(x, y)$  and  $\psi_2(x, y)$ , are required. Each is the product of two one-dimensional functions.
- Enforcing products that produce one-dimensional results, like  $\psi(x, y)$ , the four remaining products provide the separable scaling function.

$$\psi(x, y) = \phi(x) \phi(y) \quad (1)$$

$$\psi_1(x, y) = \phi(x) \psi(y) \quad (2)$$

$$\psi_2(x, y) = \psi(x) \phi(y) \quad (3)$$

$$\psi_3(x, y) = \psi(x) \psi(y) \quad (4)$$

Centre of Excellence for e-Resource De (COEERD)

Wavelets and Multi-resolution Processing

### Wavelet Transforms in Two Dimensions

- Given separable two-dimensional scaling and wavelet functions, extensions of the 1-D DWT to two dimensions is straightforward. The scaled and translated basis functions are given by:

$$\phi_{j_1, j_2, k_1, k_2}(x, y) = \phi_{j_1, k_1}(x) \phi_{j_2, k_2}(y) \quad (5)$$

$$\psi_{j_1, j_2, k_1, k_2}(x, y) = \psi_{j_1, k_1}(x) \phi_{j_2, k_2}(y) \quad (6)$$

Where index  $J$  identifies the directional wavelets:

- The discrete wavelet transforms of image  $f(x, y)$  of size  $2^J \times 2^J$  is then:

$$F_{j_1, j_2, k_1, k_2} = \int \int f(x, y) \phi_{j_1, j_2, k_1, k_2}(x, y) dx dy \quad (7)$$

Centre of Excellence for e-Resource De (COEERD)

Wavelets and Multi-resolution Processing

### Wavelet Transforms in Two Dimensions

The  $F_{j_1, j_2, k_1, k_2}$  coefficients define an approximation of  $f(x, y)$  at scale  $J$ . The  $W_{j_1, j_2, k_1, k_2}$  coefficients add horizontal, vertical, and diagonal details for scale  $J$  and

$$f(x, y) = \sum_{j_1, j_2} \sum_{k_1, k_2} W_{j_1, j_2, k_1, k_2}(x, y) F_{j_1, j_2, k_1, k_2}$$

Centre of Excellence for e-Resource De (COEERD)

Wavelets and Multi-resolution Processing

### The 2-D Fast Wavelet Transform

Centre of Excellence for e-Resource De (CGEERD)

WAVELETS AND MULTI-RESOLUTION PROCESSING

**Globetrend®** WAVELETS AND MULTI-RESOLUTION PROCESSING

- The single-scale filter bank can be "iterated" to produce a  $J$ -scale transform in which wavelets are  $2^j$  times wider than the original wavelet,  $j = 0, 1, 2, \dots, J-1$ .
- The image  $f(x, y)$  is used as the  $R(x, y, a)$  input and its rows are convolved with  $A_n$  and  $A_n(-a)$  and downsampled by its columns. We get two subimages whose horizontal resolutions are reduced by a factor of 2.
- The highpass or detail component characterizes the image's high-frequency information with vertical orientation; the lowpass approximation component contains its low-frequency, vertical information.
- Both subimages are then filtered columnwise and downsampled to yield four equally sized output subimages  $f_{2^j, 0}, f_{2^j, 1}, f_{2^j, 2}, f_{2^j, 3}$ .
- In the  $J$ -scale filter bank at each iteration, four  $2^j$ -sample long and  $2^{j-1}$ -sample high subimages are generated and convolved with two low-pass and two high-pass filters in parallel on the subimages columns and the other on its rows.

Centre of Excellence for e-Resource De (CGEERD)

WAVELETS AND MULTI-RESOLUTION PROCESSING

**Globetrend®** WAVELETS AND MULTI-RESOLUTION PROCESSING

**The 2-D Fast Wavelet Transform**

Wavelet packets

The fast wavelet transform decomposes a function into a sum of scaling and wavelet functions whose bandwidths are logarithmically related. The low frequency content is represented using functions with narrow bandwidths, while the high-frequency content is represented using functions with wider bandwidths.

If the greater control over the partitioning of the low-frequency plane is required, the FWT must be generalized to yield a more flexible decomposition called a wavelet packet.

Centre of Excellence for e-Resource De (CGEERD)

WAVELETS AND MULTI-RESOLUTION PROCESSING

**Globetrend®** WAVELETS AND MULTI-RESOLUTION PROCESSING

**The 2-D Fast Wavelet Transform**

The root node is assigned the highest-scale approximation coefficients, which are samples of the function itself, while the leaves after the transform's approximation and detail coefficients outputs.

- The low intermediate nodes  $W_{j+1,0}$  at in a filter bank approximation that is generally twice as narrow as  $W_{j,0}$ .
- The coefficients of each node are the weight of a linear expansion that produces a band limited "piece" of root node, set because by each piece of an element of a known scaling or wavelet subspaces.
- In the synthesis filter bank at each iteration, four  $2^j$ -sample long and  $2^{j-1}$ -sample high subimages are generated and convolved with two low-pass and two high-pass filters in parallel on the subimages columns and the other on its rows.

Centre of Excellence for e-Resource De (CGEERD)

WAVELETS AND MULTI-RESOLUTION PROCESSING

**Globetrend®** WAVELETS AND MULTI-RESOLUTION PROCESSING

**The 2-D Fast Wavelet Transform**

A three-scale FWT Filter Bank

Centre of Excellence for e-Resource De (CGEERD)

WAVELETS AND MULTI-RESOLUTION PROCESSING

**Globetrend®** WAVELETS AND MULTI-RESOLUTION PROCESSING

**The 2-D Fast Wavelet Transform**

In the block diagram of three-scale FWT filter bank the output of the upper-level filter is subsampled, to be accurate,  $M=2^j$  times.  $A$  has been selected by the subspace of the function that is generated by the  $H_{j+1,0}$  transform coefficients.

- The subspace corresponds to the upper-right leaf of the associated analysis tree, as well as the rightmost segment of the corresponding frequency spectrum.
- In the three-scale analysis tree shows the following three expansion systems are generally used:
 
$$f = \sum_{k=0}^{M-1} W_{j+1,0}(k) W_{j,0}(k) \dots \quad (57)$$

$$f = \sum_{k=0}^{M-1} W_{j+1,1}(k) W_{j,0}(k) \dots \quad (58)$$

In general, a  $J$ -scale FWT analysis tree supports  $J!$  unique decompositions. In this case the three-scale FWT analysis tree offers three possible decompositions. Therefore the

Centre of Excellence for e-Resource De (CGEERD)

WAVELETS AND MULTI-RESOLUTION PROCESSING

**Globetrend®** WAVELETS AND MULTI-RESOLUTION PROCESSING


**The 2-D Fast Wavelet Transform**

Center of Excellence for e-Response Learning (COEERDL)

Wavelets and Multi-resolution Processing

**Problems**

What does the following continuous wavelet transform reveal about the one-dimensional function upon which it was based?



**Solutions:**

- The Continuous wavelet transform used to calculate the "resemblance index" between the signal and the wavelet for various set of scales and translations.
- When the scales increase the resemblance is strong, else it is weak.
- If the function is similar to itself at different scales, the resemblance index will be similar at different scales.
- The CAT wavelet used will have a certain characteristic pattern.
- The function whose CWT is self similar to a fractal signal.

Wavelets and Multi-resolution Processing

**Problems**

Draw a two-dimensional four-band filter bank decoder to reconstruct input  $f(x,y)$ .

**Solutions:**

Consider a two dimensional, four band filter bank for sub-band image coding.

$f(x,y)$	$H_0(x,y)$	$H_1(x,y)$	$H_2(x,y)$	$H_3(x,y)$
Columns	Columns	Columns	Columns	Columns
Rows	Rows	Rows	Rows	Rows

The reconstruction of the input  $f(x,y)$  is achieved by reversing the decomposition process, which is achieved by:

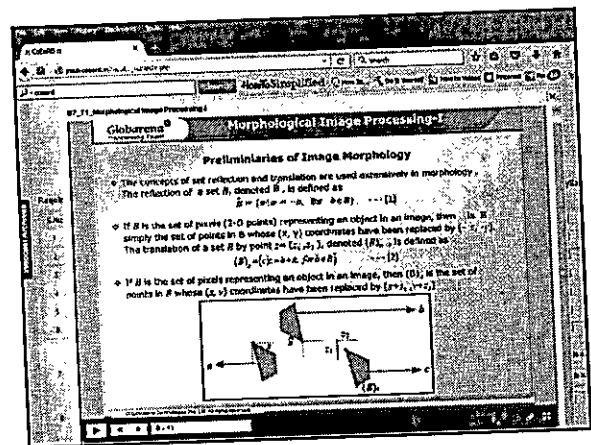
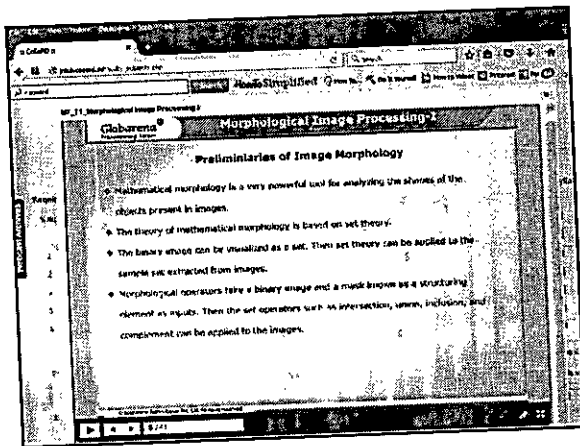
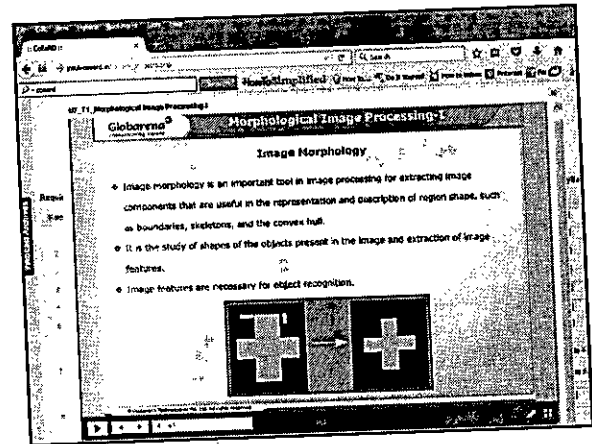
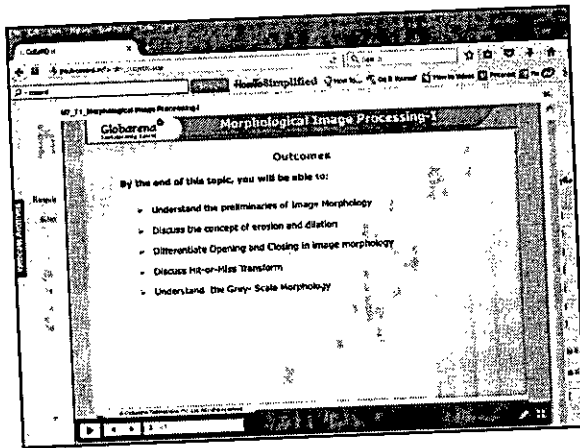
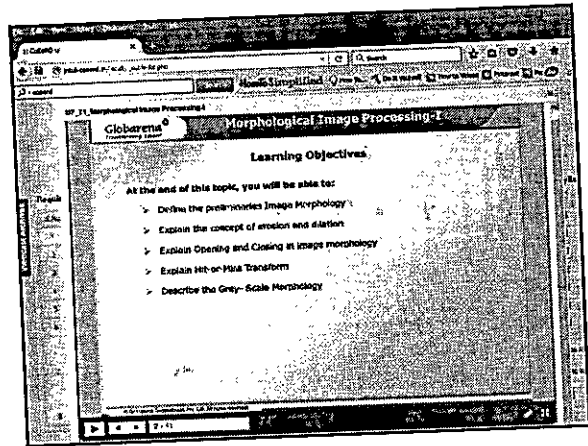
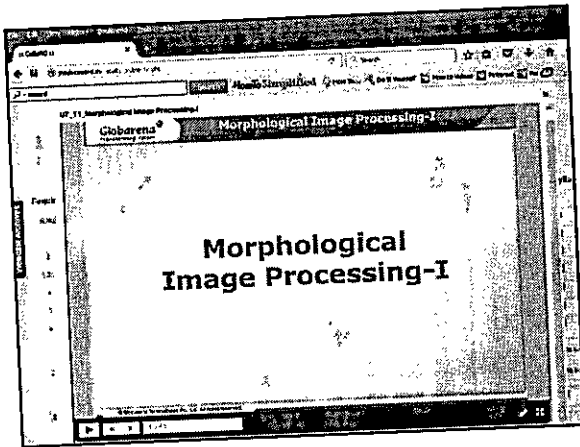
Wavelets and Multi-resolution Processing

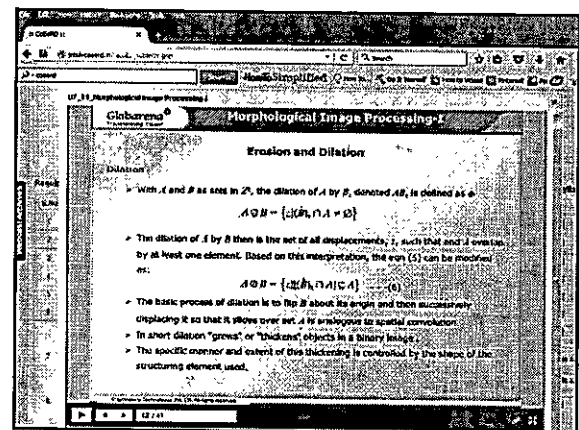
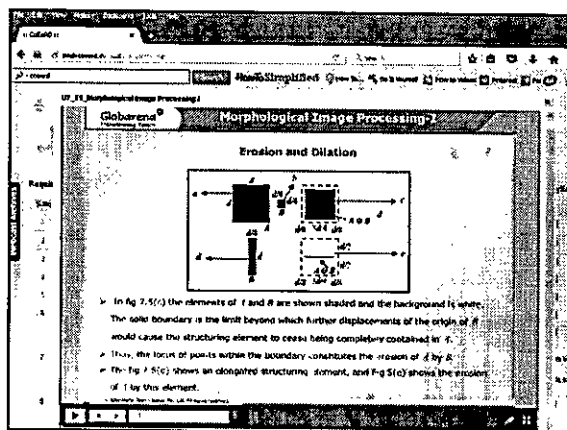
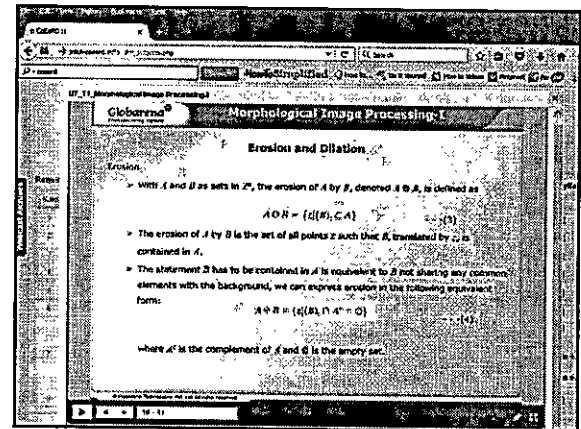
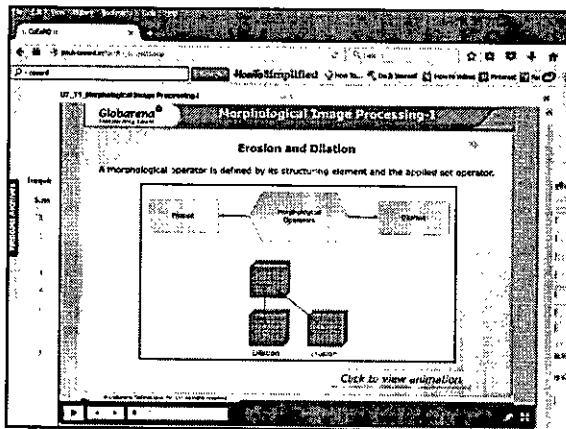
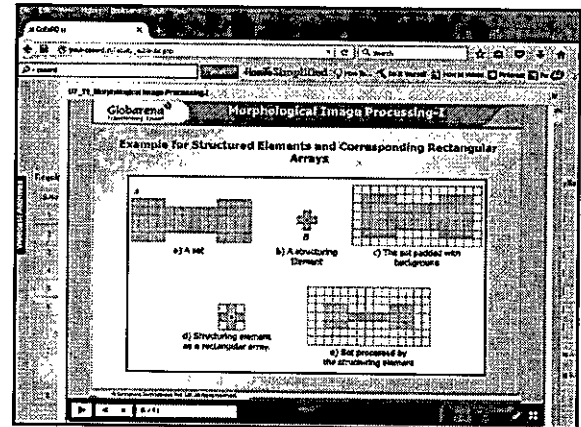
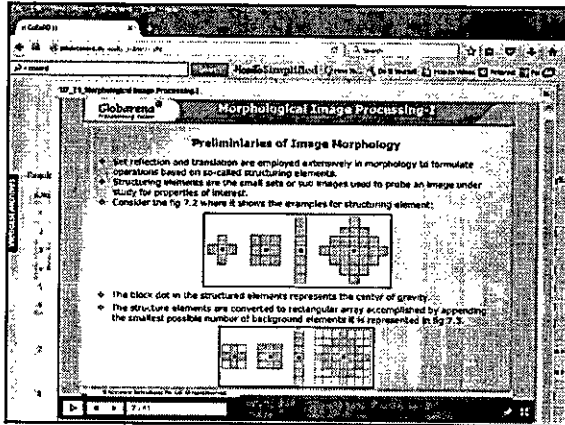
**Problems**

a) Replacing the down samplers with up samplers.  
 b) Replacing the analysis filters by their synthesis filter counterparts.

$a^2(m,n) = \frac{1}{2} \sum_k g_k(n) f_k(m)$	Columns	Rows
$d^2(m,n) = \frac{1}{2} \sum_k g_k(n) f_k(m)$	Columns	Rows
$d^2(m,n) = \frac{1}{2} \sum_k g_k(n) f_k(m)$	Columns	Rows









**Erosion and Dilation**

- The dashed line in Fig 7.9(c) shows the original set for reference, and the solid line shows the limit beyond which any further displacements of the origin of  $B$  by  $Z$  would cause the intersection of  $B$  and  $A$  to be empty.
- Therefore, all points on and inside this boundary constitute the dilation of  $A$  by  $B$ .
- Figure 7.9(d) shows a structuring element designed to achieve more dilation vertically than horizontally.
- Fig 7.9 (e) shows the dilation achieved with this element.

**Opening and Closing Morphological Operations**

- Opening generally smooths the contour of an object, breaks narrow isthmuses, and eliminates thin protrusions.
- Closing also tends to smooth sections of contours but, as opposed to opening, it generally fuses narrow breaks and long thin gaps, eliminates small holes, and fills gaps in the contour.
- The opening of set  $A$  by structuring element  $B$ , denoted  $A \circ B$ , is defined as:
 
$$A \circ B = (A \ominus B) \oplus B$$
- the opening of  $A$  by  $B$  is the erosion of  $A$  by  $B$ , followed by a dilation of the result by  $B$ .
- Similarly, the closing of set  $A$  by structuring element  $B$ , denoted  $A \bullet B$ , is defined as:
 
$$A \bullet B = (A \oplus B) \ominus B$$
- the closing of  $A$  by  $B$  is simply the erosion of  $A$  by  $B$ , followed by the erosion of the result by  $B$ .

[Click to view animation](#)

**Example for Opening Morphological Operation**

- Suppose the structuring element  $B$  is denoted as "rolling ball".
- The boundary of  $A$  is then established by the points in  $B$  that reach the furthest into the boundary of  $A$  as  $B$  is rolled around the inside of this boundary.
- The geometric fitting property of the opening operation leads to a set theoretic formulation, which states that the opening of  $A$  by  $B$  is obtained by taking the union of all translates of  $B$  that fit into  $A$ :
 
$$A \circ B = \bigcup \{ B(x) \mid B(x) \subseteq A \}$$

**Example for Closing Morphological Operation**

- Closing has a similar geometric interpretation, except that now  $B$  roll on the outside of the boundary.
- Opening and closing are duals of each other, so having to roll the ball on the outside is not unexpected.
- Geometrically, a point  $x$  is an element of  $A \bullet B$  and only if  $\exists B(x) \supseteq A$  for any translate of  $B$  that contains  $A$ .

**Hit or Miss Transform**

The morphological hit-or-miss transform is a basic tool for shape detection.

**Hit or Miss Transform**

- Let the origin of each shape be located at its center of gravity as denoted in figure 7.9(a).
- Let  $D$  be defined by a small window,  $M$ . The local background of  $D$  with respect to  $B$  is defined as the set difference  $(B^c \ominus D)$ , as shown in Fig 7.9(b). Figure 7.9(c) shows the complement of  $A$ .
- In figure 7.9(d) shows the erosion of  $A$  by  $D$ . The erosion of  $A$  by  $D$  is the set of locations of the origin of  $D$ , such that  $D$  is completely contained in  $A$ . Interpreted another way,  $B \ominus D$  may be viewed equivalently as the set of all locations of the origin of  $D$  at which  $D$  found a match in  $A$ .
- In figure 7.9(e) the erosion of the complement of  $A$  by the local background set  $(B^c \ominus D)$ . The outer shaded region is part of the erosion.
- The set of locations for which  $D$  exactly fits inside  $A$  is the intersection of the erosion of  $A$  by  $D$  and the erosion of  $(A^c)$  by  $(B^c \ominus D)$  as shown in Figure 7.9(f).

**Morphological Image Processing-1**

### Hit or Miss Transform

$A$  denotes the set composed of  $D$  and its background, the match (or set of matches) of  $B$  in  $I$ , denoted  $A * B$ , is:

$$A * B = (A \cap B) \cap (A^c \cap B^c) \quad (10)$$

- By generating the notation letting  $H = (B, B)$ , where  $B$  is the set formed from elements of  $B$  associated with an object and  $B$  is the set of elements of  $B$  associated with the corresponding background.
- From the preceding discussion,  $H = B$  and  $H = (B^c - B)$

$$A * B = (A \cap H) \cap (A \cap H^c) \quad (11)$$

- The reason for using a structuring element  $A$ , associated with objects and an element  $B$ , associated with the background is based on an assumed definition that two or more objects are distinct only if they form disjoint sets.
- The eqn (10) and eqn (11) are generally called a morphological hit-or-miss transform.

**Morphological Image Processing-1**

### Basics of Grey Scale Morphology

- A grey scale image is the input for the grey scale morphology operations. Similar to the binary morphology operation, the mask moves across the image.
- The pixel-by-pixel process is done and the resultant is produced in the output image.

$$\begin{bmatrix} X & Y & Z \\ A & X & X \\ X & X & X \end{bmatrix} \quad (12)$$

- Let  $f$  be the given image and  $A$  be the structuring element with mask weights, then the output value of erosion process is the minimum value of  $A$  at the nine factors for erosion.

$$g(x,y) = \min_{i,j \in N} \{f(x+i, y+j) + A(i,j)\} \quad (13)$$

$$g(x,y) = \min_{i,j \in N} \{f(x+i, y+j) - A(i,j)\} \quad (14)$$

- The numerical values of the pixel and its eight neighbors are evaluated and the minimal value among them next replaces the value of the central pixel in the output image.

**Morphological Image Processing-1**

### Grey Scale Erosion and Dilation Operations

- Grey scale dilation operation is given as the mask value of the structuring element can range from 0 to 255.
- However, the value is typically zero. This is used to extract the maximum of the input pixel groups. The purpose is to brighten the objects so that small objects become bigger and exaggerated.
- Grey scale erosion operation The mask value of the structuring element can range from -255 to 0. However, the value is typically zero. The value of the structuring element mask is a  $3 \times 3$  array of ones.
- This is used to extract the minimum of the input pixel group. The purpose of this is to darken the input image so that the small brighter regions would disappear.

**Morphological Image Processing-1**

### Grey Scale Erosion and Dilation Operations

Comparison of grey scale erosion and dilation

Input

Output

Figure 1.10 illustrates the effect of grey scale erosion and dilation on the input image. The erosion operation extracts the minimum value of the input image at each pixel location, while the dilation operation extracts the maximum value. The result of erosion is a darker image, and the result of dilation is a brighter image.

Example for grey scale erosion and dilation operations

**Morphological Image Processing-1**

### Generalized Opening and Closing of Grey Scale Images

- The combined operation of grey scale erosion followed by grey scale dilation is called the opening operation. It is denoted as  $J \circ B$ .
- The grey scale dilation followed by grey scale erosion is called the closing operation, denoted as  $J \bullet B$ .
- The purpose of this operation is to darken the object and to remove single-pixel objects.
- This operation can be applied multiple times and can be used to remove the larger object sometimes.

Grey Scale Images (a) Original Image, (b) Opening, (c) Closing

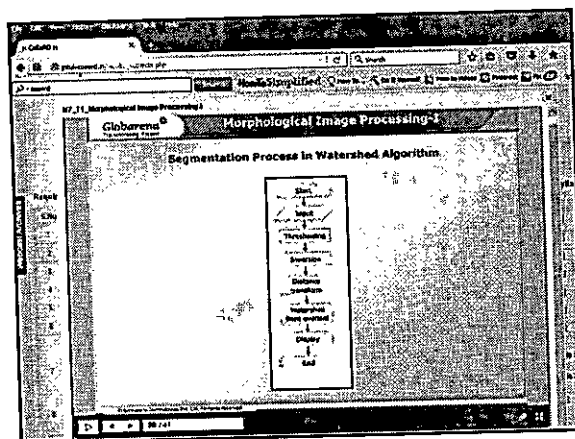
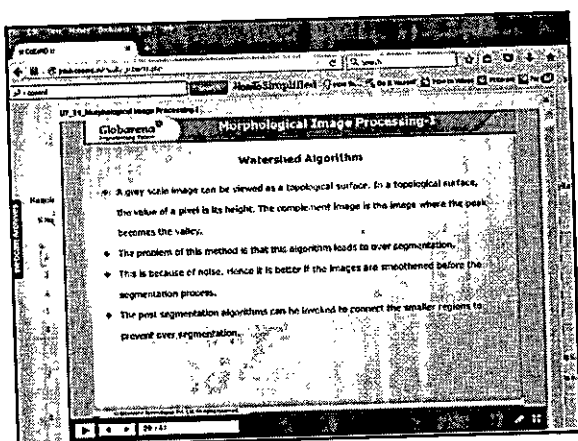
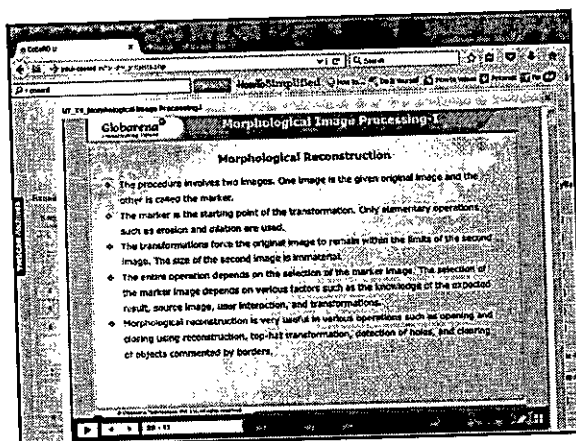
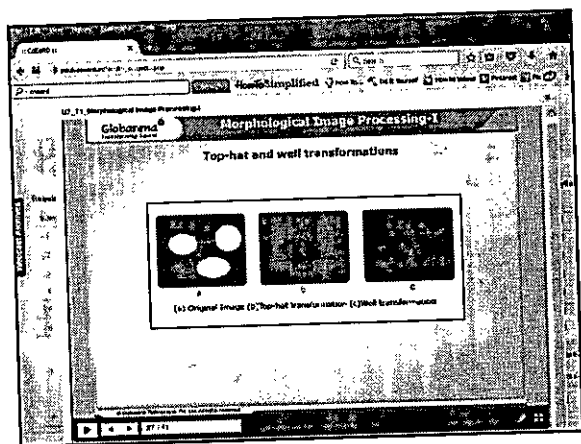
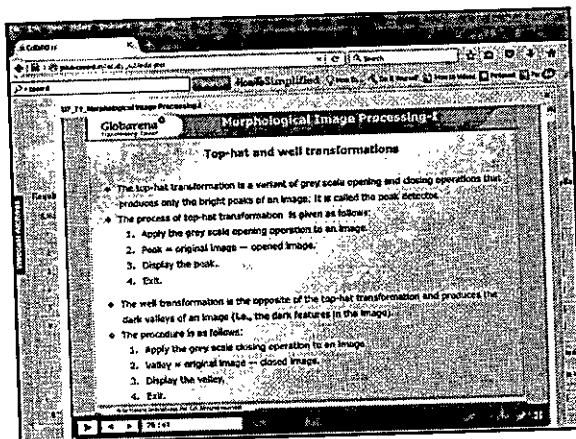
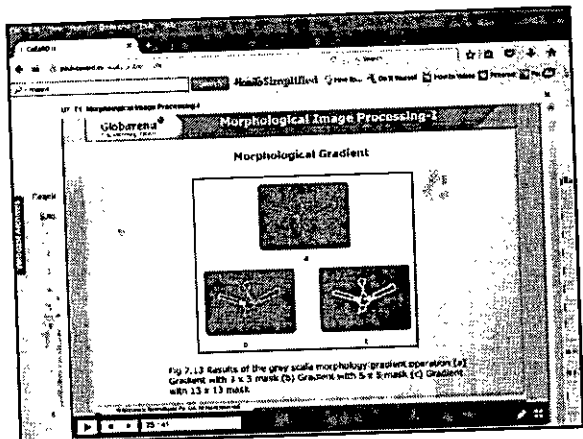
**Morphological Image Processing-1**

### Morphological Gradient

- The operation is used to create edge-enhanced images. Edges represent the transitions from dark to bright regions or vice versa in an image.
- The procedure for obtaining the morphological gradient is as follows:

1. Create a duplicate of the original image. Let it be  $I$ .
2. Apply the erosion operation to the original image.
3. Apply the dilation operation to the duplicate image.
4. Edge = dilated image - eroded image, that is,  $(I \bullet B) - (I \circ B)$ .
5. Display the gradient image.
6. E.T.C.

19-24



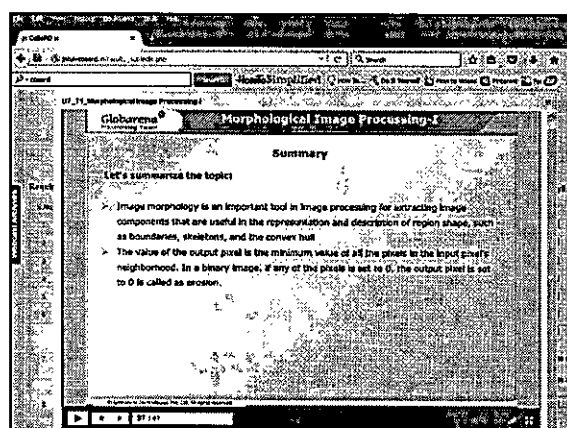
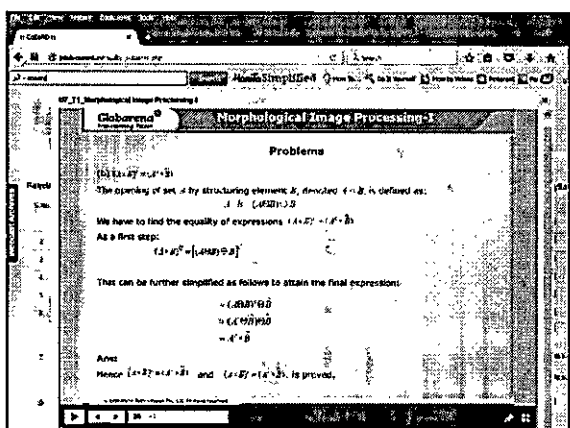
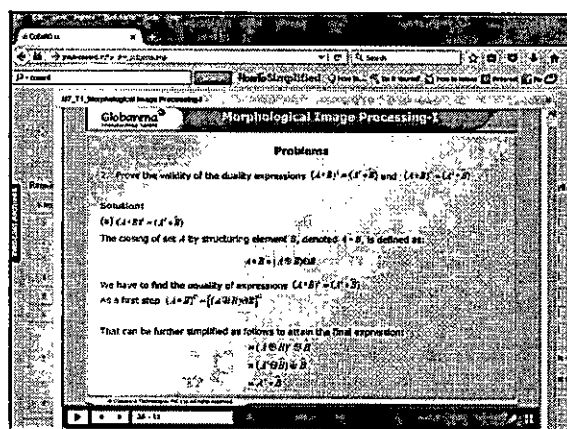
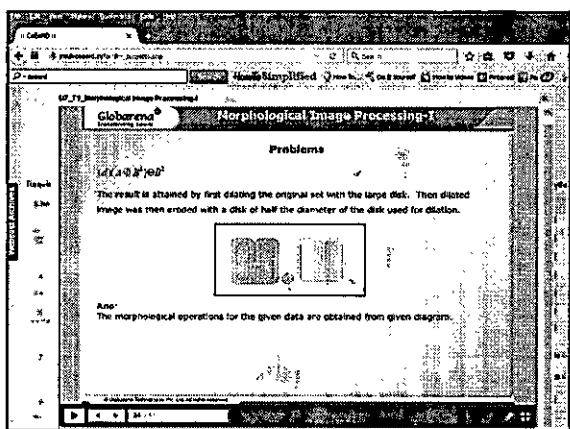
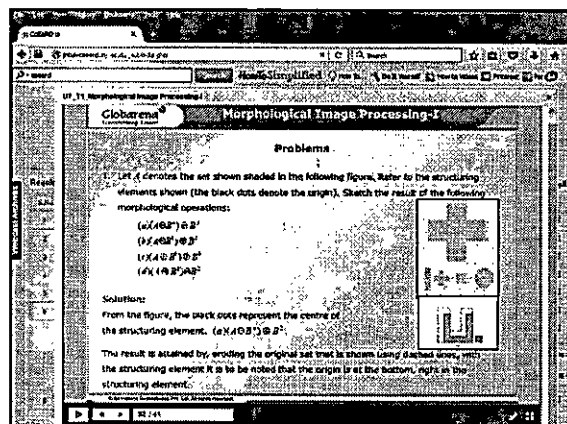
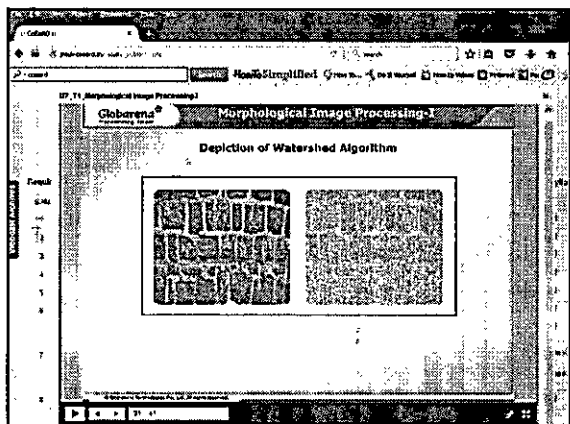


Image Segmentation - I

**Image Segmentation**

process of subdividing an image into its constituent parts or object present in the image (individual parts of image segmentation)

- Segmentation subdivides an image into its constituent regions or objects. The level of detail to which the subdivision is carried depends on the problem being solved.
- Segmentation of nontrivial images is one of the most difficult tasks in image processing. Segmentation accuracy determines the eventual success or failure of computerized analysis procedures.
- Let  $R$  represent the entire spatial region occupied by an image. The image segmentation as a process that partitions  $R$  into  $n$  subregions  $R_i$  such that
 
$$R = \bigcup_{i=1}^n R_i$$

$$R_i \cap R_j = \emptyset \text{ for } i \neq j$$

$$R_i \cap R_j = R \text{ for all } i, j$$

**Image Segmentation**

- Condition (a) indicates that the segmentation must be complete; that is, every pixel must be in a region. Condition (b) requires that points in a region be connected in some predefined sense.
- Condition (c) indicates that the regions must be disjoint. Condition (d) deals with the properties that must be satisfied by the pixels in a segmented region.
- The condition (e) indicates that two adjacent regions  $R_i$  and  $R_j$  must be different in the sense of predicate  $P$ .

The fundamental problem in segmentation is to partition an image into regions that satisfy the preceding conditions.

- Segmentation algorithms for nonstochastic images generally are based on one of two basic categories dealing with properties of intensity values: discontinuity and similarity.
- In the first category, edge-based segmentation is used where the assumption is that boundaries of regions are sufficiently different from each other and from the background to allow boundary detection based on local discontinuities in intensity.
- Region-based segmentation approaches in the second category are based on partitioning an image into regions that are similar according to a set of predefined criteria.

**Background of Point, Line, and Edge Detection**

- In segmentation there are three types of image features in which isolated points, lines, and edges are implemented.
- Edge points are pixels at which the intensity of an image function changes abruptly, and edges are sets of connected edge points.
- Edge detectors and local image processing methods designed to detect edge points. Detection of a digital function are defined in terms of differences.
- Any approximation used for a first derivative  $f'(x)$  must be zero in terms of constant intensity;  $f''(x)$  must be nonzero at points along an intensity ramp.
- For a second derivative  $f''(x)$  must be zero in areas of constant intensity;  $f''(x)$  must be nonzero at the onset and end of an intensity step or ramp; and  $f''(x)$  must be zero along intensity ramps.

**Background of Point, Line, and Edge Detection**

The first-order derivative at point  $x$  of a one-dimensional function  $f(x)$  by expanding the function  $f(x + \Delta x)$  into a Taylor series about  $x$ , letting  $\Delta x = 1$ , and keeping only the linear terms. The result is the digital difference

$$\frac{\partial f}{\partial x} = f(x+1) - f(x) \quad (1)$$

We obtain an expression for the second derivative by differentiating the equation 1

$$\frac{\partial^2 f}{\partial x^2} = \frac{\partial}{\partial x} [f(x+1) - f(x)] = f(x+2) - f(x+1) - f(x+1) + f(x) = f(x+2) - 2f(x+1) + f(x) \quad (2)$$

**Detection of Isolated Points**

From the expression we infer the following inference:

- First-order derivatives generally produce thicker edges in an image.
- Second-order derivatives have a stronger response to fine detail, such as thin lines, isolated points, and noise.
- Second-order derivatives produce a double-edge response at ramp and step transitions in intensity.
- The sign of the second derivative can be used to determine whether a transition in an edge is from light to dark or dark to light.

Detection of isolated points

- The point detection should be based on the second derivative. By using the Laplacian
 
$$\nabla^2 f(x,y) = \frac{\partial^2 f}{\partial x^2} + \frac{\partial^2 f}{\partial y^2} \quad (3)$$

Related Searches

Teaching Resources

Learning Solutions

Learning And Teaching

Learning Content Management System

Portable Workbooks

E-learning Development

Lesson Plans

E-learning Blog

Certification Programs

### Image Segmentation

#### Detection of Isolated Points

where the points are obtained from equation 3 as:

$$\frac{\partial^2 f(x,y)}{\partial x^2} = f(x+1,y) + f(x-1,y) - 2f(x,y) \quad (4)$$

$$\frac{\partial^2 f(x,y)}{\partial y^2} = f(x,y+1) + f(x,y-1) - 2f(x,y) \quad (5)$$

The Laplacian representation is given by:

$$\nabla^2 f(x,y) = f(x+1,y) + f(x-1,y) + f(x,y+1) + f(x,y-1) - 4f(x,y) \quad (6)$$

Related Searches

Teaching Resources

Learning Solutions

Learning And Teaching

Learning Content Management System

Portable Workbooks

E-learning Development

Lesson Plans

E-learning Blog

Certification Programs

### Image Segmentation

#### Line Detection & Edge Models

- In Line detection we expect second derivatives to result in a stronger response and to produce thinner lines than first derivatives.
- Thus, we can use the Laplacian mask for line detection, where the double-line effect of 1<sup>st</sup> second derivative must be handled properly.
- Edge selection is the approach used most frequently for segmenting images based on abrupt changes in intensity.
- A step edge involves a transition between two intensity levels occurring linearly over the distance of 1 pixel.
- Some edges can occur over the distance of 1 pixel, provided that no additional processing such as smoothing is used to make them look "real".
- Real edges are made of lines through a region, with the base of a real edge being determined by the background intensity of the line.
- There are 2 fundamental steps for edge detection:
  - Image processing for noise reduction.
  - Edge detection.

Related Searches

Teaching Resources

Learning Solutions

Learning And Teaching

Learning Content Management System

Portable Workbooks

E-learning Development

Lesson Plans

E-learning Blog

Certification Programs

### Image Segmentation

#### Line Detection & Edge Models

The image gradient and its properties

- The best of choice for finding edge strengths and direction at location  $(x, y)$  of an image  $f$  is the gradient, denoted by " $\nabla f$ ", and defined as the vector:

$$\nabla f = \text{grad } f = \begin{bmatrix} \frac{\partial f}{\partial x} \\ \frac{\partial f}{\partial y} \end{bmatrix} \quad (7)$$

- The magnitude (norm) of vector " $\nabla f$ ", denoted as  $M(x, y)$ :

$$M(x, y) = \text{mag}(\nabla f) = \sqrt{\left(\frac{\partial f}{\partial x}\right)^2 + \left(\frac{\partial f}{\partial y}\right)^2} \quad (8)$$

- Where,  $x$ ,  $y$ , and  $M(x, y)$  are images of the same size on the original image when  $x$  and  $y$  are allowed to vary over all pixel locations in  $f$ .
- The direction of the gradient vector is given by the angle measured with respect to the  $x$ -axis:

Related Searches

Teaching Resources

Learning Solutions

Learning And Teaching

Learning Content Management System

Portable Workbooks

E-learning Development

Lesson Plans

E-learning Blog

Certification Programs

### Image Segmentation

#### Line Detection & Edge Models

- Using the gradient to determine edge strength and direction at a point, the edge is perpendicular to the direction of the gradient vector at that point where the gradient is computed in the figure 8-1. Each square in the figure represents one pixel.

Related Searches

Teaching Resources

Learning Solutions

Learning And Teaching

Learning Content Management System

Portable Workbooks

E-learning Development

Lesson Plans

E-learning Blog

Certification Programs

### Image Segmentation

#### Line Detection & Edge Models

Gradient operators

Detecting the gradient of an image requires computing the partial derivatives  $\frac{\partial f}{\partial x}$  and  $\frac{\partial f}{\partial y}$  at every pixel location in the image.

A digital representation of the partial derivatives over a neighborhood about a point is given by:

$$G_x = \frac{\partial f(x,y)}{\partial x} = f(x+1,y) - f(x-1,y) \quad (10)$$

$$G_y = \frac{\partial f(x,y)}{\partial y} = f(x,y+1) - f(x,y-1) \quad (11)$$

These two equations can be implemented for all pertinent values of  $x$  and  $y$  by filtering  $f(x, y)$  with the 1-D masks:

$$\begin{bmatrix} -1 & 1 \\ 1 & -1 \end{bmatrix} \quad \begin{bmatrix} -1 & 1 \\ 1 & -1 \end{bmatrix}$$

Related Searches

Teaching Resources

Learning Solutions

Learning And Teaching

Learning Content Management System

Portable Workbooks

E-learning Development

Lesson Plans

E-learning Blog

Certification Programs

### Image Segmentation

#### Line Detection & Edge Models

- Filter masks used to compute the derivatives needed for the gradient are often called gradient operators, difference operators or edge operators.
- Similarly 2D masks are also used for 2x2 region using Roberts cross-gradient operators:

$$G_x = \begin{bmatrix} 1 & 0 \\ 0 & 1 \end{bmatrix} \quad G_y = \begin{bmatrix} 0 & 1 \\ 1 & 0 \end{bmatrix}$$

$$G_x = \begin{bmatrix} 1 & -1 \\ 1 & -1 \end{bmatrix} \quad G_y = \begin{bmatrix} 1 & -1 \\ 1 & -1 \end{bmatrix}$$

- The Roberts operators are based on implementing the diagonal differences:

$$G_x = \begin{bmatrix} 1 & 0 \\ 0 & 1 \end{bmatrix} \quad G_y = \begin{bmatrix} 0 & 1 \\ 1 & 0 \end{bmatrix}$$

$$G_x = \begin{bmatrix} 1 & -1 \\ 1 & -1 \end{bmatrix} \quad G_y = \begin{bmatrix} 1 & -1 \\ 1 & -1 \end{bmatrix}$$

- The edge detection can be made more selective by smoothing the image prior to the edge detection. For noise reduction.

Global processing:

- The two principal properties used for establishing continuity of edge pixels in the kind of analysis are (1) the strength (magnitude) and (2) the direction of the gradient vector.
- An edge pixel with coordinates  $(x, y)$  in  $I_0$  is similar in magnitude to the pixel at  $(x, y)$  if
- The direction angle of the gradient vector at edge pixel with coordinates  $(x, y)$  in  $I_0$  has an angle within the range of  $(\theta, \theta + \Delta\theta)$

$$\sqrt{(I_0(x, y) - I_0(x+1, y))^2 + (I_0(x, y) - I_0(x, y+1))^2} > T$$

A formulation particularly well suited for real time applications consists of the following steps:

- Compute the gradient magnitude and angle arrays,  $G(x, y)$  and  $\theta(x, y)$  of the input image,  $I_0(x, y)$
- Form a binary image,  $g$ , whose value at any pair of coordinates  $(x, y)$  is given by
 
$$g(x, y) = \begin{cases} 1 & \text{if } G(x, y) > T \\ 0 & \text{otherwise} \end{cases}$$

Where  $T$  is a threshold,  $A$  is a specified angle direction, and  $\Delta\theta$  defines a "band" of acceptable direction, about  $A$ .

- Scan the rows of  $g$  and fill (out to 1) all gaps (sets of 0s) in each row that do not exceed a specified length,  $L$ . Note that, by definition, a gap is bounded at both ends by one or more 1s. The rows are processed individually, with no continuity between them.
- To detect gaps in any direction, rotate  $g$  by the angle and apply the

Regional processing:

- One approach to the type of processing is functional approximation, where we fit a 2-D curve to the known points.
- The first executing technique that gives an approximation to essential features of the boundary, such as extreme points and concavities.

- We begin by computing the parameters of a straight line passing through  $A$  and  $B$ . Then we compute the perpendicular distance from all other points in the curve to this line and select the point that yielded the maximum distance (this is not necessarily  $C$ ).
- If this distance exceeds a specified threshold,  $T$ , the corresponding point, labeled  $C$ , is declared a vertex. Lines from  $A$  to  $C$  and from  $C$  to  $B$  are then established, and distance from all points between  $A$  and  $C$  to line  $AC$  are checked.
- The point corresponding to the maximum distance is declared a vertex,  $C$ . If the distance exceeds  $T$ , otherwise no new vertices are declared for that segment.
- A similar procedure is applied to the points between  $C$  and  $D$ . The iterative procedure is continued until the entire boundary has been processed.

Global processing using the Hough transform:

- Consider a point  $(x_0, y_0)$  in the  $x-y$  plane and the general equation of a straight line in slope-intercept form,  $y = ax + b$ .
- Infinitely many lines pass through  $(x_0, y_0)$ , but they all satisfy the equation  $y = ax + b$  for varying values of  $a$  and  $b$ .
- Hence, writing this equation as  $b = -ax + y_0$  and considering the  $a-b$  plane (also called parameter space) yields the equation of a single line for a fixed pair  $(x_0, y_0)$ .
- Furthermore, a second point  $(x_1, y_1)$  also has a line in parameter space associated with it, and, unless they are parallel, the lines intersect at the associated point  $(a, b)$  at some point  $(a, b)$ .
- When  $(x_0, y_0)$  is the same as  $(x_1, y_1)$  the intersect of the two coinciding lines  $(x_0, y_0)$  and  $(x_1, y_1)$  in the  $x-y$  plane, in fact, all the points on this line have lines in parameter space that intersect at  $(a, b)$ .

The edge-linking problem. An approach based on the Hough transform is as follows:

- Obtain a binary edge image using any of the techniques.
- Specify subregions in image plane.
- Examine the counts of the accumulator cells for each pixel coordinate.
- Examine the relationship (or quality) for matching between cells in a column and

Global Thresholding

### Image Segmentation

#### Thresholding


- Due to its intuitive properties, simplicity of implementation, and computational speed, image thresholding enjoys a central position in applications of image segmentation.
- The intensity histogram corresponds to an image,  $f(x, y)$ , composed of  $N$  objects on a dark background, as each  $x$  and  $y$  coordinate point have intensity values grouped into two conceptual modes.
- Then, any point  $(x, y)$  in the image at which  $f(x, y) > T$  is called an object point. Otherwise, the point is called a background point. In other words, the segmented image,  $g(x, y)$ , is given by:
 
$$g(x, y) = \begin{cases} f(x, y) & \text{if } f(x, y) > T \\ 0 & \text{if } f(x, y) \leq T \end{cases} \quad (24)$$
- When  $T$  is a constant applied over an entire image, the process shown in this equation is referred to as global thresholding.
- When the value of  $T$  changes over an image, we use the term variable thresholding. The term local or regional thresholding is used sometimes to denote variable thresholding in which the value of  $T$  at any point  $(x, y)$  in an image depends on properties of a neighborhood of  $(x, y)$ .

Global Thresholding

### Image Segmentation

#### Thresholding

- If  $T$  depends on the spatial coordinates  $(x, y)$  themselves, then variable thresholding is often referred to as dynamic or adaptive thresholding.
- Multiple thresholding classifies a point  $(x, y)$ , as belonging to the background if  $f(x, y) < T_1$ , to one object class if  $T_1 < f(x, y) < T_2$ , and to the other object class if  $f(x, y) > T_2$ .
 
$$g(x, y) = \begin{cases} 0 & \text{if } f(x, y) < T_1 \\ 1 & \text{if } T_1 < f(x, y) < T_2 \\ 2 & \text{if } f(x, y) > T_2 \end{cases} \quad (25)$$



Global Thresholding

### Image Segmentation

#### Thresholding

- The primary thresholding is directly related to the width and depth of the valley separating the histogram modes.
- In fact, the key factors affecting the properties of the valley are:
  - The separation between points (the further apart the peaks peak, the better the chance of separating the modes).
  - The noise content in the image (the noisier the image, the more increases).
  - The relative sizes of objects and background.
  - The uniformity of the illumination source; and
  - The uniformity of the reflectance properties of the image.

Global Thresholding

### Image Segmentation

#### Thresholding

Basic Global Thresholding

- When the intensity distributions of objects and background pixels are sufficiently distinct, it is possible to use a single (global) threshold applicable over the entire image.
- The following iterative algorithm can be used for this purpose:
  - Select an initial estimate for the global threshold  $T$ .
  - Segment the image using  $T$  in equation 22. This will provide two groups of pixels:  $C_1$ , consisting of all pixels with intensity values  $< T$ , and  $C_2$ , consisting of pixels with values  $> T$ .
  - Compute the average (mean) intensity values  $\mu_1$  and  $\mu_2$  for the pixels in  $C_1$  and  $C_2$ , respectively.
  - Compute a new threshold value:
 
$$T = \frac{\mu_1 + \mu_2}{2}$$
  - Repeat steps 2 through 4 until the difference between values of  $T$  in successive iterations is greater than a predefined parameter  $\epsilon$ .

Global Thresholding

### Image Segmentation

#### Thresholding

Optimized global thresholding using Otsu's method

- The method in question in the sense that it maximizes the between-class variance, a well-known measure used in statistical discriminant analysis.
- The basic idea is that well-thresholded classes should be distinct with respect to the intensity values of their pixels and, conversely, that a threshold giving the best separation between classes in terms of their intensity values would be the best (optimum) threshold.
- Let  $\{0, 1, 2, \dots, L-1\}$  denote the  $L$  distinct intensity levels in a digital image of size  $M \times N$  pixels, and let  $n_i$  denote the number of pixels with intensity  $i$ .
- The total number  $MN$  of pixels in the image is  $MN = n_0 + n_1 + n_2 + \dots + n_{L-1}$ . The normalized histogram has components  $P_i = n_i / MN$ , from which it follows that:
 
$$\sum_{i=0}^{L-1} P_i = 1 \quad (26)$$
- Using this threshold, the probability  $P_i$  that a pixel is assigned to the thresholded class  $C_1$  is given by the cumulative sum:
 
$$P_1(k) = \sum_{i=0}^k P_i \quad (27)$$

Global Thresholding

### Image Segmentation

#### Thresholding

- The cumulative mean (average intensity) up to level  $k$  is given by:
 
$$\mu(k) = \sum_{i=0}^k P_i i \quad (28)$$
- The average intensity of the entire image (i.e., the global mean) is given by:
 
$$\mu_0 = \sum_{i=0}^{L-1} P_i i \quad (29)$$
- In order to evaluate the "goodness" of the threshold  $k$  level, we use the normalized, dimensionless measure:
 
$$\sigma_k^2 = \frac{\mu(k) - \mu_0}{\mu_0} \quad (30)$$
- Where  $\sigma_k^2$  is the global variance is given by:
 
$$\sigma_k^2 = \sum_{i=0}^{L-1} (i - \mu_0)^2 P_i \quad (31)$$



GlobalView - Image Segmentation - 1

**Thresholding**

And  $\sigma_b^2$  is the between class variance, defined as

$$\sigma_b^2 = P_1(\mu_1 - \mu_2)^2 + P_2(\mu_2 - \mu_1)^2 \quad (32)$$

Substituting in, we have the final results:

$$\sigma_b^2 = \frac{P_1 P_2}{P_1 + P_2} \quad (33)$$

$$\sigma_b^2 = \frac{P_1 P_2}{P_1 + P_2} \left[ \frac{\mu_1 - \mu_2}{P_1 + P_2} \right]^2 \quad (34)$$

The optimal threshold is the value,  $t^*$ , that maximizes  $\sigma_b^2(t)$

$$t^* = \frac{P_1 \mu_1 + P_2 \mu_2}{P_1 + P_2} \quad (35)$$

GlobalView - Image Segmentation - 1

**Otsu's Algorithm**

1. Compute the normalized histogram of the input image. Denote the components of the histogram by  $p_i, i=0,1,2,\dots,255$ .
2. Compute the cumulative sums,  $F_i(t)$ , for  $i=0,1,2,\dots,255$ , using Equation 29.
3. Compute the cumulative means,  $m_i(t)$ , for  $i=0,1,2,\dots,255$ , using Equation 29.
4. Compute the global intensity mean,  $\mu_0$ , using Equation 29.
5. Compute the between-class variance,  $\sigma_b^2(t)$ , for  $t=0,1,2,\dots,255$ , using Equation 34.
6. Obtain the Otsu threshold,  $t^*$ , as the value of  $t$  by which  $\sigma_b^2(t)$  is maximized. The maximum is not unique; obtain  $t^*$  by choosing the value of  $t$  corresponding to the various maxima detected.
7. Obtain the separability measure,  $\sigma_b^2(t^*)$ , by evaluating Equation 35 at  $t^*$ .

GlobalView - Image Segmentation - 1

**Otsu's Algorithm**

Image smoothing to improve global thresholding

When noise cannot be reduced to the source, and thresholding by the segmentation method of choice, a technique that often enhances performance is to smooth the image prior to thresholding.

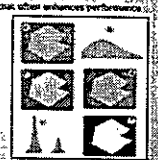


Fig. 8 (a) Noisy image (b) its histogram. (c) ASAP obtained using Otsu's method. (d) Binary image thresholded using a 3x3 3-bit histogram, (e) the histogram of (d).

GlobalView - Image Segmentation - 1

**Otsu's Algorithm**

- Every black point in the white region and every white point in the black region is a thresholding error, so the segmentation was highly unsuccessful.
- Figure 8(d) shows the result of smoothing the noisy image with an averaging mask of size  $5 \times 5$  (the image is of size  $256 \times 256$  pixels), and Figure 8(e) is its histogram.
- The improvement in the shape of the histogram due to smoothing is evident. As we would expect thresholding of the smoothed image to be nearly perfect.
- As Figure 8(c) shows, the slight distortion of the boundary between object and background in the segmented, smoothed image was caused by the blurring of the boundary.
- In fact, the more aggressively we smooth an image, the more boundary errors we should anticipate in the segmented result.

GlobalView - Image Segmentation - 1

**Otsu's Algorithm**

Using edges to improve global thresholding

An approach for improving the shape of histograms is to consider only those pixels that lie on or near the edges between objects and the background.

1. Compute an edge image as either the magnitude of the gradient, or absolute value of the Laplacian, of  $f(x,y)$ .
2. Specify a threshold value,  $t$ .
3. Threshold the image from step 1 using the threshold from step 2 to produce a binary image,  $g(x,y)$ . This image is used as a mask image in the following step to select pixels from  $f(x,y)$  corresponding to "strong" edge pixels.
4. Compute a histogram using only the pixels in  $f(x,y)$  that correspond to the locations of the 1-valued pixels in  $g(x,y)$ .
5. Use the histogram from Step 4 to determine  $t^*$  of global thresholding for binary images.

GlobalView - Image Segmentation - 1

**Otsu's Algorithm**

**Using Edges**

The thresholding method can be extended to an arbitrary number of threshold classes, because the separability measure on which it is based also extends to an arbitrary number of classes.

In the case of  $K$  classes,  $C_1, C_2, \dots, C_K$ , the between class variance, generating the expression

$$\sigma_b^2 = \sum_{i=1}^{K-1} \sum_{j=i+1}^K (m_i - m_j)^2 P_i P_j \quad (36)$$

where

$$m_i = \frac{\sum_{x,y} f(x,y) g_i(x,y)}{N_i}$$

and

$$P_i = \frac{N_i}{N}$$

The  $K$  classes are separated by  $K-1$  threshold values,  $t_1, t_2, \dots, t_{K-1}$ , and the  $i$ th class is

$$C_i = \{x,y \mid t_{i-1} < f(x,y) \leq t_i\}$$

In practice, using multiple global thresholding is considered a viable approach when

Related Searches

Teaching Resources

Learning Solutions

Learning And Teaching

Learning Content Management System

Portable Workbooks

E-learning Development

Lesson Plans

E-learning Blog

Continuing Programs

### Image Segmentation

#### Otsu's Algorithm

Applications that require more than two thresholds generally are solved using more than two intensity values.

For three classes consisting of three intensity intervals (which are separated by two thresholds) the between-class variance is given by:

$$s_b^2 = \frac{1}{N} \sum_{i=1}^3 \sum_{j=1}^3 \frac{p_i p_j}{|i-j|} \quad (36)$$

where

$$p_i = \sum_{k=1}^i p_k$$

and

$$p_j = \sum_{k=j}^L p_k$$

Related Searches

Teaching Resources

Learning Solutions

Learning And Teaching

Learning Content Management System

Portable Workbooks

E-learning Development

Lesson Plans

E-learning Blog

Continuing Programs

### Image Segmentation

#### Otsu's Algorithm

- The best optimum threshold values,  $t_1^*$  and  $t_2^*$  are the values that maximize  $s_b^2(t_1, t_2)$  the optimum thresholds are given by:
- The values of  $t_1$  and  $t_2$  corresponding to that maximum are the optimum thresholds.  $t_1^*$  and  $t_2^*$  if there are several maxima, the corresponding values of  $t_1$  and  $t_2$  are averaged to obtain the final threshold. The threshold image is then given by:
- where  $a$ ,  $b$ , and  $c$  are any three valid intensity values.
- The separability measure defined for one threshold extends directly to multiple thresholds:

Related Searches

Teaching Resources

Learning Solutions

Learning And Teaching

Learning Content Management System

Portable Workbooks

E-learning Development

Lesson Plans

E-learning Blog

Continuing Programs

### Image Segmentation

#### Otsu's Algorithm

$$g(R, C, D) = \max_{R, C, D} F(R, C, D) \quad (39)$$

$$F(R, C, D) = \begin{cases} \sqrt{f(R, C) \times A} & \text{if } \sqrt{f(R, C) \times A} > \sqrt{f(R, D) \times B} \\ \sqrt{f(R, D) \times B} & \text{if } \sqrt{f(R, D) \times B} > \sqrt{f(R, C) \times A} \end{cases} \quad (40)$$

$$f(R, C) = \frac{1}{N} \sum_{i=1}^R \sum_{j=C}^L p_i p_j \quad (41)$$

Related Searches

Teaching Resources

Learning Solutions

Learning And Teaching

Learning Content Management System

Portable Workbooks

E-learning Development

Lesson Plans

E-learning Blog

Continuing Programs

### Image Segmentation

#### Otsu's Algorithm

Variable thresholding by image partitioning.

One of the simplest approaches to variable thresholding is to subdivide an image into nonoverlapping rectangles.

- This approach is used to compensate for non-uniformities in illumination and/or reflectance. The rectangles are chosen small enough so that the illumination of each is approximately uniform.
- Image subdivision generally works well when few objects of interest and the background occupy regions of reasonably comparable size.
- When this is not the case, the method typically fails because of the inclusion of subdivisions, containing only object or background pixels.
- Although this situation can be mitigated by using additional techniques to determine when a subdivision contains both types of pixels, the logic required to address different scenarios can get complicated.

Related Searches

Teaching Resources

Learning Solutions

Learning And Teaching

Learning Content Management System

Portable Workbooks

E-learning Development

Lesson Plans

E-learning Blog

Continuing Programs

### Image Segmentation

#### Otsu's Algorithm

Example for variable thresholding by image partitioning

- Figure 10(a) shows the noisy shaded image and Fig 10 (b) shows its histogram. When discussing Fig. 10(c) we conclude that the image could not be segmented with a global threshold.
- Figure 10(c) and (d), which show the results of segmenting the image using the iterative scheme and Otsu's method, respectively.
- Both methods produced comparable results, in which numerous segmentation errors are visible.
- Figure 10(e) shows the original image, subdivided into six rectangular regions, and Fig.10 (f) is the result of applying Otsu's global method to each subimage.
- Although some errors in segmentation are visible, image subdivision produced a responsible result as an analysis that is




FIG-10 (a) Noisy shaded image and (b) its histogram, (c) Segmentation of (a) using the iterative global method, (d) Result obtained using Otsu's method, (e) Image subdivided into six subimages, (f) Result of applying Otsu's method to each subimage.

Related Searches

Teaching Resources

Learning Solutions

Learning And Teaching

Learning Content Management System

Portable Workbooks

E-learning Development

Lesson Plans

E-learning Blog

Continuing Programs

### Image Segmentation

#### Otsu's Algorithm

Variable thresholding based on local image properties

The basic approach to local thresholding using the standard deviation and mean of the pixels in a neighborhood of every point in an image.

- These two measures are quite useful for determining local thresholds because they are functions of local contrast and average intensity.
- $\mu$ ,  $\sigma$ , and  $m$  denote the standard deviation and mean value of the set of pixels contained in a neighborhood,  $S_q$ , centered at coordinates  $(x, y)$  in an image.
- The following are common forms of variable, local thresholds:

where  $a$  and  $b$  are nonnegative constants, and

where  $\mu$  is the global image mean. The segmented image is computed as

5. Significant power can be added to local thresholding by using predicates based on the parameters computed in the neighborhood of  $(x, y)$ .

where  $Q$  is a predicate based on parameters computed using the pixels in neighborhood  $S_q$ .

Related Searches

Teaching Resources

Learning And Teaching

Learning Content Management System

Portable Workbooks

Learning Development

Lesson Plans

Learning Blog

Continuing Programs

### Image Segmentation-1

Variable thresholding based on local image properties

$$T_u = \alpha T_g + \beta I_u \quad (42)$$

$$T_v = \alpha T_g + \beta I_v \quad (43)$$

$$s(x,y) = \begin{cases} 1 & \text{if } f(x,y) > T_u \\ 0 & \text{if } f(x,y) < T_v \end{cases} \quad (44)$$

$$s(x,y) = \begin{cases} 1 & \text{if } f(x,y) \text{ is in } \\ 0 & \text{if } f(x,y) \text{ is not in } \end{cases} \quad (45)$$

Related Searches

Teaching Resources

Learning And Teaching

Learning Content Management System

Portable Workbooks

Learning Development

Lesson Plans

Learning Blog

Continuing Programs

### Image Segmentation-1

Variable thresholding based on local image properties

$$T_u = \alpha T_g + \beta I_u \quad (42)$$

$$T_v = \alpha T_g + \beta I_v \quad (43)$$

$$s(x,y) = \begin{cases} 1 & \text{if } f(x,y) > T_u \\ 0 & \text{if } f(x,y) < T_v \end{cases} \quad (44)$$

$$s(x,y) = \begin{cases} 1 & \text{if } f(x,y) \text{ is in } \\ 0 & \text{if } f(x,y) \text{ is not in } \end{cases} \quad (45)$$

Related Searches

Teaching Resources

Learning And Teaching

Learning Content Management System

Portable Workbooks

Learning Development

Lesson Plans

Learning Blog

Continuing Programs

### Image Segmentation-1

Example for variable thresholding based on local image properties

Figure 11(a) shows the yeast image, this image has some prominent vertical features, so it is reasonable to assume that variable thresholding could be a good segmentation approach.

Figure 11(b) is the result of using the Otsu thresholding method, as the figure shows, it was possible to locate the bright areas from the background, but the mid-gray regions on the right side of the image were not segmented properly.

Figure 11(c) shows the result to illustrate the use of local thresholding, we computed the local statistical deviation  $T_u$  for all  $(x, y)$  in the input image using a neighborhood of size 3 x 3.

Figure 11 (d) shows the result using adaptive thresholding with the two types of intensity response dependent on the local

Fig. 11 (a) Yeast Image (b) Image segmented using the Otsu thresholding approach. (c) Image of local statistical deviation. (d) Image of local statistical deviation.

Related Searches

Teaching Resources

Learning And Teaching

Learning Content Management System

Portable Workbooks

Learning Development

Lesson Plans

Learning Blog

Continuing Programs

### Image Segmentation-1

Thresholding using moving averages

A special case of the local thresholding method is based on computing a moving average along scan lines of an image.

This implementation is quite useful in document processing, where speed is a fundamental requirement. The scanning is typically carried out by using a sliding window to reduce illumination bias.

Let  $T_u$  denote the intensity of the point encountered in the scanning sequence at step  $k = 1$ . The moving average (mean intensity) of the new point is given by:

$$m(k) = \frac{1}{n} \sum_{i=1}^n I(x, y, k-i) \quad (46)$$

where  $n$  denotes the number of points used in computing the average and  $m(k)$

Related Searches

Teaching Resources

Learning And Teaching

Learning Content Management System

Portable Workbooks

Learning Development

Lesson Plans

Learning Blog

Continuing Programs

### Image Segmentation-1

Example variable thresholding using moving averages

Figure 11(a) shows an image of handwritten text shaped by a 300° intensity pattern. This form of intensity shading is typical of images obtained with a photocopier task.

Figure 11(b) is the result of segmentation using the Otsu global thresholding method. It is not unexpected that global thresholding could not overcome the intensity variation.

Figure 11(c) shows successful segmentation with local thresholding using moving averages. A rule of thumb is to let  $n$  equal 3 times the average stroke width.

Related Searches

Teaching Resources

Learning And Teaching

Learning Content Management System

Portable Workbooks

Learning Development

Lesson Plans

Learning Blog

Continuing Programs

### Image Segmentation-1

Multi-variable thresholding

In some cases, a sensor can make available more than one variable to characterize each pixel in an image, and thus allow multi-variable thresholding.

A notable example is color imaging, where red (R), green (G), and blue (B) components are used to form a composite color image.

In this case, each "color" is characterized by three values, and can be represented as a 3-D vector:  $z = [R, G, B]^T$ , whose components are the RGB colors of a new color.

Three 3-D points often are referred to as "corners" to identify a rectangular object as opposed to image elements.

Let  $z_c$  denote the average vector color in which the  $i$ th are identified. One way to segment a color image based on the parameter is to compute a distance measure  $D_i$ , which defines an arbitrary color point,  $z$ , and the average color,  $z_c$ . Then, we segment the input image as follows:

where  $T_k$  is threshold  $T_k = \frac{1}{2} (D_{k-1} + D_k)$  (47)

Global Search

Teaching Resources

Learning Solutions

Learning And Teaching

Learning Content Management System

Private Workbooks

Learning Development

Lesson Plans

Learning Blog

Continuing Programs

Image Segmentation-1

### Otsu's Algorithm

- The condition  $(x, y) > T$  basically says that the Euclidean distance between the value of  $x$  and the origin of the real line exceeds the value of  $T$ .
- The  $n$ -dimensional Euclidean distance is defined as:
- The equation  $D(x, a) = T$  describes a sphere (called a hyper sphere) in a  $n$ -dimensional Euclidean space. A more powerful distance measure is the so-called Mahalanobis distance, defined as:
- where  $C$  is the covariance matrix of the  $x$ 's.
- $D(x, a) = T$  describes an  $n$ -dimensional hypersphere.

$$D(x, a) = \|x - a\|$$

$$D(x, a) = \sqrt{(x-a)^T(x-a)}$$

$$D(x, a) = \sqrt{(x-a)^T C^{-1}(x-a)}$$

Image Segmentation-1

### Problem

1. Prove the validity of the equation  $\frac{d}{dx} f(x) = f'(x) = f'(x) - f'(x)$ .

As a first step you expand  $f(x + \Delta x)$  into a Taylor series about  $x$ :

$$f(x + \Delta x) = f(x) + \Delta x f'(x) + \frac{\Delta x^2}{2} f''(x) + \dots$$

The increment in the spatial variable  $x$  is defined to be  $\Delta x$  hence by letting  $\Delta x \rightarrow 0$  and keeping only the linear terms we get the result as:

$$f(x) = f(x) + \Delta x f'(x)$$

Ans:  
Hence this criteria proves the validity of the given expression.

Image Segmentation-1

### Problem

1. Show that the average value of the Laplacian of a Gaussian approximates  $\Delta f(x, y)$  if  $\Delta f(x, y) = 0$ .

Solution:  
By using the expression for Laplacian of a Gaussian

$$\Delta f(x, y) = \frac{\partial^2 f}{\partial x^2} + \frac{\partial^2 f}{\partial y^2}$$

We proceed with the proof,

$$\Delta f(x, y) = \int \int \Delta f(x, y) dx dy$$

Image Segmentation-1

### Problem

$$-\frac{1}{2} (\sqrt{2\pi\sigma^2})^{-1} \sqrt{2\pi\sigma^2}$$

$$\frac{1}{2} (\sqrt{2\pi\sigma^2})^{-1} \sqrt{2\pi\sigma^2}$$

$$\frac{1}{2} (2\pi\sigma^2)^{-1/2}$$

$$= \frac{1}{2} \frac{1}{\sigma^2}$$

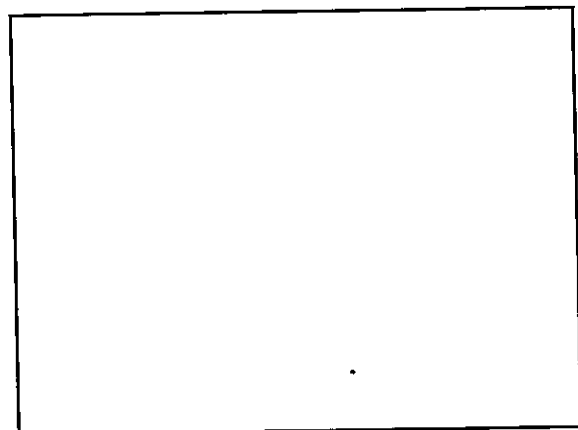
$$= 0$$

Image Segmentation-1

### Summary

Let's summarise the topic:

- Segmentation subdivides an image into its constituent regions or objects. The level of detail to which the subdivision is carried depends on the problem being solved.
- In segmentation there are three types of image features in which isolated points, lines, and edges are important.
- The point detection should be based on the second derivative. In line detection we expect second derivatives to occur in a straight line and detection to produce fewer lines than first derivatives.
- Edge detection is the approach used most frequently for segmenting images. Based on abrupt changes in intensity.
- The intensity thresholding is directly related to the width and depth of the valley separating the histogram modes.
- When the intensity distributions of edges and background pixels are sufficiently distinct, it is possible to use a single (global) threshold applicable over the entire image.
- One of the simplest approaches to variable thresholding is to subdivide an image into nonoverlapping rectangles.
- In some cases, a sensor can make mistakes more than one variable in a characteristic each pixel in an image and they affect the segmentation.



Related Searches

Teaching Resources

Learning Solutions

Learning Aid

Learning

Learning Content Management System

Practice Worksheets

Learning Development

Lesson Plans

Learning Blog

Certification Programs

### Image Segmentation I

#### Otsu's Algorithm

The condition  $f(x, y) > T$  normally says that the Euclidean distance between the value of  $f$  and the origin of the real line exceeds the value of  $T$ . The  $n$ -dimensional Euclidean distance is defined as:

The equation  $D(x, a) = T$  describes a sphere (called a hyper sphere) in  $n$ -dimensional Euclidean space. A more powerful distance measure is the so-called Mahalanobis distance, defined as:

where  $C$  is the covariance matrix of the  $x$ 's.

$D(x, a) = T$  describes an  $n$ -dimensional hypersphere.

$$D(x, a) = \sqrt{(x-a)^T C^{-1} (x-a)}$$

$$D(x, a) = \sqrt{(x-a)^T C^{-1} (x-a)}$$

$$D(x, a) = \sqrt{(x-a)^T C^{-1} (x-a)}$$

Related Searches

Teaching Resources

Learning Solutions

Learning Aid

Learning

Learning Content Management System

Practice Worksheets

Learning Development

Lesson Plans

Learning Blog

Certification Programs

### Image Segmentation I

#### Problem

Prove the validity of the equation  $\frac{d}{dx} f(x) = f'(x) + f(x) \ln f(x)$ .

**Solution:**

As a first step we expand  $f(x) = f(x) \ln f(x)$  into a Taylor series about  $x$ :

$$f(x+\Delta x) = f(x) + f'(x)\Delta x + \frac{f''(x)}{2}\Delta x^2 + \dots$$

The increment in the spatial variable  $x$  is defined to be 1 hence by letting  $\Delta x = 1$  and keeping only the linear terms we get the result as:

$$f(x+1) = f(x) + f'(x)$$

**Hint:** Hence this criteria proves the validity of the given expression.

Related Searches

Teaching Resources

Learning Solutions

Learning Aid

Learning

Learning Content Management System

Practice Worksheets

Learning Development

Lesson Plans

Learning Blog

Certification Programs

### Image Segmentation I

#### Problem

Show that the average value of the Laplacian of a Gaussian operator,  $\Delta^2 G(x, y)$  is zero.

**Solution:**

By using the expression for Laplacian of a Gaussian

$$\Delta^2 G(x, y) = \frac{\partial^2}{\partial x^2} \left[ \frac{1}{\sqrt{2\pi}} e^{-\frac{x^2+y^2}{2}} \right] + \frac{\partial^2}{\partial y^2} \left[ \frac{1}{\sqrt{2\pi}} e^{-\frac{x^2+y^2}{2}} \right]$$

We proceed on with the proof,

$$\Delta^2 G(x, y) = \int \int \left[ \frac{\partial^2}{\partial x^2} \left( \frac{1}{\sqrt{2\pi}} e^{-\frac{x^2+y^2}{2}} \right) + \frac{\partial^2}{\partial y^2} \left( \frac{1}{\sqrt{2\pi}} e^{-\frac{x^2+y^2}{2}} \right) \right] dx dy$$

Related Searches

Teaching Resources

Learning Solutions

Learning Aid

Learning

Learning Content Management System

Practice Worksheets

Learning Development

Lesson Plans

Learning Blog

Certification Programs

### Image Segmentation I

#### Problem

$$\frac{\partial}{\partial x} \left( \frac{\partial}{\partial x} \left( \frac{1}{\sqrt{2\pi}} e^{-\frac{x^2+y^2}{2}} \right) \right) + \frac{\partial}{\partial y} \left( \frac{\partial}{\partial y} \left( \frac{1}{\sqrt{2\pi}} e^{-\frac{x^2+y^2}{2}} \right) \right)$$

$$= -x \frac{1}{\sqrt{2\pi}} e^{-\frac{x^2+y^2}{2}} - y \frac{1}{\sqrt{2\pi}} e^{-\frac{x^2+y^2}{2}}$$

$$= -x \frac{1}{\sqrt{2\pi}} e^{-\frac{x^2+y^2}{2}} - y \frac{1}{\sqrt{2\pi}} e^{-\frac{x^2+y^2}{2}}$$

Related Searches

Teaching Resources

Learning Solutions

Learning Aid

Learning

Learning Content Management System

Practice Worksheets

Learning Development

Lesson Plans

Learning Blog

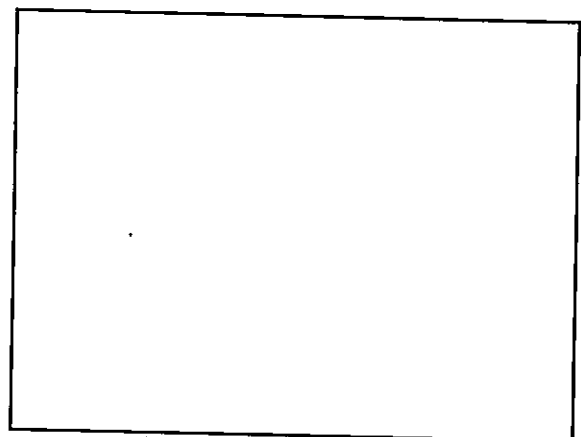
Certification Programs

### Image Segmentation I

#### Summary

Let's summarize the topics:

- Segmentation subdivides an image into its constituent regions or objects. The level of detail to which the subdivision is carried depends on the problem being solved.
- In segmentation there are three types of image features in which isolated points, lines, and edges are implemented.
- The point detectors should be based on the second derivative, in Line detection we expect second derivatives to result in a stronger response and to produce thinner lines than first derivatives.
- Edge detection is the approach used most frequently for segmenting images based on abrupt changes in intensity.
- The intensity thresholding is directly related to the width and depth of the valley separating the histogram modes.
- When the intensity distributions of objects and background pixels are sufficiently distinct, it is possible to use a single (global) threshold applied over the entire image.
- One of the simplest approaches to variable thresholding is to subdivide an image into nonoverlapping rectangles. In some cases, a sensor can make available more than one variable (color, texture, etc.) over an image, and that allows the probability of





7  
1  
2  
2  
2

# ASSIGNMENT QUESTION PAPERS

**NARASARAOPETA ENGINEERING COLLEGE::NARASARAOPET  
(AUTONOMOUS)  
DEPARTMENT OF ELECTRONICS AND COMMUNICATION ENGINEERING  
III B.TECH II-SEMESTER ASSIGNMENT TEST-I, December-2019**

<b>SUBJECT: Digital Image Processing</b>	<b>DATE: 20-12-2019</b>
<b>DURATION:30 MIN</b>	<b>MAX MARKS: 10</b>

Q. No	Questions	Course Outcome (CO)	Knowledge Level Per Bloom's Taxonomy	Marks
1	Explain the fundamental steps in Image Processing.	CO1	Understanding (K2)	10
2	Find the Haar Transformation Matrix for N=4.	CO1	Remembering (K1)	10
3	Explain the Hadamard Transform.	CO1	Understanding (K2)	10
4	Find the Slant Transform matrix for N=4	CO1	Remembering (K1)	10
5	Explain the Walsh Transform.	CO1	Understanding (K2)	10



**NARASARAOPETA ENGINEERING COLLEGE::NARASARAOPET  
(AUTONOMOUS)  
DEPARTMENT OF ELECTRONICS AND COMMUNICATION ENGINEERING  
III B.TECH II-SEMESTER ASSIGNMENT TEST-II, January-2020**

<b>SUBJECT: Digital Image Processing</b>	<b>DATE: 10-01-2020</b>
<b>DURATION:30 MIN</b>	<b>MAX MARKS: 10</b>

Q. No	Questions	Course Outcome (CO)	Knowledge Levels as Per Bloom's Taxonomy	Marks
1	Explain Histogram Processing	CO2	Understanding (K2)	10
2	Illustrate the concepts of Image negatives and Log transformation functions for Intensity Transformation	CO2	Understanding (K2)	10
3	Explain the following terms i) Bit-plane Slicing ii) Contrast Stretching	CO2	Understanding (K2)	10
4	Illustrate the concept of Smoothing spatial filter	CO2	Understanding (K2)	10
5	Utilize the concept of Laplacian operator for Sharpening spatial filter	CO2	Applying (K3)	10

Q. No	Questions	Course Outcome (CO)	Knowledge Levels as Per Bloom's Taxonomy	Marks
1	Explain Histogram Processing	CO2	Understanding (K2)	10

**NARASARAOPETA ENGINEERING COLLEGE::NARASARAOPET  
(AUTONOMOUS)  
DEPARTMENT OF ELECTRONICS AND COMMUNICATION ENGINEERING  
III B.TECH II-SEMESTER ASSIGNMENT TEST-III, February-2020**

<b>SUBJECT: Digital Image Processing</b>	<b>DATE: 22-02-2020</b>
<b>DURATION:30 MIN</b>	<b>MAX MARKS: 10</b>

Q. No	Questions	Course Outcome (CO)	Knowledge Level Per Bloom's Taxonomy	Marks
1	<b>Summarize</b> the Color Fundamentals.	CO4	Understanding (K2)	10
2	<b>Explain</b> RGB Color Model.	CO4	Understanding (K2)	10
3	<b>Develop</b> CMY model from RGB model.	CO4	Applying (K3)	10
4	<b>Explain</b> HSI Color model.	CO4	Understanding (K2)	10
5	<b>Demonstrate</b> how Wiener Filter is used for Restoration.	CO3	Understanding (K2)	10

	Course Outcome (CO)	Knowledge Levels as Per <sup>Marks</sup>
--	---------------------	--

**NARASARAOPETA ENGINEERING COLLEGE::NARASARAOPET  
(AUTONOMOUS)  
DEPARTMENT OF ELECTRONICS AND COMMUNICATION ENGINEERING  
III B.TECH II-SEMESTER ASSIGNMENT TEST-IV, June-2021**

<b>SUBJECT: Digital Image Processing</b>	<b>DATE: 25-6-2021</b>
<b>DURATION:30 MIN</b>	<b>MAX MARKS: 10</b>

Q. No	Questions	Course Outcome (CO)	Knowledge Levels as Per Bloom's Taxonomy	Marks														
1	<b>Explain Image Pyramid.</b>	CO4	Evaluating (K5)	10														
2	<b>Discuss about the Sub-band Coding.</b>	CO4	Creating (K6)	10														
3	<b>Explain General Image Compression System.</b>	CO4	Evaluating (K5)	10														
4	<b>Develop Huffman Code for the below table and explain.</b> <table border="1" style="width: 100%; border-collapse: collapse; margin-top: 5px;"> <tr> <td style="width: 15%;">Source symbols</td> <td style="width: 10%; text-align: center;">a<sub>1</sub></td> <td style="width: 10%; text-align: center;">a<sub>2</sub></td> <td style="width: 10%; text-align: center;">a<sub>3</sub></td> <td style="width: 10%; text-align: center;">a<sub>4</sub></td> <td style="width: 10%; text-align: center;">a<sub>5</sub></td> <td style="width: 10%; text-align: center;">a<sub>6</sub></td> </tr> <tr> <td>Probability</td> <td style="text-align: center;">0.1</td> <td style="text-align: center;">0.4</td> <td style="text-align: center;">0.06</td> <td style="text-align: center;">0.1</td> <td style="text-align: center;">0.04</td> <td style="text-align: center;">0.3</td> </tr> </table>	Source symbols	a <sub>1</sub>	a <sub>2</sub>	a <sub>3</sub>	a <sub>4</sub>	a <sub>5</sub>	a <sub>6</sub>	Probability	0.1	0.4	0.06	0.1	0.04	0.3	CO4	Creating (K6)	10
Source symbols	a <sub>1</sub>	a <sub>2</sub>	a <sub>3</sub>	a <sub>4</sub>	a <sub>5</sub>	a <sub>6</sub>												
Probability	0.1	0.4	0.06	0.1	0.04	0.3												
5	<b>Develop Arithmetic Code for the message a<sub>1</sub>,a<sub>2</sub>,a<sub>3</sub>,a<sub>3</sub>,a<sub>4</sub>.and explain.</b>	CO4	Creating (K6)	10														

**NARASARAOPETA ENGINEERING COLLEGE::NARASARAOPET**  
**(AUTONOMOUS)**  
**DEPARTMENT OF ELECTRONICS AND COMMUNICATION ENGINEERING**  
**III B.TECH II-SEMESTER ASSIGNMENT TEST-I, December-2019**

<b>SUBJECT: Digital Image Processing</b>	<b>DATE: 20-12-2019</b>
<b>DURATION:30 MIN</b>	<b>MAX MARKS: 10</b>

Q. No	Questions	Course Outcome (CO)	Knowledge Level Per Bloom's Taxonomy	Marks
1	Explain the fundamental steps in Image Processing.	CO1	Understanding (K2)	10
2	Find the Haar Transformation Matrix for N=4.	CO1	Remembering (K1)	10
3	Explain the Hadamard Transform.	CO1	Understanding (K2)	10
4	Find the Slant Transform matrix for N=4	CO1	Remembering (K1)	10
5	Explain the Walsh Transform.	CO1	Understanding (K2)	10

Scheme of Evaluation

1Q: Block diagram - 3m  
 Explanation - 7m } 10m

2Q: Definition - 2  
 Formulas - 3  
 Calculations - 5 } 10m

3Q: Definition - 2m  
 Formulas - 3m  
 Calculations - 5m } 10m

4Q: Definition - 2m  
 Formulas - 3m  
 Calculations - 5 } 10m

5Q: Definition - 2m  
 Formulas - 3m  
 Calculations - 5 } 10m

**NARASARAOPETA ENGINEERING COLLEGE::NARASARAOPET  
(AUTONOMOUS)  
DEPARTMENT OF ELECTRONICS AND COMMUNICATION ENGINEERING  
III B.TECH II-SEMESTER ASSIGNMENT TEST-II, January-2020**

<b>SUBJECT: Digital Image Processing</b>	<b>DATE: 10-01-2020</b>
<b>DURATION:30 MIN</b>	<b>MAX MARKS: 10</b>

Q. No	Questions	Course Outcome (CO)	Knowledge Levels as Per Bloom's Taxonomy	Marks
1	Explain Histogram Processing	CO2	Understanding (K2)	10
2	Illustrate the concepts of Image negatives and Log transformation functions for Intensity Transformation	CO2	Understanding (K2)	10
3	Explain the following terms i) Bit-plane Slicing ii) Contrast Stretching	CO2	Understanding (K2)	10
4	Illustrate the concept of Smoothing spatial filter	CO2	Understanding (K2)	10
5	Utilize the concept of Laplacian operator for Sharpening spatial filter	CO2	Applying (K3)	10

scheme of evaluation

1a: Definition — 2m  
 Explanation — 3m } 10m  
 Derivation — 5m

2a: Definition & Equations — 4m } 10m  
 Explanations — 6m

3a: Definitions & Equations — 4m } 10m  
 Explanations — 6m

4a: Definition — 2m  
 Types — 3m } 10m  
 Explanation — 5m

5a: Definitions — 4m } 10m  
 Derivation — 6m

**NARASARAOPETA ENGINEERING COLLEGE::NARASARAOPET**  
**(AUTONOMOUS)**  
**DEPARTMENT OF ELECTRONICS AND COMMUNICATION ENGINEERING**  
**III B.TECH II-SEMESTER ASSIGNMENT TEST-III, February-2020**

<b>SUBJECT: Digital Image Processing</b>	<b>DATE: 22-02-2020</b>
<b>DURATION:30 MIN</b>	<b>MAX MARKS: 10</b>

Q. No	Questions	Course Outcome (CO)	Knowledge Levels as Per Bloom's Taxonomy	Marks
1	Summarize the Color Fundamentals.	CO4	Understanding (K2)	10
2	Explain RGB Color Model.	CO4	Understanding (K2)	10
3	Develop CMY model from RGB model.	CO4	Applying (K3)	10
4	Explain HSI Color model.	CO4	Understanding (K2)	10
5	Demonstrate how Wiener Filter is used for Restoration.	CO3	Understanding (K2)	10

Scheme of Evaluation

1Q: Definition - 4m } 10m  
 explanation - 6m

2Q: Definition of color cube diagram - 4m } 10m  
 explanation - 6m

3Q: Definition of color cube diagram - 4m } 10m  
 explanation - 6m

4Q: Definition & color cube diagram - 4m } 10m  
 explanation - 6m

5Q: Definition & equation - 4m } 10m  
 Derivation & explanation - 6m

**NARASARAOPETA ENGINEERING COLLEGE::NARASARAOPET  
(AUTONOMOUS)  
DEPARTMENT OF ELECTRONICS AND COMMUNICATION ENGINEERING  
III B.TECH II-SEMESTER ASSIGNMENT TEST-IV, June-2021**

<b>SUBJECT: Digital Image Processing</b>	<b>DATE: 25-6-2021</b>
<b>DURATION:30 MIN</b>	<b>MAX MARKS: 10</b>

Q. No	Questions	Course Outcome (CO)	Knowledge Levels as Per Bloom's Taxonomy	Marks														
1	<b>Explain Image Pyramid.</b>	CO4	Evaluating (K5)	10														
2	<b>Discuss about the Sub-band Coding.</b>	CO4	Creating (K6)	10														
3	<b>Explain General Image Compression System.</b>	CO4	Evaluating (K5)	10														
4	<b>Develop Huffman Code for the below table and explain.</b> <table border="1" style="margin: 5px auto; border-collapse: collapse;"> <tr> <td style="padding: 2px;">Source symbols</td> <td style="padding: 2px;">a<sub>1</sub></td> <td style="padding: 2px;">a<sub>2</sub></td> <td style="padding: 2px;">a<sub>3</sub></td> <td style="padding: 2px;">a<sub>4</sub></td> <td style="padding: 2px;">a<sub>5</sub></td> <td style="padding: 2px;">a<sub>6</sub></td> </tr> <tr> <td style="padding: 2px;">Probability</td> <td style="padding: 2px;">0.1</td> <td style="padding: 2px;">0.4</td> <td style="padding: 2px;">0.06</td> <td style="padding: 2px;">0.1</td> <td style="padding: 2px;">0.04</td> <td style="padding: 2px;">0.3</td> </tr> </table>	Source symbols	a <sub>1</sub>	a <sub>2</sub>	a <sub>3</sub>	a <sub>4</sub>	a <sub>5</sub>	a <sub>6</sub>	Probability	0.1	0.4	0.06	0.1	0.04	0.3	CO4	Creating (K6)	10
Source symbols	a <sub>1</sub>	a <sub>2</sub>	a <sub>3</sub>	a <sub>4</sub>	a <sub>5</sub>	a <sub>6</sub>												
Probability	0.1	0.4	0.06	0.1	0.04	0.3												
5	<b>Develop Arithmetic Code for the message a<sub>1</sub>,a<sub>2</sub>,a<sub>3</sub>,a<sub>3</sub>,a<sub>4</sub>. and explain.</b>	CO4	Creating (K6)	10														

Scheme of Evaluation

- 1Q: Definition & diagram → 5m & 10m  
 Explanation — 5m
- 2Q: Definition & diagrams — 5m & 10m  
 Explanation — 5m
- 3Q: Definition & diagram — 5m & 10m  
 Explanation — 5m
- 4Q: Processing steps — 5m & 10m  
 code generation — 5m
- 5Q: Processing steps — 5m & 10m.  
 code generation — 5m

MID-EXAM  
QUESTION  
PAPERS



**NARASARAOPETA ENGINEERING COLLEGE::NARASARAOPET  
(AUTONOMOUS)  
DEPARTMENT OF ELECTRONICS AND COMMUNICATION ENGINEERING  
III B.TECH II-SEMESTER I-MID Examinations, August-2021**

<b>SUBJECT: Digital Image Processing</b>	<b>DATE: 19-08-2021</b>
<b>DURATION:90 MIN</b>	<b>MAX MARKS: 30</b>

Q. No	Questions	Course Outcome (CO)	Knowledge Marks as Per Bloom's Taxonomy	Marks
1	<b>Explain</b> the fundamental steps in Image Processing and	CO1	Evaluating (K5)	10
2	<b>Discuss</b> the concept of Smoothing spatial filters and <b>Develop</b> the Laplacian operator for image sharpening.	CO2	Creating (K6) & Creating (K6)	10
3	<b>Discuss</b> the Degradation/Restoration Process and <b>Develop</b> Inverse filtering for reconstructing the original image from degraded image.	CO3	Creating (K6) & Creating (K6)	10

J. Narasimha Rao

**NARASARAOPETA ENGINEERING COLLEGE::NARASARAOPET  
(AUTONOMOUS)  
DEPARTMENT OF ELECTRONICS AND COMMUNICATION ENGINEERING  
III B.TECH II-SEMESTER I-MID Examinations, August-2021**

<b>SUBJECT: Digital Image Processing</b>	<b>DATE: 19-08-2021</b>
<b>DURATION:90 MIN</b>	<b>MAX MARKS: 30</b>

Q. No	Questions	Course Outcome (CO)	Knowledge Marks as Per Bloom's Taxonomy	Marks
1	<b>Explain</b> the fundamental steps in Image Processing and	CO1	Evaluating (K5)	10
2	<b>Discuss</b> the concept of Smoothing spatial filters and <b>Develop</b> the Laplacian operator for image sharpening.	CO2	Creating (K6) & Creating (K6)	10
3	<b>Discuss</b> the Degradation/Restoration Process and <b>Develop</b> Inverse filtering for reconstructing the original image from degraded image.	CO3	Creating (K6) & Creating (K6)	10

J. Narasimha Rao

**NARASARAOPETA ENGINEERING COLLEGE::NARASARAOPET  
(AUTONOMOUS)  
DEPARTMENT OF ELECTRONICS AND COMMUNICATION ENGINEERING  
III B.TECH II-SEMESTER II-MID Examinations, August-2021**

<b>SUBJECT: Digital Image Processing</b>	<b>DATE: 19-08-2021</b>
<b>DURATION:90 MIN</b>	<b>MAX MARKS: 30</b>

Q. No.	Questions	Course Outcome (CO)	Knowledge Level Per Bloom's Taxonomy	Marks
1	<b>Explain</b> RGB Color Model with neat diagram.	CO4	Evaluating (K5)	10
2	<b>Discuss</b> image pyramid with neat diagram and <b>Develop</b> Huffman coding for the six source symbols with probabilities as defined below. {a1, a2, a3, a4, a5, a6}={0.1, 0.4, 0.06, 0.1, 0.04, 0.3}	CO5	Creating (K6)	10
3	<b>Discuss</b> Erosion & Dilation operations on an image.	CO6	Creating (K6)	10

**J. Narasimha Rao**

**NARASARAOPETA ENGINEERING COLLEGE::NARASARAOPET  
(AUTONOMOUS)  
DEPARTMENT OF ELECTRONICS AND COMMUNICATION ENGINEERING  
III B.TECH II-SEMESTER II-MID Examinations, August-2021**

<b>SUBJECT: Digital Image Processing</b>	<b>DATE: 19-08-2021</b>
<b>DURATION:90 MIN</b>	<b>MAX MARKS: 30</b>

Q. No.	Questions	Course Outcome (CO)	Knowledge Level Per Bloom's Taxonomy	Marks
1	<b>Explain</b> RGB Color Model with neat diagram.	CO4	Evaluating (K5)	10
2	<b>Discuss</b> image pyramid with neat diagram and <b>Develop</b> Huffman coding for the six source symbols with probabilities as defined below. {a1, a2, a3, a4, a5, a6}={0.1, 0.4, 0.06, 0.1, 0.04, 0.3}	CO5	Creating (K6)	10
3	<b>Discuss</b> Erosion & Dilation operations on an image.	CO6	Creating (K6)	10

**J. Narasimha Rao**

**NARASARAOPETA ENGINEERING COLLEGE::NARASARAOPET**  
**(AUTONOMOUS)**  
**DEPARTMENT OF ELECTRONICS AND COMMUNICATION ENGINEERING**  
**III B.TECH II-SEMESTER I-MID Examinations, August-2021**

<b>SUBJECT: Digital Image Processing</b>	<b>DATE: 19-08-2021</b>
<b>DURATION:90 MIN</b>	<b>MAX MARKS: 30</b>

Q. No	Questions	Course Outcome (CO)	Knowledge Marks as Per Bloom's Taxonomy	Marks
1	<b>Explain</b> the fundamental steps in Image Processing and	CO1	Evaluating (K5)	10
2	<b>Discuss</b> the concept of Smoothing spatial filters and <b>Develop</b> the Laplacian operator for image sharpening.	CO2	Creating (K6) & Creating (K6)	10
3	<b>Discuss</b> the Degradation/Restoration Process and <b>Develop</b> Inverse filtering for reconstructing the original image from degraded image.	CO3	Creating (K6) & Creating (K6)	10

J. Narasimha Rao

**NARASARAOPETA ENGINEERING COLLEGE::NARASARAOPET**  
**(AUTONOMOUS)**  
**DEPARTMENT OF ELECTRONICS AND COMMUNICATION ENGINEERING**  
**III B.TECH II-SEMESTER I-MID Examinations, August-2021**

<b>SUBJECT: Digital Image Processing</b>	<b>DATE: 19-08-2021</b>
<b>DURATION:90 MIN</b>	<b>MAX MARKS: 30</b>

Q. No	Questions	Course Outcome (CO)	Knowledge Marks as Per Bloom's Taxonomy	Marks
1	<b>Explain</b> the fundamental steps in Image Processing and	CO1	Evaluating (K5)	10
2	<b>Discuss</b> the concept of Smoothing spatial filters and <b>Develop</b> the Laplacian operator for image sharpening.	CO2	Creating (K6) & Creating (K6)	10
3	<b>Discuss</b> the Degradation/Restoration Process and <b>Develop</b> Inverse filtering for reconstructing the original image from degraded image.	CO3	Creating (K6) & Creating (K6)	10

J. Narasimha Rao

scheme of evaluation

1Q: Fundamental steps & diagram - 4m & 10m  
 explanation - 6m

2Q: Definitions - 5m & 10m  
 Derivation - 5m

3Q: Definition & diagram - 5m & 10m  
 Derivation - 5m

**NARASARAOPETA ENGINEERING COLLEGE::NARASARAOPET**  
**(AUTONOMOUS)**  
**DEPARTMENT OF ELECTRONICS AND COMMUNICATION ENGINEERING**  
**III B.TECH II-SEMESTER II-MID Examinations, August-2021**

<b>SUBJECT: Digital Image Processing</b>	<b>DATE: 19-08-2021</b>
<b>DURATION:90 MIN</b>	<b>MAX MARKS: 30</b>

Q. No.	Questions	Course Outcome (CO)	Knowledge Level Per Bloom's Taxonomy	Marks
1	<b>Explain RGB Color Model with neat diagram.</b>	CO4	Evaluating (K5)	10
2	<b>Discuss image pyramid with neat diagram and Develop Huffman coding for the six source symbols with probabilities as defined below.</b> $\{a_1, a_2, a_3, a_4, a_5, a_6\} = \{0.1, 0.4, 0.06, 0.1, 0.04, 0.3\}$	CO5	Creating (K6)	10
3	<b>Discuss Erosion &amp; Dilation operations on an image.</b>	CO6	Creating (K6)	10

J. Narasimha Rao

**NARASARAOPETA ENGINEERING COLLEGE::NARASARAOPET**  
**(AUTONOMOUS)**  
**DEPARTMENT OF ELECTRONICS AND COMMUNICATION ENGINEERING**  
**III B.TECH II-SEMESTER II-MID Examinations, August-2021**

<b>SUBJECT: Digital Image Processing</b>	<b>DATE: 19-08-2021</b>
<b>DURATION:90 MIN</b>	<b>MAX MARKS: 30</b>

Q. No.	Questions	Course Outcome (CO)	Knowledge Level Per Bloom's Taxonomy	Marks
1	<b>Explain RGB Color Model with neat diagram.</b>	CO4	Evaluating (K5)	10
2	<b>Discuss image pyramid with neat diagram and Develop Huffman coding for the six source symbols with probabilities as defined below.</b> $\{a_1, a_2, a_3, a_4, a_5, a_6\} = \{0.1, 0.4, 0.06, 0.1, 0.04, 0.3\}$	CO5	Creating (K6)	10
3	<b>Discuss Erosion &amp; Dilation operations on an image.</b>	CO6	Creating (K6)	10

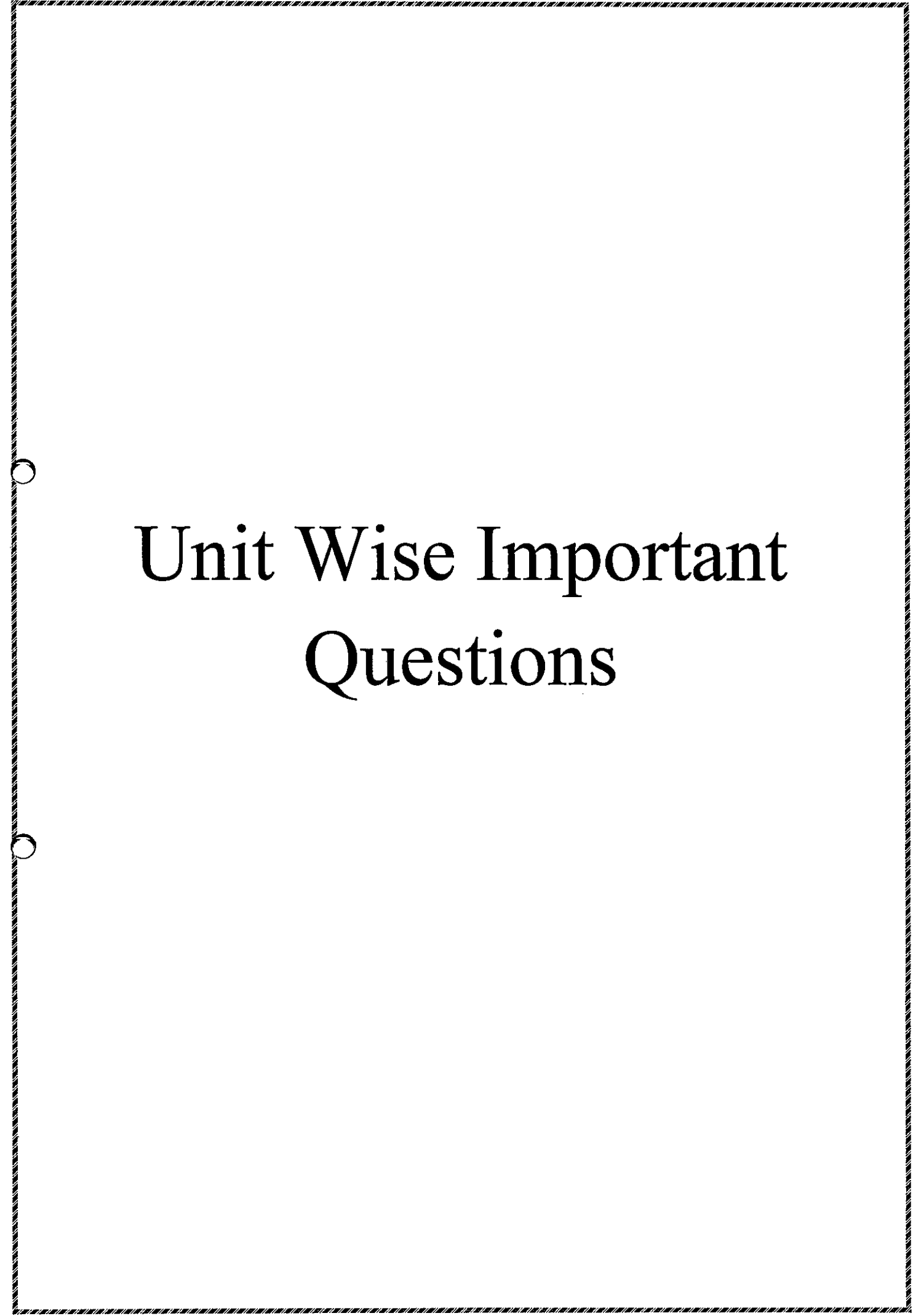
J. Narasimha Rao

*Handwritten notes:*

1Q: Definition & diagram — 15m  
Explanation — 15m  $\therefore$  10m

2Q: Definition & diagram + explanation — 15m  $\therefore$  10m  
Processing steps & Code generation — 15m

3Q: Definitions & diagrams — 15m  $\therefore$  10m  
Explanation — 15m



# Unit Wise Important Questions

**Unit wise Sample assessment questions**

S NO	QUESTION	KNOWLEDGE LEVEL	CO
<b>UNIT I</b>			
1	What is the need of image transform? List out various transform used in image processing.	K2	CO1
2	Explain the following terms: (i) Adjacency (ii) Connectivity (iii) Regions (iv) Boundaries	K2	CO1
3	Explain the basic concepts of sampling and quantization in the generation of digital image.	K2	CO1
4	Discuss about KL Transform and write its applications in image processing		
<b>UNIT 2</b>			
1	Explain the following filters: (i) Band reject and Band pass filters (ii) Notch filters	K2	CO2
2	Explain the use of histogram statistics for image enhancement.	K3	CO2
3	With an example, explain the concept of histogram equalization.	K3	CO2
4	State 2D sampling theorem and explain about aliasing in images.	K4	CO2
<b>UNIT 3</b>			
1	Explain the image degradation model	K2	CO3
2	Explain the following. a) Minimum Mean square error filtering. b) Inverse filtering.	K2	CO3
3	Define all the noise models.	K1	CO3
<b>UNIT 4</b>			
1	Explain about RGB color model and write its applications.	K1	CO3
2	State the expression for conversion of HIS to RGB color model. Explain the terms involved in it.	K1&K2	CO3
3	Demonstrate CMY and CMYK color models.	K2	CO3
<b>UNIT 5</b>			
1	Model a general image compression system and explain it.	K3	CO3
2	Explain the concept of wavelet packets and write its advantages.	K2	CO3
3	What is meant by block transform coding? Explain.	K1	CO3
<b>UNIT 6</b>			
1	Explain about morphological hit-or-miss transform.	K2	CO4
2	Distinguish Erosion & Dilation	K4	CO4
3	Explain the basics of intensity thresholding in image segmentation.	K2	CO4

UNIVERSITY  
QUESTION  
PAPERS



Subject Code: R16EC3209

III B.Tech II Semester Regular & Supple Examinations, August-2021

DIGITAL IMAGE PROCESSING

(ECE)

Time: 3 hours

Max Marks: 60

Question Paper Consists of Part-A and Part-B.

Answering the question in Part-A is Compulsory & Four Questions should be answered from Part-B

All questions carry equal marks of 12.

**PART-A**

1. a) Define basic relationships between pixels.
- b) What are the advantages of filtering in frequency domain?
- c) How the Restoration differ from Reconstruction?
- d) Define brightness, hue and saturation.
- e) What is the purpose of Image Compression?
- f) What are the applications of image segmentation?

[2M+2M+2M+2M+2M+2M]

**PART-B**

2. a. Explain the concept of sampling and quantization of an image. [6M]  
b. Find the DCT matrix for N=4. [6M]
3. a. What is meant by histogram equalization? Explain. [6M]  
b. Explain the image sharpening using ideal LPF and Butterworth LPF. [6M]
4. a. What are the different types of mean filters used for noise reduction? Explain. [6M]  
b. Explain about Restoration using inverse filtering. [6M]
5. a. What is pseudo color image processing? Explain. [6M]  
b. Explain about RGB color model. [6M]
6. a. What are the various requirements for multi-resolution analysis? Explain. [6M]  
b. What is Lossy Predictive coding? Explain. [6M]
7. a. Explain the Boundary Extraction in Morphological algorithm. [6M]  
b. Explain about edge linking using global processing. [6M]

\*\*\*



J. Narasimha Rao  
IEC-dept

## Digital Image Processing-KEY

Subject Code: R16EC3209

III B.Tech II Semester Regular & Supple Examination, August-2021

1. a) Basic Relationships Between Pixels

1. Neighborhood

2. Adjacency

3. Connectivity

4. Paths

5. Regions and boundaries

1. Neighbors of a Pixel

b) The reason for doing the filtering in the frequency domain is generally because it is **computationally faster to perform two 2D Fourier transforms and a filter multiply than to perform a convolution in the image (spatial) domain.** This is particularly so as the filter size increases.

c) Restoration depicts a property at a particular period of time in its history, while removing evidence of other periods. **Reconstruction re-creates vanished or non-surviving portions of a property** for interpretive purposes

d) Hue is determined by the dominant wavelength of the visible spectrum. ... **Saturation pertains the amount of white light mixed with a hue.** High-saturation colors, such as the circle on the left, contain little or no white light. Brightness refers to intensity, distinguished by the amount of shading mixed with the hue.

e) The objective of image compression is **to reduce irrelevance and redundancy of the image data to be able to store or transmit data in an efficient form.** It is concerned with minimizing the number of bits required to represent an image. Image compression may be lossy or lossless.

f) **Some of the practical applications of image segmentation are:**

Content-based image retrieval.

Machine vision.

Medical imaging, including volume rendered images from computed tomography and magnetic resonance imaging. ...

Object detection. ...

Recognition Tasks. ...

Traffic control systems.

Video surveillance.

Fig.5.4 An example of the digital image acquisition process (a) Energy ("illumination") source (b) An element of a scene (c) Imaging system (d) Projection of the scene onto the image plane (e) Digitized image

Explain about image sampling and quantization process.

### Image Sampling and Quantization:

The output of most sensors is a continuous voltage waveform whose amplitude and spatial behavior are related to the physical phenomenon being sensed. To create a digital image, we need to convert the continuous sensed data into digital form. This involves two processes: sampling and quantization.

### Basic Concepts in Sampling and Quantization:

The basic idea behind sampling and quantization is illustrated in Fig.6.1. Figure 6.1(a) shows a continuous image,  $f(x, y)$ , that we want to convert to digital form. An image may be continuous with respect to the x- and y-coordinates, and also in amplitude. To convert it to digital form, we have to sample the function in both coordinates and in amplitude. Digitizing the coordinate values is called sampling. Digitizing the amplitude values is called quantization.

The one-dimensional function shown in Fig.6.1 (b) is a plot of amplitude (gray level) values of the continuous image along the line segment AB in Fig. 6.1(a). The random variations are due to image noise. To sample this function, we take equally spaced samples along line AB, as shown in Fig.6.1 (c). The location of each sample is given by a vertical tick mark in the bottom part of the figure. The samples are shown as small white squares superimposed on the function. The set of these discrete locations gives the sampled function. However, the values of the samples still span (vertically) a continuous range of gray-level values. In order to form a digital function, the gray-level values also must be converted (quantized) into discrete quantities. The right side of Fig. 6.1 (c) shows the gray-level scale divided into eight discrete levels, ranging from black to white. The vertical tick marks indicate the specific value assigned to each of the eight gray levels. The continuous gray levels are quantized simply by assigning one of the eight discrete gray levels to each sample. The assignment is made depending on the vertical proximity of a sample to a vertical tick mark. The digital samples resulting from both sampling and quantization are shown in Fig.6.1 (d). Starting at the top of the image and carrying out this procedure line by line produces a two-dimensional digital image.

Sampling in the manner just described assumes that we have a continuous image in both coordinate directions as well as in amplitude. In practice, the method of sampling is determined by the sensor arrangement used to generate the image. When an image is generated by a single

2b 2b

the 1-D DCT pair

$$c(u) = \alpha(u) \sum_{x=0}^{N-1} f(x) \cos\left(\frac{(2x+1)u\pi}{2N}\right)$$

for  $u = 0, 1, 2, \dots, N-1$

### Digital Image Processing

For  $u = 0, 1, 2, \dots, N-1$ . Similarly the inverse DCT is defined as

$$f(x) = \sum_{u=0}^{N-1} \alpha(u) c(u) \cos\left[\frac{(2x+1)u\pi}{2N}\right]$$

For  $u = 0, 1, 2, \dots, N-1$

Where  $\alpha$  is

$$\alpha(u) = \begin{cases} \frac{1}{\sqrt{N}} & \text{for } u = 0 \\ \frac{2}{\sqrt{N}} & \text{for } u = 1, 2, \dots, N-1 \end{cases}$$

The corresponding 2-D DCT pair is

$$C(u, v) = \alpha(u)\alpha(v) \sum_{x=0}^{N-1} \sum_{y=0}^{N-1} f(x, y) \cos\left[\frac{(2x+1)u\pi}{2N}\right] \cos\left[\frac{(2y+1)v\pi}{2N}\right]$$

For  $u, v = 0, 1, 2, \dots, N-1$ , and

$$f(x, y) = \sum_{u=0}^{N-1} \sum_{v=0}^{N-1} \alpha(u)\alpha(v) C(u, v) \cos\left[\frac{(2x+1)u\pi}{2N}\right] \cos\left[\frac{(2y+1)v\pi}{2N}\right]$$

For  $x, y = 0, 1, 2, \dots, N-1$

### ~~9.2.1.1. The Haar Transform~~

The Haar transform is based on the Haar functions,  $h_k(z)$ , which are defined over the continuous, closed interval  $z \in [0, 1]$ , and for  $k = 0, 1, 2, \dots, N-1$ , where  $N = 2^n$ . The first step in generating the Haar transform is to note that the integer  $k$  can be decomposed uniquely as

$$k = 2^p + q - 1$$

where  $0 \leq p \leq n-1$ ,  $q = 0$  or  $1$  for  $p = 0$ , and  $1 \leq q \leq 2^p$  for  $p \neq 0$ . For example, if  $N = 4$ ,  $k, q, p$  have following values

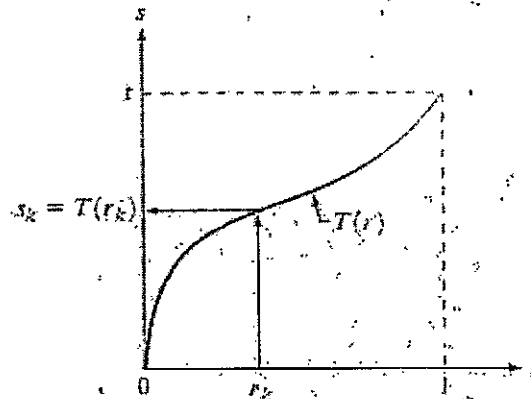


Fig.4.1 A gray-level transformation function that is both single valued and monotonically increasing.

The gray levels in an image may be viewed as random variables in the interval  $[0, 1]$ . One of the most fundamental descriptors of a random variable is its probability density function (PDF). Let  $p_r(r)$  and  $p_s(s)$  denote the probability density functions of random variables  $r$  and  $s$ , respectively, where the subscripts on  $p$  are used to denote that  $p_r$  and  $p_s$  are different functions. A basic result from an elementary probability theory is that, if  $p_r(r)$  and  $T(r)$  are known and  $T^{-1}(s)$  satisfies condition (a), then the probability density function  $p_s(s)$  of the transformed variable  $s$  can be obtained using a rather simple formula:

$$p_s(s) = p_r(r) \left| \frac{dr}{ds} \right|$$

Thus, the probability density function of the transformed variable,  $s$ , is determined by the gray-level PDF of the input image and by the chosen transformation function. A transformation function of particular importance in image processing has the form

$$s = T(r) = \int_0^r p_r(w) dw$$

where  $w$  is a dummy variable of integration. The right side of Eq. above is recognized as the cumulative distribution function (CDF) of random variable  $r$ . Since probability density functions are always positive, and recalling that the integral of a function is the area under the function, it follows that this transformation function is single valued and monotonically increasing, and, therefore, satisfies condition (a). Similarly, the integral of a probability density function for variables in the range  $[0, 1]$  also is in the range  $[0, 1]$ , so condition (b) is satisfied as well.

Where  $G$ ,  $H$  and  $F$  are the Fourier transforms of  $g$ ,  $h$  and  $f$  respectively. In the terminology of linear system the transform  $H(u, v)$  is called the transfer function of the process. The edges in  $f(x, y)$  can be boosted by using  $H(u, v)$  to emphasize the high frequency components of  $F(u, v)$ .

### 3. Explain about Ideal Low Pass Filter (ILPF) in frequency domain.

#### Lowpass Filter:

The edges and other sharp transitions (such as noise) in the gray levels of an image contribute significantly to the high-frequency content of its Fourier transform. Hence blurring (smoothing) is achieved in the frequency domain by attenuating us the transform of a given image.

$$G(u, v) = H(u, v) F(u, v)$$

where  $F(u, v)$  is the Fourier transform of an image to be smoothed. The problem is to select a filter transfer function  $H(u, v)$  that yields  $G(u, v)$  by attenuating the high-frequency components of  $F(u, v)$ . The inverse transform then will yield the desired smoothed image  $g(x, y)$ .

#### Ideal Filter:

A 2-D ideal lowpass filter (ILPF) is one whose transfer function satisfies the relation

$$H(u, v) = \begin{cases} 1 & \text{if } D(u, v) \leq D_0 \\ 0 & \text{if } D(u, v) > D_0 \end{cases}$$

where  $D$  is a specified nonnegative quantity, and  $D(u, v)$  is the distance from point  $(u, v)$  to the origin of the frequency plane; that is,

$$D(u, v) = (u^2 + v^2)^{1/2}$$

Figure 3 (a) shows a 3-D perspective plot of  $H(u, v)$  as a function of  $u$  and  $v$ . The name ideal filter indicates that only frequencies inside a circle of radius

3b

4. Discuss about Butterworth lowpass filter with a suitable example.

Butterworth filter:

The transfer function of the Butterworth lowpass (BLPF) of order n and with cutoff frequency locus at a distance  $D_0$  from the origin is defined by the relation

$$H(u, v) = \frac{1}{1 + [D(u, v)/D_0]^n}$$

A perspective plot and cross section of the BLPF function are shown in figure 4.

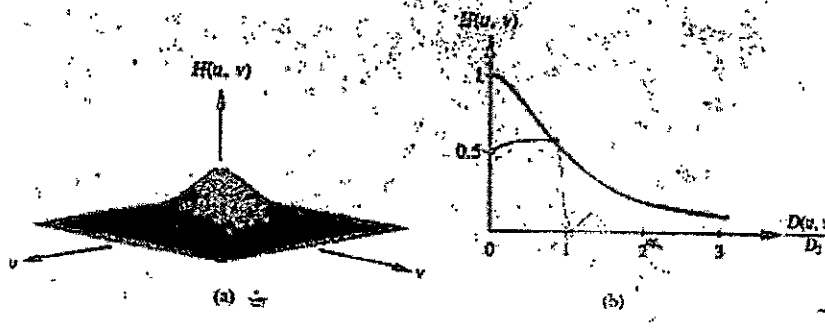


Fig.4 (a) A Butterworth lowpass filter (b) radial cross section for  $n = 1$ .

Unlike the ILPF, the BLPF transfer function does not have a sharp discontinuity that establishes a clear cutoff between passed and filtered frequencies. For filters with smooth transfer functions, defining a cutoff frequency locus at points for which  $H(u, v)$  is down to a certain fraction of its maximum value is customary. In the case of above Eq.  $H(u, v) = 0.5$  (down 50 percent from its maximum value of 1) when  $D(u, v) = D_0$ . Another value commonly used is  $1/\sqrt{2}$  of the maximum value of  $H(u, v)$ . The following simple modification yields the desired value when  $D(u, v) = D_0$ :

$$H(u, v) = \frac{1}{1 + [\sqrt{2} - 1][D(u, v)/D_0]^2}$$

$$= \frac{1}{1 + 0.414[D(u, v)/D_0]^2}$$

$$\hat{f}(x, y) = \left[ \prod_{(s, t) \in S_{xy}} g(s, t) \right]^{1/mn}$$

Here, each restored pixel is given by the product of the pixels in the subimage window, raised to the power  $1/mn$ . A geometric mean filter achieves smoothing comparable to the arithmetic mean filter, but it tends to lose less image detail in the process.

### (iii) Harmonic mean filter

The harmonic mean filtering operation is given by the expression

$$\hat{f}(x, y) = \frac{mn}{\sum_{(s, t) \in S_{xy}} \frac{1}{g(s, t)}}$$

The harmonic mean filter works well for salt noise, but fails for pepper noise. It does well also with other types of noise like Gaussian noise.

### (iv) Contra harmonic mean filter

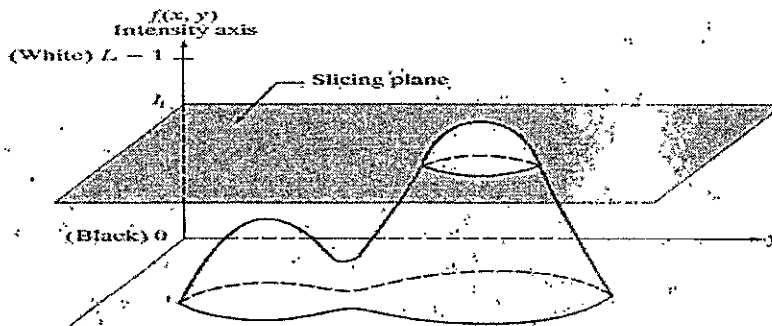
The contra harmonic mean filtering operation yields a restored image based on the expression

$$\hat{f}(x, y) = \frac{\sum_{(s, t) \in S_{xy}} g(s, t)^{Q+1}}{\sum_{(s, t) \in S_{xy}} g(s, t)^Q}$$

where  $Q$  is called the order of the filter. This filter is well suited for reducing or virtually eliminating the effects of salt-and-pepper noise. For positive values of  $Q$ , the filter eliminates pepper noise. For negative values of  $Q$  it eliminates salt noise. It cannot do both simultaneously. Note that the contra harmonic filter reduces to the arithmetic mean filter if  $Q = 0$ , and to the harmonic mean filter if  $Q = -1$ .

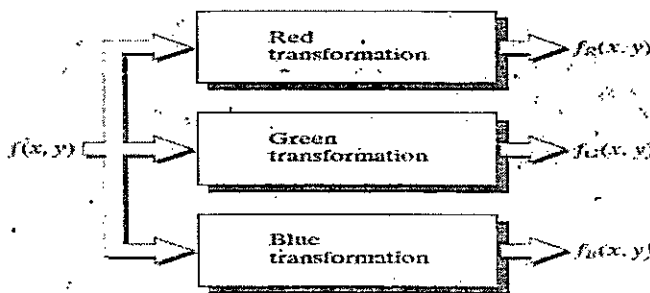
5 a) Pseudocolor images are originally grayscale which are assigned colors based on the intensity values. Typical usage of these images is for thermography where the only available is infrared radiation instead of lights. Another example is elevation map.

Intensity Slicing: This is a simple case of pseudocolor image processing. It's also called density slicing or color coding. Imagine a grayscale image as a 3D function with the intensity being the third dimension. Placing a plane parallel to the horizontal plane for the pixel position coordinates would "slice" the image into two parts. After that we can assign different colors to different levels.



We are not constrained to use only one plane. Multiple slices result in more flexible representations of the grayscale images. In this case, the grayscale is parted into intervals and each one is assigned a different color.

Intensity to Color Transformation: We can generalize the above technique by performing three independent transformations on the intensity of the image, resulting in three images which are the red, green, blue component images used to produce a color image.



Functional block diagram for pseudo color image processing.

The flexibility can be even more enhanced by using more than one monochrome images, for example, the three components of an RGB and the thermal image.



6a

6 a) Requirements for MRA

1. The scaling function is orthogonal to its integer translates.
2. The subspaces spanned by the scaling function at low scales are nested within those spanned at higher scales.  $V_{-\infty} \subset \dots \subset V_{-1} \subset V_0 \subset V_1 \subset V_2 \subset \dots \subset V_{\infty}$
3. The only function that is common to all  $V_j$  is  $f(x) = 0$ .
4. Any function can be represented with arbitrary precision.

7a

7a) Boundary Extraction:

If A is an image and structuring element is B then Boundary Extraction can be given as,  
 Boundary (A) = A - (A  $\ominus$  B)

It means subtracting the erode image of A from the original image. Let A =

0	0	0	0	0	0	0	0	0	0
0	0	0	0	0	0	0	0	0	0
0	0	0	0	0	0	0	0	0	0
0	0	0	0	0	0	0	0	0	0
0	0	0	0	0	0	0	0	0	0
0	0	0	0	0	0	0	0	0	0
0	0	0	0	0	0	0	0	0	0
0	0	0	0	0	0	0	0	0	0
0	0	0	0	0	0	0	0	0	0
0	0	0	0	0	0	0	0	0	0

If B =

1	1	1
1	1	1
1	1	1

Then A  $\ominus$  B would be same as A except one pixel, A  $\ominus$  B =

0	0	0	0	0	0	0	0	0	0
0	0	0	0	0	0	0	0	0	0
0	0	0	0	0	0	0	0	0	0
0	0	0	0	0	0	0	0	0	0
0	0	0	0	0	0	0	0	0	0
0	0	0	0	0	0	0	0	0	0
0	0	0	0	0	0	0	0	0	0
0	0	0	0	0	0	0	0	0	0
0	0	0	0	0	0	0	0	0	0
0	0	0	0	0	0	0	0	0	0

Now Boundary (A) =

0	0	0	0	0	0	0	0	0	0
0	0	0	0	0	0	0	0	0	0
0	0	0	0	0	0	0	0	0	0
0	0	0	0	0	0	0	0	0	0
0	0	0	0	0	0	0	0	0	0
0	0	0	0	0	0	0	0	0	0
0	0	0	0	0	0	0	0	0	0
0	0	0	0	0	0	0	0	0	0
0	0	0	0	0	0	0	0	0	0
0	0	0	0	0	0	0	0	0	0

Hence, it would give a pixel difference.

## Digital Image Processing

where each subscripted variable is now expressed explicitly as a function of spatial coordinates  $x$  and  $y$ . The Eq. indicates that the 1-D linear prediction  $f(x, y)$  is a function of the previous pixels on the current line alone. In 2-D predictive coding, the prediction is a function of the previous pixels in a left-to-right, top-to-bottom scan of an image. In the 3-D case, it is based on these pixels and the previous pixels of preceding frames. Equation above cannot be evaluated for the first  $m$  pixels of each line, so these pixels must be coded by using other means (such as a Huffman code) and considered as an overhead of the predictive coding process. A similar comment applies to the higher-dimensional cases.

66 Explain about lossy predictive coding.

### Lossy Predictive Coding:

In this type of coding, we add a quantizer to the lossless predictive model and examine the resulting trade-off between reconstruction accuracy and compression performance. As Fig.9 shows, the quantizer, which absorbs the nearest integer function of the error-free encoder, is inserted between the symbol encoder and the point at which the prediction error is formed. It maps the prediction error into a limited range of outputs, denoted  $e_n^*$  which establish the amount of compression and distortion associated with lossy predictive coding.

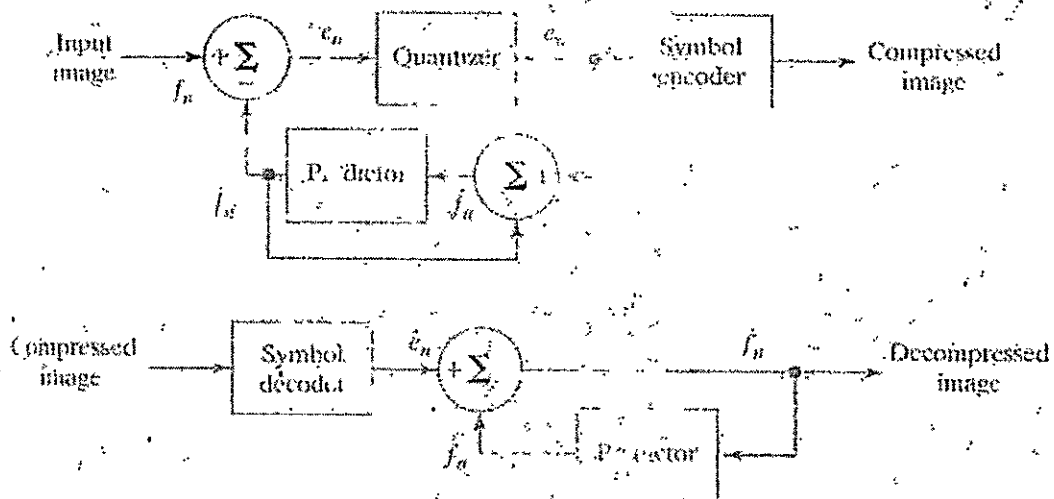


Fig. 9 A lossy predictive coding model: (a) encoder and (b) decoder.

**3. Explain about the edge linking procedures.**

The different methods for edge linking are as follows

- (i) Local processing
- (ii) Global processing via the Hough Transform.
- (iii) Global processing via graph-theoretic techniques.

**(i) Local Processing:**

One of the simplest approaches for linking edge points is to analyze the characteristics of pixels in a small neighborhood (say, 3 X 3 or 5 X 5) about every point  $(x, y)$  in an image that has been labeled an edge point. All points that are similar according to a set of predefined criteria are linked, forming an edge of pixels that share those criteria.

The two principal properties used for establishing similarity of edge pixels in this kind of analysis are (1) the strength of the response of the gradient operator used to produce the edge pixel; and (2) the direction of the gradient vector. The first property is given by the value of  $|\nabla f|$ .

Thus an edge pixel with coordinates  $(x_0, y_0)$  in a predefined neighborhood of  $(x, y)$ , is similar in magnitude to the pixel at  $(x, y)$  if

$$|\nabla f(x, y) - \nabla f(x_0, y_0)| \leq A$$

The direction (angle) of the gradient vector is given by Eq. An edge pixel at  $(x_0, y_0)$  in the predefined neighborhood of  $(x, y)$  has an angle similar to the pixel at  $(x, y)$  if

$$|\alpha(x, y) - \alpha(x_0, y_0)| \leq A$$

where  $A$  is a nonnegative angle threshold. The direction of the edge at  $(x, y)$  is perpendicular to the direction of the gradient vector at that point.

A point in the predefined neighborhood of  $(x, y)$  is linked to the pixel at  $(x, y)$  if both magnitude and direction criteria are satisfied. This process is repeated at every location in the image. A record must be kept of linked points as the center of the neighborhood is moved from pixel to pixel. A simple bookkeeping procedure is to assign a different gray level to each set of linked edge pixels.



Subject Code: R16EC3209

**III B.Tech II Semester Regular & Supple Examinations, November-2020**

**DIGITAL IMAGE PROCESSING**

**(ECE)**

**Time: 3 hours**

**Max Marks: 60**

Question Paper Consists of **Part-A** and **Part-B**.

Answering the question in **Part-A** is Compulsory & Four Questions should be answered from **Part-B**

All questions carry equal marks of 12.

**PART-A**

1. (a) List fundamental steps involved in the digital image processing.
- (b) Consider the continuous function  $f(t) = \sin(2\pi mt)$ . What is the period of  $f(t)$ ?
- (c) What is projection? And give its classification.
- (d) write a short note on CMY to RGB conversion
- (e) Provide the formula for total number of pixels required in a  $P+1$  level pyramid of  $P > 0$ .
- (f) Define Segmentation

[2+2+2+2+2+2]

**PART-B**

**4 X 12 = 48**

2. (a) What is pixel and explain all basic relationships between pixels. [6 M]  
(b) Write image transform advantages and disadvantages, also compare Walsh and Hadamard transform. [6M]
3. (a) Prove that the 2-D continuous Fourier transform is linear Operation. [4 M]  
(b) Give a single intensity transformation function for spreading the intensities of an image so the lowest intensity is 0 and the highest is  $L-1$ . [4 M]  
(c) What would be the effect on the histogram if we set to zero the higher-order bit planes instead? [4 M]
4. (a) Explain some important noise models and show their response curves. [8M]  
(b) What is inverse filtering and explain its concept clearly. [4M]
5. (a) With formulation explain color transformation techniques. [6M]  
(b) Provide details of color image compression concept. [6M]
6. (a) Obtain the Haar transformation matrix for  $N = 8$ . [6M]  
(b) Write the analysis of fast wavelet transform. [6M]
7. (a) Explain dilation and erosion operations in morphological image processing [6M]  
(b) Describe point, line and edge detection in image segmentation. [6M]

\*\*\*



Subject Code: R16EC3209

III B.Tech II Semester Supple Examinations, November-2019

DIGITAL IMAGE PROCESSING

(ECE)

Time: 3 hours

Max Marks: 60

Question Paper Consists of Part-A and Part-B.

Answering the question in Part-A is Compulsory & Four Questions should be answered from Part-B  
All questions carry equal marks of 12.

PART-A

1. a) Define the following terms: (i) Resolution (ii) Pixel
- b) Write any two properties of DCT.
- c) List out different noises in images.
- d) Write any two colour models.
- e) What is Compression Ratio?
- f) Define image segmentation.

[2+2+2+2+2+2]

PART-B

2. a) What is meant by a digital image? Explain how digital images can be represented [6M]
- b) Explain about components of an image processing system. [6M]
3. Briefly explain about image enhancement using point processing techniques. [12M]
4. Explain the following filters in detail  
a) Arithmetic mean filter  
b) Geometric mean filter  
c) Harmonic mean filter  
d) Contra harmonic mean filter [3M+3M+3M+3M]
5. a) Explain about RGB colour Model [6M]
- b) Discuss the concept of converting colours from RGB to HSI. [6M]
6. a) Explain about wavelet transform in two dimensions. [6M]
- b) What is meant by block transform coding? Explain. [6M]
7. a) Explain briefly the following morphological operations:  
(i) Erosion (ii) Dilation [6M]
- b) Discuss about region based segmentation [6M]

\*\*\*

Missing Topics(Course  
gaps) and Topics  
beyond Syllabus

### TOPICS BEYOND SYLLABUS/ADVANCED TOPICS

SNO	DESCRIPTION	Associated PO & PSO
1	Image Segmentation techniques	PO4 & PSO1
2	Principle Component analysis	PO1,PO3& PO4

# Remedial/corrective actions



1

# RESULTS

NARASARAOPETA ENGINEERING COLLEGE: NARASARAOPET (AUTONOMOUS)

(R16) 2018 BATCH III B.TECH II SEM I - ASSIGNMENT TEST MARKS AWARD LIST

- 2021

Branch : ECE - A

SUBJECT: DIP

DATE:

Sl.No.	H.T.NO	CO No.	1	Total (10M)
		Max. Marks		
		Sub Q.No.		
1	18471A0401	1		10
2	18471A0402	2		10
3	18471A0403	3		10
4	18471A0405	4		10
5	18471A0406	5		A
6	18471A0407	1		10
7	18471A0408	2		A
8	18471A0409	3		10
9	18471A0410	4		10
10	18471A0411	5		10
11	18471A0412	1		10
12	18471A0413	2		10
13	18471A0414	3		10
14	18471A0415	4		10
15	18471A0416	5		10
16	18471A0417	1		10
17	18471A0418	2		10
18	18471A0419	3		10
19	18471A0420	4		10
20	18471A0421	5		10
21	18471A0422	1		10
22	18471A0423	2		10
23	18471A0424	3		A
24	18471A0425	4		A
25	18471A0426	5		10
26	18471A0427	1		10
27	18471A0428	2		10
28	18471A0429	3		10
29	18471A0430	4		10
30	18471A0431	5		10

Sl.No.	H.T.NO	CO No.	Total (10M)
		Max. Marks	
		Sub Q.No.	
31	18471A0432	1	10
32	18471A0433	2	10
33	18471A0434	3	10
34	18471A0435	4	10
35	18471A0436	5	10
36	18471A0437	1	10
37	18471A0438	2	10
38	18471A0439	3	10
39	18471A0440	4	10
40	18471A0441	5	10
41	18471A0442	1	A
42	18471A0443	2	10
43	18471A0444	3	A
44	18471A0445	4	10
45	18471A0446	5	10
46	18471A0447	1	10
47	18471A0448	2	10
48	18471A0449	3	10
49	18471A0450	4	10
50	18471A0451	5	10
51	18471A0452	1	10
52	18471A0453	2	10
53	18471A0454	3	10
54	18471A0455	4	10
55	18471A0456	5	10
56	18471A0457	1	10
57	18471A0458	2	10
58	18471A0459	3	10
59	18471A0460	4	10
60			

NAME OF THE STAFF MEMBER J. Narasimha Rao

SIGNATURE OF THE STAFF MEMBER

SIGNATURE OF THE HOD

19/6/21

Branch : ECE - A

SUBJECT: DLP

DATE:

Sl.No.	H.T.NO	CO No.	2	Total (10M)
		Max. Marks		
		Sub Q.No.		
1	18471A0401	1		10
2	18471A0402	2		10
3	18471A0403	3		10
4	18471A0405	4		A
5	18471A0406	5		A
6	18471A0407	1		10
7	18471A0408	2		10
8	18471A0409	3		10
9	18471A0410	4		A
10	18471A0411	5		10
11	18471A0412	1		10
12	18471A0413	2		A
13	18471A0414	3		A
14	18471A0415	4		10
15	18471A0416	5		A
16	18471A0417	1		A
17	18471A0418	2		10
18	18471A0419	3		A
19	18471A0420	4		10
20	18471A0421	5		10
21	18471A0422	1		10
22	18471A0423	2		10
23	18471A0424	3		10
24	18471A0425	4		10
25	18471A0426	5		10
26	18471A0427	1		A
27	18471A0428	2		10
28	18471A0429	3		10
29	18471A0430	4		10
30	18471A0431	5		10

Sl.No.	H.T.NO	CO No.	Total (10M)
		Max. Marks	
		Sub Q.No.	
31	18471A0432	1	A
32	18471A0433	2	10
33	18471A0434	3	10
34	18471A0435	4	10
35	18471A0436	5	10
36	18471A0437	1	10
37	18471A0438	2	10
38	18471A0439	3	10
39	18471A0440	4	10
40	18471A0441	5	A
41	18471A0442	1	10
42	18471A0443	2	10
43	18471A0444	3	A
44	18471A0445	4	A
45	18471A0446	5	A
46	18471A0447	1	10
47	18471A0448	2	10
48	18471A0449	3	A
49	18471A0450	4	A
50	18471A0451	5	10
51	18471A0452	1	10
52	18471A0453	2	A
53	18471A0454	3	A
54	18471A0455	4	A
55	18471A0456	5	10
56	18471A0457	1	A
57	18471A0458	2	10
58	18471A0459	3	10
59	18471A0460	4	A
60			

NAME OF THE STAFF MEMBER J. Narasimha Rao

SIGNATURE OF THE STAFF MEMBER

19/6/21  
SIGNATURE OF THE HOD

Branch : ECE - A

SUBJECT: D&P

DATE:

Sl.No.	H.T.NO	CO No.	Total (10M)	
		4		
		Max. Marks		
		Sub Q.No.		
1	18471A0401	3	10	
2	18471A0402	4	10	
3	18471A0403	5	10	
4	18471A0405	1	10	
5	18471A0406	2	10	
6	18471A0407	3	10	
7	18471A0408	4	A	
8	18471A0409	5	10	
9	18471A0410	1	10	
10	18471A0411	2	10	
11	18471A0412	3	10	
12	18471A0413	4	10	
13	18471A0414	5	10	
14	18471A0415	1	A	
15	18471A0416	2	10	
16	18471A0417	3	A	
17	18471A0418	4	10	
18	18471A0419	5	A	
19	18471A0420	1	10	
20	18471A0421	2	10	
21	18471A0422	3	10	
22	18471A0423	4	10	
23	18471A0424	5	A	
24	18471A0425	1	A	
25	18471A0426	2	A	
26	18471A0427	3	10	
27	18471A0428	4	A	
28	18471A0429	5	10	
29	18471A0430	1	10	
30	18471A0431	2	10	

Sl.No.	H.T.NO	CO No.	Total (10M)	
		Max. Marks		
		Sub Q.No.		
31	18471A0432	3	A	
32	18471A0433	4	10	
33	18471A0434	5	10	
34	18471A0435	1	10	
35	18471A0436	2	10	
36	18471A0437	3	10	
37	18471A0438	4	10	
38	18471A0439	5	10	
39	18471A0440	1	A	
40	18471A0441	2	10	
41	18471A0442	3	10	
42	18471A0443	4	10	
43	18471A0444	5	10	
44	18471A0445	1	10	
45	18471A0446	2	10	
46	18471A0447	3	10	
47	18471A0448	4	10	
48	18471A0449	5	A	
49	18471A0450	1	10	
50	18471A0451	2	10	
51	18471A0452	3	10	
52	18471A0453	4	A	
53	18471A0454	5	10	
54	18471A0455	1	10	
55	18471A0456	2	10	
56	18471A0457	3	10	
57	18471A0458	4	10	
58	18471A0459	5	10	
59	18471A0460	1	A	
60				

NAME OF THE STAFF MEMBER J. Narasimha Rao

SIGNATURE OF THE STAFF MEMBER

SIGNATURE OF THE HOD

19/6/21

NARASARAOPETA ENGINEERING COLLEGE: NARASARAOPET (AUTONOMOUS)

(R16) 2018 BATCH III B.TECH II SEM IV ASSIGNMENT TEST MARKS AWARD LIST JUNE - 2021

Branch : ECE - A

SUBJECT: DCA

DATE: 25/6/21 <sup>JNR</sup>

Sl.No.	H.T.NO	CO No.		Total (10M)	Sl.No.	H.T.NO	CO No.		Total (10M)
		Max. Marks					Max. Marks		
		Sub Q.No.					Sub Q.No.		
1	18471A0401			A	31	18471A0432	3		10
2	18471A0402			A	32	18471A0433			A
3	18471A0403	5		8	33	18471A0434	5		10
4	18471A0405	1		10	34	18471A0435			A
5	18471A0406			A	35	18471A0436			A
6	18471A0407	3		10	36	18471A0437			A
7	18471A0408	4		10	37	18471A0438			A
8	18471A0409	5		10	38	18471A0439			A
9	18471A0410			A	39	18471A0440	1		10
10	18471A0411			A	40	18471A0441			A
11	18471A0412			A	41	18471A0442			A
12	18471A0413			A	42	18471A0443			A
13	18471A0414			A	43	18471A0444			A
14	18471A0415			A	44	18471A0445			A
15	18471A0416			A	45	18471A0446			A
16	18471A0417	3		10	46	18471A0447			A
17	18471A0418			A	47	18471A0448			A
18	18471A0419	5		10	48	18471A0449	5		10
19	18471A0420			A	49	18471A0450			A
20	18471A0421	2		10	50	18471A0451			A
21	18471A0422			A	51	18471A0452			A
22	18471A0423	4		10	52	18471A0453	4		5
23	18471A0424	5		9	53	18471A0454			A
24	18471A0425	3		6	54	18471A0455			A
25	18471A0426	4		5	55	18471A0456			A
26	18471A0427			A	56	18471A0457			A
27	18471A0428	4		10	57	18471A0458			A
28	18471A0429			A	58	18471A0459			A
29	18471A0430	1		10	59	18471A0460			A
30	18471A0431	2		10					

NAME OF THE STAFF MEMBER

J. Narasimha Rao

SIGNATURE OF THE STAFF MEMBER

SIGNATURE OF THE HOD

26/6/21

NARASARAOPETA ENGINEERING COLLEGE: NARASARAOPET (AUTONOMOUS)

(R16) 2018 BATCH III B.TECH II SEM

ASSIGNMENT TEST MARKS AWARD LIST

- 2021

Branch : ECE - B

SUBJECT: D&P

DATE:

Sl.No.	H.T.NO	CO No.	1	Total (10M)
		Max. Marks		
		Sub Q.No.		
1	18471A0461	5		10
2	18471A0463	1		10
3	18471A0464	2		10
4	18471A0465	3		A
5	18471A0466	4		10
6	18471A0467	5		A
7	18471A0468	1		10
8	18471A0470	2		10
9	18471A0471	3		10
10	18471A0472	4		10
11	18471A0473	5		10
12	18471A0474	1		10
13	18471A0475	2		10
14	18471A0476	3		10
15	18471A0477	4		10
16	18471A0478	5		10
17	18471A0479	1		10
18	18471A0480	2		10
19	18471A0481	3		10
20	18471A0482	4		10
21	18471A0483	5		10
22	18471A0484	1		10
23	18471A0485	2		10
24	18471A0486	3		10
25	18471A0487	4		10
26	18471A0488	5		10
27	18471A0489	1		10
28	18471A0490	2		10
29	18471A0491	3		10
30	18471A0492	4		10

Sl.No.	H.T.NO	CO No.	Total (10M)
		Max. Marks	
		Sub Q.No.	
31	18471A0493	5	10
32	18471A0494	1	10
33	18471A0495	2	10
34	18471A0496	3	10
35	18471A0497	4	A
36	18471A0498	5	10
37	18471A0499	1	10
38	18471A04A1	2	10
39	18471A04A2	3	10
40	18471A04A3	4	10
41	18471A04A4	5	10
42	18471A04A5	1	A
43	18471A04A6	2	10
44	18471A04A7	3	A
45	18471A04A8	4	10
46	18471A04A9	5	A
47	18471A04B0	1	10
48	18471A04B1	2	10
49	18471A04B2	3	A
50	18471A04B3	4	10
51	18471A04B4	5	10
52	18471A04B5	1	10
53	18471A04B6	2	10
54	18471A04B7	3	A
55	18471A04B8	4	10
56	18471A04B9	5	10
57	18471A04C0	1	A
58			
59			
60			

NAME OF THE STAFF MEMBER J. Narasimha Rao

SIGNATURE OF THE STAFF MEMBER

19/6/21

SIGNATURE OF THE HOD

NARASARAOPETA ENGINEERING COLLEGE: NARASARAOPET (AUTONOMOUS)

(R16) 2018 BATCH III B.TECH II SEM

II ASSIGNMENT TEST MARKS AWARD LIST

- 2021 ✓

Branch : ECE - B

SUBJECT: D&P

DATE:

Sl.No.	H.T.NO	CO No.	2	Total (10M)
		Max. Marks		
		Sub Q.No.		
1	18471A0461	5		10
2	18471A0463	1		10
3	18471A0464	2		A
4	18471A0465	3		A
5	18471A0466	4		10
6	18471A0467	5		10
7	18471A0468	1		A
8	18471A0470	2		10
9	18471A0471	3		10
10	18471A0472	4		10
11	18471A0473	5		10
12	18471A0474	1		A
13	18471A0475	2		10
14	18471A0476	3		A
15	18471A0477	4		10
16	18471A0478	5		10
17	18471A0479	1		A
18	18471A0480	2		10
19	18471A0481	3		10
20	18471A0482	4		A
21	18471A0483	5		10
22	18471A0484	1		10
23	18471A0485	2		10
24	18471A0486	3		10
25	18471A0487	4		10
26	18471A0488	5		10
27	18471A0489	1		A
28	18471A0490	2		10
29	18471A0491	3		A
30	18471A0492	4		10

Sl.No.	H.T.NO	CO No.		Total (10M)
		Max. Marks		
		Sub Q.No.		
31	18471A0493	5		A
32	18471A0494	1		A
33	18471A0495	2		10
34	18471A0496	3		10
35	18471A0497	4		A
36	18471A0498	5		10
37	18471A0499	1		10
38	18471A04A1	2		10
39	18471A04A2	3		10
40	18471A04A3	4		A
41	18471A04A4	5		10
42	18471A04A5	1		A
43	18471A04A6	2		A
44	18471A04A7	3		A
45	18471A04A8	4		10
46	18471A04A9	5		A
47	18471A04B0	1		10
48	18471A04B1	2		10
49	18471A04B2	3		10
50	18471A04B3	4		10
51	18471A04B4	5		10
52	18471A04B5	1		10
53	18471A04B6	2		10
54	18471A04B7	3		A
55	18471A04B8	4		A
56	18471A04B9	5		A
57	18471A04C0	1		10
58				
59				
60				

NAME OF THE STAFF MEMBER J. Narasimha Rao

SIGNATURE OF THE STAFF MEMBER

19/6/21  
SIGNATURE OF THE HOD

NARASARAOPETA ENGINEERING COLLEGE: NARASARAOPET (AUTONOMOUS)

(R16) 2018 BATCH III B.TECH II SEM

III ASSIGNMENT TEST MARKS AWARD LIST

- 2021

Branch : ECE - B

SUBJECT: DSP

DATE: .

Sl.No.	H.T.NO	CO No.	4	Total (10M)
		Max. Marks		
		Sub Q.No.		
1	18471A0461	2		10
2	18471A0463	3		10
3	18471A0464	4		10
4	18471A0465	5		A
5	18471A0466	1		10
6	18471A0467	2		10
7	18471A0468	3		10
8	18471A0470	4		10
9	18471A0471	5		10
10	18471A0472	1		10
11	18471A0473	2		10
12	18471A0474	3		A
13	18471A0475	4		10
14	18471A0476	5		A
15	18471A0477	1		10
16	18471A0478	2		10
17	18471A0479	3		10
18	18471A0480	4		10
19	18471A0481	5		10
20	18471A0482	1		10
21	18471A0483	2		10
22	18471A0484	3		10
23	18471A0485	4		A
24	18471A0486	5		10
25	18471A0487	1		10
26	18471A0488	2		10
27	18471A0489	3		10
28	18471A0490	4		10
29	18471A0491	5		A
30	18471A0492	1		A

Sl.No.	H.T.NO	CO No.	Total (10M)
		Max. Marks	
		Sub Q.No.	
31	18471A0493	2	10
32	18471A0494	3	10
33	18471A0495	4	10
34	18471A0496	5	10
35	18471A0497	1	A
36	18471A0498	2	10
37	18471A0499	3	10
38	18471A04A1	4	10
39	18471A04A2	5	10
40	18471A04A3	1	10
41	18471A04A4	2	10
42	18471A04A5	3	A
43	18471A04A6	4	10
44	18471A04A7	5	A
45	18471A04A8	1	10
46	18471A04A9	2	A
47	18471A04B0	3	10
48	18471A04B1	4	10
49	18471A04B2	5	10
50	18471A04B3	1	10
51	18471A04B4	2	10
52	18471A04B5	3	10
53	18471A04B6	4	10
54	18471A04B7	5	10
55	18471A04B8	1	10
56	18471A04B9	2	10
57	18471A04C0	3	A
58			
59			
60			

NAME OF THE STAFF MEMBER J. Narasimha Rao

SIGNATURE OF THE STAFF MEMBER

19/6/21  
SIGNATURE OF THE HOD



NARASARAOPETA ENGINEERING COLLEGE: NARASARAOPET (AUTONOMOUS)

(R16) 2018 BATCH III B.TECH II SEM IV ASSIGNMENT TEST MARKS AWARD LIST JUNE - 2021

Branch : ECE - B

SUBJECT: D&P

DATE: 25/6/21 JNR

Sl.No.	H.T.NO	CO No.		Total (10M)
		Max. Marks		
		Sub Q.No.		
1	18471A0461	2		10
2	18471A0463			A
3	18471A0464			A
4	18471A0465			A
5	18471A0466			A
6	18471A0467			A
7	18471A0468			A
8	18471A0470	5		10
9	18471A0471			A
10	18471A0472			A
11	18471A0473			A
12	18471A0474			A
13	18471A0475	4		10
14	18471A0476	5		10
15	18471A0477	1		10
16	18471A0478	2		10
17	18471A0479			A
18	18471A0480			A
19	18471A0481	5		10
20	18471A0482			A
21	18471A0483			A
22	18471A0484			A
23	18471A0485	4		10
24	18471A0486			A
25	18471A0487			A
26	18471A0488	2		10
27	18471A0489			A
28	18471A0490			A
29	18471A0491	5		10
30	18471A0492			A

Sl.No.	H.T.NO	CO No.		Total (10M)
		Max. Marks		
		Sub Q.No.		
31	18471A0493			A
32	18471A0494			A
33	18471A0495			A
34	18471A0496	5		10
35	18471A0497			A
36	18471A0498			A
37	18471A0499	3		10
38	18471A04A1			A
39	18471A04A2	5		9
40	18471A04A3			A
41	18471A04A4	2		10
42	18471A04A5			A
43	18471A04A6			A
44	18471A04A7			A
45	18471A04A8			A
46	18471A04A9			A
47	18471A04B0			A
48	18471A04B1	4		10
49	18471A04B2	5		10
50	18471A04B3	1		10
51	18471A04B4	2		10
52	18471A04B5			A
53	18471A04B6			A
54	18471A04B7			A
55	18471A04B8			A
56	18471A04B9			A
57	18471A04C0			A

NAME OF THE STAFF MEMBER: J. abhisimha Reddy

SIGNATURE OF THE STAFF MEMBER

26/6/21

SIGNATURE OF THE HOD

NARASARAOPETA ENGINEERING COLLEGE : NARASARAOPET  
(AUTONOMOUS).

(R16) 17 Batch III B.Tech II Sem I Assignment Test Marks - Award List (DECEMBER-2019)

Branch :ECE-C

Subject: D&P

Date: 20/12/19

Sl. No.	H.T.NO	CO No.	Total (10M)
		Max. Marks Sub Q.No.	
1	17471A04C1	3	9
2	17471A04C2	1	9
3	17471A04C3	3	9
4	17471A04C4	2	6
5	17471A04C5	5	0
6	17471A04C6	4	09
7	17471A04C7	5	10
8	17471A04C8	3	10
9	17471A04C9	4	10
10	17471A04D0	2	00
11	17471A04D1	3	09
12	17471A04D2	3	9
13	17471A04D3	2	8
14	17471A04D4	3	08
15	17471A04D5	3	10
16	17471A04D6	1	5
17	17471A04D7	—	A
18	17471A04D8	4	10
19	17471A04D9	3	09
20	17471A04E0	4	10
21	17471A04E1	2	0
22	17471A04E2	2	8
23	17471A04E3	5	10
24	17471A04E4	1	9
25	17471A04E5	1	10
26	17471A04E6	4	01
27	17471A04E7	2	09
28	17471A04E8	4	10
29	17471A04E9	5	00
30	17471A04F0	2	10
31	17471A04F1	4	10
32	17471A04F2	2	10
33	17471A04F3	3	10
34	17471A04F4	—	A

Sl. No.	H.T.NO	CO No.	Total (10M)
		Max. Marks Sub Q.No.	
35	17471A04F5	3	10
36	17471A04F6	5	10
37	17471A04F7	4	10
38	17471A04F8	3	10
39	17471A04F9	5	9
40	17471A04G0	1	9
41	17471A04G1	5	10
42	17471A04G2	4	9
43	17471A04G3	2	10
44	17471A04G4	2	00
45	17471A04G5	5	09
46	17471A04G6	—	A
47	17471A04G8	2	06
48	17471A04G9	4	10
49	17471A04H0	2	00
50	17471A04H1	—	A
51	17471A04H2	1	06
52	17471A04H3	5	00
53	17471A04H4	1	06
54	17471A04H5	4	01
55	17471A04H6	1	05
56	17471A04H7	—	A
57	17471A04H8	—	A
58	17471A04H9	—	A
59	17471A04I0	5	10
60	18475A0401	1	09
61	18475A0402	1	09
62	18475A0403	1	10
63	18475A0404	1	09
64	18475A0405	3	09
65	18475A0406	2	10
66	18475A0407	5	10
67	18475A0408	4	03
68	18475A0409	—	A

Name of the Staff Member Narasimha Rao

Signature of the Staff Member [Signature]

Signature of the HOD [Signature]  
21/1/2020

NARASARAOPETA ENGINEERING COLLEGE : NARASARAOPET  
(AUTONOMOUS)

(R16) 17.Batch III B.Tech II Sem II Assignment Test Marks - Award List (JAN-2020)

Branch :ECE-C

Subject: DLP

Date: 10/1/2020

Sl. No.	H.T.NO	CO No.	Total (10M)
		Max. Marks Sub Q.No.	
1	17471A04C1	1	2
2	17471A04C2	15	00
3	17471A04C3	3	10
4	17471A04C4	4	10
5	17471A04C5	3	10
6	17471A04C6	3	06
7	17471A04C7	15	5
8	17471A04C8	1	8
9	17471A04C9	5	10
10	17471A04D0	15	8
11	17471A04D1		A
12	17471A04D2	2	2
13	17471A04D3	4	10
14	17471A04D4	15	09
15	17471A04D5	3	5
16	17471A04D6	2	10
17	17471A04D7	1	10
18	17471A04D8		A
19	17471A04D9	15	3
20	17471A04E0	3	2
21	17471A04E1	3	10
22	17471A04E2	2	8
23	17471A04E3	15	00
24	17471A04E4	1	10
25	17471A04E5		A
26	17471A04E6	2	10
27	17471A04E7	2	10
28	17471A04E8	3	9
29	17471A04E9	2	10
30	17471A04F0	4	00
31	17471A04F1	15	3
32	17471A04F2		A
33	17471A04F3	4	10
34	17471A04F4	1	10

Sl. No.	H.T.NO	CO No.	Total (10M)
		Max. Marks Sub Q.No.	
35	17471A04F5	3	00
36	17471A04F6	4	8
37	17471A04F7	3	00
38	17471A04F8	2	00
39	17471A04F9	4	00
40	17471A04G0	1	10
41	17471A04G1	15	3
42	17471A04G2	4	10
43	17471A04G3	2	00
44	17471A04G4	1	9
45	17471A04G5	4	09
46	17471A04G6	1	15
47	17471A04G8	2	9
48	17471A04G9	15	00
49	17471A04H0	4	10
50	17471A04H1	4	9
51	17471A04H2	15	10
52	17471A04H3	3	10
53	17471A04H4	3	10
54	17471A04H5	1	10
55	17471A04H6	2	10
56	17471A04H7	1	10
57	17471A04H8	3	10
58	17471A04H9	4	10
59	17471A04I0	3	10
60	18475A0401	2	00
61	18475A0402	2	8
62	18475A0403	4	10
63	18475A0404	15	00
64	18475A0405	1	00
65	18475A0406		A
66	18475A0407	4	06
67	18475A0408	4	9
68	18475A0409	1	10

Name of the Staff Member J. Narasimha Rao Signature of the Staff Member [Signature]

[Signature] 21/1/2020  
Signature of the HOD

NARASARAOPETA ENGINEERING COLLEGE : NARASARAOPET  
(AUTONOMOUS)

(R16) 17 Batch III B.Tech II Sem III Assignment Test Marks - Award List (FEB-2020)

Branch :ECE-C

Subject: DEP

Date: 26/2/2020

Sl.No	H.T.NO	CO No.	4	Total (10M)	
		Max. Marks	10		
		Sub Q.No.			
1	17471A04C1	← Absent →			
2	17471A04C2	5		10	
3	17471A04C3	2		9	
4	17471A04C4	1		4	
5	17471A04C5	3		9	
6	17471A04C6	1		6	
7	17471A04C7	1		10	
8	17471A04C8	3		10	
9	17471A04C9	2		10	
10	17471A04D0	1		10	
11	17471A04D1	2		10	
12	17471A04D2	1		10	
13	17471A04D3	3		10	
14	17471A04D4	2		10	
15	17471A04D5	1		10	
16	17471A04D6	← Absent →			
17	17471A04D7	5		10	
18	17471A04D8	← Absent →			
19	17471A04D9	2		10	
20	17471A04E0	5		10	
21	17471A04E1	2		10	
22	17471A04E2	1		10	
23	17471A04E3	5		10	
24	17471A04E4	3		10	
25	17471A04E5	← Absent →			
26	17471A04E6	← Absent →			
27	17471A04E7	2		10	
28	17471A04E8	2		10	
29	17471A04E9	1		10	
30	17471A04F0	4		10	
31	17471A04F1	5		10	
32	17471A04F2	2		10	
33	17471A04F3	4		10	
34	17471A04F4	← Absent →			

Sl. No.	H.T.NO	CO No.	4	Total (10M)	
		Max. Marks	10		
		Sub Q.No.			
35	17471A04F5	4		10	
36	17471A04F6	1		10	
37	17471A04F7	2		10	
38	17471A04F8	3		9	
39	17471A04F9	2		10	
40	17471A04G0	2		9	
41	17471A04G1	3		10	
42	17471A04G2	3		10	
43	17471A04G3	2		9	
44	17471A04G4	4		10	
45	17471A04G5	3		10	
46	17471A04G6	2		10	
47	17471A04G8	1		10	
48	17471A04G9	5		10	
49	17471A04H0	3		10	
50	17471A04H1	4		9	
51	17471A04H2	3		9	
52	17471A04H3	3		9	
53	17471A04H4	1		10	
54	17471A04H5	2		10	
55	17471A04H6	2		10	
56	17471A04H7	3		10	
57	17471A04H8	← Absent →			
58	17471A04H9	4		10	
59	17471A04I0	2		10	
60	18475A0401	2		10	
61	18475A0402	← Absent →			
62	18475A0403	1		10	
63	18475A0404	1		10	
64	18475A0405	← Absent →			
65	18475A0406	1		10	
66	18475A0407	1		10	
67	18475A0408	3		10	
68	18475A0409	← Absent →			

Name of the Staff Member J. Narasimharao

Signature of the Staff Member 

07/3/2020  
Signature of the HOD

NARASARAOPETA ENGINEERING COLLEGE : NARASARAOPET  
(AUTONOMOUS)

(R16) 17 Batch III B.Tech II Sem IV Assignment Test Marks - Award List (MARCH-2020)

Branch : ECE-C

Subject: DEF

Date: 13/3/20

Sl.No	H.T.NO	CO No. 6		Total (10M)
		Max. Marks	Sub Q.No.	
1	17471A04C1	10		09
2	17471A04C2			A
3	17471A04C3	2		07
4	17471A04C4	1		10
5	17471A04C5	4		00
6	17471A04C6	2		08
7	17471A04C7	1		02
8	17471A04C8	2		01
9	17471A04C9	3		05
10	17471A04D0	4		01
11	17471A04D1	1		00
12	17471A04D2	2		09
13	17471A04D3	3		10
14	17471A04D4	3		07
15	17471A04D5	1		08
16	17471A04D6	2		10
17	17471A04D7			A
18	17471A04D8	4		08
19	17471A04D9	1		00
20	17471A04E0	2		00
21	17471A04E1	3		02
22	17471A04E2	4		03
23	17471A04E3	1		02
24	17471A04E4	2		00
25	17471A04E5	3		03
26	17471A04E6	4		10
27	17471A04E7	1		10
28	17471A04E8	2		09
29	17471A04E9	3		09
30	17471A04F0			A
31	17471A04F1	1		10
32	17471A04F2	2		06
33	17471A04F3	3		05
34	17471A04F4	4		10

Sl.No	H.T.NO	CO No. 8		Total (10M)
		Max. Marks	Sub Q.No.	
35	17471A04F5	1		01
36	17471A04F6	2		08
37	17471A04F7	3		00
38	17471A04F8	4		00
39	17471A04F9	1		03
40	17471A04G0	2		00
41	17471A04G1	3		02
42	17471A04G2	4		06
43	17471A04G3			A
44	17471A04G4			A
45	17471A04G5	4		2
46	17471A04G6	10		00
47	17471A04G8	4		00
48	17471A04G9	3		00
49	17471A04H0	2		00
50	17471A04H1	1		00
51	17471A04H2	10		00
52	17471A04H3	4		00
53	17471A04H4	3		00
54	17471A04H5	2		00
55	17471A04H6	1		10
56	17471A04H7	10		01
57	17471A04H8	4		10
58	17471A04H9	3		00
59	17471A04I0	2		00
60	18475A0401	1		10
61	18475A0402			A
62	18475A0403	4		05
63	18475A0404	3		00
64	18475A0405	10		10
65	18475A0406	3		2
66	18475A0407	10		8
67	18475A0408	10		00
68	18475A0409	4		07

Name of the Staff Member J. Narasimha Rao

Signature of the Staff Member [Signature]

16/3/2020  
Signature of the HOD

NARASARAOPETA ENGINEERING COLLEGE : NARASARAOPET  
(AUTONOMOUS).

(R16) 17 Batch III B.Tech II Sem I Assignment Test Marks - Award List (DECEMBER-2019)

Branch :ECE-D

Subject: DGP

Date: 20/12/19

Sl. No.	H.T.NO	CO No. Max. Marks Sub Q.No.	Total (10M)
1	16475A0415	5	09
2	16471A04D2	2	02
3	16471A04G1	3	8
4	17471A04I1	4	9
5	17471A04I2	4	8
6	17471A04I3	3	05
7	17471A04I4	4	10
8	17471A04I5	4	09
9	17471A04I6	2	10
10	17471A04I7	3	10
11	17471A04I8	4	9
12	17471A04I9	4	10
13	17471A04J0	5	10
14	17471A04J1	2	05
15	17471A04J2	2	10
16	17471A04J3	5	10
17	17471A04J4	1	10
18	17471A04J5	2	9
19	17471A04J6	3	10
20	17471A04J7	4	10
21	17471A04J8	3	10
22	17471A04J9	3	10
23	17471A04K0	1	9
24	17471A04K1	4	10
25	17471A04K2	5	8
26	17471A04K3	1	9
27	17471A04K4	5	5
28	17471A04K5	4	9
29	17471A04K6	2	8
30	17471A04K7	1	07
31	17471A04K8	—	A
32	17471A04K9	2	10
33	17471A04L0	5	08
34	17471A04L1	4	10

Sl. No.	H.T.NO	CO No. Max. Marks Sub Q.No.	Total (10M)
35	17471A04L2	—	A
36	17471A04L4	1	10
37	17471A04L5	5	9
38	17471A04L6	3	10
39	17471A04L8	4	00
40	17471A04M0	2	09
41	17471A04M1	2	10
42	17471A04M2	1	05
43	17471A04M3	—	A
44	17471A04M4	—	A
45	17471A04M5	3	09
46	17471A04M6	2	10
47	17471A04M7	5	05
48	17471A04M8	3	10
49	17471A04N0	5	9
50	17471A04N1	1	09
51	17471A04N2	2	10
52	17471A04N3	3	09
53	18475A0410	2	02
54	18475A0411	5	08
55	18475A0412	5	09
56	18475A0413	3	9
57	18475A0414	3	10
58	18475A0415	1	8
59	18475A0416	—	A
60	18475A0417	2	5
61	18475A0418	4	02
62	18475A0419	1	09
63	18475A0420	3	09
64	18475A0421	1	02
65	18475A0422	1	05
66	18475A0423	5	10
	18475A0424	3	10

Name of the Staff Member J. Narasimhan Rao

Signature of the Staff Member [Signature]

[Signature] 21/11/2020  
Signature of the HOD

NARASARAOPETA ENGINEERING COLLEGE : NARASARAOPET  
(AUTONOMOUS).

(R16) 17 Batch III B.Tech II Sem II Assignment Test Marks - Award List (JAN-2020)

Branch :ECE-D

Subject: DLP

Date: 10/1/20

Sl. No.	H.T.NO	CO No.		Total (10M)
		Max. Marks	Sub Q.No.	
1	16475A0415	3		2
2	16471A0424			A
3	16471A04D2	1		9
4	16471A04G1			A
5	17471A04I1	3		5
6	17471A04I2	5		10
7	17471A04I3	2		08
8	17471A04I4	5		9
9	17471A04I5	2		05
10	17471A04I6	3		10
11	17471A04I7	1		5
12	17471A04I8	1		10
13	17471A04I9	1		08
14	17471A04J0			A
15	17471A04J1	2		10
16	17471A04J2	4		10
17	17471A04J3	1		09
18	17471A04J4	3		10
19	17471A04J5			A
20	17471A04J6	2		08
21	17471A04J7	4		8
22	17471A04J8	5		05
23	17471A04J9			A
24	17471A04K0	5		10
25	17471A04K1			A
26	17471A04K2	2		10
27	17471A04K3			A
28	17471A04K4	2		9
29	17471A04K5	4		9
30	17471A04K6	5		9
31	17471A04K7	5		00
32	17471A04K8	1		10
33	17471A04K9	4		9
34	17471A04L0	1		10

Sl. No.	H.T.NO	CO No.		Total (10M)
		Max. Marks	Sub Q.No.	
35	17471A04L1	3		5
36	17471A04L2	1		10
37	17471A04L4	4		04
38	17471A04L5	5		10
39	17471A04L6	5		03
40	17471A04L8	1		9
41	17471A04M0	1		07
42	17471A04M1	2		3
43	17471A04M2	1		10
44	17471A04M3	3		10
45	17471A04M4	1		9
46	17471A04M5	3		03
47	17471A04M6	2		03
48	17471A04M7	5		10
49	17471A04M8	4		03
50	17471A04N0	3		10
51	17471A04N1			A
52	17471A04N2			A
53	17471A04N3	3		10
54	18475A0410	4		10
55	18475A0411	1		10
56	18475A0412	2		9
57	18475A0413			A
58	18475A0414	3		02
59	18475A0415			A
60	18475A0416	5		9
61	18475A0417	1		8
62	18475A0418	3		9
63	18475A0419	1		10
64	18475A0420	3		10
65	18475A0421	2		9
66	18475A0422	2		9
67	18475A0423	4		9

Name of the Staff Member J. Narasimha Rao

Signature of the Staff Member 

10/1/2020  
Signature of the HOD

NARASARAOPETA ENGINEERING COLLEGE : NARASARAOPET  
(AUTONOMOUS)

(R16) 17 Batch III B.Tech II Sem III Assignment Test Marks - Award List (FEB-2020)

Branch :ECE-D

Subject: D&P

Date: 26/2/2020

Sl.No	H.T.NO	CO No.	4	Total (10M)
		Max. Marks	10	
		Sub Q.No.		
1	16475A0415			A
2	16471A0424	3		05
3	16471A04D2			A
4	16471A04G1			A
5	17471A04I1	1		02
6	17471A04I2	3		05
7	17471A04I3			A
8	17471A04I4	5		9
9	17471A04I5			A
10	17471A04I6	2		10
11	17471A04I7			A
12	17471A04I8			A
13	17471A04I9	3		7
14	17471A04J0	4		04
15	17471A04J1	4		00
16	17471A04J2	4		3
17	17471A04J3	5		9
18	17471A04J4	3		05
19	17471A04J5			A
20	17471A04J6	2		2
21	17471A04J7	5		2
22	17471A04J8	1		2
23	17471A04J9			A
24	17471A04K0			A
25	17471A04K1	4		04
26	17471A04K2			A
27	17471A04K3	4		05
28	17471A04K4	1		06
29	17471A04K5			A
30	17471A04K6			A
31	17471A04K7	2		00
32	17471A04K8	3		6
33	17471A04K9	2		9
34	17471A04L0			A

Sl. No.	H.T.NO	CO No.	4	Total (10M)
		Max. Marks	10	
		Sub Q.No.		
35	17471A04L1	3		02
36	17471A04L2	2		08
37	17471A04L4	2		06
38	17471A04L5			A
39	17471A04L6	5		9
40	17471A04L8	3		3
41	17471A04M0			A
42	17471A04M1	1		00
43	17471A04M2	1		05
44	17471A04M3			A
45	17471A04M4	3		2
46	17471A04M5			A
47	17471A04M6	1		05
48	17471A04M7	2		2
49	17471A04M8	2		00
50	17471A04N0			A
51	17471A04N1	3		6
52	17471A04N2			A
53	17471A04N3	3		7
54	18475A0410			A
55	18475A0411	1		02
56	18475A0412			A
57	18475A0413			A
58	18475A0414			A
59	18475A0415			A
60	18475A0416			A
61	18475A0417	5		00
62	18475A0418	4		05
63	18475A0419	1		05
64	18475A0420	4		05
65	18475A0421			A
66	18475A0422			A
67	18475A0423	4		5

Name of the Staff Member J Nageswara Rao

Signature of the Staff Member [Signature]

3/3/2020

Signature of the HOD



NARASARAOPETA ENGINEERING COLLEGE : NARASARAOPET  
(AUTONOMOUS)

(R16) 17 Batch III B.Tech II Sem IV Assignment Test Marks - Award List (MARCH-2020)

Branch : ECE-D

Subject: D&P

Date: 13/3/20

Sl.No	H.T.NO	CO No.6		Total (10M)
		Max. Marks 10	Sub Q.No.	
1	16475A0415	3		08
2	16471A0424	2		08
3	16471A04D2			A
4	16471A04G1			A
5	17471A04I1	2		08
6	17471A04I2	4		07
7	17471A04I3	2		07
8	17471A04I4	1		09
9	17471A04I5	1		02
10	17471A04I6	5		03
11	17471A04I7	4		10
12	17471A04I8	3		09
13	17471A04I9	2		07
14	17471A04J0	5		09
15	17471A04J1	3		08
16	17471A04J2	5		09
17	17471A04J3	5		10
18	17471A04J4	4		10
19	17471A04J5	1		03
20	17471A04J6	1		10
21	17471A04J7	2		09
22	17471A04J8	3		10
23	17471A04J9	1		07
24	17471A04K0	4		10
25	17471A04K1	5		09
26	17471A04K2	3		08
27	17471A04K3	3		10
28	17471A04K4	1		04
29	17471A04K5	4		09
30	17471A04K6	2		08
31	17471A04K7	5		08
32	17471A04K8	4		04
33	17471A04K9	1		10
34	17471A04L0	1		10

Sl. No.	H.T.NO	CO No.6		Total (10M)
		Max. Marks 10	Sub Q.No.	
35	17471A04L1	2		09
36	17471A04L2	1		09
37	17471A04L4	1		02
38	17471A04L5			A
39	17471A04L6	4		3
40	17471A04L8	2		10
41	17471A04M0	5		10
42	17471A04M1	1		07
43	17471A04M2	1		08
44	17471A04M3	2		00
45	17471A04M4	5		08
46	17471A04M5	2		00
47	17471A04M6	2		10
48	17471A04M7	4		10
49	17471A04M8	3		08
50	17471A04N0	2		09
51	17471A04N1	4		01
52	17471A04N2	1		02
53	17471A04N3	2		06
54	18475A0410	2		06
55	18475A0411	2		10
56	18475A0412	4		10
57	18475A0413			A
58	18475A0414	1		10
59	18475A0415	4		09
60	18475A0416	1		09
61	18475A0417	3		10
62	18475A0418			A
63	18475A0419	3		09
64	18475A0420	5		09
65	18475A0421	1		09
66	18475A0422	4		07
67	18475A0423	3		10

Name of the Staff Member J. Narasimha Rao

Signature of the Staff Member [Signature]

Signature of the HOD [Signature]  
16/3/2020

NARASARAOPETA ENGINEERING COLLEGE (AUTONOMOUS) : : NARASARAOPET  
(R16) 2018 BATCH III B.TECH II SEM I MID & I QUIZ AWARD LIST, AUG - 2021

Branch : ECE - A      Subject CODE & NAME: DEP      Date: 19/8/21

Sl.No.	H.T.NO.	CO No.						MID - I	MID- I	QUIZ - I MARKS (10)	
		Max.Marks						Total	REDUCED		
		Q.No.	1(a)	1(b)	2(a)	2(b)	3(a)	3(b)	Marks (30M)		MARKS (20M)
1	18471A0401		10		10		9		29	20	5
2	18471A0402		9		8		7		21	14	1
3	18471A0403		10		10		9		29	20	5
4	18471A0405		10		10		8		28	19	6
5 ✓	18471A0406		8		8		4		20	14	2
6	18471A0407		10		10		9		29	20	4
7	18471A0408		7		6		3		16	11	2
8	18471A0409		7		8		7		22	15	3
9	18471A0410		10		10		8		28	19	5
10	18471A0411		10		10		5		25	17	6
11	18471A0412		10		10		9		29	20	7
12	18471A0413		10		10		8		28	19	5
13	18471A0414		10		10		8		28	19	4
* 14	18471A0415		← AB B B N C →					AB	AB	A	
15	18471A0416		10		10		9		29	20	5
16	18471A0417		9		8		6		23	16	2
17	18471A0418		10		9		7		26	18	3
18	18471A0419		10		10		8		28	19	4
19	18471A0420		10		10		8		28	19	4
20	18471A0421		10		10		9		29	20	5
21	18471A0422		10		10		9		29	20	5
22	18471A0423		10		10		9		29	20	4
23	18471A0424		10		10		9		29	20	5
24	18471A0425		6		6		6		18	12	5
25	18471A0426		7		7		7		21	14	1
26	18471A0427		9.5		9.5		9		28	19	4
27	18471A0428		10		10		8		28	19	5
28	18471A0429		10		10		8		28	19	5
29	18471A0430		10		10		10		30	20	6
30	18471A0431		10		10		10		30	20	6
31	18471A0432		9		8		7		24	16	4
32	18471A0433		10		9		8		27	18	6

Branch : ECE - B

Subject CODE & NAME: D&P

Date: 19/8/21

Sl.No.	H.T.NO.	CO No.							MID - I Total Marks (30M)	MID- I REDUCED MARKS (20M)	QUIZ - I MARKS (10)
		Max.Marks	10		10		10				
		Q.No.	1(a)	1(b)	2(a)	2(b)	3(a)	3(b)			
1	18471A0461		9		9		6		24	16	3
2	18471A0463		10		10		10		30	20	6
3	18471A0464		10		10		8		28	19	4
4+	18471A0465		0		0		2		02	02	3
5	18471A0466		10		10		7		27	18	5
6	18471A0467		10		5		8		23	16	2
7	18471A0468		10		6		6		22	15	3
8	18471A0470		10		10		9		29	20	6
9	18471A0471		10		7		7		24	16	6
10	18471A0472		10		9		9		28	19	5
11	18471A0473		10		10		10		30	20	4
12	18471A0474		9		9		5		23	16	6
13	18471A0475		10		10		9		29	20	7
14	18471A0476		9		6		6		21	14	6
15	18471A0477		9		8		8		25	17	6
16	18471A0478		8		6		6		20	14	4
17	18471A0479		10		10		8		28	19	6
18	18471A0480		8		8		6		22	15	6
19	18471A0481		10		10		9		29	20	4
20	18471A0482		9		8		6		23	16	6
21	18471A0483		10		8		8		26	18	6
22	18471A0484		10		10		8		28	19	6
23	18471A0485		9		10		9		28	19	6
24	18471A0486		10		10		8		28	19	4
25	18471A0487		10		10		8		28	19	5
26	18471A0488		10		10		8		28	19	5
27	18471A0489		10		10		7		27	18	6
28	18471A0490		10		10		10		30	20	7
29	18471A0491		10		10		9		29	20	7
30	18471A0492		7.5		7.5		6		21	14	4
31	18471A0493		10		10		7		27	18	5

NARASARAOPETA ENGINEERING COLLEGE (AUTONOMOUS) : : NARASARAOPET  
(R16) 2018 BATCH III B.TECH II SEM I MID & I QUIZ AWARD LIST, AUG - 2021

Branch : ECE - C

Subject CODE & NAME: D&P

Date: 19/8/21

Sl.No.	H.T.NO.	CO No.							MID - I Total Marks (30M)	MID- I REDUCED MARKS (20M)	QUIZ - I MARKS (10)
		Max.Marks	10		10		10				
		Q.No.	1(a)	1(b)	2(a)	2(b)	3(a)	3(b)			
1 ✓	18471A04C1		0		0		0		00	00	4
2	18471A04C2		10		10		9		29	20	5
3	18471A04C3		8		7		7		22	18	3
4	18471A04C4		9		10		9		28	19	6
5	18471A04C5		10		10		9		29	20	6
6	18471A04C6		9		7		0		16	11	5
7	18471A04C7		10		10		10		30	20	5
8	18471A04C9		8		10		9		27	18	7
9	18471A04D0		10		10		9		29	20	6
10	18471A04D1		9		10		9		28	19	2
11	18471A04D2		9		10		9		28	19	6
12	18471A04D3		10		10		9		29	20	5
13	18471A04D4		10		9		8		27	18	6
14	18471A04D5		10		10		9		29	20	5
15	18471A04D6		10		10		8		28	19	5
16	18471A04D7		10		10		9		29	20	5
17	18471A04D8		10		10		9		29	20	5
18 ✓	18471A04D9		2		8		0		10	07	1
19	18471A04E0		9		10		8		27	18	5
20	18471A04E1		10		10		9		29	20	6
21	18471A04E2		9		10		9		28	19	2
22	18471A04E3		10		10		7		27	18	5
23	18471A04E4		10		10		9		29	20	5
24	18471A04E5		9		10		9		28	19	3
25	18471A04E7		8		8		8		24	16	6
26	18471A04E8		10		10		9		29	20	6
27	18471A04E9		10		10		0		20	14	5
28	18471A04F0		10		10		10		30	20	5
29	18471A04F1		10		10		9		29	20	7
30	18471A04F2		10		10		9		29	20	5
31	18471A04F3		9		10		9		28	19	5
32	18471A04F4		10		10		7		27	18	5

NARASARAOPETA ENGINEERING COLLEGE (AUTONOMOUS) : : NARASARAOPET  
(R16) 2018 BATCH III B.TECH II SEM I MID & I QUIZ AWARD LIST, AUG - 2021

Branch : ECE - D

Subject CODE & NAME: DLP

Date: 19/8/21

Sl.No.	H.T.NO.	CO No.							MID - I Total Marks (30M)	MID- I REDUCED MARKS (20M)	QUIZ - I MARKS (10)
		Max.Marks	10	10	10						
		Q.No.	1(a)	1(b)	2(a)	2(b)	3(a)	3(b)			
1	17471A0402		0		10		1		11	08	7
2	18471A04I1		10		9		9		28	19	6
3	18471A04I2		9		9		6		26	16	7
4	18471A04I3		9		10		8		27	18	7
5	18471A04I4		9		9		2		20	14	3
6	18471A04I5		10		10		8		28	19	5
7	18471A04I6		9		9		7		27	17	4
8	18471A04I7		9		9		5		23	16	4
9	18471A04I8		10		10		8		28	19	5
10	18471A04I9		10		10		8		28	19	3
11	18471A04J0		10		10		8		28	19	7
12	18471A04J1		10		10		8		28	19	4
13	18471A04J2		9		9		5		23	16	4
14	18471A04J3		9		10		8		27	18	5
15	18471A04J4		10		10		8		28	19	6
16✓	18471A04J5		8		6		6		20	14	4
17	18471A04J6		8		8		7		23	16	4
18	18471A04J7		10		10		8		28	19	6
19	18471A04J8		10		8		5		23	16	6
20	18471A04J9		8		7		6		21	14	6
21	18471A04K0		8		7		7		22	15	4
22	18471A04K1		9		9		7		25	17	6
23	18471A04K2		10		9		7		26	18	3
24	18471A04K3		10		10		7		27	18	6
25	18471A04K4		10		10		6		26	18	4
26	18471A04K5		10		10		7		27	18	6
27	18471A04K6		10		9		7		26	18	6
28	18471A04K7		10		10		8		28	19	5
29	18471A04K8		9		9		6		24	16	6
30	18471A04K9		7		6.5		6.5		20	14	7
31	18471A04L0		6		10		6		22	15	4
32	18471A04L1		10		10		9		29	20	4
33✓	18471A04L2		6.5		6.5		7		20	14	3
34	18471A04L3		7		6.5		6.5		20	14	4
35	18471A04L4		10		10		8		28	19	5
36	18471A04L5		10		10		8		28	19	8
37	18471A04L6		10		10		8		28	19	5
38	18471A04L7		9		9		7		25	17	4

NARASARAOPETA ENGINEERING COLLEGE (AUTONOMOUS) : : NARASARAOPETA  
(R16) 2018 BATCH III B.TECH II SEM II MID & II QUIZ AWARD LIST, AUG - 2021

Branch : ECE - A

Subject CODE & NAME: DEP

Date: 19/8/21

Sl.No.	H.T.NO.	CO No.							MID - II Total Marks (30M)	MID- II REDUCED MARKS (20M)	QUIZ - II MARKS (10)
		Max.Marks	10		10		10				
		Q.No.	1(a)	1(b)	2(a)	2(b)	3(a)	3(b)			
1	18471A0401		10		10		8		28	19	6
2	18471A0402		8		8		6		22	17	2
3	18471A0403		10		10		9		29	20	5
4	18471A0405		10		10		8		28	19	4
5	18471A0406		8		8		4		20	14	2
6	18471A0407		10		10		0		20	14	5
7	18471A0408		8		8		0		16	11	2
8	18471A0409		10		10		6		26	18	2
9	18471A0410		10		0		10		20	14	3
10	18471A0411		10		9.5		9.5		29	20	4
11	18471A0412		10		9		10		29	20	5
12	18471A0413		10		10		9		29	20	4
13	18471A0414		9		9		9		27	18	3
14	18471A0415		8		8		8		24	16	2*
15	18471A0416		10		10		9		29	20	4
16	18471A0417		← AB B B N 5 →						AB	AB	A
17	18471A0418		10		10		10		30	20	5
18	18471A0419		10		10		10		30	20	4
19	18471A0420		10		10		10		30	20	5
20	18471A0421		10		10		10		30	20	5
21	18471A0422		10		10		10		30	20	6
22	18471A0423		10		10		10		30	20	3
23	18471A0424		10		9		10		29	20	4
24	18471A0425		0		0		0		00	00	03
25	18471A0426		8		2		0		10	07	02
26	18471A0427		10		10		10		30	20	3
27	18471A0428		7		10		4		21	14	4
28	18471A0429		10		8		8		26	18	6
29	18471A0430		10		10		10		30	20	7
30	18471A0431		10		10		9		29	20	5
31	18471A0432		← AB B B N 5 →						AB	AB	A
32	18471A0433		10		8.5		8.5		27	18	5

NARASARAOPETA ENGINEERING COLLEGE (AUTONOMOUS) : : NARASARAOPET  
(R16) 2018 BATCH III B.TECH II SEM II MID & II QUIZ AWARD LIST, AUG - 2021

Branch : ECE - B

Subject CODE & NAME: DEP

Date: 19/8/21

Sl.No.	H.T.NO.	CO No.						MID - II Total Marks (30M)	MID- II REDUCED MARKS (20M)	QUIZ - II MARKS (10)
		Max.Marks								
		Q.No.	1(a)	1(b)	2(a)	2(b)	3(a)			
1	18471A0461		8.5		8.5		8	25	17	4
2	18471A0463		10		10		9	29	20	7
3	18471A0464		10		10		9	29	20	5
4	18471A0465		3		2		0	05	04	3
5	18471A0466		9		10		8	27	18	3
6	18471A0467		9		7		8	26	16	2
7	18471A0468		10		10		10	30	20	4
8	18471A0470		10		10		9	29	20	5
9	18471A0471		10		10		9	29	20	4
10	18471A0472		9		10		10	29	20	7
11	18471A0473		10		10		10	30	20	5
12	18471A0474		9		10		7	26	18	5
13	18471A0475		10		10		9	29	20	4
14	18471A0476		10		10		8	28	19	4
15	18471A0477		8		8		8	26	16	5
16	18471A0478		8		8		8	26	16	2
17	18471A0479		10		10		9	29	20	5
18	18471A0480		10		10		9	29	20	5
19	18471A0481		10		10		6	26	18	3
20	18471A0482		9		5		7	21	14	4
21	18471A0483		10		10		9	29	20	5
22	18471A0484		10		5		7	22	15	4
23	18471A0485		9		1		5	15	10	4
24	18471A0486		10		10		9	29	20	4
25	18471A0487		10		10		9	29	20	3
26	18471A0488		5		0		5	10	07	4
27	18471A0489		10		9		8	27	18	4
28	18471A0490		10		10		10	30	20	6
29	18471A0491		10		10		10	30	20	6
30	18471A0492		0		0		0	00	00	4
31	18471A0493		10		10		9	29	20	5
32	18471A0494		0		0		0	00	00	04

NARASARAOPETA ENGINEERING COLLEGE (AUTONOMOUS) : : NARASARAOPET  
(R16) 2018 BATCH III B.TECH II SEM II MID & II QUIZ AWARD LIST, AUG - 2021

Branch : ECE - C

Subject CODE & NAME: DGP

Date: 19/8/21

Sl.No.	H.T.NO.	CO No.						MID - II Total Marks (30M)	MID- II REDUCED MARKS (20M)	QUIZ - II MARKS (10)	
		Max.Marks	10	10	10						
		Q.No.	1(a)	1(b)	2(a)	2(b)	3(a)	3(b)			
1	18471A04C1		0		2		5		07	05	4
2	18471A04C2		10		6		9		25	17	5
3	18471A04C3		6		4		6		16	11	4
4	18471A04C4		10		10		9		29	20	4
5	18471A04C5		10		10		9		29	20	5
6	18471A04C6		9		9		4		22	15	4
7	18471A04C7		8		10		10		28	19	3
8	18471A04C9		10		10		9		29	20	5
9	18471A04D0		10		10		9		29	20	4
10	18471A04D1		10		5		6		21	14	4
11	18471A04D2		10		9		5		24	16	4
12	18471A04D3		10		10		9		29	20	4
13	18471A04D4		9		10		9		28	19	6
14	18471A04D5		10		9		9		28	19	4
15	18471A04D6		8		8		8		24	16	5
16	18471A04D7		10		10		9		29	20	4
17	18471A04D8		10		10		9		29	20	6
18	18471A04D9		8		0		9		17	12	4
19	18471A04E0		10		10		9		27	18	4
20	18471A04E1		10		10		9		29	20	5
21	18471A04E2		10		10		9		29	20	2
22	18471A04E3		10		10		9		29	20	5
23	18471A04E4		10		10		10		30	20	4
24	18471A04E5		9.5		6		9.5		25	17	2
25	18471A04E7		9		0		8		17	12	4
26	18471A04E8		10		7		10		27	18	4
27	18471A04E9		7		0		0		07	05	2
28	18471A04F0		10		10		10		30	20	4
29	18471A04F1		10		10		9		29	20	6
30	18471A04F2		10		10		9		29	20	5
31	18471A04F3		9		9		9		27	18	4
32	18471A04F4		10		5		10		25	17	4



NARASARAOPETA ENGINEERING COLLEGE (AUTONOMOUS) : : NARASARAOPETA  
(R16) 2018 BATCH III B.TECH II SEM II MID & II QUIZ AWARD LIST, AUG - 2021

Branch : ECE - D

Subject CODE & NAME: D&P

Date: 19/8/21

Sl.No.	H.T.NO.	CO No.							MID - II	MID- II	QUIZ - II
		Max.Marks	10		10		10	Total	REDUCED	MARKS	
		Q.No.	1(a)	1(b)	2(a)	2(b)	3(a)	3(b)	(30M)	(20M)	(10)
1	17471A0402	←			AB			AB	AB	AB	
2	18471A04I1		9		5		0	14	10	4 ✓	
3	18471A04I2		9		7		0	16	11	5 ✓	
4	18471A04I3		9		3		3	15	10	3 ✓	
5	18471A04I4		10		5		0	15	10	3 ✓	
6	18471A04I5		8		7		8	23	16	5 ✓	
7	18471A04I6		8		0		0	08	06	4 ✓	
8	18471A04I7		3		0		3	06	04	2 ✓	
9	18471A04I8		9		0		7	16	11	3 ✓	
10	18471A04I9		10		10		0	20	14	5 ✓	
11	18471A04J0		10		10		0	20	14	5 ✓	
12	18471A04J1		10		10		0	20	14	4 ✓	
13	18471A04J2		9		3		2	14	10	2 ✓	
14	18471A04J3		9		2		4	15	10	4 ✓	
15	18471A04J4		10		10		9	29	20	3 ✓	
16	18471A04J5		8		5		6	19	13	4 ✓	
17	18471A04J6		9		9		3	21	14	4 ✓	
18	18471A04J7		10		2		5	15	10	5 ✓	
19	18471A04J8		9		5		2	16	11	6 ✓	
20	18471A04J9		10		10		7	27	18	4 ✓	
21	18471A04K0		10		10		0	20	14	2 ✓	
22	18471A04K1		9		9		2	20	14	4 ✓	
23	18471A04K2		10		0		0	10	07	3 ✓	
24	18471A04K3		9		3		5	20	14	3 ✓	
25	18471A04K4		10		0		0	10	07	7 ✓	
26	18471A04K5	←			AB			AB	AB	AB ✓	
27	18471A04K6		10		5		0	15	10	6 ✓	
28	18471A04K7		10		10		5	25	17	4 ✓	
29	18471A04K8		10		10		0	20	14	4 ✓	
30	18471A04K9		10		0		0	10	07	2 ✓	
31	18471A04L0		0		0		0	00	00	5 ✓	
32	18471A04L1		10		10		5	25	17	5 ✓	
33	18471A04L2		1		4		0	05	04	6 ✓	
34	18471A04L3		0		3		3	06	04	4 ✓	
35	18471A04L4		8		0		0	08	06	4 ✓	
36	18471A04L5		10		0		0	10	07	2 ✓	
37	18471A04L6		10		5		2	17	12	4 ✓	
38	18471A04L7		8		7		0	15	10	5 ✓	

# EXTERNAL RESULTS

**(R16) 2018 BATCH III B.TECH II SEMESTER RESULTS BEFORE REVALUATION AUGUST - 2021**

BRANCH : ECE

DATE : 16.11.2021

SLNO	HTNO	NAME	R16CC32MNC2		R16CC320E19		R16EC3201		R16EC3202		R16EC3203		R16EC3204		R16EC3209		R16EC32L1		R16EC32L2		R16EC32NO		SGPA	
			GR	GP	CR	GP	CR	GP	CR	GP	CR	GP	CR	GP	CR	GP	CR	GP	CR	GP	CR	GP		CR
1	17471A0402	ANAM PRABHU CHAITANYA	S	0	0	F	0	0	F	0	0	F	0	0	F	0	0	AB	0	0	S	0	0	NA
2	18471A0401	ANUMALASETTY DHARAMI	S	0	0	A	8	3	A	8	3	E	9	3	A	8	3	0	10	2	S	0	0	8.5
3	18471A0402	AVULA NAVEEN	S	0	0	P	5	3	B	7	3	B	7	3	C	6	3	E	9	2	S	0	0	6.82
4	18471A0403	BADUGU PRAKASH BABU	S	0	0	E	9	3	E	9	3	O	10	3	B	7	3	E	9	2	S	0	0	8.95
5	18471A0405	BALLI PALLI SAI VENKAT	S	0	0	A	8	3	A	8	3	E	9	3	B	7	3	0	10	2	S	0	0	8.09
6	18471A0406	BANDARU SAI KUMAR	S	0	0	F	0	0	F	0	0	B	7	3	P	5	3	E	9	2	S	0	0	NA
7	18471A0407	BATHULA SRINU	S	0	0	E	9	3	A	8	3	C	6	3	B	7	3	0	10	2	S	0	0	8.23
8	18471A0408	BEERAM UPENDRA REDDY	S	0	0	F	0	0	B	7	3	F	0	0	F	0	0	E	9	2	S	0	0	NA
9	18471A0409	BHUVANAM NAGA VAMSI	S	0	0	C	6	3	B	7	3	C	6	3	B	7	3	A	8	2	S	0	0	7.23
10	18471A0410	BOBBILLA KARTHIK	S	0	0	B	7	3	B	7	3	A	8	3	B	7	3	A	8	2	S	0	0	7.41
11	18471A0411	BODLAPATI SRAVYA	S	0	0	A	8	3	A	8	3	C	6	3	B	7	3	0	10	2	S	0	0	7.95
12	18471A0412	BURRI MAGAVENI	S	0	0	B	7	3	A	8	3	A	8	3	A	8	3	0	10	2	S	0	0	8.36
13	18471A0413	CHAKKA MANOJ KUMAR	S	0	0	B	7	3	A	8	3	C	6	3	B	7	3	0	10	2	S	0	0	7.95
14	18471A0414	CHITTINENI SIDDHARDHA	S	0	0	C	6	3	C	6	3	B	7	3	B	7	3	0	10	2	S	0	0	6.95
15	18471A0415	CHOPPARA MANOJ KUMAR	S	0	0	P	5	3	F	0	0	F	0	0	P	5	3	F	0	0	A	8	2	NA
16	18471A0416	DASIREDDY NAGI REDDY	S	0	0	A	8	3	A	8	3	E	9	3	A	8	3	E	9	3	A	8	2	8.32
17	18471A0417	DEVARAKOOTA NITESH KUMAR REDDY	S	0	0	P	5	3	B	7	3	B	7	3	P	5	3	P	5	3	E	9	2	6.27
18	18471A0418	DEVARAPALLI KUSUMITHA	S	0	0	A	8	3	E	9	3	E	9	3	A	8	3	0	10	2	S	0	0	8.5
19	18471A0419	GADIBOYINA JAYENDRA KUMAR	S	0	0	A	8	3	B	7	3	C	6	3	A	8	3	0	10	2	S	0	0	7.73
20	18471A0420	GAYAM RAMYA	S	0	0	A	8	3	O	10	3	E	9	3	A	8	3	0	10	2	S	0	0	8.77
21	18471A0421	GOPU GANESH SIVA SAI	S	0	0	A	8	3	A	8	3	E	9	3	A	8	3	0	10	2	S	0	0	8.77
22	18471A0422	GOPU SAI MOULI	S	0	0	A	8	3	A	8	3	E	9	3	A	8	3	0	10	2	S	0	0	8.5
23	18471A0423	GOTTIPATI VAMSI	S	0	0	A	8	3	A	8	3	E	9	3	A	8	3	E	9	2	S	0	0	7.95
24	18471A0424	GUPPALAMPATI MANOJ KUMAR	S	0	0	A	8	3	E	9	3	A	8	3	E	9	3	E	9	2	S	0	0	8.59
25	18471A0425	INAGANTI BHARATH TEJA	S	0	0	P	5	3	B	7	3	A	8	3	P	5	3	P	5	3	A	8	2	6.14
26	18471A0426	JALADI SAI KRISHNA	S	0	0	C	6	3	B	7	3	C	6	3	C	6	3	E	9	2	S	0	0	6.86
27	18471A0427	JILLELLAMUDI SRINIVASU	S	0	0	B	7	3	A	8	3	E	9	3	A	8	3	A	8	2	S	0	0	7.95

**(R16) 2018 BATCH III B.TECH II SEMESTER RESULTS BEFORE REVALUATION AUGUST - 2021**

SLNO	HTNO	NAME	R16CC32MNC2		R16CC320E19		R16EC3201		R16EC3202		R16EC3203		R16EC3204		R16EC3209		R16EC32L1		R16EC32L2		R16EC32NO			
			GR	CR	GR	CR	GR	CR	GR	CR	GR	CR	GR	CR	GR	CR	GR	CR	GR	CR	GR	CR	GR	CR
1	18471A0402	ANNAM PRABHU CHAITANYA	S	0	0	F	0	0	F	0	0	F	0	0	F	0	0	AB	0	0	S	0	0	NA
2	18471A0401	ANUMALASETTY DHARANI	S	0	0	A	8	3	A	8	3	E	9	3	A	8	3	0	10	2	S	0	0	8.5
3	18471A0402	AVULA NAVEEN	S	0	0	P	5	3	C	6	3	B	7	3	C	6	3	E	9	2	S	0	0	6.82
4	18471A0403	BADUGU PRAKASH BABU	S	0	0	E	9	3	E	9	3	O	10	3	E	9	3	E	9	2	S	0	0	8.95
5	18471A0405	BALLI PALLI SAI VENKAT	S	0	0	A	8	3	E	9	3	E	9	3	B	7	3	O	10	2	S	0	0	8.09
6	18471A0406	BANDARU SAI KUMAR	S	0	0	F	0	0	F	0	0	B	7	3	P	5	3	E	9	2	S	0	0	NA
7	18471A0407	BATHULA SRINU	S	0	0	E	9	3	C	6	3	A	8	3	B	7	3	O	10	2	S	0	0	8.23
8	18471A0408	BEERAM UPENDRA REDDY	S	0	0	F	0	0	F	0	0	B	7	3	F	0	0	E	9	2	S	0	0	NA
9	18471A0409	BHUVANAM NAGA VAMSI	S	0	0	C	6	3	C	6	3	A	8	3	B	7	3	A	8	2	S	0	0	7.23
10	18471A0410	BOBBILLA KARTHICK	S	0	0	B	7	3	B	7	3	A	8	3	B	7	3	A	8	2	S	0	0	7.41
11	18471A0411	BODLAPATI SRAVYA	S	0	0	A	8	3	C	6	3	A	8	3	B	7	3	O	10	2	S	0	0	7.95
12	18471A0412	BURRI NAGAVENI	S	0	0	B	7	3	A	8	3	A	8	3	A	8	3	O	10	2	S	0	0	8.36
13	18471A0413	CHAKKA MANOJ KUMAR	S	0	0	B	7	3	C	6	3	A	8	3	E	9	3	O	10	2	S	0	0	7.95
14	18471A0414	CHITTINENI SIDDHARDHA	S	0	0	C	6	3	C	6	3	B	7	3	C	6	3	A	8	2	S	0	0	6.95
15	18471A0415	CHOPPARA MANOJ KUMAR	S	0	0	P	5	3	F	0	0	F	0	0	P	5	3	A	8	2	S	0	0	NA
16	18471A0416	DASIREDDY NAGI REDDY	S	0	0	A	8	3	A	8	3	E	9	3	A	8	3	A	8	2	S	0	0	8.32
17	18471A0417	DEVARAKOOTA NITESH KUMAR REDDY	S	0	0	P	5	3	P	5	3	B	7	3	P	5	3	E	9	2	S	0	0	6.27
18	18471A0418	DEVARAPALLI KUSUMITHA	S	0	0	A	8	3	E	9	3	E	9	3	A	8	3	O	10	2	S	0	0	8.5
19	18471A0419	GADIBOYINA JAVENDRA KUMAR	S	0	0	A	8	3	A	8	3	A	8	3	A	8	3	E	9	2	S	0	0	7.73
20	18471A0420	GAYAM RAMYA	S	0	0	A	8	3	A	8	3	E	9	3	A	8	3	O	10	2	S	0	0	8.77
21	18471A0421	GOPU GANESH SIVA SAI	S	0	0	A	8	3	A	8	3	E	9	3	A	8	3	O	10	2	S	0	0	8.77
22	18471A0422	GOPU SAI MOULI	S	0	0	A	8	3	A	8	3	E	9	3	A	8	3	O	10	2	S	0	0	8.5
23	18471A0423	GOTTIPATI VAMSI	S	0	0	A	8	3	A	8	3	E	9	3	B	7	3	A	8	2	S	0	0	7.95
24	18471A0424	GUWALAMPATI MANOJ KUMAR	S	0	0	A	8	3	A	8	3	A	8	3	E	9	3	E	9	2	S	0	0	8.59
25	18471A0425	INAGANTI BHARATH TEJA	S	0	0	P	5	3	P	5	3	A	8	3	P	5	3	B	7	2	S	0	0	6.14
26	18471A0426	JALADI SAI KRISHNA	S	0	0	C	6	3	C	6	3	A	8	3	C	6	3	A	8	2	S	0	0	6.86
27	18471A0427	JILLELLAMUDI SRINIVASU	S	0	0	B	7	3	B	7	3	E	9	3	A	8	3	E	9	2	S	0	0	7.95

BRANCH : ECE

DATE : 16.11.2021











184	18471A0419	GATTIPALLI LAKSHMI PRAVALIKA	S	0	0	A	8	3	3	7	3	A	8	3	3	A	8	3	3	7	3	0	10	2	5	0	0	7.95
185	18471A0420	JUNUBOYINA SRINIVASARAO	S	0	0	E	9	3	3	8	3	A	8	3	3	E	9	3	3	8	3	0	10	2	5	0	0	8.77
186	18471A0421	KAMBALA NAVYA HARIKA	S	0	0	E	9	3	3	7	3	B	7	3	3	E	9	3	3	7	3	0	10	2	5	0	0	8.77
187	18471A0422	KAMEPALLI HARISH	S	0	0	A	8	3	3	6	3	C	6	3	3	A	8	3	3	6	3	0	10	2	5	0	0	7.59
188	18471A0423	KANAPARTHI ROHITH	S	0	0	A	8	3	3	7	3	B	7	3	3	E	9	3	3	7	3	E	9	2	5	0	0	8.05
189	18471A0424	KARANAM GOPI CHANDHD	S	0	0	E	9	3	3	8	3	A	8	3	3	O	10	3	3	8	3	E	9	2	5	0	0	8.82
190	18471A0425	LINGGAKANTLA SHAIK AMEER BASHA	S	0	0	C	6	3	3	6	3	P	5	3	3	C	6	3	3	6	3	MP	0	2	5	0	0	NA
191	18471A0426	MALAMPATI NAVEEN	S	0	0	A	8	3	3	7	3	C	6	3	3	E	9	3	3	7	3	B	7	2	5	0	0	7.86
192	18471A0427	MANDAVA PRANAY KUMAR	S	0	0	A	8	3	3	8	3	B	7	3	3	E	9	3	3	8	3	B	7	2	5	0	0	7.91
193	18471A0428	MARRIKANTI VEERA CHARY	S	0	0	A	8	3	3	6	3	C	6	3	3	E	9	3	3	6	3	C	6	2	5	0	0	7.55
194	18471A0429	MUDDAPATI SAI TEJA	S	0	0	E	9	3	3	8	3	A	8	3	3	E	9	3	3	8	3	E	9	2	5	0	0	8.59
195	18471A0430	NARNE PAVANESWAR	S	0	0	A	8	3	3	6	3	C	6	3	3	A	8	3	3	6	3	B	7	2	5	0	0	7.5
196	18471A0431	PASAM JAYA SAI REDDY	S	0	0	B	7	3	3	6	3	C	6	3	3	A	8	3	3	6	3	F	0	2	5	0	0	NA
197	18471A0432	PERIGSETTY SURESH	S	0	0	A	8	3	3	7	3	B	7	3	3	A	8	3	3	7	3	E	9	2	5	0	0	7.95
198	18471A0433	PERLA BHAVANI	S	0	0	B	7	3	3	6	3	C	6	3	3	A	8	3	3	6	3	B	7	2	5	0	0	7.55
199	18471A0434	POLURI HARI PRIYA REDDY	S	0	0	A	8	3	3	7	3	B	7	3	3	A	8	3	3	7	3	B	7	2	5	0	0	7.77
200	18471A0435	PONUKOTI SIVA MANIKANTA SAI	S	0	0	C	6	3	3	6	3	C	6	3	3	B	7	3	3	6	3	C	6	2	5	0	0	7.05
201	18471A0436	RAJANALA KARTHIKEYA	S	0	0	A	8	3	3	7	3	B	7	3	3	A	8	3	3	7	3	A	8	2	5	0	0	8.09
202	18471A0437	SARANGI VENKATA SAI	S	0	0	E	9	3	3	8	3	A	8	3	3	E	9	3	3	8	3	A	8	2	5	0	0	8.68
203	18471A0438	SHAIK ABDUL BASHA	S	0	0	E	9	3	3	7	3	B	7	3	3	A	8	3	3	7	3	B	7	2	5	0	0	8
204	18471A0439	SHAIK BAJI	S	0	0	C	6	3	3	6	3	C	6	3	3	C	6	3	3	6	3	B	7	2	5	0	0	6.55
205	18471A0440	SHAIK FAREED BABA	S	0	0	P	5	3	3	5	3	P	5	3	3	P	5	3	3	5	3	F	0	2	5	0	0	NA
206	18471A0441	SHAIK HAPPSA	S	0	0	A	8	3	3	6	3	E	9	3	3	E	9	3	3	6	3	A	8	2	5	0	0	8.68
207	18471A0442	SHAIK SADDAM HUSSAIN	S	0	0	B	7	3	3	6	3	C	6	3	3	B	7	3	3	6	3	MP	0	2	5	0	0	NA
208	18471A0443	SHAIK TANVIR	S	0	0	P	5	3	3	6	3	C	6	3	3	F	0	0	3	6	3	C	6	2	5	0	0	NA
209	18471A0444	SHAIK UMRE FAROOQ	S	0	0	A	8	3	3	7	3	B	7	3	3	B	7	3	3	7	3	A	8	2	5	0	0	7.45
210	18471A0445	SYED MOHAMMAD ALI	S	0	0	B	7	3	3	6	3	C	6	3	3	C	6	3	3	6	3	C	6	2	5	0	0	6.86
211	18471A0446	TAVVA KANAKA TEJA	S	0	0	A	8	3	3	7	3	C	6	3	3	B	7	3	3	7	3	A	8	2	5	0	0	7.77
212	18471A0447	THANGUDALA RAJASEKHAR REDDY	S	0	0	A	8	3	3	6	3	C	6	3	3	C	6	3	3	6	3	B	7	2	5	0	0	7.27
213	18471A0448	THIMMISETTY ANIL KUMAR	S	0	0	E	9	3	3	7	3	B	7	3	3	A	8	3	3	7	3	B	7	2	5	0	0	8.23
214	18471A0449	VEERLA TRINADH	S	0	0	C	6	3	3	6	3	P	5	3	3	P	5	3	3	6	3	B	7	2	5	0	0	6.32
215	18471A0450	YARLAGADDA NAVYA SAI	S	0	0	A	8	3	3	7	3	B	7	3	3	E	9	3	3	7	3	A	8	2	5	0	0	8.5
216	18471A0451	LAKKAKULA AKASH	S	0	0	B	7	3	3	6	3	C	6	3	3	C	6	3	3	6	3	P	5	2	5	0	0	6.77
217	18471A0452	NELAKURTHI HARITHA	S	0	0	A	8	3	3	7	3	B	7	3	3	E	9	3	3	7	3	A	8	2	5	0	0	8.36
218	18471A0453	ANAMITHA LAKSHMI RISHITHA	S	0	0	E	9	3	3	6	3	B	7	3	3	E	9	3	3	6	3	B	7	2	5	0	0	8.5
219	18471A0454	PATHAN BALASAJDA	S	0	0	A	8	3	3	6	3	C	6	3	3	B	7	3	3	6	3	B	7	2	5	0	0	7.27
220	19475A0401	KOLAGANI TEJANJALI	S	0	0	E	9	3	3	8	3	E	9	3	3	E	9	3	3	8	3	A	8	2	5	0	0	8.91
221	19475A0402	SHAIK MASUDA	S	0	0	A	8	3	3	7	3	E	9	3	3	E	9	3	3	7	3	A	8	2	5	0	0	8.64
222	19475A0403	MUTLURI DAVID	S	0	0	A	8	3	3	6	3	B	7	3	3	A	8	3	3	6	3	B	7	2	5	0	0	7.95

223	19475A0404	VINUKONDA PRIYANKA	S	0	0	A	8	3	3	E	9	3	A	8	3	A	8	3	3	0	10	2	S	0	0	8.41
224	19475A0405	BANDARU HARIKA	S	0	0	A	8	3	3	E	9	3	B	7	3	A	8	3	3	0	10	2	S	0	0	8.23
225	19475A0406	BANTUPALLI SUDHEER KUMAR	S	0	0	E	9	3	3	E	9	3	B	7	3	A	8	3	3	0	10	2	S	0	0	8.55
226	19475A0407	KATTAPURI JAGADEESH KUMAR	S	0	0	B	7	3	3	C	6	3	F	7	3	B	7	3	3	0	10	2	S	0	0	NA
227	19475A0408	TELAGATHOTI NAVEEN	S	0	0	B	7	3	3	B	7	3	C	6	3	C	6	3	3	0	10	2	S	0	0	7.52
228	19475A0409	UDATHA NARENDRA	S	0	0	A	8	3	3	B	7	3	B	7	3	B	7	3	3	0	10	2	S	0	0	7.82
229	19475A0410	PEDDISETTI PRABHU KUMAR	S	0	0	E	9	3	3	B	7	3	A	8	3	A	8	3	3	0	10	2	S	0	0	8.5
230	19475A0411	EEMANI LAKSHMI NARAYANA	S	0	0	A	8	3	3	A	8	3	C	6	3	A	8	3	3	0	10	2	S	0	0	7.64
231	19475A0412	MANNEM SAMBASIVA RAO	S	0	0	C	6	3	3	B	7	3	C	6	3	B	7	3	3	E	9	2	S	0	0	6.95
232	19475A0413	PARITALA SREEKANTH	S	0	0	E	9	3	3	A	8	3	C	6	3	A	8	3	3	0	10	2	S	0	0	8.36
233	19475A0414	VADDI MAGALAKSHMI	S	0	0	E	9	3	3	A	8	3	B	7	3	A	8	3	3	0	10	2	S	0	0	8.5
234	19475A0415	BOLE SRINU	S	0	0	E	9	3	3	E	9	3	C	6	3	E	9	3	3	0	10	2	S	0	0	8.55
235	19475A0416	ARIKATLA VENU GOPALA REDDY	S	0	0	A	8	3	3	B	7	3	A	8	3	A	8	3	3	E	9	2	S	0	0	7.91
236	19475A0417	KATTEKOTA JAGANNATHA SAI KOTESWAR	S	0	0	E	9	3	3	B	7	3	E	9	3	E	9	3	3	0	10	2	S	0	0	8.64
237	19475A0418	PAMIDIMALLA SAMUEL JOE	S	0	0	E	9	3	3	O	10	3	A	8	3	AB	0	0	0	0	10	2	S	0	0	NA
238	19475A0419	GALIDINNE PAVAN KALYAN	S	0	0	E	9	3	3	B	7	3	P	5	3	B	7	3	3	E	9	2	S	0	0	7.36
239	19475A0420	PALAPARTHI CHANDRABABU	S	0	0	A	8	3	3	A	8	3	C	6	3	B	7	3	3	0	10	2	S	0	0	7.77
240	19475A0421	ALAKUNTA SRIHARI	S	0	0	B	7	3	3	A	8	3	C	6	3	B	7	3	3	0	10	2	S	0	0	7.5
241	19475A0422	BALIJEPALETTI GANGAMMA	S	0	0	E	9	3	3	B	7	3	A	8	3	A	8	3	3	0	10	2	S	0	0	8
242	19475A0423	GUDURI RAJASREE	S	0	0	A	8	3	3	E	9	3	B	7	3	A	8	3	3	0	10	2	S	0	0	8.36
243	19475A0424	KATIKAM MAHESH BABU	S	0	0	C	6	3	3	A	8	3	C	6	3	F	0	0	0	E	9	2	S	0	0	NA
244	19475A0425	KOLA JAYANTH SAI GANESH	S	0	0	A	8	3	3	E	9	3	C	6	3	B	7	3	3	E	9	2	S	0	0	7.77
245	19475A0426	KOTTAPALLI SAIKUMAR	S	0	0	E	9	3	3	A	8	3	B	7	3	A	8	3	3	E	9	2	S	0	0	8.32

*M/S*

CHIEF CONTROLLER OF EXAMINATIONS

